CEPHALOPODS FROM THE CRETACEOUS/ TERTIARY BOUNDARY INTERVAL ON THE ATLANTIC COASTAL PLAIN, WITH A DESCRIPTION OF THE HIGHEST AMMONITE ZONES IN NORTH AMERICA. PART III. MANASQUAN RIVER BASIN, MONMOUTH COUNTY, NEW JERSEY

NEIL H. LANDMAN
Division of Paleontology (Invertebrates)
American Museum of Natural History
(landman@amnh.org)

RALPH O. JOHNSON
Monmouth Amateur Paleontologist's Society
57 Oceanport Avenue, West Long Branch, NJ 07764
(paleotrog@webtv.net)

MATTHEW P. GARB
Department of Geology
Brooklyn College and Graduate School of the City
University of New York, Brooklyn, NY 11210
(mgarb@brooklyn.cuny.edu)

LUCY E. EDWARDS
U.S. Geological Survey
Mail Stop 926A, Reston, VA 20192
(leedward@usgs.gov)

FRANK T. KYTE
Institute of Geophysics and Planetary Physics
University of California, Los Angeles, CA 90095-1567
(kyte@igpp.ucla.edu)

BULLETIN OF THE AMERICAN MUSEUM OF NATURAL HISTORY
CENTRAL PARK WEST AT 79TH STREET, NEW YORK, NY 10024
Number 303, 122 pp., 56 figures, 12 tables
Issued April 10, 2007

 ISSN 0003-0090

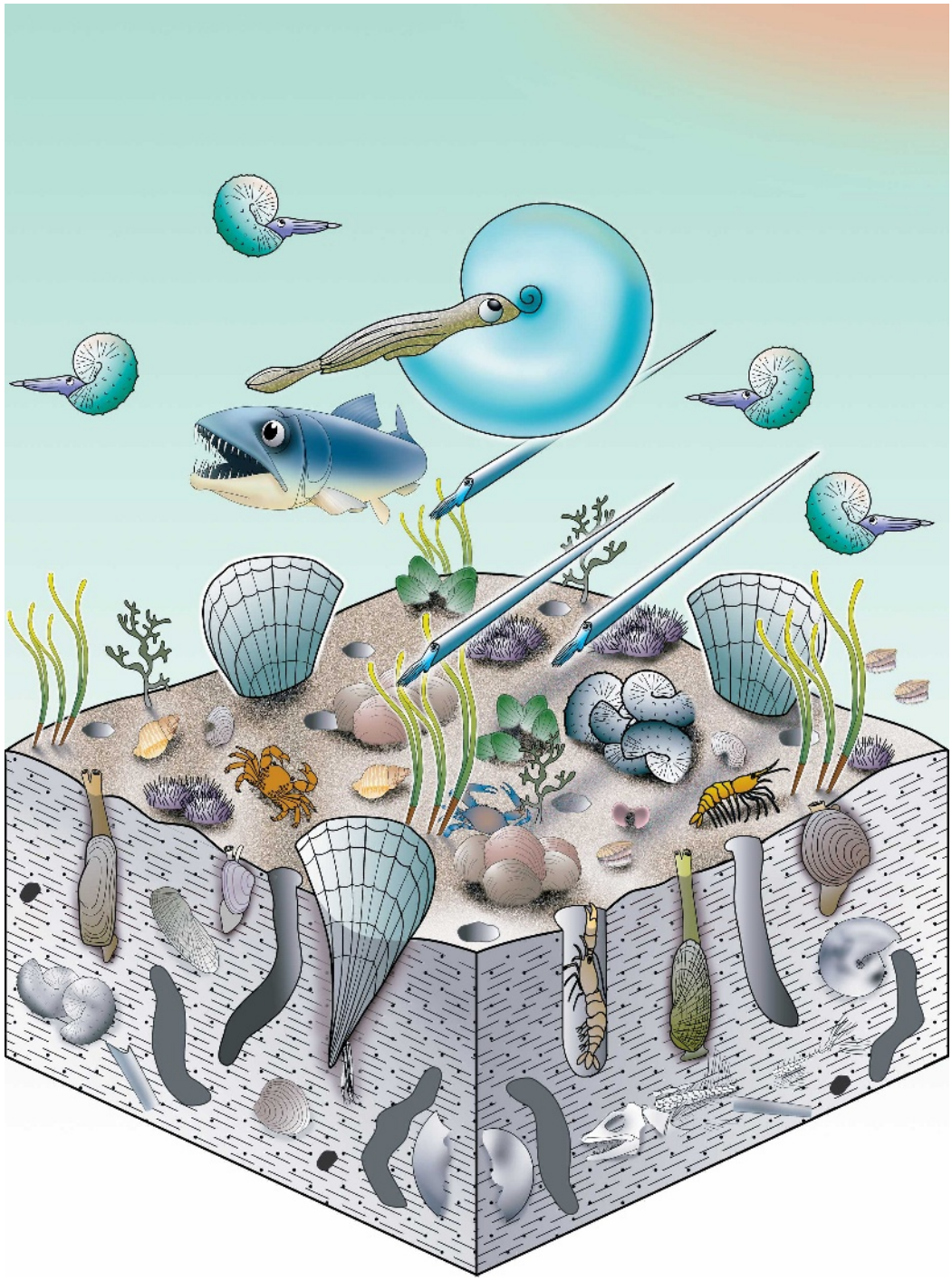

Frontispiece. Reconstruction of the sea bottom on the Atlantic Coast at the end of the Cretaceous, as inferred from sections in the Manasquan River Basin, Monmouth County, New Jersey, just before the meteor impact (upper right). Some of the animals shown are the fish *Enchodus*, the ammonites *Sphenodiscus lobatus*, *Eubaculites latecarinatus*, and *Discoscaphites iris* (with accumulations of dead shells on the sea floor), the bivalves *Pinna laqueata* (in vertical life position), *Cucullaea vulgaris* (in clusters, as in life), *Pycnodonte convexa* (in clusters, as in life), and *Pecten venustus* (in swimming and resting mode), and the echinoid *Hemiaster dalli* (singly and in aggregations).

CONTENTS

ABSTRACT

Geological investigations in the upper Manasquan River Basin, central Monmouth County, New Jersey, reveal a Cretaceous/Tertiary (= Cretaceous/Paleogene) succession consisting of approximately 2 m of the Tinton Formation overlain by 2 m of the Hornerstown Formation. The top of the Tinton Formation consists of a very fossiliferous unit, approximately 20 cm thick, which we refer to as the *Pinna* Layer. It is laterally extensive and consists mostly of glauconitic minerals and some angular quartz grains. The *Pinna* Layer is truncated at the top and is overlain by the Hornerstown Formation, which consists of nearly equal amounts of glauconitic minerals and siderite. The base of the Hornerstown Formation is marked by a concentration of siderite nodules containing reworked fossils. This layer also contains a few fossils of organisms that were living in the environment during the time of reworking. At some downdip sites, there is an additional layer (the Burrowed Unit), which is sandwiched between the top of the *Pinna* Layer and the concentrated bed of nodules. This unit is very thin and is characterized by large burrows piping down material from above.

The *Pinna* Layer is abundantly fossiliferous and represents a diverse, nearshore marine community. It contains approximately 110 species of bivalves, gastropods, cephalopods, echinoids, sponges, annelids, bryozoans, crustaceans, and dinoflagellates. The cephalopods include *Eutrephoceras dekayi* (Morton, 1834), *Pachydiscus* (*Neodesmoceras*) *mokotibensis* Collignon, 1952, *Sphenodiscus lobatus* (Tuomey, 1856), *Eubaculites carinatus* (Morton, 1834), *Eubaculites latecarinatus* (Brunnschweiler, 1966), *Discoscaphites iris* (Conrad, 1858), *Discoscaphites sphaeroidalis* Kennedy and Cobban, 2000, *Discoscaphites minardi* Landman et al., 2004b, *Discoscaphites gulosus* (Morton, 1834), and *Discoscaphites jerseyensis*, n.sp. The dinoflagellates include *Palynodinium grallator* Gocht, 1970, *Thalassiphora pelagica* (Eisenack, 1954) Eisenack & Gocht, 1960, *Deflandrea galeata* (Lejeune-Carpentier, 1942) Lentin & Williams, 1973, and *Disphaerogena carposphaeropsis* Wetzel, 1933. These ammonites and dinoflagellates are indicative of the uppermost Maastrichtian, corresponding to the upper part of calcareous nannofossil Subzone CC26b.

The mode of occurrence of the fossils in the *Pinna* Layer suggests an autochthonous accumulation with little or no postmortem transport. Many of the benthic organisms are preserved in life position. For example, specimens of *Pinna laqueata* Conrad, 1858, are oriented in a vertical position, similar to that of modern members of this genus. The echinoids also occur in aggregations of hundreds of individuals, suggesting gregarious feeding behavior. In addition, there are monospecific clusters of baculites and scaphites. These clusters are biological in origin and could not have been produced by hydraulic means. Scaphite jaws are also present, representing the first reports of these structures in the Upper Cretaceous of the Atlantic Coastal Plain. They occur both as isolated specimens and inside the body chamber, and indicate little or no postmortem transport.

The *Pinna* Layer represents a geologically short interval of time. The fact that most of the animals are mature suggests that the community persisted for at least 5–10 years. If multiple generations of animals are present, perhaps reflecting multiple episodes of colonization and burial, then this unit probably represents more time, amounting to several tens of years. The fact that the *Pinna* Layer is truncated at the top implies a still longer period of time, amounting to hundreds of years. These age estimates are consistent with observed rates of sedimentation in nearshore environments.

Iridium analyses of 37 samples of sediment from three sites in the Manasquan River Basin reveal an elevated concentration of iridium of 520 pg/g, on average, at the base of the *Pinna* Layer. The iridium profile is aymmetric with an abrupt drop off above the base of this unit and a gradual decline below the base. The elevated concentration of iridium is not as high as that recorded from some other Cretaceous/Tertiary boundary sections. However, it is sufficiently above background level to suggest that it is related to the global Ir anomaly documented at many other localities, and attributed to a bolide impact.

The position of the iridium anomaly at the base of the *Pinna* Layer is inconsistent with the biostratigraphic data, because this anomaly occurs below the unit containing fossils indicative of

the uppermost Maastrichtian. We present two alternative hypotheses:

(1) If the enriched concentration of iridium is in place, it marks the Cretaceous/Tertiary boundary by reference to the global stratotype section and point at El Kef, Tunisia. The position of the iridium anomaly further implies that the *Pinna* community was living at the moment of impact and may even have flourished in its immediate wake. Subsequently, the community may have been buried by pulses of mud-rich sediment, possibly associated with enhanced riverine discharge following the impact. The Burrowed Unit may represent a subsequent pulse of riverine discharge that scoured the top of the *Pinna* Layer.

(2) The iridium anomaly was originally located at the top of the *Pinna* Layer and was displaced downward due to bioturbation and/or chemical diffusion. This hypothesis implies that the *Pinna* Layer was deposited prior to the deposition of the iridium. The *Pinna* community may have died before or at the moment of impact. Erosion of the top of the *Pinna* Layer and deposition of the Burrowed Unit may have been associated with events immediately following the impact.

In both hypotheses, the sea floor experienced an extended period of erosion and reworking in the early Danian, which may have lasted for several hundred thousand years, producing a concentrated lag of siderite nodules containing reworked fossils in the basal part of the Hornerstown Formation. This lag deposit is equivalent to the Main Fossiliferous Layer at the base of the Hornerstown Formation elsewhere in New Jersey. This period of erosion and reworking was probably associated with a transgression in the early Danian. The post-impact community was greatly reduced in diversity, with most of the species representing Cretaceous survivors.

INTRODUCTION

Sediments spanning the Cretaceous/Tertiary (=Cretaceous/Paleogene) boundary in New Jersey crop out in a belt extending from the Sandy Hook embayment in the northeast to the Delaware embayment in the southwest. These sediments have been extensively studied in both surface exposures and cores (Olsson, 1960, 1963, 1975, 1987; Minard et al., 1969; Owens and Sohl, 1969; Gallagher, 1986, 1993, 2002; Gallagher et al., 1986; Olsson et al., 1997, 2002; Miller et al., 2004). Recently, Landman et al. (2004b) described the stratigraphic section in northeastern Monmouth County and compared it with well-known localities in the Crosswicks Creek Basin, southwestern Monmouth County, and the Inversand Pit, near Sewell, Gloucester County.

One of the missing pieces of the geologic puzzle was the area between northeastern and southwestern Monmouth County (''the Black Hole''), which was hardly treated in the literature at all. The geologic map of New Jersey by Lewis and Kümmel (1910–1912) indicated that the Manasquan River Basin, southwest of Freehold, central Monmouth County, exposed the Hornerstown Formation overlying the combined Tinton and Red Bank formations, suggesting that this area was an interesting place to look (figs. 1, 2). During the course of these investigations, serendipity intervened in the guise of a bridge construction. This excavation revealed a beautiful section of Upper Cretaceous and Paleocene rocks spanning the K/T boundary and containing the most abundant and diverse invertebrate assemblage ever discovered from this interval in New Jersey. Although the bridge excavation activities only lasted a week, they provided us with enough background to further explore and document the same section in the natural exposures along the adjacent stream banks. However, without stumbling upon the original construction site and the generous assistance of the construction crew, these sections might not have been discovered.

This is the third in a series of four papers on the K/T boundary interval on the Atlantic Coastal Plain. The reader is referred to Part 2 (Landman et al., 2004b) for a general overview of the Upper Cretaceous stratigraphy of New Jersey. Our primary focus in these papers is to document the diversity and

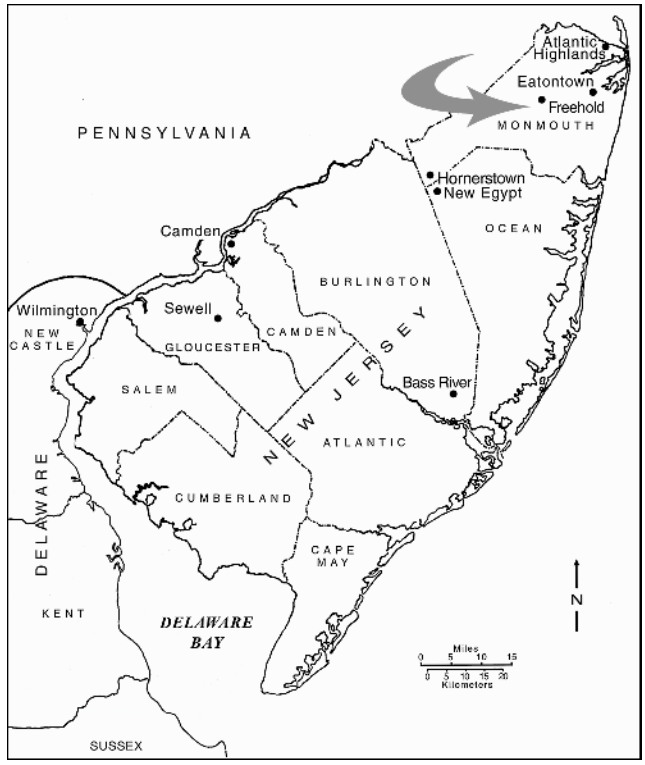

Fig. 1. Map of parts of New Jersey showing localities mentioned in the text. The Manasquan River Basin is indicated by an arrow.

distribution of cephalopods at the top of the Cretaceous. One of the most astonishing outcomes of this project is the discovery of a richly ammonitiferous unit spanning the K/T boundary in New Jersey that somehow managed to escape notice till now. This unit promises to furnish interesting and rare fossils for years to come.

METHODS

Samples for sedimentological, mineralogical, geochemical, and microfossil analyses were taken at 2-, 5-, and 10-cm intervals across the outcrop using plastic spoons. The sediments were wet sieved for grain size analysis. Results are reported as mud ($X < 0.0625$ mm), very fine sand ($0.0625 \text{ mm} \leq X < 0.125$ mm), fine sand ($0.125 \text{ mm} \leq X < 0.25$ mm), and medium and coarser sediments ($X \geq 0.25$ mm). It is important to emphasize that much of the sediment consists of glauconitic minerals in the form of pellets. The sediment was treated to disaggregate it, as described in Landman et al. (2004b). However, many pellets remained intact after treatment and did not disintegrate into mud. As a result, the reported grain size distribution does not necessarily reflect the original size distribution of the sediment as it settled to the bottom. For the mineralogical analysis, at least 100 grains within each size fraction were examined under the microscope. The number of grains of glauconitic minerals, mica, quartz, siderite, and other minerals was counted and reported as a percentage of the total. These values may also be biased due to incomplete disaggregation of the sediment, as described above. It is important to note that some of the minerals (e.g., quartz) are authigenic in origin.

LIST OF LOCALITIES

Localities are indicated in figure 2. They are reported as American Museum of Natu-

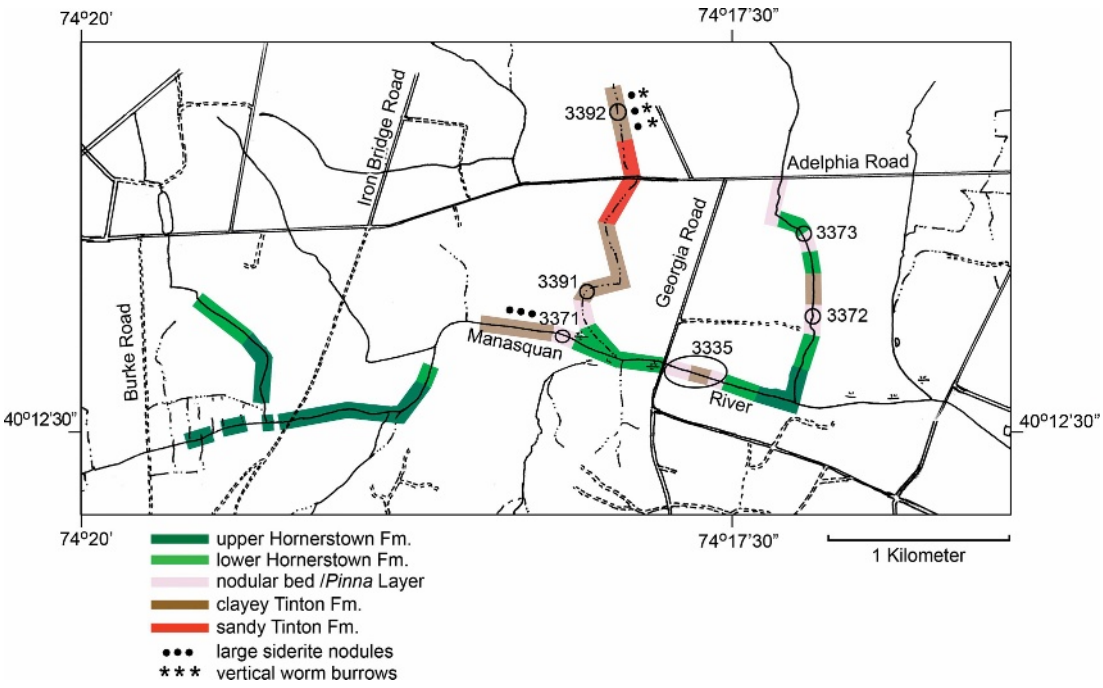

Fig. 2. Detailed locality map of the Manasquan River Basin, central Monmouth County, New Jersey, showing the Tinton Formation and overlying Hornerstown Formation. Numbers correspond to AMNH localities described in the text.

ral History (AMNH) and U.S. Geological Survey Paleobotanical locality numbers (preceded with an R).

AMNH loc. 3335, upper part of the Tinton Formation and lower part of the Hornerstown Formation, Manasquan River, for a distance of 250 m east of the bridge on Georgia Road, including the original construction site, 4.3 km southwest of Freehold, Monmouth County, New Jersey (R6367A: Tinton Formation, 0–25 cm below the *Pinna* Layer; R6367B, R6416A: *Pinna* Layer; R6367C, R6416B: nodular bed, basal Hornerstown Formation).

AMNH loc. 3371, upper part of the Tinton Formation and lower part of the Hornerstown Formation, Manasquan River, 0.6 km upstream (northwest) of the bridge on Georgia Road ("*Cucullaea* Heaven"), 4.4 km southwest of Freehold, Monmouth County, New Jersey.

AMNH loc. 3372, upper part of the Tinton Formation and lower part of the Hornerstown Formation, 0.5 km north of the Manasquan River, on a south-flowing tributary ("Lower Agony Creek"), 0.8 km northeast of the bridge on Georgia Road, and 3.8 km south-southwest of Freehold, Monmouth County, New Jersey (R6435AA: 10 cm above formational contact [Burrowed Unit, mixed]; R6435BA: ~10 cm above formational contact [Burrowed Unit, sediment around burrows]; R6435BB: ~10 cm above formational contact [Burrowed Unit, burrows]; R6435AE: siderite nodules 15 cm above formational contact [just above Burrowed Unit]; R6435AB: 20 cm above formational contact; R6435A: 30 cm above formational contact; R6435B: 40 cm above formational contact; R6435C: 50 cm above formational contact; R6435AC: 60 cm above formational contact; R6435AD: 70 cm above formational contact.)

AMNH loc. 3373, upper part of the Tinton Formation and lower part of the Hornerstown Formation, 0.7 km north of the Manasquan River, on a south-flowing tributary ("Upper Agony Creek"), 0.9 km northeast of the bridge on Georgia Road, and 3.6 km southwest of Freehold, Monmouth County, New Jersey.

AMNH loc. 3391, upper part of the Tinton Formation, 0.35 km north of the Manasquan River, on a south-flowing tributary (''Lower Iron Canyon''), 0.6 km northwest of the bridge on Georgia Road, and 4.1 km southwest of Freehold, Monmouth County, New Jersey.

AMNH loc. 3392, upper part of the Tinton Formation, south-flowing tributary of the Manasquan River (''Upper Iron Canyon''), 0.25 km north of its intersection with Adelphia Road, and 3.8 km southwest of Freehold, Monmouth County, New Jersey.

GEOLOGIC DESCRIPTION

The temporary construction site at Georgia Road and the Manasquan River, 4.3 km southwest of Freehold, Monmouth County, New Jersey (AMNH loc. 3335), revealed the upper part of the Tinton Formation overlain by the lower part of the Hornerstown Formation. This led to an investigation of natural outcrops over an area of approximately 6.5 km^2 (AMNH locs. 3371–3373, 3391, and 3392), confirming the same stratigraphic succession (figs. 2, 3).

Most of the upper Manasquan River is floored by the basal part of the Hornerstown Formation. However, the river has cut through the Hornerstown Formation and extensively exposed the underlying Tinton Formation in at least six areas (fig. 2). It is actually possible to walk along the K/T boundary for tens of meters along some parts of the stream bed. Collectively, the exposures in the Manasquan River Basin comprise the upper 2 m of the Tinton Formation and the lower 2 m of the Hornerstown Formation (figs. 3–5). The lower portion of this section, which is well exposed at AMNH loc. 3392, is rusty red in weathered exposures and dark grayish brown in unweathered exposures. It is sandy and contains abundant siderite nodules, which range up to 20 cm in diameter. Vertical and inclined tubular burrows are present throughout this part of the section, and were presumably produced by worms, crustaceans, or bivalves. The oyster *Ostrea nasuta* Morton, 1834, is a common faunal element but disappears a short distance below the top of the Tinton Formation.

The Tinton Formation gradually becomes clayier upsection. The upper portion, which is 1.0–1.3 m thick, is orange-red in weathered exposures and dark grayish brown in unweathered exposures. It consists of 49% mud, 11% very fine sand, 21% fine sand, and 19% medium and coarser sediments. The mud is not uniformly distributed throughout but occurs in small patches, suggesting bioturbation. Mineralogically, the sediment is composed mostly of glauconitic minerals (93%) and quartz (3.5%). This part of the section, which is well exposed at AMNH loc. 3371 (fig. 2), also contains abundant orange-weathering, siderite nodules, which range in diameter from 4 to 12 cm. These nodules sometimes accumulate on point bars along the stream.

This part of the Tinton Formation is fairly well indurated and hard to break. The fauna is diverse but not abundant, although this impression may be misleading due to nonintensive collecting. The thickness of this fossil-bearing portion is unclear. The fossils are blackish gray to black in color. Many of the bivalves are articulated. Lignite and bone are not preserved and no calcareous material is present.

Overlying this part of the Tinton Formation is a very fossiliferous unit approximately 20 cm thick, which we refer to as the *Pinna* Layer (figs. 3–5). The thickness of the *Pinna* Layer is remarkably constant throughout the Manasquan River Basin. The transition from the underlying part of the Tinton Formation to the *Pinna* Layer is conformable. The boundary between these units is a hard surface and was probably a firm ground at the time of deposition. Today, it is an aquitard, and ground water percolates down through cracks in the *Pinna* Layer and occasionally forms an accumulation of mud at its base.

The *Pinna* Layer is less lithified than the underlying part of the Tinton Formation. It is gray-green on fresh exposures, but weathers orange-brown, and is commonly covered with an orange algal slime. It contains small siderite nodules 1–5 cm in diameter, some of which are fossiliferous, scattered throughout the unit. It is bioturbated without any evidence of bedding. Although it is homogeneous, it tends to break along horizontal planes.

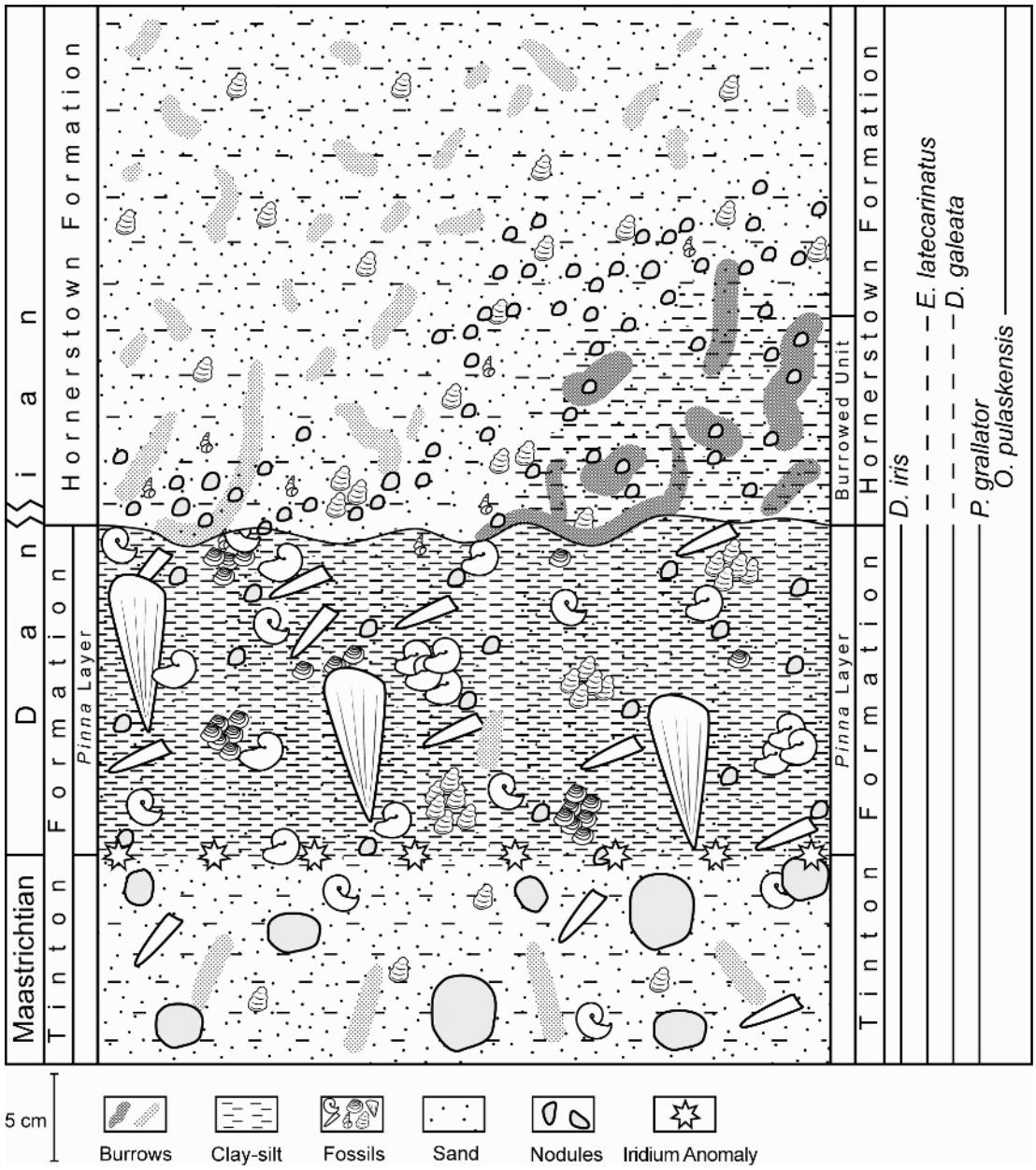

Fig. 3. Simplified stratigraphic section in the Manasquan River Basin, central Monmouth County, New Jersey, showing the upper part of the Tinton Formation and the lower part of the Hornerstown Formation. The unit at the top of the Tinton Formation (the *Pinna* Layer) contains a rich assemblage of fossils and represents an autochthonous deposit. (The fossils are not as abundant as illustrated.) The iridium spike occurs at the base of the *Pinna* Layer, and represents the Cretaceous/Tertiary boundary, assuming no postdepositional remobilization of iridium (but see text). A concentration of siderite nodules occurs at the base of the Hornerstown Formation and is associated with a hiatus. A ''Burrowed Unit'' is present at some downdip sites and is sandwiched between the top of the *Pinna* Layer and the overlying part of the Hornerstown Formation. The biostratigraphic ranges of five key species are illustrated on the right (*D. iris* = *Discoscaphites iris*; *E. latecarinatus* = *Eubaculites latecarinatus*; *D. galeata* = *Deflandrea galeata*; *P. grallator* = *Palynodinium grallator*; *O. pulaskensis* = *Ostrea pulaskensis*).

Fig. 4. Stratigraphic section at AMNH loc. 3372, Manasquan River Basin, Monmouth County, New Jersey, showing the upper part of the Tinton Formation, including the *Pinna* Layer, and the overlying Hornerstown Formation, including the Burrowed Unit. The reworked nodules (arrows) in the basal Hornerstown Formation contain Cretaceous fossils. The position of the iridium spike at the base of the *Pinna* Layer is indicated by an asterisk.

The *Pinna* Layer differs from the underlying part of the Tinton Formation in having a higher percentage of mud (62% vs. 49%) and a correspondingly lower percentage of coarser sediments (38% vs. 51%). The sediment in the *Pinna* Layer is poorly sorted and consists mostly of glauconitic minerals (92%), quartz (7%), and siderite (1%). Most of the glauconite grains are tan, with a few pale green to dark green grains. The quartz

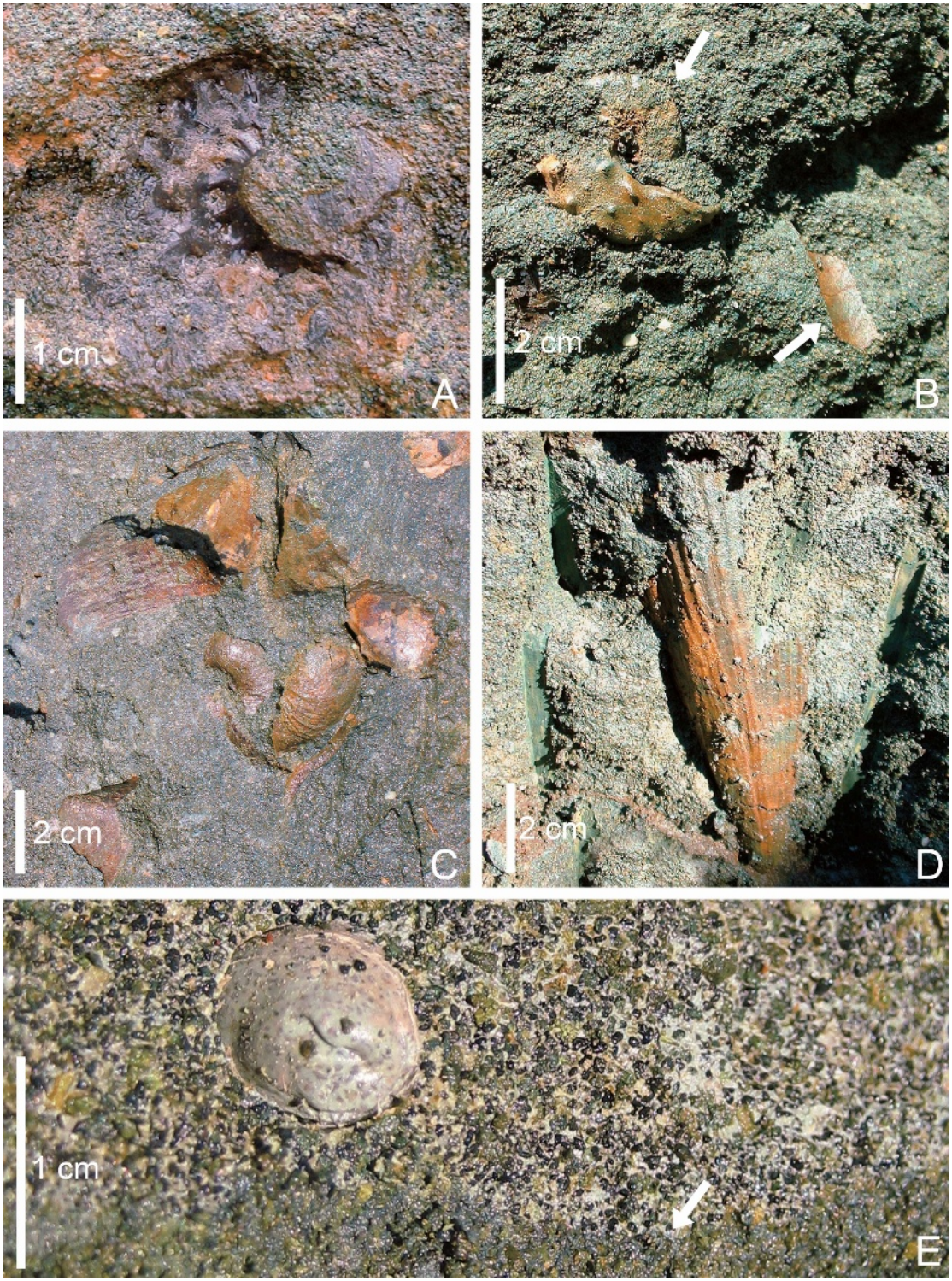
1 cm
A
2 cm
B
2 cm
C
2 cm
D
1 cm
E

TABLE 1
Invertebrates, Upper Part of the Tinton Formation, Manasquan River Basin, Monmouth County, New Jersey

Taxon	Mode of life[a]
CEPHALOPODA	
Discoscaphites gulosus (Morton, 1834)	mobile planktivore
Discoscaphites iris (Conrad, 1858)	mobile planktivore
Discoscaphites jerseyensis, n.sp.	mobile planktivore
Discoscaphites minardi Landman et al., 2004a	mobile planktivore
Discoscaphites sphaeroidalis Kennedy and Cobban, 2000	mobile planktivore
Eubaculites carinatus (Morton, 1834)	mobile planktivore
Eubaculites latecarinatus (Brunnschweiler, 1966)	mobile planktivore
Eutrephoceras dekayi (Morton, 1834)	mobile omnivore
Pachydiscus (*Neodesmoceras*) *mokotibensis* Collignon, 1952	mobile omnivore
Sphenodiscus lobatus (Tuomey, 1856)	mobile omnivore
PELECYPODA	
Anatimya lata (Whitfield, 1886)	infaunal facultatively mobile suspension feeder
Anomia sp.[b]	epifaunal stationary suspension feeder
Aphrodina tippana Whitfield, 1886	infaunal facultatively mobile suspension feeder
Arca obesa (Whitfield, 1886)	epifaunal stationary suspension feeder
Breviarca sp.	semi-infaunal facultatively mobile suspension feeder
Crassatella sp.	infaunal facultatively mobile suspension feeder
Crenella serica Conrad, 1860	semi-infaunal stationary suspension feeder
Cucullaea vulgaris Morton, 1830	infaunal facultatively mobile suspension feeder
Eriphyla parilis (Conrad, 1853)	infaunal facultatively mobile suspension feeder
Exogyra costata Say, 1820	epifaunal stationary suspension feeder
Granocardium (*Ethmocardium*) sp.	infaunal facultatively mobile suspension feeder
Granocardium sp.	infaunal facultatively mobile suspension feeder
Inoceramus sp.	epifaunal stationary suspension feeder
Legumen ellipticum Conrad, 1858	infaunal facultatively mobile suspension feeder
Lima reticulata Lyell and Forbes, 1845[b?]	epifaunal stationary suspension feeder
Liopistha protexta (Conrad, 1853)	infaunal facultatively mobile suspension feeder
Ostrea pulaskensis Harris, 1894[c]	epifaunal stationary suspension feeder
Ostrea tecticosta Gabb, 1860	epifaunal stationary suspension feeder
Pecten argillensis Conrad, 1860[b]	epifaunal facultatively mobile suspension feeder
Pecten venustus Morton, 1833[b]	epifaunal facultatively mobile suspension feeder
Perrisonota littlii Gardner, 1916	infaunal stationary suspension feeder
Pinna laqueata Conrad, 1858	semi-infaunal stationary suspension feeder
Pycnodonte convexa (Say, 1820)[b]	epifaunal stationary suspension feeder
Solemya lineolatus Conrad, 1870	infaunal stationary suspension feeder
Tellina sp.	infaunal facultatively mobile deposit feeder
Tenuipteria argentea (Conrad, 1858)	epifaunal stationary suspension feeder
Trigonia cerulia Whitfield, 1886	infaunal facultatively mobile suspension feeder
Unicardium concentricum Wade, 1926	infaunal facultatively mobile suspension feeder
Veniella conradi Morton, 1833	infaunal facultatively mobile suspension feeder
Xylophagella irregularis (Gabb, 1860)[b]	infaunal stationary suspension feeder

←

Fig. 5. **A–D.** Invertebrate fossils at AMNH loc. 3335, Manasquan River Basin, Monmouth County, New Jersey. **A.** Impression of *Discoscaphites iris* (Conrad, 1858) in the nodular layer at the base of the Hornerstown Formation. **B.** *Discoscaphites iris* (upper arrow) and *Eubaculites latecarinatus* (Brunnschweiler, 1966) (lower arrow) in the *Pinna* Layer at the top of the Tinton Formation. **C.** Cluster of *Cucullaea vulgaris* Morton, 1830, in the *Pinna* Layer at the top of the Tinton Formation. **D.** *Pinna laqueata* Conrad, 1858, in life position, in the *Pinna* Layer at the top of the Tinton Formation. **E.** Contact (arrow) between the top of the *Pinna* Layer and the base of the Hornerstown Formation at AMNH loc. 3371, Manasquan River Basin, with a small specimen of *Ostrea pulaskensis* Harris, 1894, immediately above the contact.

TABLE 1
(Continued)

Taxon	Mode of life[a]
GASTROPODA	
Anchura substriata? Wade, 1926	semi-infaunal mobile deposit feeder/suspension feeder
Anchura sp.	semi-infaunal mobile deposit feeder/suspension feeder
Arrhoges sp.	semi-infaunal mobile deposit feeder/suspension feeder
Bellifusus sp.	epifaunal mobile carnivore
Belliscala? sp.	semi-infaunal/epifaunal mobile carnivore
Bullopsis demersus Sohl, 1964	semi-infaunal/epifaunal mobile herbivore
Calliomphalus sp.	epifaunal mobile carnivore
Cylichna sp.	epifaunal mobile carnivore
Deussenia sp.	epifaunal mobile carnivore
Ellipsoscapha sp.	epifaunal mobile carnivore
Epitonium sp.[b]	semi-infaunal/epifaunal mobile carnivore
Euspira sp.[b]	epifaunal mobile carnivore
Gyrodes spillmani Gabb, 1861	epifaunal mobile carnivore
Gyrodes supraplicatus (Conrad, 1858)	epifaunal mobile carnivore
Latiaxis sp.	epifaunal mobile carnivore
Margaritella pumila Stephenson, 1941[b]	epifaunal mobile carnivore
Napulus sp.	epifaunal mobile carnivore
Pseudomalaxis sp.	epifaunal mobile carnivore
Pterocerella sp.	semi-infaunal mobile deposit feeder/suspension feeder
Pyropsis trochiformis (Tuomey, 1854)	epifaunal mobile carnivore
Pyropsis sp.	epifaunal mobile carnivore
Turritella bilira Stephenson, 1941	infaunal mobile deposit feeder/suspension feeder
Turritella sp.[c]	infaunal mobile deposit feeder/suspension feeder
Xenophora leprosa (Morton, 1834)	epifaunal mobile carnivore
Undescribed gastropod	
ECHINODERMATA	
Cardiaster marylandica Clark, 1916	semi-infaunal mobile detritivore
Hemiaster dalli Clark, 1891[b]	semi-infaunal mobile detritivore
Hemiaster delawarensis Clark, 1916[b]	semi-infaunal mobile detritivore
BRYOZOA	
Heteropora americana Richards, 1962	epifaunal stationary suspension feeder
PORIFERA	
Cliona cretacica Fenton and Fenton, 1932	epifaunal stationary suspension feeder
ANNELIDA	
Hamulus squamosus Gabb, 1859	epifaunal stationary suspension feeder
Longitubus lineatus (Weller, 1907)	epifaunal stationary suspension feeder
Serpula rotula (Morton, 1834)	epifaunal stationary suspension feeder
Serpula pervermiformis (Wade, 1926)[d]	epifaunal stationary suspension feeder
ARTHROPODA	
Notopocorystes cf. *N. tridens* (Roberts, 1962)	mobile carnivore
Protocallianassa mortoni (Pilsbry, 1901)[b]	mobile carnivore
Undescribed crab	mobile carnivore
Undescribed lobster[d]	mobile carnivore

[a]Data on mode of life are drawn from The Paleobiology Database @ http://paleodb.org/cgi-bin/bridge.pl and Beesley et al. (1998).

[b]These species also occur as non-reworked fossils in the basal Hornerstown Formation.

[c]These species are restricted to the basal Hornerstown Formation, above the Burrowed Unit.

[d]These species occur in the basal Hornerstown Formation, but have not yet been recovered from the *Pinna* Layer, although they are known from slightly older strata elsewhere in New Jersey.

grains, which are characteristic of the entire Tinton Formation, attain diameters of as much as 3.5 mm and range from glassy to sugarlike in appearance. George Harlow (AMNH) analyzed these grains using X-ray diffraction and polarized light microscopy and concluded that they were probably authigenic rather than detrital in origin.

The *Pinna* Layer is abundantly fossiliferous with a spectacular diversity (frontispiece; tables 1, 2). The fauna seems to be a continuation of that in the underlying part of the Tinton Formation with two notable exceptions, *Cucullaea vulgaris* Morton, 1830, and *Pinna laqueata* Conrad, 1858, which only first appear in the *Pinna* Layer. Conversely, *Ostrea nasuta*, which occurs in the underlying part of the Tinton Formation, is absent in the *Pinna* Layer.

In general, fossils in the *Pinna* Layer are much more abundant than in the underlying Tinton Formation. This increased abundance may be partly due to ease of recovery–the *Pinna* Layer breaks more readily and is more easily collected than the underlying Tinton Formation. There is also an abrupt change in fossil preservation at the transition to the *Pinna* Layer. This change is visible within single clusters of scaphites, baculites, and bivalves that straddle the transition. The fossils in the *Pinna* Layer are orange-brown in color whereas those in the underlying Tinton Formation are blackish to blackish gray in color. In addition, the fossils in the *Pinna* Layer are usually better preserved, with more detail and less distortion, than those in the underlying Tinton Formation.

All of the fossils in the *Pinna* Layer are internal or external molds, without any calcareous shell. Neither aragonite nor calcite is preserved. In general, the fossils are composed of the same material as the matrix itself. A small percentage (≈10%) of the fossils is sideritized, forming small nodules. Some fossils are completely sideritized, for example, completely sideritized specimens of *Cucullaea vulgaris*, whereas others are only partially sideritized, for example, only parts of baculites. The external ornamentation of many of the gastropods is preserved, which is unusual for the Upper Cretaceous of New Jersey. Lignite and bone (e.g., turtle fragments) are very rare (fig. 6F). Fish scales are common, but fish teeth are rare, and only the blades of the teeth are usually preserved (fig. 7).

Bivalves are the most common macrofossils in the *Pinna* Layer, both in terms of number of species and number of individuals. Nearly all of the bivalves are suspension feeders, comprising 11 species of epifauna and 18 species of infauna (table 1). *Cucullaea vulgaris* is very abundant and occurs in large concentrations, with most specimens articulated. *Pinna laqueata* (after which the layer is named) is almost always preserved in an upright life position and is nearly as tall as the *Pinna* Layer is thick. It occasionally occurs in clusters but never forms a dense framework.

The cephalopods include *Eutrephoceras dekayi* (Morton, 1834), *Pachydiscus* (*Neodesmoceras*) *mokotibensis* Collignon, 1952, *Sphenodiscus lobatus* (Tuomey, 1856), *Eubaculites carinatus* (Morton, 1834), *Eubaculites latecarinatus* (Brunnschweiler, 1966), *Discoscaphites iris* (Conrad, 1858), *Discoscaphites sphaeroidalis* Kennedy and Cobban, 2000, *Discoscaphites minardi* Landman et al., 2004a, *Discoscaphites gulosus* (Morton, 1834), and *Discoscaphites jerseyensis*, n.sp.

Altogether, the *Pinna* Layer contains 10 species of cephalopods, 29 species of bivalves, 24 species of gastropods, 3 species of echinoids, 1 species of sponge, 3 species of annelids, 3 species of crustaceans, and 1 species of bryozoans (figs. 8–16). The noncephalopod molluscs are illustrated in figures 8–14 but require further taxonomic study.

Dinoflagellates in the *Pinna* Layer are very diverse and include *Thalassiphora pelagica* (Eisenack, 1954) Eisenack & Gocht, 1960, *Palynodinium grallator* Gocht, 1970, *Deflandrea galeata* (Lejeune-Carpentier, 1942) Lentin & Williams, 1973 (consistently misspelled as *galatea* in Landman et al., 2004a, 2004b), and *Disphaerogena carposphaeropsis* Wetzel, 1933 (figs. 17–19, table 2). The assemblage of dinoflagellates in the *Pinna* Layer is more diverse than that in the underlying Tinton Formation, but this may be due in part to the fact that more material was analyzed from the *Pinna* Layer than from the underlying Tinton Formation.

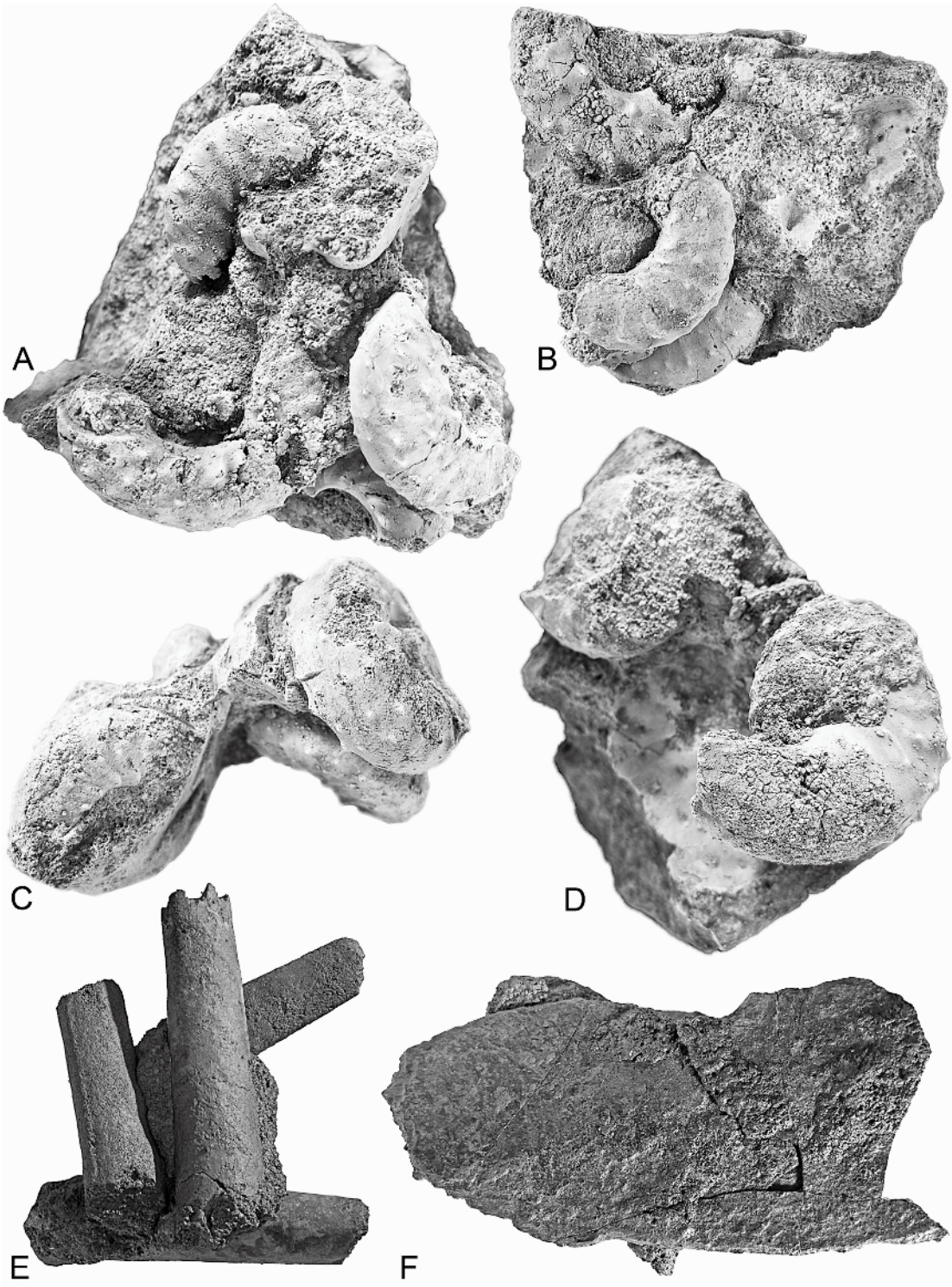

Fig. 6. **A–D.** Cluster of *Discoscaphites iris* (Conrad, 1858), *Pinna* Layer, Tinton Formation, Manasquan River Basin, Monmouth County, New Jersey. All of the pieces fit together and form the

The distribution of fossils in the *Pinna* Layer is patchy. In some areas, the fossils are very abundant whereas in others, they are scarce. For example, at downdip sites (AMNH locs. 3335 and 3372), fossils are common, especially scaphites. However, *Cucullaea vulgaris* is most abundant at AMNH loc. 3371, where it occurs in dense concentrations. In contrast, fossils are relatively rare at AMNH loc. 3373.

Many fossils occur in clusters, the most notable of which is *Cucullaea vulgaris*. In addition, echinoids, gastropods, baculites, and scaphites sometimes occur in clusters of as few as 2 or 3 specimens to as many as 30 or more (fig. 6A–E). In a few instances, one cluster sits above another; for example, we have observed a cluster of *C. vulgaris* lying above a cluster of *Discoscaphites iris*.

The top of the *Pinna* Layer is truncated, with some specimens of *P. laqueata* and other fossils cut in half. The contact is an irregular, slightly undulating surface (fig. 3). It usually appears as a narrow indentation in the rock face, emphasized by an orange rusty stain. This unconformity is the single most conspicuous feature in the Manasquan River Basin, and, therefore, we selected it as the boundary marking the base of the overlying Hornerstown Formation (figs. 3, 4).

At most outcrops in the Manasquan River Basin, there is a concentrated bed of siderite nodules, 10–15 cm thick, at the base of the Hornerstown Formation. The top of this bed is nearly horizontal. In areas where it is extensively exposed, it is indurated and much harder than the underlying *Pinna* Layer. As a result, the section usually splits along the formational boundary. At some localities, e.g., AMNH loc. 3371, this nodular bed protrudes as a shelf from the stream bank, and at other localities, it forms the bed of the stream.

The basal Hornerstown Formation is grayish green in fresh exposures. The difference between it and the *Pinna* Layer is evident in hand samples (fig. 5E). The basal Hornerstown Formation consists of 38% mud, 5% very fine sand, 12% fine sand, and 45% medium sand and coarser grains (average of two samples). Mineralogically, it is composed of glauconitic minerals (55%) and siderite (45%) (average of two samples). The glauconite grains are light to dark green. The siderite nodules are similar to those in the *Pinna* Layer, although some of them are lighter in color, probably due to weathering.

The majority of fossils in the basal Hornerstown Formation show evidence of reworking from the *Pinna* Layer. Most of them are preserved as siderite nodules. The most abundant fossil is *Cucullaea vulgaris*, which is never in life position. Other fossils include reworked scaphites, baculites, and crustaceans. Several nodules contain specimens of *Discoscaphites iris* with hollow phragmocones (fig. 20).

The basal Hornerstown Formation also contains non-reworked fossils, indicating a living community (table 1). However, the number of species and individuals is markedly reduced relative to that in the *Pinna* Layer. Altogether, there are approximately 16 invertebrate species: four species of gastropods, including *Margaritella pumila* Stephenson, 1941, seven species of bivalves including *Pecten argillensis* Conrad, 1860, *Pecten venustus* Morton, 1833, *Ostrea pulaskensis* Harris, 1894, and *Pycnodonte convexa* (Say, 1820), abundant fragments of *Protocallianassa mortoni* (Pilsbry, 1901) and an undescribed lobster, several worm colonies, and a cluster of echinoids composed of *Hemiaster dalli* Clark, 1891, and *Hemiaster delawarensis* Clark, 1916. Benthic foraminifera, shark teeth, and bone fragments are also present. Dinoflagellates are very scarce and mostly belong to the *Areoligera* group (table 2). These specimens are well preserved and represent a reduced assemblage.

At several downdip sites, e.g., AMNH locs. 3335 and 3372, there is an additional unit, which we call the Burrowed Unit, which

←

central core of the cluster. Nearly all of the specimens are mature microconchs. **E.** Cluster of four specimens of *Eubaculites carinatus* (Morton, 1834), MAPS A2058b3, same locality as **A–D**. The specimens are oriented at various angles. **F.** Bone, possibly from a turtle, MAPS A1238a1, same locality as **A–D**. All figures ×1.

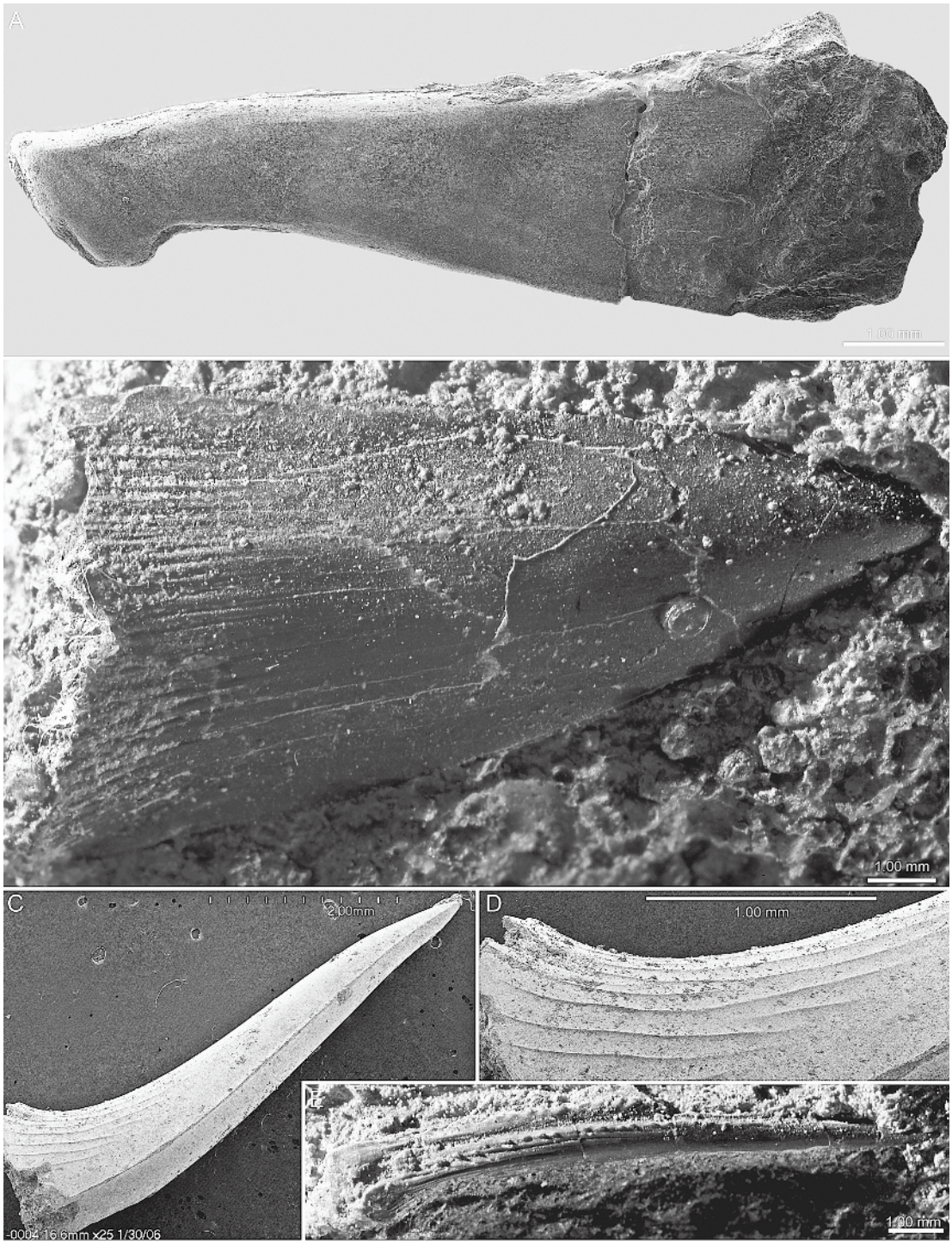

Fig. 7. Fish teeth and spines, *Pinna* Layer, upper part of the Tinton Formation, Manasquan River Basin, Monmouth County, New Jersey. **A.** Rostral tooth of a sawfish (photo mosaic of two images), AMNH 51310. **B.** Fish tooth, probably not of a shark, MAPS A1043a1. **C, D.** Tooth of a lamniform

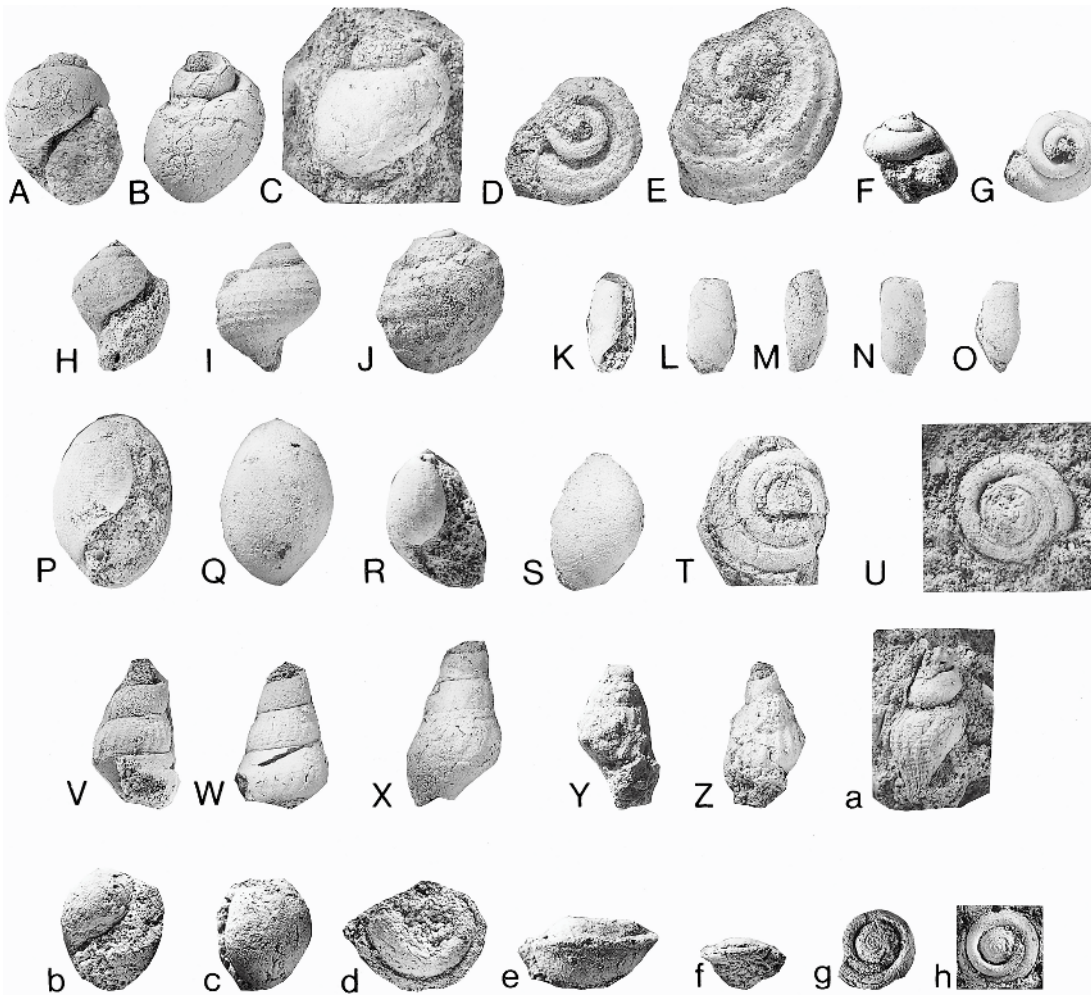

Fig. 8. Gastropods from the top of the Tinton Formation, Manasquan River Basin, Monmouth County, New Jersey. **A–C.** *Euspira* sp. **A, B.** MAPS A2809e1. **C.** MAPS A2809e2. **D, E.** *Pyropsis* sp. **D.** MAPS A2800k1. **E.** MAPS A2800k2. **F, G.** *Calliomphalus* sp., MAPS A2897b1. **H–J.** *Napulus* sp. **H, I.** MAPS A2859d1. **J.** MAPS A2859d2. **K–O.** *Cylichna* sp. **K, L.** MAPS A2908a1. **M.** MAPS A2908a2. **N.** MAPS A2908a3. **O.** MAPS A2908a4. **P–S.** *Ellipsoscapha* sp. **P, Q.** MAPS A2833f1. **R, S.** MAPS A2833f2. **T, U.** *Pseudomalaxis* sp. **T.** MAPS A2907a1. **U.** MAPS A2907a2. **V–X.** *Anchura* sp. **V, W.** MAPS A2909a1. **X.** MAPS A2909a2. **Y, Z, a.** *Belliscala*? sp. **Y, Z.** MAPS A2888c1. **a.** MAPS A2888c2. **b, c**. *Bullopsis demersus* Sohl, 1964, MAPS A2949a1. **d, e**. *Latiaxis* sp., MAPS A2948a1. **f–h**. *Margaritella pumila* Stephenson, 1941. **f, g**. MAPS A2911d2. **h**. MAPS A2911d1. All figures ×1.

is sandwiched between the truncated top of the *Pinna* Layer and the concentrated bed of siderite nodules (figs. 3, 4). This layer is very thin and discontinuous, attaining a maximum thickness of 15–20 cm. It is still thinner or absent altogether at updip sites, e.g., AMNH locs. 3371, 3373, and 3391. We consider the Burrowed Unit as part of the Hornerstown

←

shark, probably a juvenile of *Scapanorhynchus texanus* (Roemer, 1849), MAPS A1045a1. **E.** Spine, probably from the dorsal fin of a squirrel(?) fish, MAPS A1044a1.

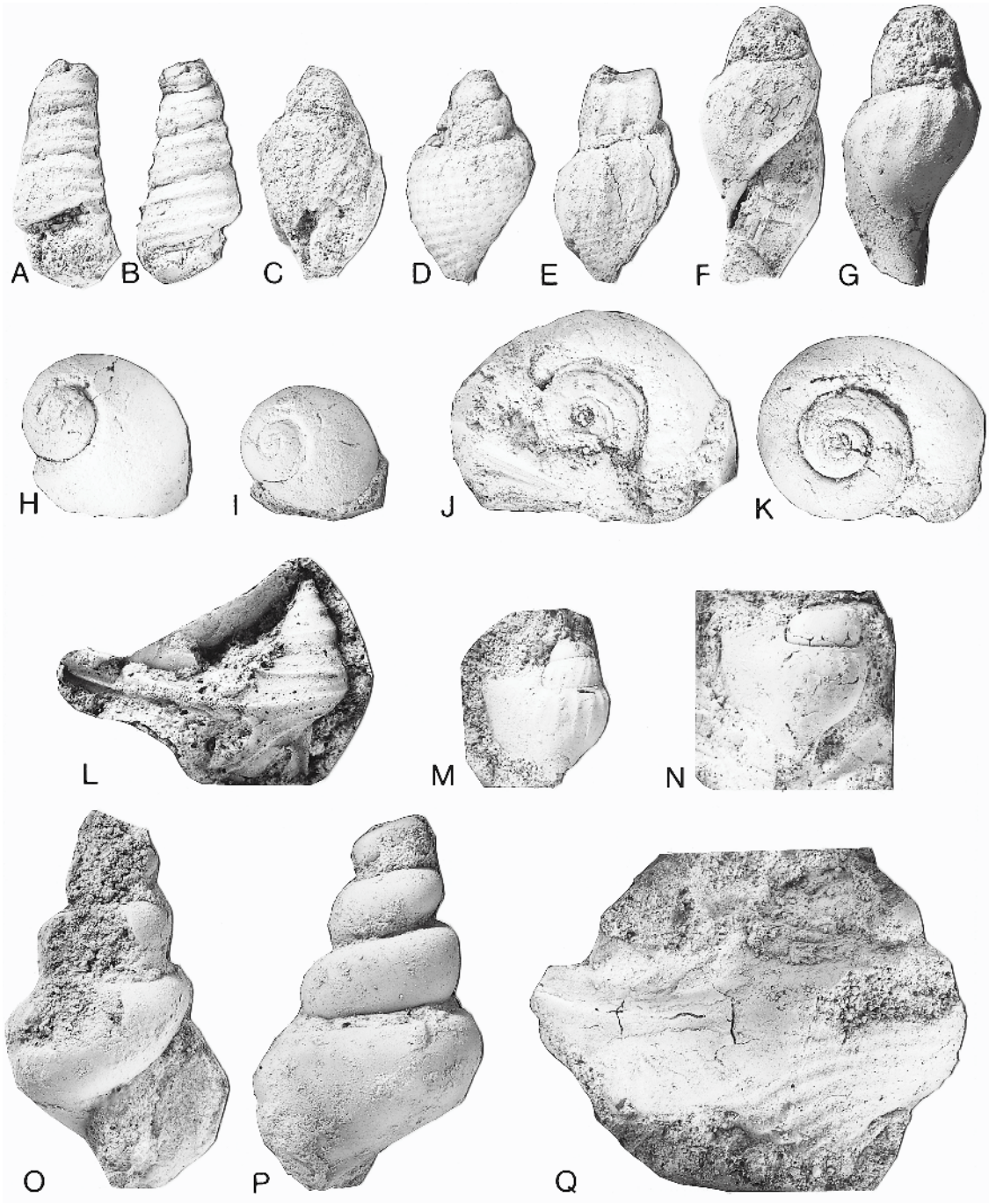

Fig. 9. Gastropods from the top of the Tinton Formation, Manasquan River Basin, Monmouth County, New Jersey. **A, B.** *Turritella bilira* Stephenson, 1941, MAPS A2838e1. **C, D.** *Deussenia* sp., MAPS A2821b1. **E–G.** *Bellifusus* sp. **E.** MAPS A2889e1. **F, G.** MAPS A2889e2. **H, I.** *Gyrodes spillmani* Gabb, 1861. **H.** MAPS A2873c1. **I.** MAPS A2873c2. **J, K.** *Gyrodes supraplicatus* (Conrad, 1858). **J.** MAPS A2872f1. **K.** MAPS A2872f2. **L.** *Pterocerella* sp., MAPS A2877d1. **M, N.** *Arrhoges* sp. **M.** MAPS A2906a1. **N.** MAPS A2906a2. **O–Q.** *Anchura substriata*? Wade, 1926. **O, P.** MAPS A2905b1. **Q.** MAPS A2905b2. All figures ×1.

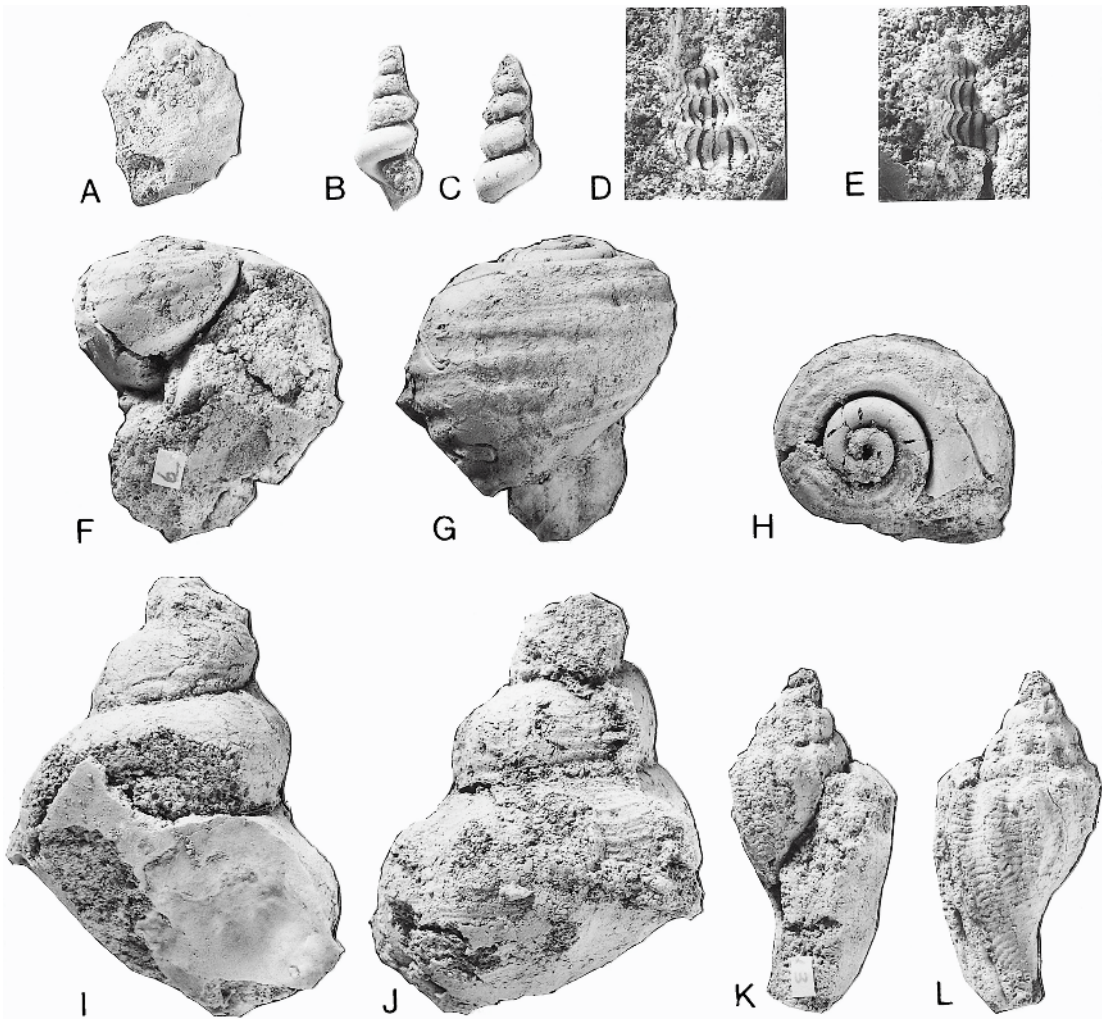

Fig. 10. Gastropods from the top of the Tinton Formation, Manasquan River Basin, Monmouth County, New Jersey. **A.** *Xenophora leprosa* (Morton, 1834), MAPS A2801j1. **B–E.** *Epitonium*? sp. **B, C.** MAPS A2874f1. **D.** MAPS A2874f3. **E.** MAPS A2874f2. **F–H.** *Pyropsis trochiformis* (Toumey, 1854), MAPS A2862b1. **I–L.** Unidentified gastropods. **I, J.** MAPS A2950a1. **K, L.** MAPS A2951a1. All figures ×1.

Formation because it consists mostly of material piped down from the overlying portion of this formation.

The upper boundary of the Burrowed Unit is usually difficult to detect. Where visible, it consists of an undulating surface just below the bed of concentrated nodules. More commonly, however, the upper part of the Burrowed Unit blends into the overlying part of the Hornerstown Formation, and the boundary between them is difficult to differentiate. In fresh exposures, the Burrowed Unit is grayish green in color with patches of darker, grayish black material representing burrows from the overlying part of the Hornerstown Formation.

The burrows in the Burrowed Unit are very large, e.g., 10 cm long by 2.5 cm wide, and are part of an extensive anastomozing complex piping down material from above. In general, burrows do not penetrate into the *Pinna* Layer (fig. 3). In some instances,

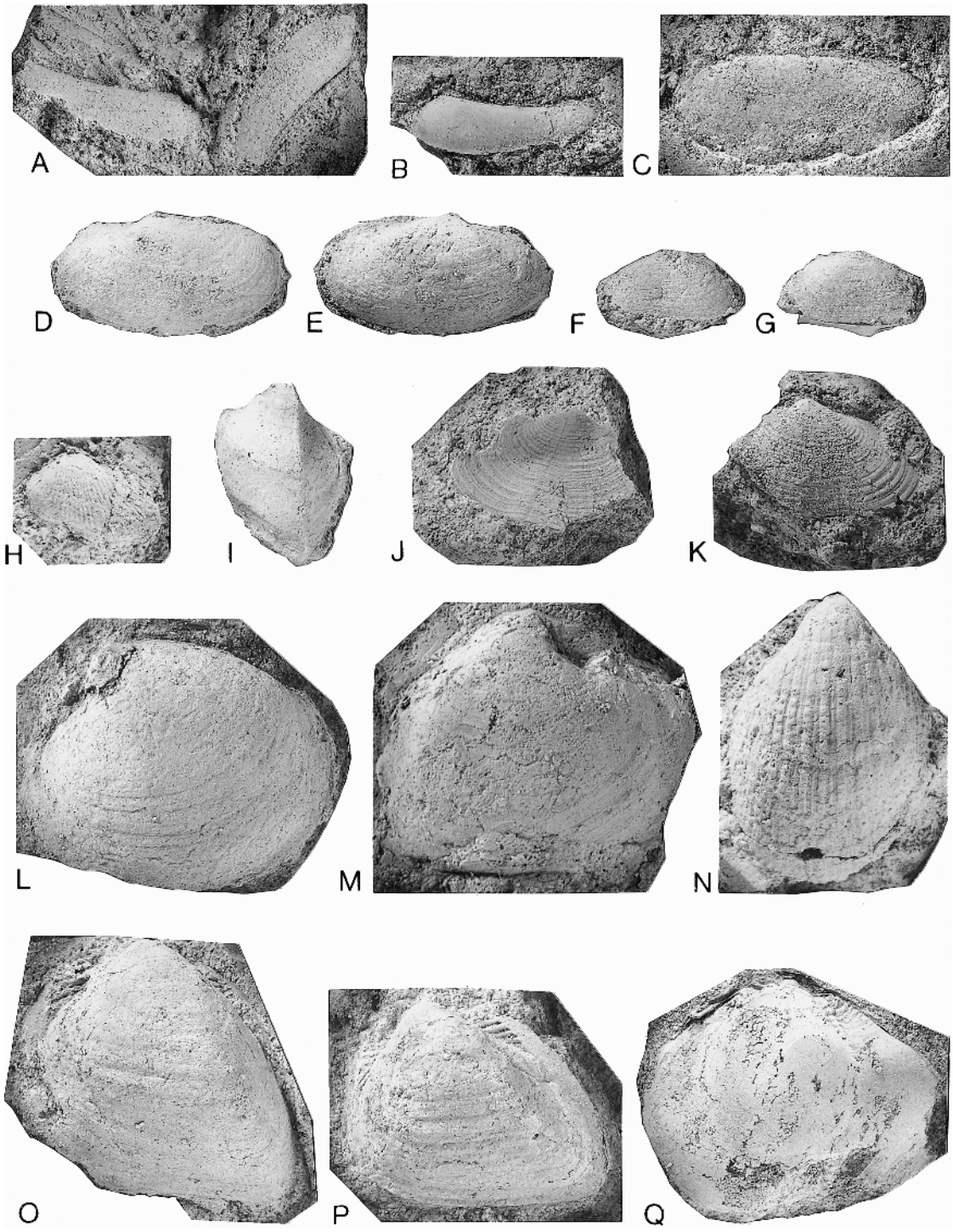
A
B
C
D
E
F
G
H
I
J
K
L
M
N
O
P
Q

downward trending burrows encounter the *Pinna* Layer and turn abruptly to follow the formational contact.

The sediment surrounding the burrows consists of 50% mud, 10% very fine sand, 20% fine sand, and 20% medium and coarser grains (average of two analyses). This grain size distribution is similar to that in the *Pinna* Layer. Mineralogically, however, the sediment more closely resembles that in the overlying part of the Hornerstown Formation, consisting of glauconitic minerals (63%) and siderite (37%) (average of two analyses).

The sediment in the burrows consists of 22% mud, 5% very fine sand, 10% fine sand, and 63% medium sand and coarser grains (average of two analyses). This grain size distribution is similar to that in the overlying part of the Hornerstown Formation. Mineralogically, the sediment also resembles that in the overlying part of the Hornerstown Formation with an abundance of glauconitic minerals (68%) and siderite (30%), although some quartz (2%) is also present (average of two analyses). Most of the glauconite grains are greenish black, shiny, and botryoidal, similar to those in the overlying part of the Hornerstown Formation.

The Burrowed Unit contains numerous siderite nodules, almost all of which occur adjacent to or in the burrows extending down from above. These nodules are identical to those that occur sporadically throughout the *Pinna* Layer and as a concentrated accumulation in the overlying part of the Hornerstown Formation.

Fossils are rare in the Burrowed Unit. The burrows themselves contain *Ostrea pulaskensis*, which is present in the overlying part of the Hornerstown Formation. The sediment surrounding the burrows has yielded a few fossil fragments, some of which are sideritized, and others that are composed of the same material as the matrix itself. These fossils include *Eubaculites latecarinatus*, and, possibly, *Discoscaphites iris*. *Cucullaea vulgaris*, the most common fossil in the *Pinna* Layer, is absent, but this may be due to collecting failure. One group of *E. latecarinatus* consists of at least four specimens, three of which are oriented nearly parallel to each other. One of these specimens contains one or even two additional specimens telescoped inside it.

Dinoflagellates are also rare in the Burrowed Unit. In a mixed sample from this bed, we detected a fragment of what may be *Damassadinium californicum* (Drugg, 1967) Fensome et al., 1993, or some closely related form (fig. 19N), probably from one of the burrows, and *Deflandrea galeata* (fig. 19L, M), probably from the sediments surrounding the burrows. In a sample restricted to the burrows, we detected *Diphyes colligerum* (Deflandre & Cookson, 1955) Cookson, 1965, and specimens of the *Areoligera senonensis* Lejeune-Carpentier, 1938, species complex, and in a sample restricted to the sediments surrounding the burrows, we detected *Alisogymnium/Dinogymnium* sp. and ?*Disphaerogena carposphaeropsis*.

Approximately 2 m of the Hornerstown Formation are exposed above the basal bed of concentrated nodules. This part of the Hornerstown Formation is dark green in fresh exposures with a salt-and-pepper appearance. Burrows tend to be smaller than those in the Burrowed Unit. This part of the Hornerstown Formation is sparsely fossiliferous, with occasional siderite nodules.

←

Fig. 11. Bivalves from the top of the Tinton Formation (**A–P**) and base of the Hornerstown Formation (**Q**), Manasquan River Basin, Monmouth County, New Jersey. **A, B.** *Perissonata littlii* Gardner, 1916. **A.** MAPS A2536b1. **B.** MAPS A2536b2. **C.** *Legumen ellipticum* Conrad, 1858, MAPS A2484c1. **D, E.** *Solemya lineolatus* Conrad, 1870, MAPS A2499f1. **F, G.** *Tellina* sp. **F.** MAPS A2531f1. **G.** MAPS A2531f2. **H.** *Arca obesa* (Whitfield, 1886), MAPS A2460f1. **I.** *Veniella conradi* Morton, 1833, MAPS A2436h1. **J, K.** *Anatimya lata* (Whitfield, 1886). **J.** MAPS A2404h1. **K.** MAPS A2404h2. **L, M.** *Aphrodina tippana* Whitfield, 1886. **L.** MAPS A2485k1. **M.** MAPS A2485k2. **N.** *Granocardium* sp., MAPS A2443a1. **O, P.** *Cucullaea vulgaris* Morton, 1830. **O.** MAPS A2486j1. **P.** MAPS A2486j2. **Q.** *Pycnodonte convexa* (Say, 1870), MAPS A2471l1. All figures ×1.

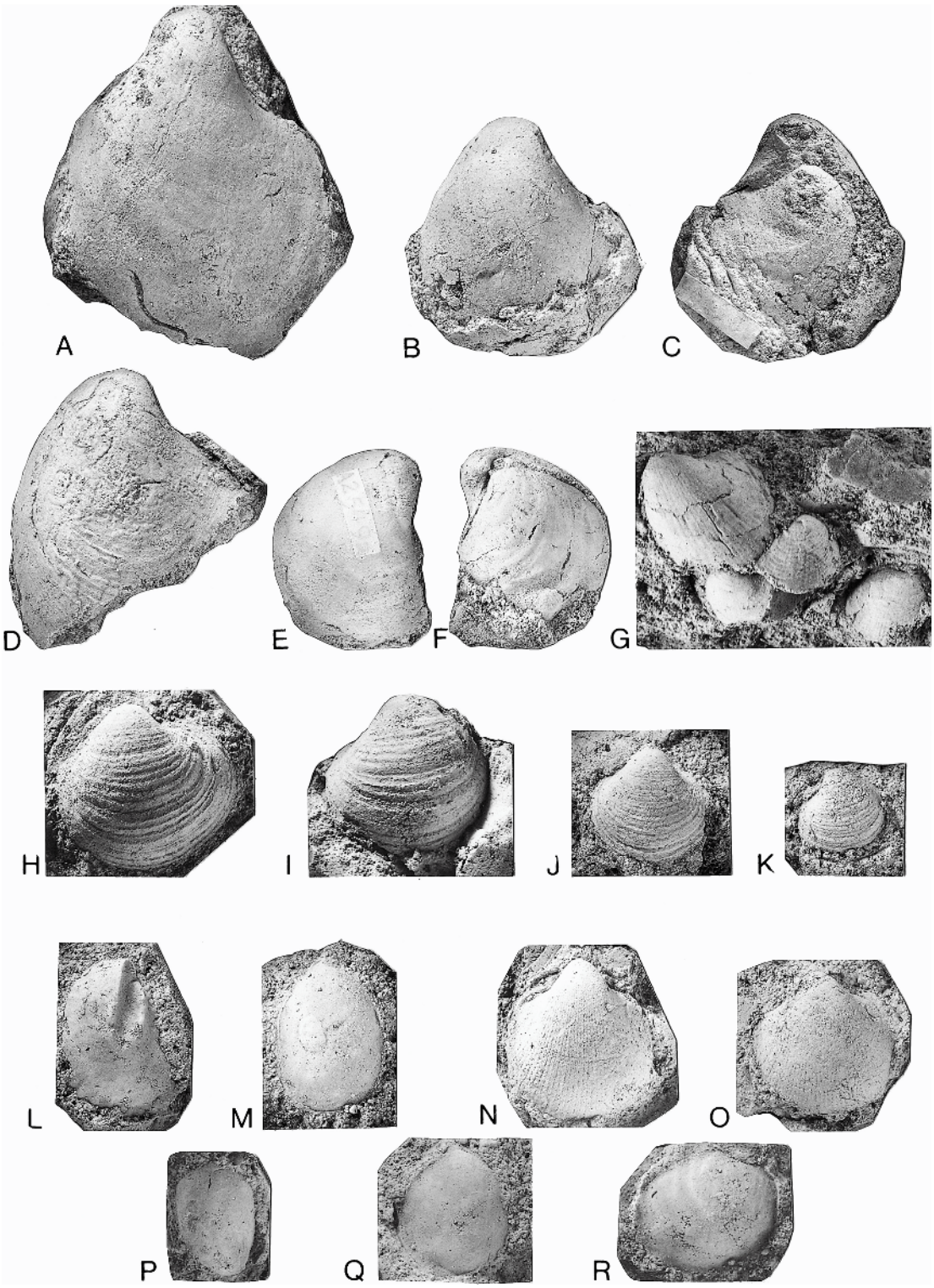
A
B
C
D
E
F
G
H
I
J
K
L
M
N
O
P
Q
R

IRIDIUM ANALYSIS

We initially analyzed eight samples of sediment for iridium from the upper part of the Tinton Formation and lower part of the Hornerstown Formation at AMNH loc. 3335. We subsequently analyzed a set of 29 closely spaced samples from this same interval at AMNH locs. 3372 and 3391.

Samples were prepared from approximately 1 g of material by manual grinding, with a new, high purity, aluminum oxide mortar and pestle that were cleaned with crushed synthetic quartz and methanol before using. Samples were crushed to a gravel, placed in cleaned borosilicate glass vials, and heated overnight at 105°C. Samples were then ground to a powder, placed into quartz glass crucibles and heated in steps to 100, 350, and 850°C to destroy all organic matter. This process also decomposes carbonates and oxidizes all the Fe to Fe_2O_3. Step-heating was performed in crucibles that were used in previous experiments that did not involve high iridium concentrations. Separate splits of samples from AMNH loc. 3372 (300–400 mg) were also step-heated and weighed so mass loss could be estimated. This is reported as Loss on Ignition (LOI). LOI was not determined on samples from AMNH loc. 3335, so we assumed a value of approximately 10%, which is characteristic of the samples from AMNH loc. 3372. LOI values were used to correct elemental concentrations for mass loss during preparation. Splits of these powders (≈100 mg) were sealed in quartz-glass vials (2 mm inner diameter; 3 mm outer diameter) and irradiated at the University of Missouri Research Reactor Facility for 30 hours at a neutron flux of 5×10^{13} n cm^{-2} sec^{-1}. Approximately 2 months after irradiation, sample powders were counted for approximately 6 hours with intrinsic Ge, gamma-ray detectors to determine Sc, Cr, Fe, Co, Ni, Zn, Cs, Ce, Eu, Tb, Yb, Ha, Ta, and Th. Samples were then processed using a chemical procedure similar to that described in Schellenberg et al. (2004) to purify iridium (Ir). These Ir concentrates were counted for 24 hours. Chemical yields were measured by re-irradiating aliquots of the Ir solutions.

The results for iridium are reported in table 3. At AMNH loc. 3335, the highest concentration of iridium is 589 pg/g [reported as ≈800 ppt in Landman et al. (2004b) before correction for mass loss during preparation]. This elevated concentration occurs at the contact between the *Pinna* Layer and the underlying part of the Tinton Formation. A sample from part of the Tinton Formation immediately below the *Pinna* Layer also shows a slightly elevated concentration (220 pg/g). In contrast, the values of iridium from samples above the base of the *Pinna* Layer are relatively low (82–151 pg/g).

The analyses at AMNH locs. 3372 and 3391 show a similar pattern (fig. 21, table 3). At AMNH loc. 3372, the concentration of iridium at the contact between the *Pinna* Layer and the underlying part of the Tinton Formation is 457 pg/g. The concentration of iridium from a sample 4 cm below this contact is also relatively high (276 pg/g). The concentrations of two samples from approximately 30 and 60 cm below this horizon at AMNH loc. 3391 are lower (188 and 176 pg/g, respectively). The concentrations of iridium in all of the samples from above the contact are very low and range from 76 to 143 pg/g.

In summary, the analysis of iridium in the Manasquan River Basin shows an elevated concentration at the contact between the *Pinna* Layer and the underlying part of the Tinton Formation. The average concentra-

←

Fig. 12. Bivalves from the top of the Tinton Formation, Manasquan River Basin, Monmouth County, New Jersey. **A–G.** *Tenuipteria argentea* (Conrad, 1858). **A.** MAPS A2549a2. **B, C.** MAPS A2549a3. **D.** MAPS A2549a4. **E, F.** MAPS A2549a5. **G.** MAPS A2549a6. **H–K.** *Unicardium concentricum* Wade, 1926. **H.** MAPS A2554a1. **I.** MAPS A2554a2. **J.** MAPS A2554a3. **K.** MAPS A2554a4. **L, M.** *Ostrea tecticosta* Gabb, 1860. **L.** MAPS A2520c1. **M.** MAPS A2520c2. **N, O.** *Granocardium* (*Ethmocardium*) sp. **N.** MAPS A2544d1. **O.** MAPS A2544d2. **P–R.** *Anomia* sp. **P.** MAPS A2494c1. **Q.** MAPS A2494c2. **R.** MAPS 2494c3. All figures ×1.

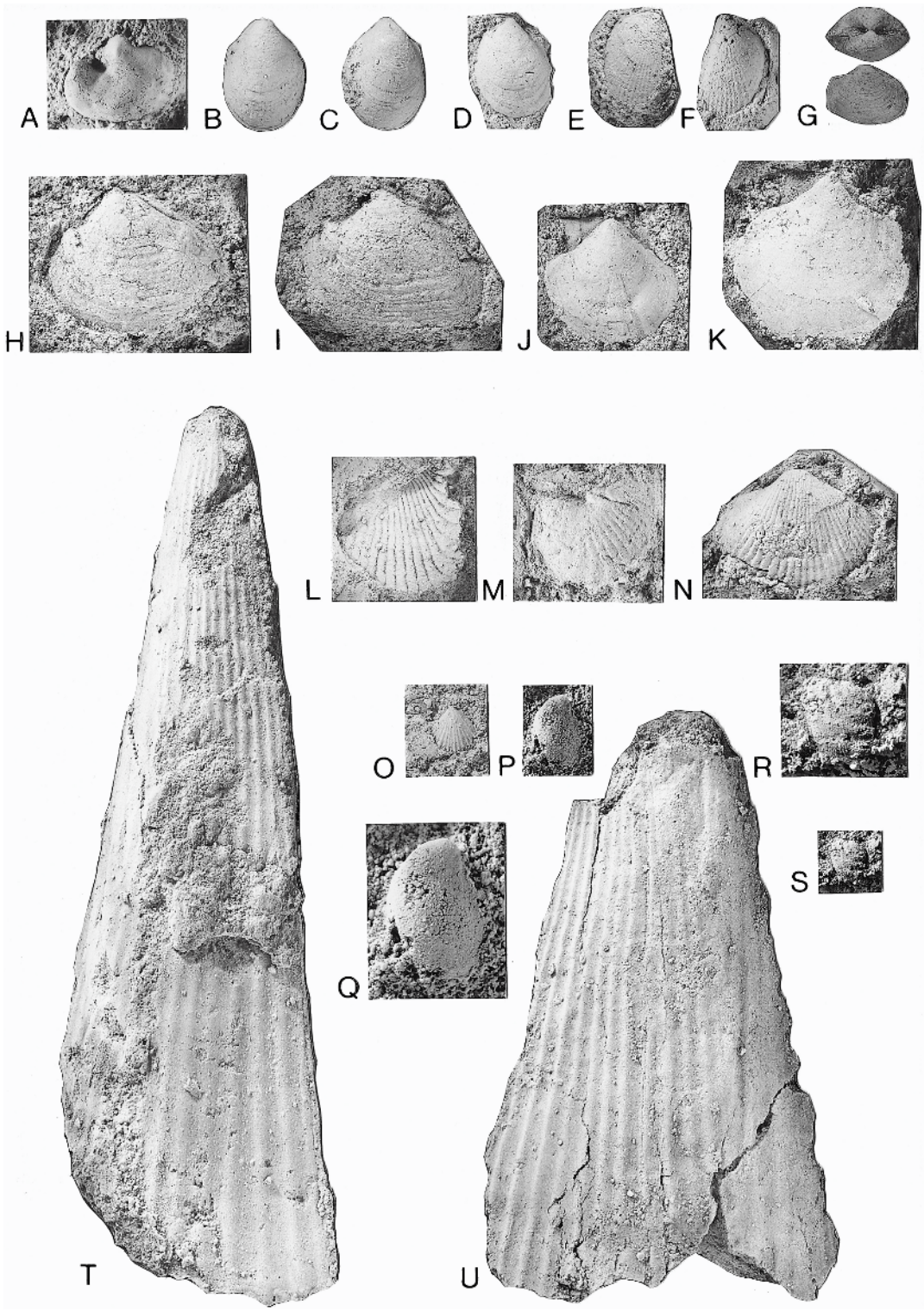
A
B
C
D
E
F
G
H
I
J
K
L
M
N
O
P
R
S
Q
T
U

tion of two samples from this horizon at AMNH locs. 3335 and 3372 is 520 pg/g. The iridium profile is asymmetric with an abrupt drop off above the contact and a more gradual decline below the contact. The maximum concentration of iridium is not as high as that reported from some other Cretaceous/Tertiary boundary sections (Kiessling and Claeys, 2001; Claeys et al., 2002; Olsson et al., 2002).

The concentration and distribution of iridium can be altered after deposition due to a variety of processes. Claeys et al. (2002: 62) noted that "bioturbation, reworking, diagenesis, and chemical diffusion can cause the remobilization of Ir and its spread over as much as several meters of section." Along these same lines, Sawlowicz (1993: 261) wrote that "extensive postdepositional PGE [Platinum Group Element] mobilization in sediments can be generated by low-temperature aqueous solutions, hydrothermal fluids, and oxidation fronts." He added, however, that "the mechanism of PGE behavior and transport in low-temperature solutions is still poorly known, but chemical fractionation among the PGE certainly occurs." In addition, DeLange et al. (1991) demonstrated that a sharp Ir anomaly can be produced by postdepositional mobilization and redox-controlled precipitation at distinct depths in the sediment. [See Guinasso and Schink (1975) and Rocchia and Robin (1996) for additional discussions about the effects of bioturbation and diffusion on the redistribution of iridium and other elements].

These arguments have been used elsewhere to explain ostensibly inconsistent relationships betwen the position of the iridium anomaly and other stratigraphic features at the K/T boundary. For example, Olsson et al. (2002: 105), in their study of the Bass River Borehole, observed an iridium anomaly below a layer of spherules, although the reverse situation would have been expected based on the timing of deposition. However, they argued that "the higher concentration of iridium at the base of the spherule layer is believed to be due to the postdepositonal downward diffusion of iridium through pore water in the highly permeable and porous spherule layer; the underlying Maastrichtian clayey silts act as an aquitard."

The concentration and distribution of iridium in the Manasquan River Basin may also have been modified after deposition. Accordingly, we present two alternative hypotheses:

Hypothesis 1: The iridium anomaly is in place. The best evidence for this hypothesis is that the Ir peak is very sharp and the concentrations above the base of the *Pinna* Layer are uniformly low. If the iridum were displaced downward from a stratigraphically higher position, it is puzzling that there is no evidence of elevated concentrations above the present anomaly. In contrast, the broad tail below the base of the *Pinna* Layer may reflect postdepositional remobilization, implying that the concentration of iridium has been effectively diluted. In fact, the iridium can be integrated over this interval of elevated concentrations to obtain the iridium inventory. This may provide a more precise means of comparing the iridium profile in the Manasquan River Basin with profiles at other K/T boundary sites.

If the iridium is in place, then the horizon at which it occurs marks the Cretaceous/

←

Fig. 13. Bivalves from the top of the Tinton Formation (**A–O**, **R–U**) and base of the Hornerstown Formation (**P,Q**), Manasquan River Basin, Monmouth County, New Jersey. **A.** *Exogyra costata* Say, 1820, MAPS A2555a1. **B–D.** *Crenella serica* Conrad, 1860. **B, C.** MAPS A2553a1. **D.** MAPS A2553a2. **E, F.** *Lima reticulata* Lyell and Forbes, 1845, MAPS A2552a1. **G.** *Breviarca* sp., MAPS A2479c1. **H, I.** *Crassatella* sp. **H.** MAPS A2556a1. **I.** MAPS A2556a2. **J, K.** *Pecten argillensis* Conrad, 1860. **J.** MAPS A2512b1. **K.** MAPS A2512b2. **L, M.** *Trigonia cerulia* Whitfield, 1886. **L.** MAPS A2528c2. **M.** MAPS A2528c1. **N.** *Liopistha protexta* (Conrad, 1853), MAPS A2439g1. **O.** *Pecten venustus* Morton, 1833, MAPS A2521f1. **P, Q**. *Ostrea pulaskensis* Harris, 1894, AMNH 51304. **R, S**. *Eriphyla parilis* (Conrad, 1853), MAPS A2557b1. **T, U.** *Pinna laqueata* Conrad, 1858. **T.** MAPS A2402p1. **U.** MAPS A2402p2. All figures ×1; Q, R ×2.

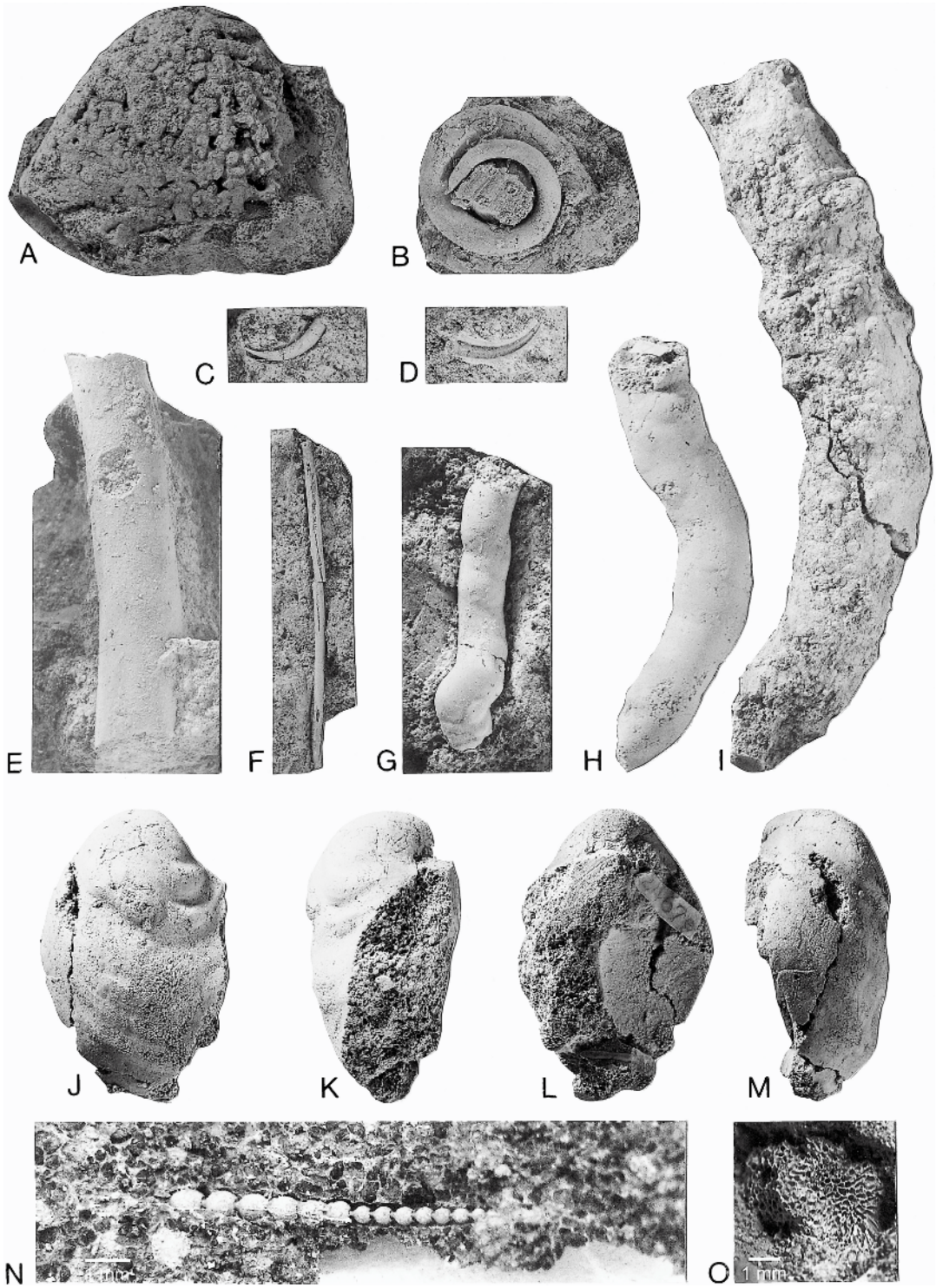
A
B
C
D
E
F
G
H
I
J
K
L
M
N
O
1 mm

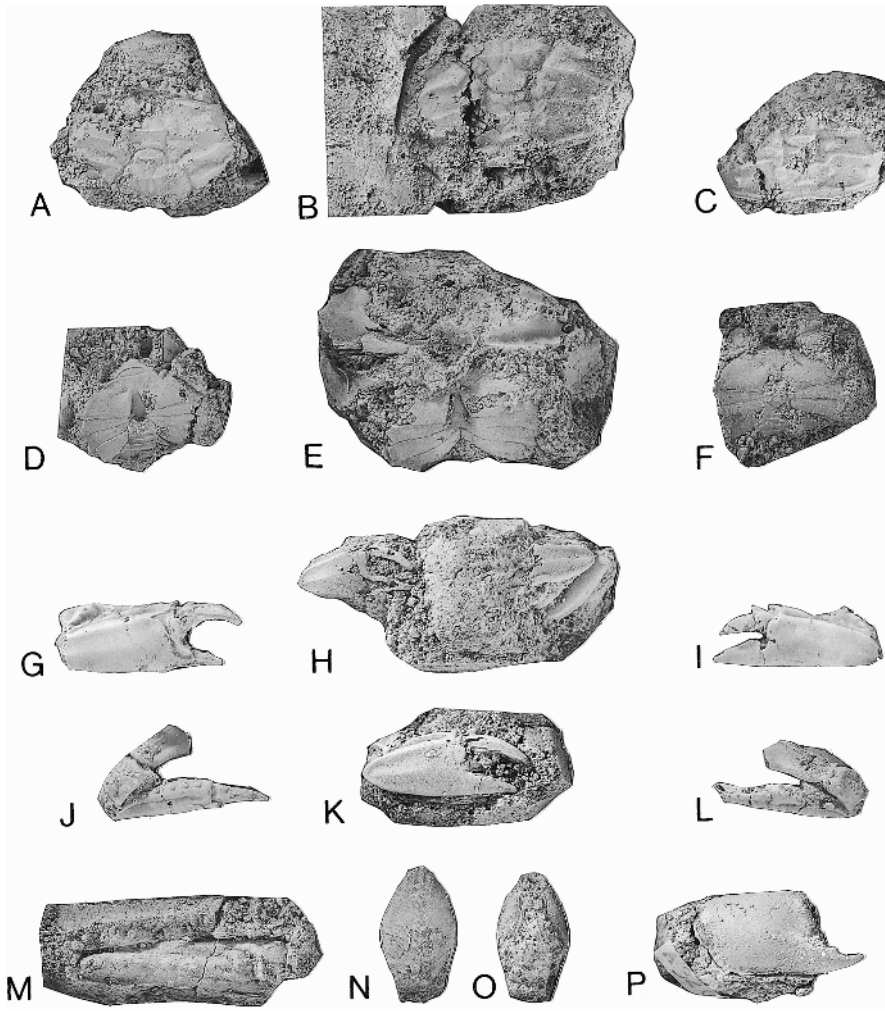

Fig. 15. Crustaceans from the top of the Tinton Formation, Manasquan River Basin, Monmouth County, New Jersey. **A–L.** Unidentified crab. **A.** MAPS A3229a1. **B.** MAPS A3229a2. **C, D.** MAPS A3229a3. **E.** MAPS A3229a4. **F.** MAPS A3229a5. **G, J.** AMNH 50426. **H.** MAPS A3229a6. **I, L.** AMNH 50428. **K.** MAPS A3229a7. **M.** Unidentified crustacean, MAPS A3230a1. **N, O.** *Notopocorystes* cf. N. *tridens* (Roberts, 1962), AMNH 50421. **P.** *Protocallianassa mortoni* (Pilsbry, 1901), MAPS A3205j1. All figures ×1.

←

Fig. 14. Miscellaneous invertebrates from the top of the Tinton Formation (**A–M**) and the base of the Hornerstown Formation (**N, O**), Manasquan River Basin, Monmouth County, New Jersey. **A.** *Cliona cretacica* Fenton and Fenton, 1932, MAPS A3900j1. **B.** *Serpula rotula* (Morton, 1834), MAPS A3926e1. **C, D.** *Hamulus squamosus* Gabb, 1859. **C.** MAPS A3933b1. **D.** MAPS A3933b2. **E.** Unidentified smooth burrow, AMNH 50738. **F.** *Longitubus lineatus* (Weller, 1907), MAPS A3925e1. **G, H.** *Xylophagella irregularis* (Gabb, 1860). **G.** MAPS A2476j2. **H.** MAPS A2476j3. **I.** Unidentified rough burrow, MAPS A3228a1. **J–M.** *Inoceramus* sp., MAPS A2467e1. **N**. Benthic foraminifera, AMNH 51323. **O**. *Heteropora americana* Richards, 1962, AMNH 51309. **A–M**. ×1.

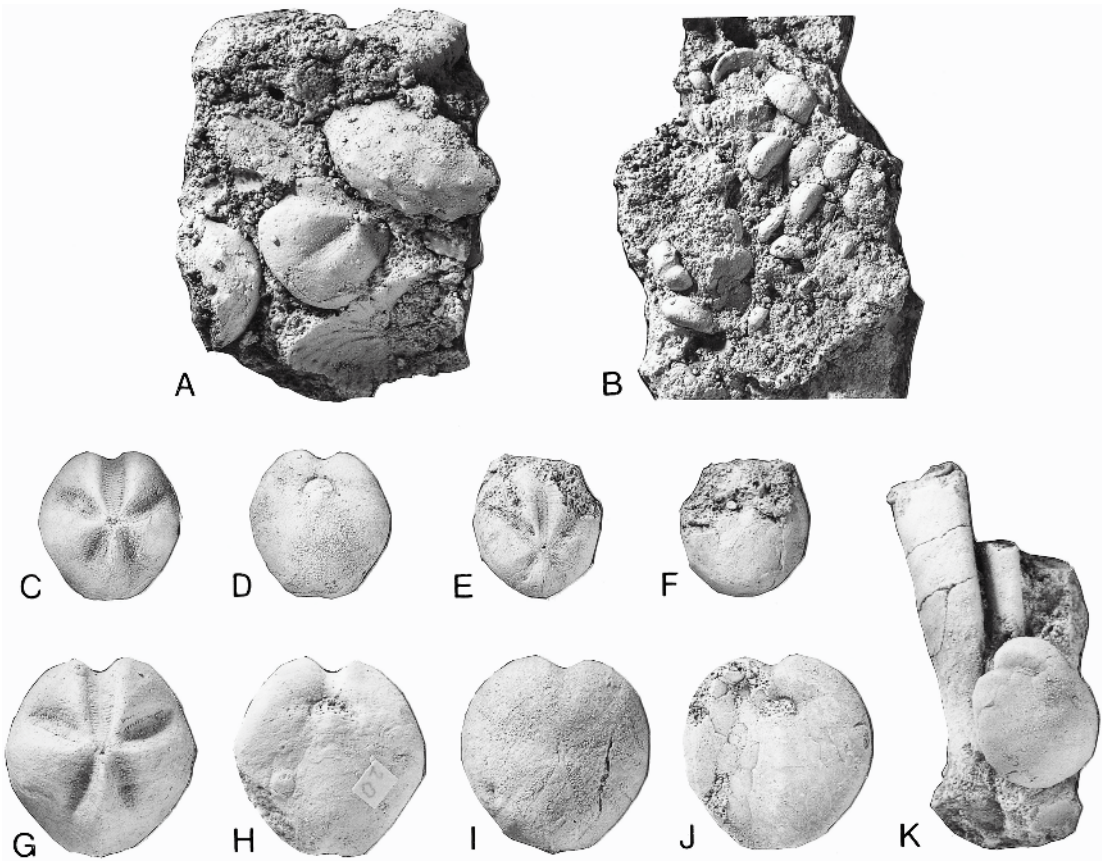

Fig. 16. Echinoids from the top of the Tinton Formation, Manasquan River Basin, Monmouth County, New Jersey. **A, C, D, G, H.** *Hemiaster dalli* Clark, 1891. **A.** Association with a fragment of *Discoscaphites iris* (Conrad, 1858), MAPS A3609a3. **C, D.** MAPS A3609a1. **G, H.** MAPS A3609a2. **B, I–K.** *Cardiaster marylandica* Clark, 1916. **B.** Cluster of juveniles, MAPS A3601g3. **I, J.** MAPS A3601g1. **K.** Association with *Eubaculites latecarinatus* (Brunnschweiler, 1966), MAPS A3601g2. **E, F.** *Hemiaster delawarensis* Clark, 1916, MAPS A3605f1. All figures ×1.

Tertiary boundary (fig. 3), by reference to the global stratotype section and point at El Kef, Tunisia (Cowie et al., 1989). However, this conclusion is inconsistent with the biostratigraphy in the Manasquan River Basin (see below). The *Pinna* Layer, which occurs stratigraphically above the iridium anomaly, contains species indicative of the uppermost Maastrichtian. This kind of inconsistency is not uncommon in Cretaceous/Tertiary boundary sections elsewhere. For example, Bralower et al. (1989) cautioned that biostratigraphic data in K/T sections from the Gulf of Mexico and the Caribbean provide

→

Fig. 17. Dinoflagellates from the *Pinna* Layer, upper part of the Tinton Formation, R6416A, AMNH loc. 3335, 4.3 km southwest of Freehold, Monmouth County, New Jersey. **A, B.** *Disphaerogena carposphaeropsis* Wetzel, 1933 (= *Cyclapophysis monmouthensis*). **A.** Dorsal view of dorsal surface; **B.** dorsal view at midfocus. **C, F.** *Deflandrea galeata* (Lejeune-Carpentier, 1942) Lentin & Williams, 1973. **C.**

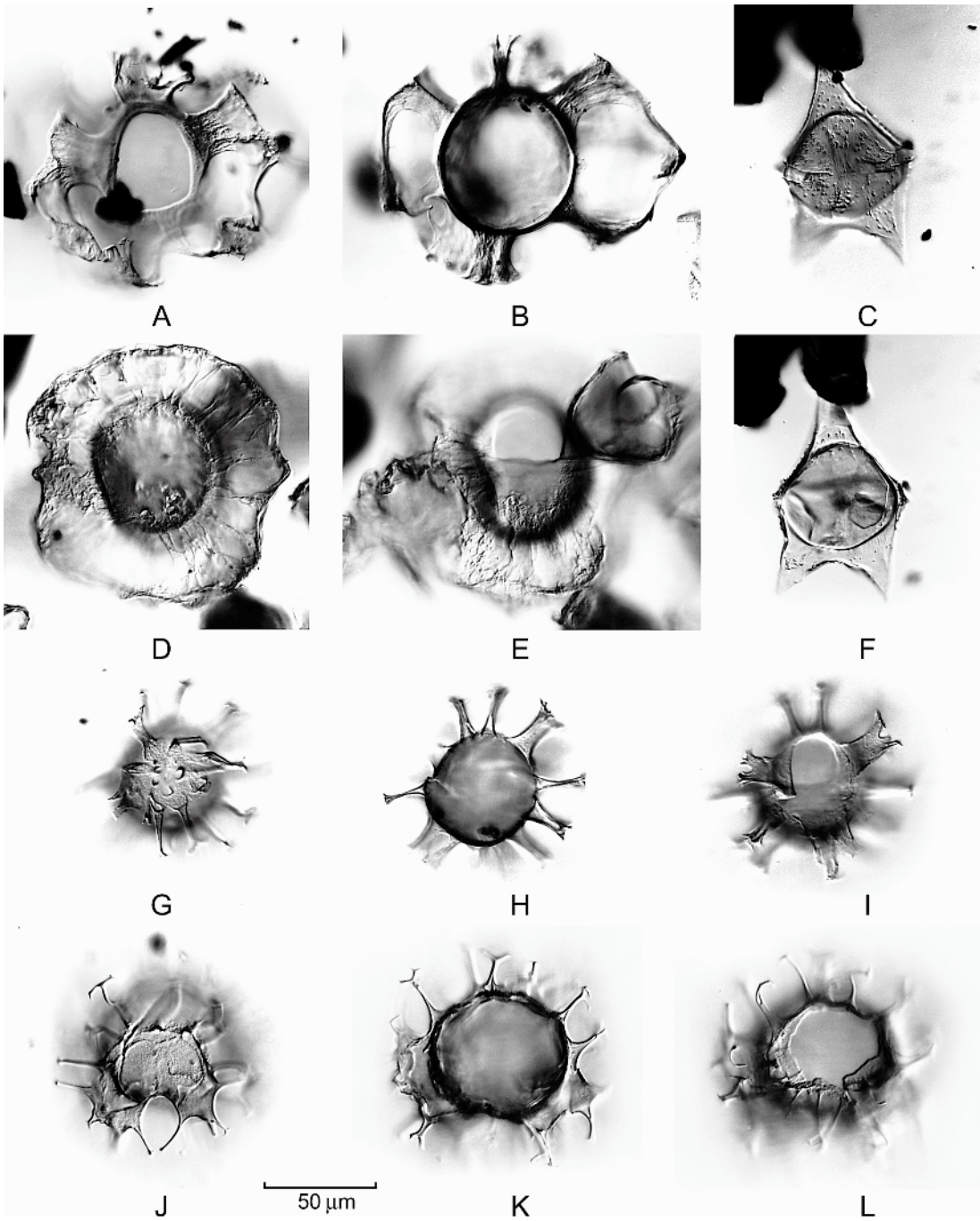

Ventral view of ventral surface; **F.** ventral view at midfocus. **D, E.** *Thalassiphora pelagica* (Eisenack, 1954) Eisenack & Gocht, 1960. **D.** Ventral view of ventral surface; **E.** ventral view of dorsal surface. **G–I.** *Kleithriasphaeridium truncatum* (Benson, 1976) Stover & Evitt, 1978. **G.** Ventral view of ventral surface; **H.** ventral view at midfocus; **I.** ventral view of dorsal surface. **J–L.** *Palynodinium grallator* Gocht, 1970. **J.** Antapical view of antapex; **K.** antapical view at midfocus; **L.** antapical view of apex.

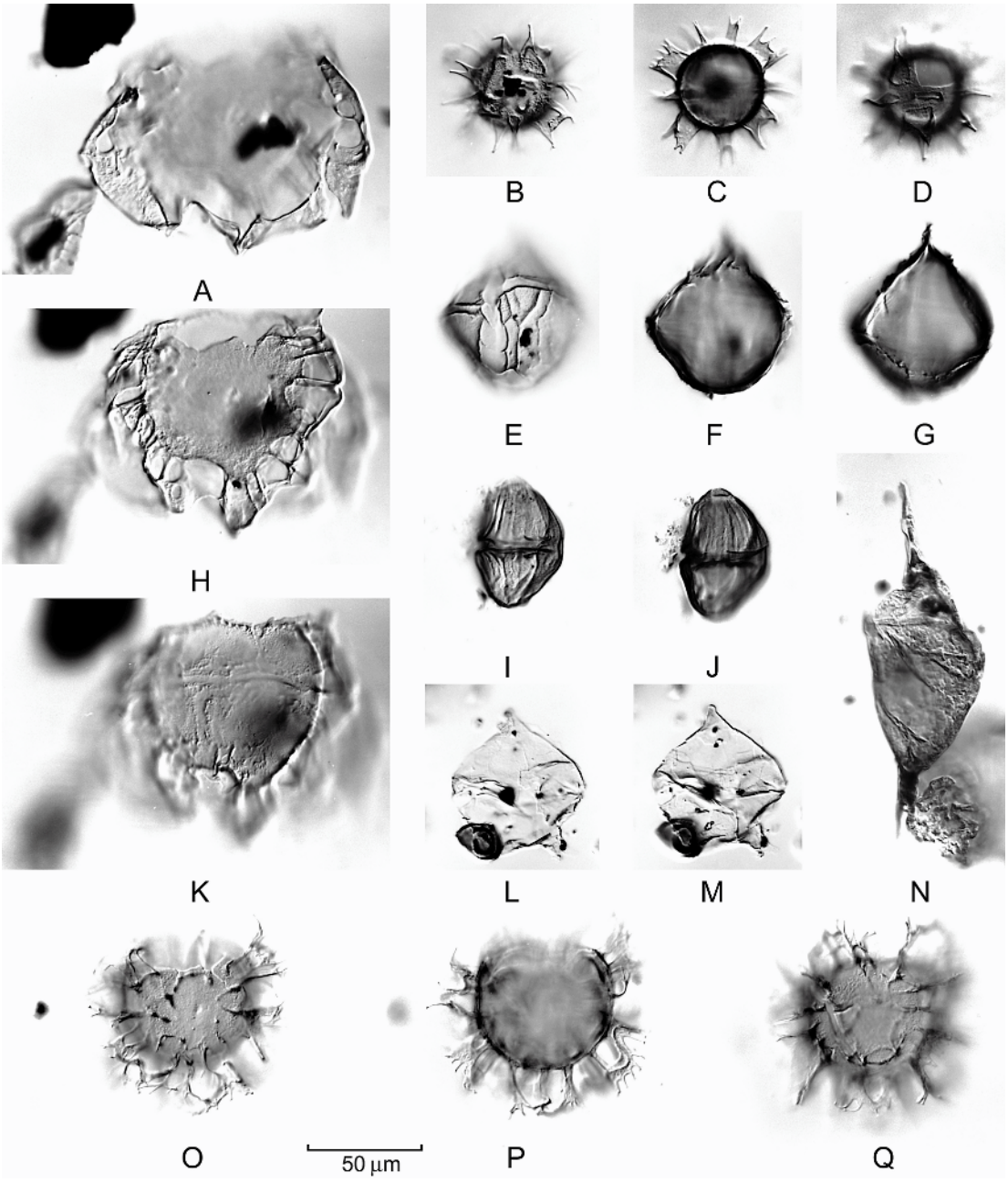

Fig. 18. Dinoflagellates from the upper part of the Tinton Formation and lower part of the Hornerstown Formation, Manasquan River Basin, Monmouth County, New Jersey. **A, H, K.** *Glaphyrocysta expansa* (Corradini, 1973) Roncaglia & Corradini, 1997 (? = *G. perforata* sensu Schiøler et al., 1997), R6416A, *Pinna* Layer, AMNH loc. 3335, 4.3 km southwest of Freehold, Monmouth County. **A.** Ventral view of ventral ectophragm; **H.** ventral view of ventral surface; **K.** ventral view of dorsal surface. **B–D**. *Florentinia ferox* (Deflandre, 1937) Duxbury, 1980, R6416A, *Pinna* Layer, AMNH loc. 3335, 4.3 km southwest of Freehold, Monmouth County. **B.** Ventral view of ventral surface; **C.** ventral view at midfocus; **D.** ventral view of dorsal surface. **E–G.** *Cribroperidinium* sp. (species group includes the *C.*

only maximum ages because of extensive redeposition in these areas at the end of the Cretaceous and beginning of the Paleocene.

Hypothesis 2: The iridium anomaly has been displaced downward. The most logical choice for the original position of the enriched layer of iridium is at the top of the *Pinna* Layer. Downward displacement of the iridium could have resulted from at least two processes. Soon after deposition of the iridium, it could have been translated downward due to bioturbation of the animals living at the time. Alternatively, it may have been remobilized due to chemical diffusion, either early or late in diagenesis. In this context, we note that the contact between the *Pinna* Layer and the underlying part of the Tinton Formation is presently an aquitard, with ground water flowing through the *Pinna* Layer, possibly via cracks, and emerging at the contact. This horizon may thus represent a chemical boundary, causing a secondary enrichment of iridium. Loss during remobilization could also account for the relatively low concentration of iridium relative to that at other K/T boundary sites.

If the iridium has been displaced downward from the top of the *Pinna* Layer, then this higher horizon would, in theory, correspond to the K/T boundary, by reference to the global stratotype section and point at El Kef, Tunisia. This interpretation is in better agreement with the biostratigraphic data, because this horizon occurs just above the unit containing fossils indicative of the uppermost Maastrichtian.

Choosing between these two hypotheses requires additional analyses. In particular, examination of the concentration and distribution of other elements may provide insights into the probability of remobilization, although the behavior of these other elements may differ from that of iridium. Additional analyses of iridium, especially in the stratigraphic interval containing few data below the base of the *Pinna* Layer, would also help answer questions about the shape of the iridium profile. The implications of these two hypotheses are further discussed in the section on the Cretaceous/Tertiary boundary.

We have not identified a specific fallout layer containing spherules or shocked quartz in the Manasquan River Basin, although such structures have been commonly reported at other K/T boundary sites (e.g., Smit, 1999; Olsson et al., 2002). Spherules may have been deposited and subsequently destroyed. Indeed, work in progress has suggested the presence of spherules at nearby outcrops in New Jersey (Landman et al., in prep). However, the absence of spherules in the Manasquan River Basin implies that this section does not preserve the full spectrum of depositional events associated with the K/T impact. Nevertheless, it is reasonable to assume that the small Ir anomaly that we observe is related to the global Ir anomaly documented at many other localities, although the stratigraphic position of this anomaly in the Manasquan River Basin is subject to debate.

BIOSTRATIGRAPHIC ANALYSIS

The presence of *Discoscaphites iris* in the upper part of the Tinton Formation, including the *Pinna Layer*, in the Manasquan

←

edwardsi / *wetzelii* / *ventriosum* complex), R6416A, *Pinna* Layer, AMNH loc. 3335, 4.3 km southwest of Freehold, Monmouth County. **E.** Ventral view of ventral surface; **F, G.** ventral view of ventral surface at successively lower foci. **I, J.** *Alisogymnium*/*Dinogymnium* sp., R6367B, *Pinna* Layer, AMNH loc. 3335, 4.3 km southwest of Freehold, Monmouth County. Upper (**I**) and lower (**J**) surfaces, orientation uncertain. **L, M.** *Piercites pentagonum* (May, 1980) Habib & Drugg, 1987, R6367A, Tinton Formation, 0–25 cm below the *Pinna* Layer, AMNH loc. 3335, 4.3 km southwest of Freehold, Monmouth County. Ventral views of ventral (**L**) and dorsal surfaces (**M**). **N.** *Palaeocystodinium australinum* (Cookson, 1965) Lentin & Williams, 1976, species complex, orientation uncertain, midfocus, R6416A, *Pinna* Layer, AMNH loc. 3335, 4.3 km southwest of Freehold, Monmouth County. **O–Q.** *Areoligera*/*Glaphyrocysta* complex, R6435AD, Hornerstown Formation, 70 cm above the base, AMNH loc. 3372, 3.8 km southwest of Freehold, Monmouth County. **O.** Ventral view of ventral surface; **P.** ventral view at midfocus; **Q.** ventral view of dorsal processes.

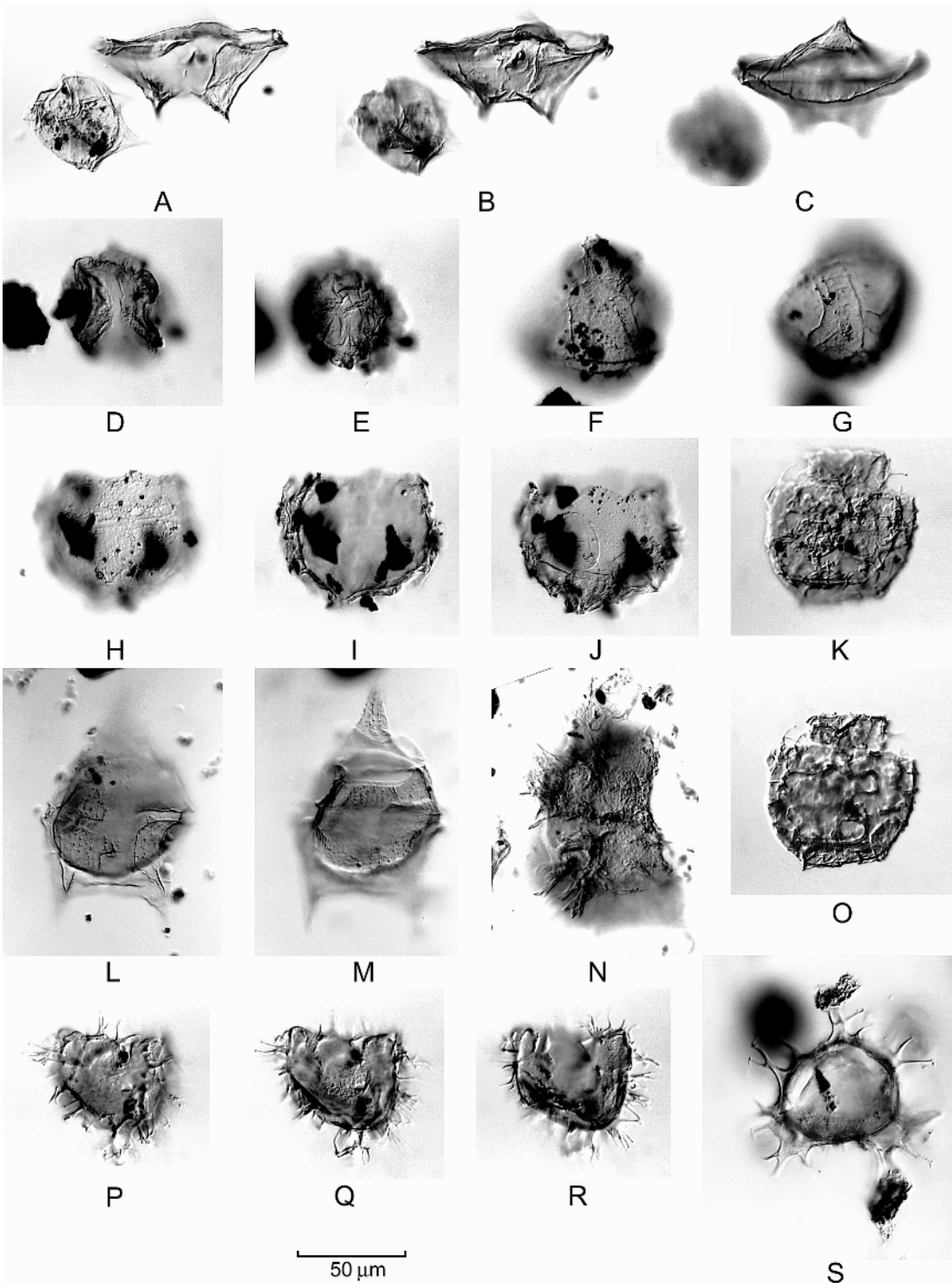
A
B
C
D
E
F
G
H
I
J
K
L
M
N
O
P
Q
R
S
50 µm

River Basin indicates the *D. iris* Assemblage Zone. This zone is approximately 1 m thick in this area, although its lower limit is not well documented. This is the highest ammonite zone in North America, representing the uppermost Maastrichtian, and correlates with the upper part of calcareous nannofossil Zone CC26b (Landman et al., 2004a).

The *Pinna* Layer also contains other macrofossils indicative of the uppermost Maastrichtian. For example, *Tenuipteria argentea* (Conrad, 1858) is present, which represents the first report of this species on the Atlantic Coastal Plain. This species is known elsewhere from the uppermost Maastrichtian of northern Europe (Abdel-Gawad, 1986; Jagt, 1996) and the Gulf Coastal Plain (Stephenson, 1955; Speden, 1970). In addition, the *Pinna* Layer contains rare specimens of *Exogyra costata* Say, 1820, suggesting that this species may also have extended to the top of the Maastrichtian, contrary to traditional interpretations. Similarly, a specimen of *Inoceramus* sp. is present in the *Pinna* Layer (fig. 14J–M). It shows a pronounced geniculation with comarginal ribs and bears a close resemblance to species from lower in the Maastrichtian (P. J. Harries, personal commun., 2006; I. Walaszczyk, personal commun., 2006). If correctly identified as an inoceramid, this discovery contradicts previous reports that inoceramids disappeared 1.5 million years before the end of the Cretaceous (Kauffman et al., 1993; MacLeod et al., 1996; Chauris et al., 1998).

Cucullaea vulgaris is abundant in the *Pinna* Layer and commonly occurs in dense concentrations (figs. 5C, 11O, P). This species was previously considered as an ''index fossil'' for the Main Fossiliferous Layer (MFL) at the base of the Hornerstown Formation (Gallagher, 1993). However, *C. vulgaris* is also present in the upper part of the New Egypt Formation below the MFL at Eatontown, northeastern Monmouth County (Landman et al., 2004a), and at Crosswicks Creek, southwestern Monmouth County (Landman et al., in prep.).

The dinoflagellates in the upper part of the Tinton Formation in the Manasquan River Basin are illustrated in figures 17–19 and listed in table 2. The biostratigraphic significance of these dinoflagellates was evaluated with reference to the zonation established by

←

Fig. 19. Dinoflagellates from the upper part of the Tinton Formation and lower part of the Hornerstown Formation, Manasquan River Basin, Monmouth County, New Jersey. **A–C.** *Phelodinium magnificum* (Stanley, 1965) Stover & Evitt, 1978, R6416A, *Pinna* Layer, AMNH loc. 3335, 4.3 km southwest of Freehold, Monmouth County. Oblique ventral views of ventral surface (**A**), at midfocus (**B**), and of dorsal surface (**C**); note small peridiniacean form in focus in **A**. **D, E.** *Rugubivesiculites* pollen, R6435AE, siderite nodules, 15 cm above base of Hornerstown Formation (just above Burrowed Unit), AMNH loc. 3372, 3.8 km southwest of Freehold, Monmouth County. Distal views of distal (**D**) and proximal (**E**) surfaces; this form is undoubtably reworked. **F, G.** *Cribroperidinium graemei* William et al., 1998, R6435AE, siderite nodules, 15 cm above base of Hornerstown Formation (just above Burrowed Unit), loc. 3372, 3.8 km southwest of Freehold, Monmouth County. Oblique right-lateral views of upper (**F**) and lower (**G**) surfaces. **H–J.** *Areoligera*/*Glaphyrocysta* complex, R6435AE, siderite nodules, 15 cm above base of Hornerstown Formation (just above Burrowed Unit), AMNH loc. 3372, 3.8 km southwest of Freehold, Monmouth County. Dorsal views of dorsal surface (**H**), at midfocus (**I**), and of ventral surface (**J**); note poorly preserved ectophragm. **K, O, P–R.** *Areoligera*/*Glaphyrocysta* complex, R6435AD, 70 cm above base of Hornerstown Formation, AMNH loc. 3372, 3.8 km southwest of Freehold, Monmouth County. Orientation uncertain, upper focus (**K**) and lower focus (**O**), poorly preserved specimen; dorsal views of dorsal surface (**P**), at midfocus (**Q**), and of ventral processes (**R**), better preserved specimen. **L, M.** *Deflandrea galeata* (Lejeune-Carpentier, 1942) Lentin & Williams, 1973, R6435AA, 10 cm above base of Hornerstown Formation (Burrowed Unit), AMNH loc. 3372, 3.8 km southwest of Freehold, Monmouth County. Ventral views of ventral surface (**L**) and dorsal surface (**M**). **N.** *Damassadinium californicum* (Drugg, 1967) Fensome et al., 1993, questionably identified fragment, upper surface, R6435AA, 10 cm above the base of the Hornerstown Formation (Burrowed Unit), AMNH loc. 3372, 3.8 km southwest of Freehold, Monmouth County. **S.** *Palynodinium grallator* Gocht, 1970, R6435AB, 20 cm above base of Hornerstown Formation, AMNH loc. 3372, 3.8 km southwest of Freehold, Monmouth County. Antapical view at midfocus, presumably reworked.

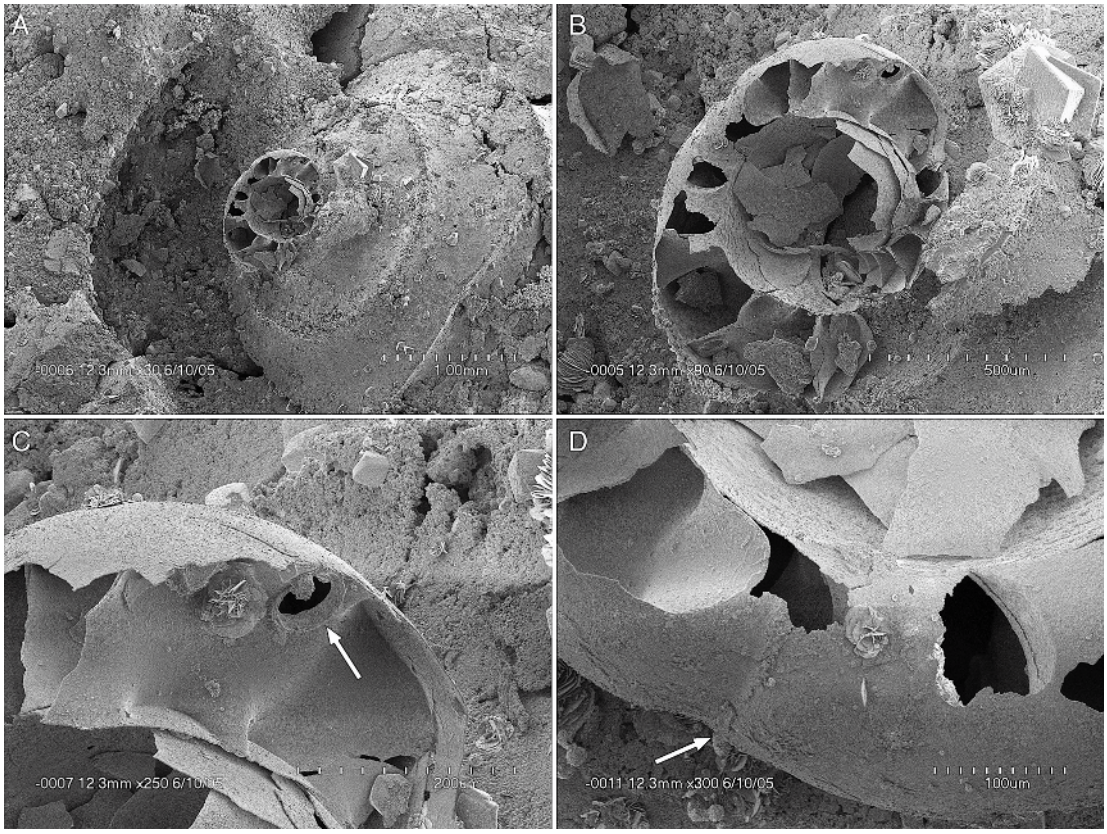

Fig. 20. Scaphite with hollow inner whorls, AMNH 50777, from a nodule at the base of the Hornerstown Formation, AMNH loc. 3372, Monmouth County, New Jersey. **A.** Overview. **B.** Close-up. **C.** Close-up of septal neck (arrow). **D.** Close-up of primary constriction (arrow) marking the point of hatching.

Firth (1987, 1993) and Edwards et al. (1999) for the Atlantic Coastal Plain, in the context of the broader compilation assembled by Brinkhuis et al. (2003).

The age of the dinoflagellates is consistent with that of the ammonites in the same strata. The upper part of the Tinton Formation, including the *Pinna* Layer, contains *Palynodinium grallator* and *Thalassiphora pelagica*. The presence of these two species indicates the uppermost Maastrichtian *P. grallator* Zone, probably the Tpe (*T. pelagica*) Subzone of Schiøler and Wilson (1993). This zone correlates with the upper part of calcareous nannofossil Subzone CC26b (Landman et al., 2004b).

The Burrowed Unit at the base of the Hornerstown Formation contains a few ammonite fragments in the sediments surrounding the burrows. A sample of sediment from this unit also contains *Deflandrea galeata* (fig. 19L, M), indicating the upper Maastrichtian, and a single fragment of ?*Damassadinium californicum*, or some closely related form (fig. 19N), indicating the Danian. As stated previously, the specimen of *D. galeata* may have been derived from the sediments surrounding the burrows and the specimen of ?*D. californicum* may have been derived from the burrows themselves. Analysis of a sample (R6435BA) restricted to the sediments surrounding the burrows yielded ?*Disphaerogena carposphaeropsis*, indicating the upper Maastrichtian. These results suggest that the age of the Burrowed Unit is similar to that of the *Pinna* Layer, albeit slightly younger, inasmuch as the Burrowed Unit occurs above the *Pinna* Layer.

The siderite nodules at the base of the Hornerstown Formation contain reworked

TABLE 2
Dinocysts from the Manasquan River Basin, Monmouth Country, New Jersey

	AMNH loc. 3335 (Tinton Formation)			AMNH loc. 3372 (Hornerstown Formation) R6435						
	R6367A	R6416A	R6367B	AA	AE	AB	A	C	AC	AD
Alisogymnium/Dinogymnium spp.	X	X	X	.	.	.	.	.	.	.
Amphorosphaeridium/Cordosphaeridium complex	X	X	.	.	.	.	.	.	.	.
?*Andalusiella rhombohedra* of Edwards et al., 1984	X	.	.	.	.	.	.	.	.	.
Areoligera senonensis Lejeune-Carpentier, 1938 species complex	.	X	X	X	.	.	.	X	X	X
Areoligera sp. indet.	.	.	X	.	.	X	X	X	X	X
Cerodinium striatum/diebelii complex	X	X	.	.	.	.	.	.	.	.
Conneximura fimbriata (Morgenroth, 1968) May, 1980	.	X	.	.	.	.	.	.	.	.
Cordosphaeridium fibrospinosum Davey & Williams, 1966	.	X	.	.	.	.	.	.	.	.
Coronifera granulata Slimani, 1994	.	X	.	.	.	.	.	.	.	.
Coronifera oceanica Cookson & Eisenack, 1958	X	X	.	.	.	.	.	.	.	.
Cribroperidinium graemei Williams et al., 1998	X	X	X	.	.	.	.	.	.	.
Cribroperidinium spp.(includes *C. edwardsi/wetzelii/ventriosum* complex)	X	X	X	.	X	.	.	.	.	X
Cyclopsiella ? sp. Drugg & Loeblich, 1967	.	X	.	.	.	.	.	.	.	.
Deflandrea galeata (Lejeune-Carpentier, 1942) Lentin & Williams, 1973	X	X	X	R?	.	.	.	.	.	.
Diphyes colligerum (Deflandre & Cookson, 1955) Cookson, 1965	.	X	.	.	.	.	.	.	.	.
Disphaerogena carposphaeropsis Wetzel, 1933 (=*Cyclapophysis monmouthensis*)	X	X	.	.	.	.	.	.	.	.
Exochosphaeridium sp.	?	X	.	.	.	?	.	.	.	.
Fibradinium annetorpense Morgenroth, 1968	X[a]	X	.	.	.	X[a]	.	.	.	.
Fibrocysta radiata (Morgenroth, 1966) Stover & Evitt, 1978	X	X	.	.	.	?	.	.	.	.
Florentinia ferox (Deflandre, 1937) Duxbury, 1980	.	X	.	.	.	.	.	.	.	.
Fromea fragilis (Cookson & Eisenack, 1962) Stover & Evitt, 1978	.	X	.	.	.	.	.	.	.	.
"*Glaphyrocysta expansa* (Corradini, 1973) Roncaglia & Corradini, 1997 (?=*G. perforata* sensu Schiøler et al., 1997)"	.	X	.	.	X	.	.	.	.	.
Glaphyrocysta spp. (misc. or indet.)	X	X	.	X	.	.	.	.	.	.
Hafniasphaera fluens Hansen, 1977	X	X	.	.	.	.	.	.	.	.
Hystrichosphaeridium spp. Deflandre, 1937	.	X	.	.	.	.	.	.	.	.
Impagidinium sp.	.	X	.	.	.	.	.	.	.	.
Kleithriasphaeridium truncatum (Benson, 1976) Stover & Evitt, 1978	X	X	.	.	.	.	.	.	.	.
Microdinium cretaceum Slimani, 1994	.	X	.	.	.	.	.	.	.	.
Microdinium mariae Slimani, 1994	.	X	.	.	.	.	.	.	.	.
Oligosphaeridium sp. Davey & Williams, 1966	?	?	.	.	.	.	.	.	.	.
Operculodinium sp. (large)	X	.	.	.	.	X	.	.	.	.
Palaeocystodinium australinum (Cookson, 1965) Lentin & Williams, 1976, species complex	.	X	.	.	.	.	.	.	.	.
Palaeocystodinium sp. (fat)	.	.	.	.	.	X	.	.	.	.
Palaeotetradinium caudatum (Benson, 1976) Stover & Evitt, 1978	X	X	.	.	.	.	.	.	.	.
Palynodinium grallator Gocht, 1970	X	X	X	.	R?	R	.	.	.	.
Pervosphaeridium tubuloaculeatum Slimani, 1994	.	?	.	.	.	.	.	.	.	.
Phelodinium magnificum (Stanley, 1965) Stover & Evitt, 1978	.	X	.	.	.	.	.	.	.	.
Piercites pentagonum (May, 1980) Habib & Drugg, 1987	X	X	.	.	.	.	.	.	.	.
Senegalinium microgranulatum (Stanley, 1965) Stover & Evitt, 1978	X	.	.	.	.	.	.	.	.	.
Senoniasphaera protrusa Clark & Verdier, 1967	?	.	.	.	.	.	.	.	.	.
Spiniferites spp.	X	X	?	.	.	X	.	.	.	.
Thalassiphora pelagica (Eisenack, 1954) Eisenack & Gocht, 1960	X	X	.	.	.	.	.	.	.	.
Trigonopyxidia ginella (Cookson & Eisenack, 1960) Downie & Sarjeant, 1965	.	X	.	.	.	.	.	.	.	.
Turnhosphaera hypoflata (Yun, 1981) Slimani, 1994	.	X	.	.	.	.	.	.	.	.
Yolkinigymium elongatum (May, 1977) Lentin & Vozzhennikova, 1990	X	.	.	.	.	.	.	.	.	.
misc. cladopyxidiaceans	X	.	.	.	.	.	.	X	.	.
misc. small peridiniceans	X	X	X	.	?	.	.	X	.	.
misc. bumpy sphere	.	.	X	.	.	.	.	.	.	.
unidentifiable fragments	.	.	.	X	X	X	.	X	X	.

[a]*Fibradinium* cf. *annetorpense*
R = reworked.

TABLE 3
Elemental Concentrations across the Cretaceous/Tertiary Boundary Interval, Manasquan River Basin, New Jersey

AMNH loc. no.	Sample no.	Position[a]	Fe, mg/g	Ir, pg/g	LOI, wt%
3372	AC:27	30 cm	206	94	11.7
3372	AC:26	24 cm	205	76	11.3
3372	AC:25	22 cm	213	104	11.5
3372	AC:24	20 cm	206	131	12.0
3372	AC:23	18 cm	213	113	8.0
3372	AC:22	16 cm	209	104	12.4
3372	AC:21	14 cm	202	108	12.4
3372	AC:20	12 cm	208	83	9.0
3372	AC:19	10 cm	204	101	7.3
3372	AC:18	8 cm	236	126	10.6
3372	AC:17	6 cm	224	110	9.8
3372	AC:16	4 cm	215	132	9.5
3372	AC:15	2 cm	213	130	8.1
3372	AC:14	0.5 cm	236	139	9.8
3372	AC:13	−0.5 cm	228	120	9.4
3372	AC:12	−2 cm	228	132	10.0
3372	AC:11	−4 cm	226	118	10.6
3372	AC:10	−6 cm	237	127	12.7
3372	AC:9	−8 cm	211	99	8.9
3372	AC:8	−10 cm	232	126	9.4
3372	AC:7	−12 cm	235	143	10.1
3372	AC:6	−14 cm	229	117	9.5
3372	AC:5	−16 cm	238	120	9.5
3372	AC:4	−18 cm	223	116	10.0
3372	AC:3	−20 cm	222	129	9.2
3372	AC:2	−21 cm	203	457	10.5
3372	AC:1	−25 cm	209	276	9.1
3391	IC:2	−50 cm	255	188	13.6
3391	IC:1	−80 cm	224	176	10.7
3335	5	15 cm	233	82	10.0[e]
3335	A	2.5 cm	219	131	10.0[e]
3335	4	~2 cm	228	93	10.0[e]
3335	B	−2.5 cm	231	151	10.0[e]
3335	C	−15 cm	218	143	10.0[e]
3335	2[b]	−20 cm	206	589	10.0[e]
3335	1[c]	Mud	230	244	10.0[e]
3335	3[d]	−22 cm	202	220	10.0[e]

[a]The values are plotted relative to the Tinton/Hornerstown formational boundary (0 cm). The Burrowed Unit is present at AMNH loc. 3372 but absent at AMNH locs. 3335 and 3391. The enriched concentration of iridium occurs at the contact between the *Pinna* Layer and the underlying part of the Tinton Formation.

[b]The value of Ir represents an average of the original sample (545 pg/g), a split from the same powder (671 pg/g), and newly prepared powder from additional material from the same sample (552 pg/g). The value of Fe represents an average of 211, 210, and 196 mg/g from the same three samples, respectively.

[c]This sample represents a discontinuous layer of mud at the contact between the *Pinna* Layer and the underlying part of the Tinton Formation. This mud probably accumulated diagenetically due to water flow along the contact because the underlying part of the Tinton Formation is an aquitard. The value of Ir represents an average of the original sample (225 pg/g) and a split from the same powder (262 pg/g). The value of Fe represents an average of 229 and 230 mg/g from the same two samples, respectively.

[d]The value of iridium represents an average of the original sample (207 pg/g) and a split from the same powder (233 pg/g). The value of Fe represents an average of 204 and 199 mg/g from the same two samples, respectively.

[e]Assuming 10% LOI.

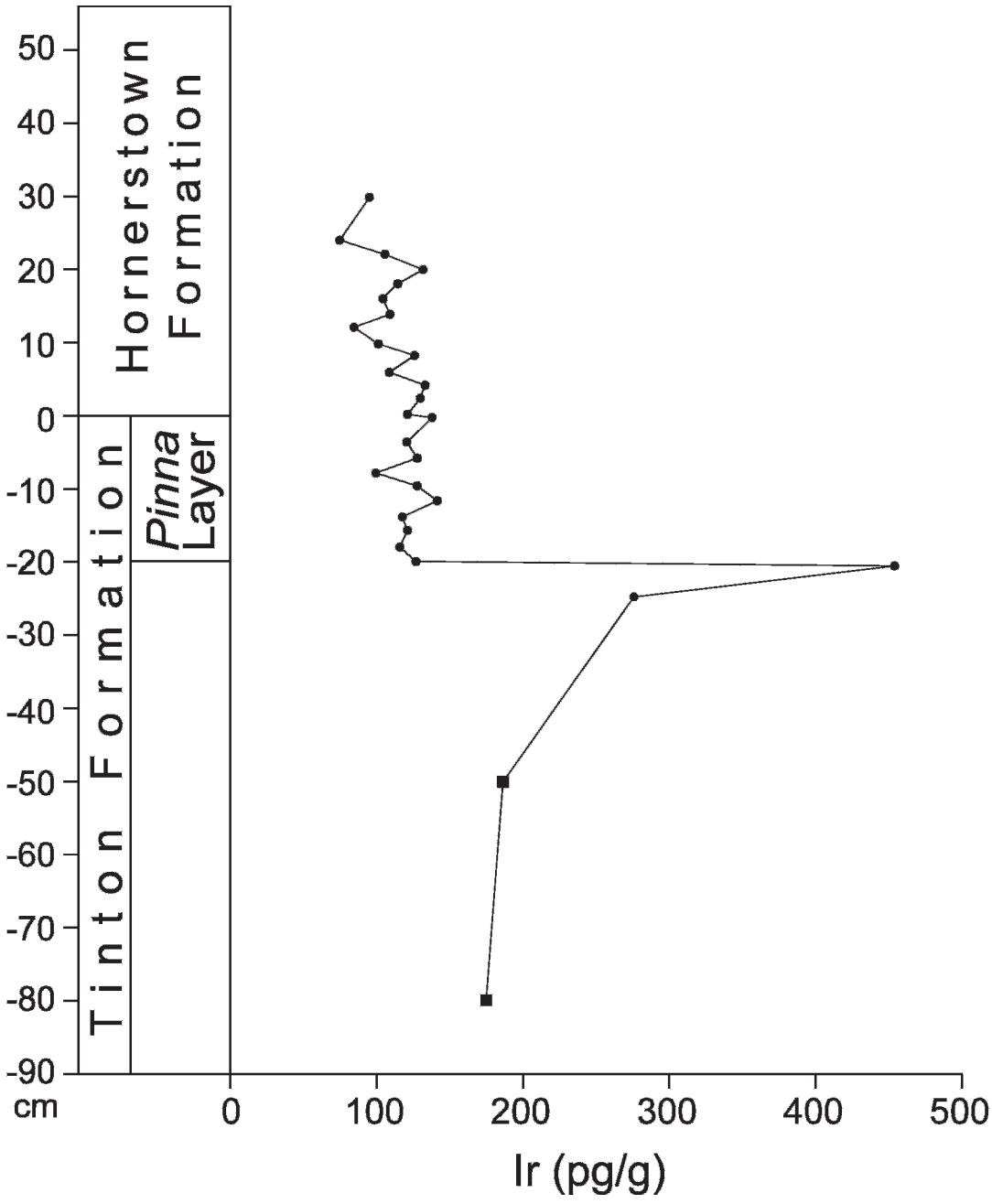

Fig. 21. Concentration of iridium (pg/g) at AMNH locs. 3372 (●) and 3391 (■), Manasquan River Basin, central Monmouth County, New Jersey. The scale (cm) is drawn such that 0 cm marks the boundary between the Tinton and Hornerstown formations. The highest concentration of iridium occurs at the base of the *Pinna* Layer, but the highest non-reworked ammonites occur approximately 20 cm higher up, at the top of the *Pinna* Layer.

fossils from the *Pinna* Layer, including *Cucullaea vulgaris* and *Discoscaphites iris*. In addition, the nodules contain poorly preserved dinoflagellate cysts (fig. 19F–J) and *Rugubivesiculites* pollen (fig. 19D, E), supporting the interpretation that these nodules were reworked.

The overlying part of the Hornerstown Formation is sparsely fossiliferous. Palynomorphs are rare, with most sediment samples containing only a few, poorly preserved specimens, even though more raw material than usual was processed. Samples R6435AB, AC, and AD are the only samples with more than a dozen specimens, the majority of which represent members of the *Areoligera* group. *Palynodinium grallator* in sample R6345AB from 20 cm above the base of the Hornerstown Formation, just above the Burrowed Unit, is probably reworked (fig. 19S). Higher samples (30 cm above the formational boundary and higher) do not show obvious reworking.

In contrast to the rarity of dinoflagellates, the bivalve *Ostrea pulaskensis* is relatively abundant in the basal Hornerstown Formation. This species is known from the Danian part of the Clayton Formation in southern Illinois (Cope et al., 2005). It also occurs in beds 7–9 in the basal Pine Barren Member of the Clayton Formation at Braggs, Alabama (Bryan and Jones, 1989), which, according to Moshkovitz and Habib (1993), corresponds to the upper part of calcareous nannofossil Zone NP1. At the Brazos River section in east Texas, the lowest occurrence of this species is at sample level 16 in the Littig Member of the Kincaid Formation (Hansen et al., 1993b). According to the recent analysis of Schulte et al. (2006), this level corresponds to foraminiferal Zone P1a, but the dating of this section is still in dispute (T. Yancey, personal commun., 2006).

Thus, the presence of *Ostrea pulaskensis* in the basal Hornerstown Formation indicates that these strata are lower Danian. If it is further assumed that the lowest occurrence of this species in the Manasquan River Basin corresponds to the upper part of calcareous nannofossil Zone NP1, it implies that there is a hiatus of no more than several hundred thousand years between the top of the *Pinna* Layer and the basal Hornerstown Formation, based on the time scale of Berggren et al. (1995) and Luterbacher et al. (2004). This is consistent with previous interpretations at other sites in New Jersey. For example, in northeastern Monmouth County, where the Hornerstown Formation overlies the New Egypt Formation, Landman et al. (2004b) postulated a hiatus of approximately 100,000 years at the formational boundary.

STRATIGRAPHIC RELATIONSHIPS

What we refer to as the Tinton Formation in the Manasquan River Basin was mapped as a single unit consisting of the Tinton and Red Bank formations in the geologic map of New Jersey by Lewis and Kümmel (1910–1912). In the most recently published map by Owens et al. (1998), the main part of the upper Manasquan River Basin is mapped as the Hornerstown Formation. However, we observed that large sections of the Manasquan River and its tributaries are floored by the Tinton Formation with the Cretaceous/Tertiary boundary widely exposed.

The type locality of the Tinton Formation is at Tinton Falls in northeastern Monmouth County. The exposures of the Tinton Formation in the Manasquan River Basin are 11.3 km along strike southwest of the southwesternmost outcrops of this formation, as reported by Weller (1907), in the head waters of Yellow Brook at Colts Neck. Nevertheless, the Tinton Formation in the Manasquan River Basin is lithologically identical in almost every respect, including the presence of large angular quartz grains. Another common feature is the abundance of fossil oysters, particularly *Ostrea nasuta* and *Pycnodonte convexa*. However, the Tinton Formation in the Manasquan River Basin differs from the Tinton Formation at its type locality in two respects: the scattered occurrence of large siderite nodules in the upper part of the formation and, especially, the presence of the *Pinna* Layer at the top.

The Tinton Formation, including the *Pinna* Layer, is present at Ivanhoe Brook in the northeasternmost part of the Crosswicks Creek Basin, 14 km southwest of the Manasquan River outcrops. The upper part of the Tinton Formation at this site has yielded *Ostrea nasuta*, *Sphenodiscus lobatus*, *Eubacu-*

lites latecarinatus, and *Discoscaphites iris*, all of which are also present in the Manasquan River Basin. However, the Tinton Formation at Ivanhoe Brook is muddier, perhaps reflecting the increasing influence of the deeper-water facies represented by the New Egypt Formation, into which it grades toward the southwest. As in the Manasquan River Basin, *Ostrea pulaskensis* is relatively abundant in the basal Hornerstown Formation at Ivanhoe Brook.

Approximately 7.5 km north of Ivanhoe Brook is the Perrineville Borrow Pit. It is over 40 m above sea level and thus represents one of the most updip depositional environments available for study. (It would have been interesting to compare this site to the borrow pit on Rt. 36 in Atlantic Highlands, which was also an extremely updip site but, unfortunately, both localities are now lost to development.) The Hornerstown Formation at the Perrineville Pit unconformably overlies approximately 2 m of silty clay and sand. Lithologically, this unit does not resemble either the Tinton or New Egypt Formation and may represent a local, very nearshore equivalent of the Tinton Formation. This unit is presumably equivalent in age to the Tinton and New Egypt formations but, unfortunately, there are no fossils to confirm this (P. J. Sugarman, personal commun., 2004). Several meters of unconsolidated massive quartz sand underlie this unit and weather to a bright orange-red color. This part of the section strongly resembles the Shrewsbury Member of the Red Bank Formation.

The top of the Tinton Formation in the Manasquan River Basin is approximately equivalent to the top of the New Egypt Formation just below the Main Fossiliferous Layer in the Crosswicks Creek Basin, southwestern Monmouth County, and at Parkers Creek, near Eatontown, northeastern Monmouth County, and represents the nearshore equivalent of these sites. The New Egypt Formation is absent in the Manasquan River Basin but is present at Parkers Creek. The elevations of the two sites are approximately 30 m and 3 m, respectively. If a southeast dip of approximately 4.7 m/km (Landman et al., 2004b) is assumed, it implies that the Manasquan River Basin is approximately 5.7 km farther updip than Parkers Creek. (Assuming a more gentle dip, the distance would be even greater.) This difference helps explain the absence of the New Egypt Formation in the Manasquan River Basin and its presence at Parkers Creek even though Parkers Creek is 23 km northeast of the Manasquan River Basin and nearer to the presumed source of riverine sediments, i.e., the clastic wedge represented by the Tinton and Red Bank formations.

The concentrated bed of nodules with reworked fossils at the base of the Hornerstown Formation in the Manasquan River Basin is equivalent to the Main Fossiliferous Layer elsewhere in New Jersey (Landman et al., 2004b). This bed indicates a widespread episode of erosion and reworking in response to fluctuations in sea level (see below).

ORIGIN OF THE *PINNA* LAYER

The environment of deposition of the *Pinna* Layer was relatively shallow. Olsson et al. (2002) estimated that sea level at the K/T boundary was approximately 50 m above the present level. Using this estimate, Landman et al. (2004b) calculated the paleodepth at the Manasquan River Basin. Assuming little tectonic movement of the New Jersey Coastal Plain since the end of the Cretaceous (Miller et al., 2004), they subtracted out the current elevation at this site and concluded that the water was approximately 20 m deep at the time of deposition. [This estimate does not take into account compaction, loading, and thermal subsidence. For a discussion of these factors, as well as backstripping, see Miller et al. (2006)]. This estimate is consistent with observations of the depth of modern *Pinna*, as documented by Yonge (1953) and Turner and Rosewater (1958).

The fauna in the *Pinna* Layer consists of benthic, nektobenthic, and nektic organisms, totaling approximately 70 species. The benthic organisms include both epi- and infauna. The majority of bivalves are suspension feeders including *Cucullaea vulgaris*, *Pycnodonte convexa*, and *Pinna laqueata* (table 1). The presence of *C. vulgaris* and *P. laqueata* distinguishes the community in the *Pinna* Layer from that in the underlying part of the Tinton Formation, in which these species are

absent. Most of the gastropods are mobile carnivores, with the exception of the Aporrhaidae and Turritellidae, which are deposit and/or suspension feeders, and the Bullidae, which are herbivores. The nektobenthic and nektic organisms include fish, turtles, and cephalopods.

This nearshore, subtidal environment was probably nutrient rich and, as a result, sustained a diverse community. The predominance of suspension feeders over deposit feeders indicates that during most of the time, the rate of sedimentation was low and the substrate was relatively firm (Jablonski and Bottjer, 1983; Hansen et al., 1993a; Kidwell, 1993). Perhaps even more critically, the amount of material in suspension did not overwhelm the filtering capacity of these organisms (S. Stanley, personal commun., 2006). However, because of its nearshore setting, this environment was probably subject to occasional episodes of rapid sedimentation, probably from riverine influx.

The mode of occurrence of the specimens in the *Pinna* Layer suggests an autochthonous accumulation, which was buried rapidly, with little or no postmortem transport. The animals may have been buried in several episodes, alternating with periods of little or no deposition, thus promoting the development of a suspension-feeding community.

Most of the benthic organisms in the *Pinna* Layer are preserved in life position. Specimens of *Pinna laqueata* are oriented vertically in the sediment, similar to the position of living members of this genus (see Young, 1953; Turner and Rosewater, 1968; Chinzei et al., 1982; Seilacher, 1984). *Cucullaea vulgaris*, which is semi-infaunal, occurs in living associations of up to 50 specimens, with both valves commonly attached. Echinoids also occur in aggregations of hundreds of individuals, suggesting gregarious feeding behavior.

The mode of occurrence of the scaphites and baculites also indicates that these animals lived and died near or at the site:

(1) Both kinds of ammonites are abundant and well preserved, representing all stages of growth from juveniles to adults.
(2) Many of the scaphites show signs of predatory damage, characterized by breaks in the adapical part of the body chamber (see Keupp, 2006; Larson, in press). In many instances, the damaged shells are preserved intact, implying that the animals died and sank to the bottom and were buried soon thereafter.
(3) Scaphite jaws (aptychi) are present, representing the first record of these structures in the Upper Cretaceous of New Jersey. Most of the jaws are isolated, but one specimen occurs inside the adoral part of a body chamber. Two other specimens are closely associated with their shells. The presence of these jaws indicates minimal transport and rapid burial.
(4) Both the scaphites and baculites commonly occur as clusters of dead shells. Many of the scaphite clusters consist almost entirely of microconchs (males) and may, thus, represent accumulations resulting from postmating fatality (see below). In any event, such accumulations could not have been produced by hydraulic processes.
(5) The phragmocones of the scaphites are commonly crushed whereas the body chambers are whole and filled with sediment. This preservational bias implies an early stage in taphonomic history when the siphuncular tube of the ammonite was still present, preventing infiltration of sediment into the phragmocone (Maeda and Seilacher, 1996). As a consequence, the hollow phragmocone was crushed during later compaction. The only exception to this rule is specimens in which the adapical end of the body chamber was broken due to predation. In these specimens, both the phragmocone and body chamber were filled with sediment.

In contrast, the eutrephoceratids, sphenodiscids, and pachydiscid are rarer and more fragmentary than the scaphites and baculites. This may indicate that these shells drifted in from elsewhere. Alternatively, it is possible that the larger size of the sphenodiscids and pachydiscid worked against their complete preservation. In this context, it is worth noting that the pieces of sphenodiscid shells are commonly sharp with jagged edges, suggesting that they were broken due to predation.

The *Pinna* Layer probably reflects a geologically short interval of time. The fact that most of the animals in the *Pinna* Layer are mature suggests that the community persisted for at least 5–10 years. According to Bucher

et al. (1996), shallow water ammonites such as baculites and scaphites probably reached maturity in approximately 5 years. *Cucullaea vulgaris* may have lived for 1–2 years, based on growth studies of related species of this genus from the late Maastrichtian of South Dakota (Pannella et al. 1968). There are no estimates available for *Pinna laqueata*, but this species probably reached maturity in 5–10 years, based on analogy with modern forms (Richardson et al., 1999; Katsanevakis, 2005). If multiple generations of animals are present in the *Pinna* Layer, reflecting multiple episodes of colonization and burial, this unit could represent more time, perhaps several tens of years. It is also important to note that the *Pinna* Layer is truncated at the top and may have originally been thicker, implying a still longer period of time, amounting to hundreds of years. However, the *Pinna* Layer is capped in places by the Burrowed Unit, which contains fossils indicative of the uppermost Maastrichtian.

These time estimates are consistent with the rate of sedimentation in nearshore environments. For example, Nittrouer et al. (1984) reported that the rate of accumulation of fine grained sediment in coastal environments ranges from millimeters to centimeters per year, as measured over a time span of 100 years. Schindel (1980: table 1) reported an average rate of approximately 1 cm/yr in coastal wetlands and tidal flats, as measured over longer time spans. Using these estimates and neglecting the effects of sediment compaction, the *Pinna* Layer, which is approximately 20 cm thick, would represent less than 200 years. If the *Pinna* Layer accumulated over tens of thousands of years, in contrast, it is unlikely that the monospecific clusters of scaphites, baculites, and other organisms would have survived intact at or below the sediment-water interface. It is equally unlikely that the scaphite aptychi would have remained in close association with the shells from which they were derived.

The sediments in the *Pinna* Layer are similar to those in the underlying part of the Tinton Formation, but contain a higher percentage of mud. The sediments in both units were probably derived from riverine discharge. However, there is no evidence of graded bedding in the *Pinna* Layer, due perhaps to pelletization of the sediment during formation of glauconite.

The presence of glauconitic minerals in the *Pinna* Layer seems inconsistent with our interpretation of multiple episodes of rapid burial, possibly with intervening periods of little or no deposition, amounting, in total, to hundreds of years. Glaucony is usually associated with much slower rates of sedimentation and much longer periods of time (see Odin, 1988, for an extensive review of the subject). However, glaucony has also been reported under regimes of more rapid sedimentation, as observed in the modern Amazon delta. The formation of glauconite is dependant on a number of geochemical conditions, including a source of abundant iron, and the existence of an oxic/suboxic interface, and may be completely independent of depositional rates (Aller, 2004).

ORIGIN OF THE BASAL HORNERSTOWN FORMATION

The Burrowed Unit that overlies the *Pinna* Layer at downdip sites may represent a pulse of riverine discharge associated with reworking of the bottom. This unit shares a few faunal elements in common with the *Pinna* Layer. The fossils are rare and most of them are fragmentary, suggesting postmortem transport. The presence of telescoped baculites indicates a high energy environment (see Histon, 2002). Some fossils may have been reworked from the underlying *Pinna* Layer. However, most of the baculites in the Burrowed Unit are filled with the same material as the matrix, indicating that any reworking would have occurred before the shells were fossilized.

The concentrated lag of siderite nodules in the basal Hornerstown Formation reflects an extensive period of reworking. There are many indications that these nodules were derived from the *Pinna* Layer. The size and lithology of the nodules are the same in both units. In addition, the nodules in the basal Hornerstown Formation contain specimens of *Discoscaphites iris*, *Cucullaea vulgaris*, *Rugubivesiculites* pollen, and other species that are present in the *Pinna* Layer. Several nodules also contain hollow specimens of *D. iris*, implying that the entire nodules were

reworked without destroying the delicate specimens inside (fig. 20).

The nodules in the basal Hornerstown Formation may have been eroded in place, as well as eroded at more updip sites and then transported seaward. It is difficult to estimate the amount of material removed during this process. However, one clue may be the number of siderite nodules in the basal Hornerstown Formation relative to that in the *Pinna* Layer. Siderite nodules are fairly common in the *Pinna* Layer, implying that the amount of material that must have been removed to yield the observed concentration of siderite nodules in the basal Hornerstown Formation may have been relatively modest. This process also involved the removal of most of the Burrowed Unit, which must have originally been more widely distributed.

Winnowing and reworking may also explain the reduction in the percentage of mud in the basal Hornerstown Formation (38% in the basal Hornerstown Formation vs. 62% in the *Pinna* Layer). The paucity of dinoflagellates in this unit may also result from winnowing, although they are scarce in age-equivalent sites elsewhere, possibly reflecting an impoverished flora (Landman et al., 2004b).

The presence of non-reworked echinoids, gastropods, bivalves, foraminifera, and crustaceans in parts of the basal Hornerstown Formation indicates that animals were living in the environment during the initial depositional phase of the formation. This admixture of reworked and non-reworked material is a hallmark of the Main Fossiliferous Layer elsewhere in New Jersey (Landman et al., 2004b). Even with respect to vertebrates, there is a mixture of material. Mosasaur teeth from the upper Maastrichtian show evidence of reworking, whereas turtle and bird fossils from the Paleocene are much better preserved (W. B. Gallagher, personal commun., 2006).

Subsequent to and simultaneous with the deposition of the basal Hornerstown Formation, the sea floor experienced extensive bioturbation. The sediments must have been relatively cohesive to maintain the integrity of the burrows. The burrows in the Burrowed Unit contain bivalves and nodules from the overlying part of the Hornerstown Formation. Interestingly, the burrows almost never penetrate into the *Pinna* Layer, which must have been more indurated than the Burrowed Unit. This induration must have occurred before the deposition of the overlying part of the Hornerstown Formation.

CRETACEOUS/TERTIARY BOUNDARY

The main features of the stratigraphic section in the Manasquan River Basin consist, in ascending order, of an enriched concentration of iridium, the fossiliferous *Pinna* Layer, the Burrowed Unit (in places), and a concentration of reworked siderite nodules. We interpret this stratigraphic sequence in the context of the known events at the close of the Cretaceous, as described by Koeberl and MacLeod (2002). In particular, we attribute the iridium anomaly to the Chicxulub impact, as suggested by many other studies [but see Keller et al. (2003, 2004) for a different point of view]. We present two alternative hypotheses, depending on whether the iridium anomaly is in place or has migrated downward.

Hypothesis 1: The iridium anomaly is in place.

If the iridium has not migrated downward, then the enriched concentration of iridium at the base of the *Pinna* Layer marks the Cretaceous/Tertiary boundary, by reference to the global stratotype section and point at El Kef, Tunisia (Cowie et al., 1989). Many of the faunal elements in the *Pinna* Layer are also present in the underlying part of the Tinton Formation, suggesting that the *Pinna* community was already established at the time of impact. In addition, the composition of the *Pinna* community, with its abundance of ammonites, is very similar to that of other late Maastrichtian communities, for example, in the Brazos River region, Texas (Hansen et al. 19993a, b), and at several sites in Poland (Abdel-Gawad, 1986).

The position of the iridium anomaly at the base of the *Pinna* Layer further implies that the community survived the impact. The organisms may even have flourished in its immediate wake due to greater nutrient runoff from the continent (Kump, 1991). The abundance of *Cucullaea vulgaris* in the *Pinna* Layer, as opposed to its absence in the

underlying part of the Tinton Formation, may reflect a post-impact explosion of suspension feeders. Altogether, the community may have persisted for up to hundreds of years after the impact, based on estimates of the rate of sedimentation and the age composition of the fauna (see above). This interpretation contrasts with the hypothesis of a substantially longer period (300,000 years) between impact and widespread extinction, as proposed by Keller et al. (2003, 2004), based on studies of the Brazos River section in Texas.

The sediments in the *Pinna* Layer may have been deposited in association with enhanced weathering following the impact. The impact would have injected tremendous amounts of dust, water vapor, and sulfur dioxide into the atmosphere, leading to acid rain (Pope et al., 1997). Wildfires on land would also have destroyed vegetation and further enhanced weathering and runoff (Robertson et al., 2004). Thus, the *Pinna* community may have been buried by pulses of mud-rich sediment from overflowing rivers in the early Danian (for a description of analogous plumes of mud on the modern Amazon delta, see Trowbridge and Kineke, 1994; Kineke and Sternberg, 1995; Kineke et al., 1996). The Burrowed Unit may represent a subsequent pulse of riverine discharge that scoured the top of the *Pinna* Layer, perhaps associated with an initial phase of the Danian transgression.

Hypothesis 2: The iridium anomaly has migrated downward from its original position at the top of the Pinna Layer

If the iridium anomaly originally occurred at the top of the *Pinna* Layer, it could have migrated downward due to the burrowing activities of animals living at the time, or due to chemical diffusion later in diagenesis. Either way, it implies that the top of the *Pinna* Layer more closely corresponds to the Cretaceous/Tertiary boundary, by reference to the global stratotype section and point at El Kef, Tunisia (Cowie et al., 1989). This interpretation is more consistent with the biostratigraphic data because the *Pinna* Layer contains fossils indicative of the uppermost Maastrichtian.

According to this hyothesis, the *Pinna* Layer would have been deposited prior to the deposition of the iridium. As noted above, the *Pinna* community strongly resembles late Maastrichtian communities on the Gulf Coast. The development of this fauna may have coincided with a warming trend in the Late Cretaceous. Olsson et al. (2002) documented an increase in $\delta^{18}O$ and a poleward shift in the distribution of subtropical foraminifera, implying an increase in sea surface temperatures of 4–5°C. They attributed this warming trend to increased release of greenhouse gases associated with Deccan volcanism. Based on sedimentation rates in the Bass River Borehole, they estimated that this warming period lasted from 500,000 to18,000 years before the end of the Cretaceous.

The *Pinna* community may have died before or at the moment of impact. It may have been ultimately buried in the immediate aftermath of the impact due to enhanced riverine discharge. Erosion of the top of the *Pinna* Layer and the subsequent deposition of the Burrowed Unit may have been associated wth events immediately following the impact. The few, fragmentary fossils in the Burrowed Unit suggest postmortem transport and breakage. In addition, the diversity of dinoflagellates in this unit is severely reduced, suggesting an impoverished flora.

Choosing between these two hypotheses requires further investigation of other elements to evaluate the probability of chemical remobilization. In addition, it is possible that analyses of carbon and oxygen isotopes may provide clues to the age of the *Pinna* Layer and the overlying part of the Hornerstown Formation. A marked decrease in carbon isotopes has been reported from just above the Cretaceous/Tertiary boundary at many sites, and has been attributed to unusually low biological productivity (Hsü and McKenzie, 1985) or changes in the structure of the ecosystem of the oceans following the impact (D'Hondt, 2005).

After the impact, the sea floor, in the area of what is now the Manasquan River Basin, experienced an extended period of reworking. Part of the *Pinna* Layer and most of the Burrowed Unit were eroded, producing a lag deposit of siderite nodules. A new depositional regime was established, marked by

a change in lithology. This period of erosion and reworking may have begun hundreds of years after the bolide impact and extended for hundreds of thousands of years afterward. The fossils in the basal Hornerstown Formation in the Manasquan River Basin indicate a hiatus of several hundred thousand years. At age-equivalent sites in northeastern Monmouth County, Landman et al. (2004b) estimated that this period may have lasted for approximately 100,000 years.

Two possibilities have been proposed to explain this period of erosion and reworking. Based on studies of sections at the Inversand Pit in Gloucester County, New Jersey, Gallagher (2002) attributed the erosion and reworking to a tsunami that immediately followed the impact. However, the outwash from a tsunami would presumably have produced a thick layer of debris from the land mixed with eroded chunks of the sea floor. Such deposits are absent in the section in the Manasquan River Basin. In addition, at sites where tsunami deposits are present, e.g., along the Brazos River, Texas, the iridium anomaly occurs stratigraphically above these deposits (Hansen et al., 1993a). In the Manasquan River Basin, in contrast, the iridium anomaly occurs approximately 20 cm below the erosional contact. Even if the iridium anomaly were originally located at the top of the *Pinna* Layer, it would still lie below the concentration of siderite nodules.

A more plausible explanation is that the erosion and reworking were due to a transgression in the early Danian. Olsson et al. (2002), based on their study of the Bass River Borehole, hypothesized a sea level rise of approximately 20 m over several hundred thousand years in the early Danian. This transgression may have produced the lag deposit of siderite nodules. Similar lag deposits have been documented at other K/T boundary sites and have been attributed to a Danian transgression (Smit et al., 1996; Machalski, 1998).

The presence of non-reworked echinoids, bivalves, gastropods, foraminifera, and crustaceans in the basal Hornerstown Formation points to the continuity of an early Danian community. However, the number of species and individuals is greatly reduced relative to the late Maastrichtian. Of the 16 species present in the basal Hornerstown Formation (excluding dinoflagellates and foraminifera), 12 of them are Cretaceous survivors. In contrast, *Ostrea pulaskensis* is a Danian species, and is recorded elsewhere from the Brazos River region, Texas (Hansen et al., 1993a, b), Braggs, Alabama (Bryan and Jones, 1989), and southern Illinois (Cope et al., 2005). It is relatively abundant in the Manasquan River Basin, suggesting an opportunistic species.

Comparison of the fauna in the *Pinna* Layer with that in the basal Hornerstown Formation allows us to evaluate the hypothesis of a decrease in the size of species above the K/T boundary. This hypothesis is known as the ''Lilliput Effect'' and argues that the fauna following a mass extinction is dwarfed (Bralower, 2006; Harries, 2006; Lockwood, 2006; MacLeod, 2006; Twitchett, 2006). Of the 12 species that persist into the basal Hornerstown Formation, only one of them, *Pycnodonte convexa*, shows a decrease in size, that is, the average size of a specimen in the basal Hornerstown Formation is smaller than one in the *Pinna* Layer. The average size of the other 11 species remains the same.

The larger-size species in the *Pinna* Layer, such as *Pinna laqueata*, do not extend into the basal Hornerstown Formation, possibly implying the differential extinction of larger species, or conversely, the differential survival of smaller species. In addition, *Ostrea pulaskensis*, which is the most abundant species in the basal Hornerstown Formation, is relatively small, approximately 1 cm in length, and may reflect post-extinction selection for small size.

Studies of the K/T extinction have also suggested that the post-impact marine ecosystem was degraded, with an associated change in trophic composition (D'Hondt, 2005). For example, Hansen et al. (1993b), based on their studies in the Brazos River region, Texas, reported that the Danian section in this area contained fewer species and individuals than the Maastrichtian section, and was dominated by deposit feeders rather than suspension feeders. In addition, Gallagher (2002: 297), on the basis of his investigations of the Inversand Pit in Gloucester County, New Jersey, described an assemblage approximately 2 m above the

Main Fossiliferous Layer consisting mainly of sponges, brachipods, and solitary corals. He interpreted this assemblage as representing "a resetting of the evolutionary clock in Danian marine ecosystems, which are dominated by faunas of Paleozoic aspect."

Analysis of the fauna in the Manasquan River Basin yields slightly different results, assuming that the fossils are equally well preserved on either side of the boundary. The fauna in the basal Hornerstown Formation immediately above the *Pinna* Layer is species poor and relatively sparse. Of the 74 species in the *Pinna* Layer, only 12 extend into the basal Hornerstown Formation, indicating a survival rate of only approximately 15%. The fauna largely consists of molluscs, not brachipods or sponges. It is dominated by *Ostrea pulaskensis* and *Pycnodonte convexa.* In addition, there is little change in trophic composition; the bivalves consist exclusively of suspension feeders, without any deposit feeders. These observations are more consistent with those of Heinberg (1999), who studied the change in bivalves across the K/T boundary at Stevns Klint, Denmark.

AMMONITE ECOLOGY

The ammonite fauna of the *Discoscaphites iris* Zone is present in New Jersey, Maryland, Mississippi, Missouri, Tennessee, and Texas. The principal species in common are *Discoscaphites iris*, *D. sphaeroidalis*, *D. gulosus*, *Eubaculites carinatus*, and *E. latecarinatus*. In addition, one species of *Sphenodiscus* and one species of *Pachydiscus* are present at several sites. Kennedy et al. (2001) also reported a specimen of *Glyptoxoceras* cf. *G. rugatum* (Forbes, 1846) from the upper part of the Corsicana Formation in Texas.

This fauna is part of a diverse, neashore community that extended along the Gulf and Atlantic Coastal Plains during the late Maastrichtian. Although this community has not previously been recorded from New Jersey, it is very similar to the late Maastrichtian community described by Hansen et al. (1993a, b) from Texas, which is dominated by suspension feeding bivalves. Sohl (1964: 160–164) remarked on the similarity of the gastropod fauna throughout this area during the Campanian to Maastrichtian. He wrote "we must of necessity include New Jersey within the same faunal province as that of the gulf coast" and noted that "the similarity to the gulf coast fauna would no doubt increase if better preserved material were to be found in New Jersey." (See Koch and Sohl, 1983, for a more expanded treatment of preservational bias and its effect on biogeographic inferences in this region.)

The Gulf and Atlantic Coastal Plains represented a subtropical to temperate fauna. The fauna became more tropical toward the south and more temperate toward the north. Because peninsular Florida was submerged at the time, there must have been relatively unobstructed migration along the entire coast.

The abundance and composition of the ammonite fauna in the Manasquan River Basin is slightly different from that of age-equivalent sites elsewhere in New Jersey. *Discoscaphites iris* is very abundant in the Manasquan River Basin—altogether we have collected nearly 300 specimens of this species from the upper part of the Tinton Formation. In contrast, we have collected approximately 70 specimens of this species in the upper part of the New Egypt Formation at Parkers Creek, northeastern Monmouth County (Landman et al., 2004b), and six specimens in approximately the same stratigraphic interval in the Crosswicks Creek Basin, southwestern Monmouth County (Landman et al., in prep.). This species has not been recovered at all from the Inversand Pit at Sewell, Gloucester County (Kennedy and Cobban, 1996).

On the other hand, there is only a single septate pachydiscid from the Manasquan River Basin whereas Kennedy and Cobban (1996) reported 14 specimens of this species at Sewell. In addition, nautilids are rare and fragmentary in the Manasquan River Basin whereas they are more abundant and better preserved at Sewell and Parkers Creek.

The noncephalopod molluscan fauna also shows differences between the Manasquan River Basin and other age-equivalent sites in New Jersey. There are 29 species of bivalves and 24 species of gastropods in the Manasquan River Basin whereas Landman et al. (2004b) reported only 8 species of bivalves and 5 species of gastropods in age-equivalent strata at Parkers Creek.

These faunal differences are probably related to differences in the environment, namely water depth, proximity to shore, and abundance of nutrients. As stated, the depth at the Manasquan River Basin was approximately 20 m. This depth estimate is consistent with that of living species of *Pinna*, as described by Turner and Rosewater (1958) and Chinzei et al. (1982). It is also consistent with the inferred habitat depths of scaphites and sphenodiscids (Hewitt, 1996; Ifrim et al., 2005). In contrast, Landman et al. (2004b) estimated a depth of approximately 30–50 m at other age-equivalent sites in New Jersey. It is possible that *Discoscaphites iris* favored the more shallow water environment of the Manasquan River Basin whereas pachydiscids and nautilids preferred slightly deeper, more offshore settings.

One of the most characteristic features of the *Pinna* Layer is the presence of monospecific clusters of scaphites and baculites consisting of up to 30 specimens or more. Some of these specimens are broken whereas others are intact. Sometimes a cluster is composed exclusively of adults whereas other times, it is composed mainly of juveniles.

We dissected one scaphite cluster approximately 25 cm in diameter (fig. 6). There is no lithologic boundary between it and the surrounding matrix. The bottom of the cluster is flat and coincides with the bottom of the *Pinna* Layer. The cluster does not form a concretion nor does it rest in a depression or burrow. Specimens are concentrated at the center of the cluster (the core), which is approximately 11 cm $\times$ 8.5 cm $\times$ 6 cm. The core was broken into pieces to determine the number of specimens inside. Seven small satellite clusters, each composed of three to six specimens, surround the core. The satellite clusters were collected in separate chunks of matrix.

There are a total of 35 specimens in the cluster, including seven impressions. This number is probably an underestimate because additional specimens may be embedded in the core, which are not visible on the outside. All of the specimens are *Discoscaphites iris* (although five specimens are too small or incomplete for species identification). The 35 specimens consist of 30 adults, 3 pieces of phragmocones, and 2 juveniles. There are 13 microconchs and 1 macroconch. The rest of the specimens are too fragmentary to determine the dimorph.

The distribution of specimens in the cluster is visible on the outside of the core. Specimens are oriented at random, including nearly horizontal, nearly vertical, and everything in between. Most specimens are partly touching, either lying almost on top of each other or vertically next to each other. The rest of the space between specimens is filled with matrix. The single macroconch is in a satellite cluster next to a specimen whose dimorph is indeterminate.

Most of the specimens are complete, consisting of both the body chamber and phragmocone. The body chambers are usually intact, with even the apertures preserved, whereas the phragmocones are usually crushed, implying that they were still hollow at the time of burial. There is no evidence of predatory damage, as opposed to postmortem breakage [for a discussion of predatory damage, see Keupp (2006)].

This cluster is biological in origin and could not have been produced by hydraulic means. There are several lines of evidence in support of this interpretation:

(1) The fauna consists almost exclusively of *Discoscaphites iris*. The only other specimens include a small scallop in the core and parts of a baculite and oyster in one of the satellite pieces. (There is also the impression of a small juvenile scaphite in the aperture of one of the adults.) Otherwise, the cluster is monospecific.

(2) The specimens of *Discoscaphites iris* in the cluster show less morphological variation than that of the total sample of this species in the *Pinna* Layer. For example, the maximum length of the microconchs in the cluster (n = 5 measurable specimens) ranges from 31–34 mm. In contrast, the maximum length of a larger sample of microconchs in the *Pinna* Layer (n = 12 measurable specimens) ranges from 29–41 mm. In addition, all of the specimens in the cluster are very similar in morphology. They are characterized by a robust body chamber with a nearly subquadrate whorl section, four rows of fairly prominent tubercles, and coarse ribs at the aperture. This implies that these animals were rapidly buried after death, preserving a snapshot of a living community.

(3) Most of the scaphites are adults, and of those whose dimorph can be determined, nearly all

of them are microconchs. Scaphite microconchs are generally interpreted as males (Davis et al., 1996). In many modern coleoids, males die soon after mating and their bodies accumulate on the sea floor (Boyle and Rodhouse, 2005). Thus, this cluster could represent the result of postmating fatality, if scaphites followed a behavioral pattern similar to that of many modern coleoids.

After the scaphites accumulated on the sea floor, the body chambers and the spaces between specimens were filled in with sediment. A few, small extraneous shells were also swept into the mix. This implies sufficient current velocity to bury the cluster, but not enough to redistribute the scaphites. In addition, the scaphites must have been buried rapidly because the prhragmocones are crushed, implying that they were still hollow at the time of burial.

Other clusters in the *Pinna* Layer contain scaphites and sea urchins. One such cluster contains nine specimens of *Discoscaphites iris* (eight microconchs and one macroconch) plus several fragments, two large specimens of *Hemiaster dalli*, and a small fragment of *Pinna laqueata*. It is possible that this cluster represents a feeding association in which the urchins were feeding on scaphites that had recently died after mating.

Scaphite clusters have been reported elsewhere from the late Maastrichtian of New Jersey. Landman et al. (2004b) described a large cluster from the top of the New Egypt Formation at Parkers Creek, northeastern Monmouth County. This cluster consists exclusively of *Discoscaphites iris*. There are 67 specimens, many of which are fragments, representing approximately 40 adults. The number of microconchs is approximately equal to that of macroconchs. The presence of *D. iris* to the exclusion of all other species suggests that this accumulation is also biological in origin. The fact that both dimorphs are equally abundant in the cluster argues against postmating fatality of males as the likely cause. However, in some species of modern coleoids, spawning follows mating in rapid succession, with both males and females dying immediately thereafter, and accumulating on the sea floor (Norman, 2000).

Assuming that these accumulations are, in fact, due to scaphite behavior, it provides a clue to many of the scaphite accumulations described elsewhere, for example, in the Upper Cretaceous Fox Hills Formation of the U.S. Western Interior (Waage, 1964; Landman and Waage, 1993). The scaphites in this formation sometimes occur in a single layer of concretions consisting exclusively of the macroconchs or microconchs of a single species. However, it is unclear if the distribution of concretions in such a layer matches the original distribution of shells on the sea floor. One possibility is that the shells occurred everywhere on the sea floor but were only preserved at the sites of concretion formation. A second possibility is that the shells occurred in clusters, which later formed the nuclei of concretions. The evidence in the *Pinna* Layer suggests the second explanation—the scaphites originally accumulated as clusters, and subsequently developed into concretions.

AMMONITES AT THE CRETACEOUS/TERTIARY BOUNDARY

It is interesting to compare the ammonite record in the Manasquan River Basin with other ammonite-bearing K/T boundary sections from elsewhere (fig. 22, table 4). We summarize 10 of the best known sites. Such a comparison permits an assessment of the number of ammonite species alive at the end of the Cretaceous.

On the Atlantic Coastal Plain, the *Discoscaphites iris* Zone is present in Maryland and New Jersey. Landman et al. (2004a) described five species from the upper part of the Severn Formation in Anne Arundel County, Maryland: *D. iris*, *D.* cf. *D. iris*, *D.* cf. *D. minardi*, *Eubaculites carinatus*, and *E.* cf. *E. carinatus* (table 4). In New Jersey, Landman et al. (2004b) described eight species from the top of the New Egypt Formation in northeastern Monmouth County. The ammonites occur in the uppermost 20 cm of this unit, corresponding to the upper part of calcareous nannofossil zone CC26b, and as reworked material at the base of the overlying Hornerstown Formation. The ammonites consist of *D. iris*, *D. sphaer-*

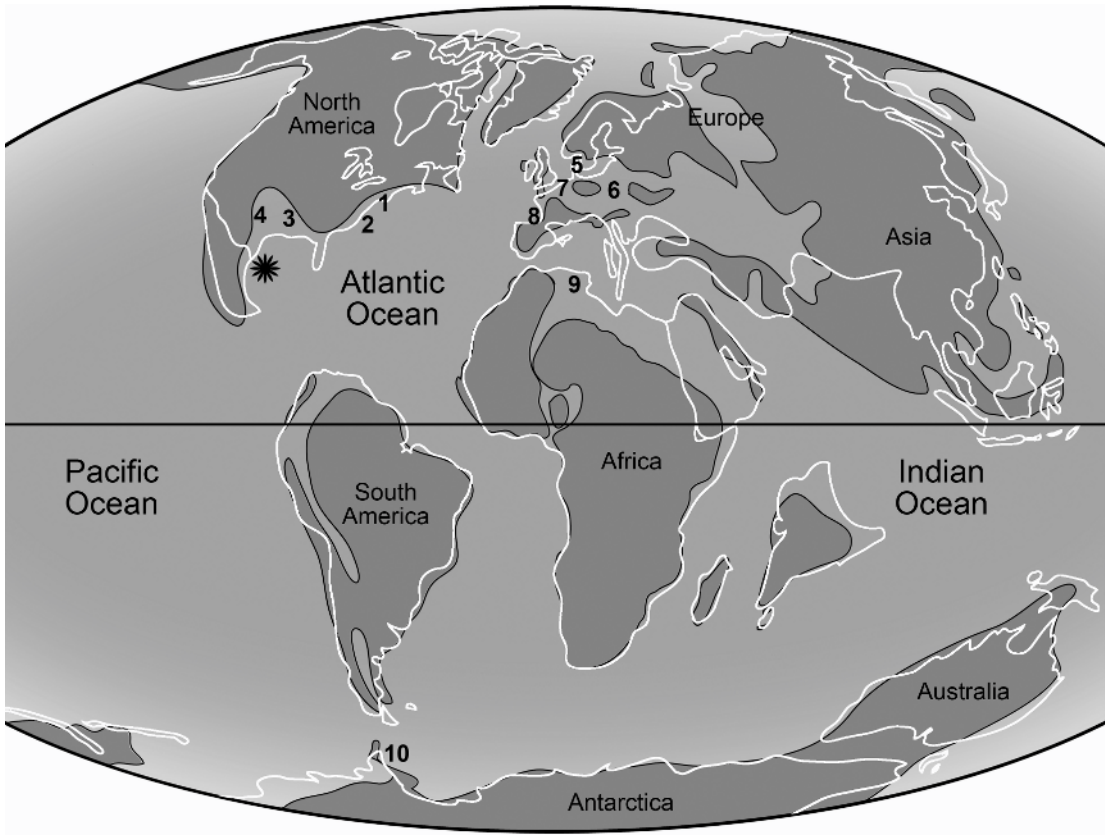

Fig. 22. Paleogeographic map at the Cretaceous/Tertiary boundary (after C.R. Scotese at http://www.scotese.com/K/t.htm). The white lines indicate the present configuration of the continents. The star marks the Chicxulub impact crater in the northern Yucatan Peninsula, Mexico (Arenillas et al., 2006). The numbers denote sites with ammonites preserved near or at the K/T boundary: 1 = New Jersey; 2 = Maryland; 3 = Mississippi, Tennessee, Missouri; 4 = Texas; 5 = Denmark; 6 = Poland; 7 = The Netherlands; 8 = Bay of Biscay, France, Spain; 9 = Tunisia; 10 = Antarctica (for references, see table 4).

oidalis (originally described as *D. iris*), *D. minardi*, *D. gulosus*, *E. carinatus*, *E. latecarinatus*, *Sphenodiscus pleurisepta* (Conrad, 1857), and *Sphenodiscus* sp. Fewer species are present in Gloucester County, New Jersey (Kennedy and Cobban, 1996; Kennedy et al., 1997), but include *Sphenodiscus lobatus* (Tuomey, 1856) and *Pachydiscus* (*Neodesmoceras*) *mokotibensis*. Nearly all of these species, with the addition of *D. jerseyensis*, occur at the top of the Tinton Formation and as reworked material at the base of the Hornerstown Formation in the Manasquan River Basin, central Monmouth County (this report).

On the Gulf Coast, Kennedy and Cobban (2000) described the ammonite species from the Owl Creek Formation in Tippah County, northeastern Mississippi (table 4). The Owl Creek Formation is unconformably overlain by the Paleocene Clayton Formation. There are seven ammonite species: *Sphenodiscus pleurisepta*, *Baculites* cf. *B. claviformis* Stephenson, 1941, *Baculites* cf. *B. undatus* Stephenson, 1941, *Eubaculites carinatus*, *Discoscaphites. iris*, *D. sphaeroidalis*, and *D.* cf. *D. conradi* (Morton, 1834). These species belong to the *Discoscaphites iris* Zone, but their stratigraphic ranges relative to the top of the Owl Creek Formation were not given. Stephenson (1955) reported four of these species, *E. carinatus*, *D. iris*, *D. sphaeroidalis* (originally described as *D.* sp.), and *S. pleurisepta* from the top of the Owl Creek Formation and as reworked material at the

base of the overlying Clayton Formation at Crowley's Ridge in Stoddard and Scott counties, southeastern Missouri.

Kennedy et al. (2001) described the ammonites from the upper Corsicana Formation along the Brazos River, Falls County, Texas (table 4). Hansen et al. (1987) interpreted the erosional surface at the top of this formation as the Cretaceous/Tertiary boundary, but this interpretation has been disputed by others. Kennedy et al. (2001) identified five ammonite species in the uppermost 11.5 m of the Corsicana Formation: *Eubaculites carinatus*, *Discoscaphites sphaeroidalis*, *D.* cf. *gulosus*, *Pachydiscus* (*P.*) *jacquoti jacquoti* Seunes, 1890, and *Glyptoxoceras* cf. *G. rugatum*. Two of these species, *E. carinatus* and *D.* cf. *D. gulosus*, extend into the uppermost 1 m of the formation. In addition, G. Keller (personal commun., 2005) reported a specimen of *D. iris* in a core from the upper part of the Corsicana Formation in the same general vicinity. Phosphatized fragments of scaphites and baculites occur as reworked material at the base of the overlying Kincaid Formation.

The ammonite record in Denmark has been extensively studied by Birkelund (1979, 1993), Kennedy (1993), and Machalski (2005). Ammonites occur in the upper Maastrichtian Grey Chalk, which was deposited in a shelf sea ranging from the euphotic zone to several hundred meters deep (Surlyk and Birkelund, 1977). At Kjølby Gård, two ammonite species, *Hoploscaphites constrictus* (Sowerby, 1817) and *Baculites vertebralis* Lamarck, 1801, extend to within 20 cm of the K/T boundary. A richer fauna is present at Stevns Klint, perhaps due to more extensive collecting. This section is complex, and it is possible that it contains a hiatus at the top of the Maastrichtian (Hansen, 1979; Hultberg, 1986; Hultberg and Malmgren, 1987; Surlyk and Håkansson, 1999; Rocchia et al., 2001). Most ammonites occur in a hardground at the top of the Grey Chalk, which was probably produced by early diagenetic submarine cementation (Hansen, 1990). The ammonite fauna consists of seven species dominated by adults and juveniles of *H. constrictus*, including *H. constrictus* var. *johnjagti* Machalski, 2005b, and *B. vertebralis*. Embryonic shells of *Baculites* and *Hoploscaphites* are very abundant in the hardground. Specimens of *H. constrictus* and *B. vertebralis* also occasionally occur in the overlying Cerithium Limestone (Birkelund, 1979, 1993; Surlyk and Nielsen, 1999; Machalski, 2002). These specimens have generally been interpreted as reworked material, but Machalski and Heinberg (2005) argued that some of them may represent early Danian survivors.

The K/T boundary is exposed in Nasiłów, Poland (Machalski and Walaszczyk, 1987, 1988; Kennedy, 1993; Machalski, 2005a). The ammonites occur in a hard limestone layer at the top of the Kazimierz Opoka. This unit passes into a thin layer of soft opoka, which is penetrated by burrows filled with glauconite derived from the overlying Danian unit (Siwak). According to Machalski (2005a), this section contains a hiatus of approximately 500,000 years representing parts of the uppermost Maastrichtian and the lowermost Danian. The ammonite fauna is dominated by *Baculites* spp. including *Baculites anceps* Lamarck, 1822, followed by *Hoploscaphites constrictus crassus* (Łopuski, 1911). The rest of the ammonite fauna consists mostly of *Menuites terminus* (Ward and Kennedy, 1993), *Pachydiscus* (*P.*) *jacquoti jacquoti*, and *Sphenodiscus binckhorsti* Böhm, 1898. The section at Mełgiew, Poland, is more complete than that at Nasiłów with a hiatus of only a few thousand years at the K/T boundary (Machalski, 2005a). The ammonites include *Baculites* spp. and *H. constrictus johnjagti*.

In the Maastricht region, the Netherlands, eight species of ammonites extend into the top of the upper Maastrichtian Meerssen Member of the Maastricht Formation (Jagt and Kennedy, 1989; Jagt, 1996, 2002; Jagt et al., 2006; Machalski, 2005b): *Menuites terminus*, *Sphenodiscus binckhorsti*, *Phylloptychoceras* cf. *P. sipho* (Forbes, 1846), *Baculites vertebralis*, *B. anceps*, *Eubaculites carinatus*, *Hopoloscaphites constrictus johnjagti*, and *Hoploscaphites* ex. gr. *waagei-angmartussutensis*. This part of the formation is interpreted as having been deposited on a shallow carbonate platform. Jagt et al. (2003) also reported several scaphites and baculites in Unit IVf-7 of the Meerssen Member above the Berg en Teblijt Horizon at the Guelhem-

TABLE 4
Ammonite Species at or near the Cretaceous/Tertiary Boundary[a]

Species	NJ	MD	MS, TE, MO	TX	DNK	POL	NLD	BISCAY	TUN	ATA
Anagaudryceras politissimum? (Kossmat, 1895)	.	.	.	.	.	.	.	X	.	.
Baculites anceps Lamarck, 1822	.	.	.	.	.	X	X	.	.	.
Baculites cf. *anceps* Lamarck, 1822	.	.	.	.	.	.	.	.	.	.
Baculites cf. *B. claviformis* Stephenson, 1941	.	.	X	.	.	.	.	.	.	.
Baculites cf. *B. undatus* Stephenson, 1941	.	.	X	.	.	.	.	.	.	.
"*Baculites*" *paradoxus* Pervinquière, 1907	.	.	.	.	.	.	.	.	X	.
Baculites vertebralis Lamarck, 1801	.	.	.	.	X	.	X	.	.	.
Baculites sp. of Goolaerts et al., 2004	.	.	.	.	.	.	.	.	X	.
Baculites sp. (nov?) of Jagt et al., 2003	.	.	.	.	.	.	X	.	.	.
Baculites spp. of Machalski, 2005a	.	.	.	.	.	X	.	.	.	.
Brahmaites (*Brahmaites*) *brahma* (Forbes, 1846)	.	.	.	.	.	.	.	X	X	.
Desmoceratac eae spp. 1–5 of Goolaerts et al., 2004	.	.	.	.	.	.	.	.	X	.
Desmoceratac eae indet. of Goolaerts et al., 2004	.	.	.	.	.	.	.	.	X	.
Diplomoceras cylindraceum (DeFrance, 1816)	.	.	.	.	X	.	.	X	X	.
Diplomoceras maximum Olivero and Zinsmeister, 1989	.	.	.	.	.	.	.	.	.	X
Discoscaphites cf. *D. conradi* (Morton, 1834)	.	.	X	.	.	.	.	.	.	.
Discoscaphites gulosus (Morton, 1834)	X	.	.	.	.	.	.	.	.	.
Discoscaphites cf. *D. gulosus* (Morton, 1834)	.	.	.	X	.	.	.	.	.	.
Discoscaphites iris (Conrad, 1858)	X	X	X	.	.	.	.	.	.	.
Discoscaphites cf. *D. iris* (Conrad, 1858)	.	X	.	.	.	.	.	.	.	.
Discoscaphites jerseyensis, n.sp.	X	.	.	.	.	.	.	.	.	.
Discoscaphites minardi Landman et al., 2004a	X	.	.	.	.	.	.	.	.	.
Discoscaphites cf. *D. minardi* Landman et al., 2004a	.	X	.	.	.	.	.	.	.	.
Discoscaphites sphaeroidalis Kennedy and Cobban, 2000	X	.	X	X	.	.	.	.	.	.
Discoscaphites spp. of Landman et al., 2004b	X	.	.	.	.	.	.	.	.	.
Eubaculites carinatus (Morton, 1834)	X	X	X	X	.	.	X	.	.	.
Eubaculites cf. *E. carinatus* (Morton, 1834)	.	X	.	.	.	.	.	.	.	.
Eubaculites latecarinatus (Brunnschweiler, 1966)	X	.	.	.	.	.	.	.	.	.
Glyptoxoceras cf. *G. rugatum* (Forbes, 1846)	.	.	.	X	.	.	.	.	.	.
Hauericeras cf. *H. rembda* (Forbes, 1846)	.	.	.	.	.	.	.	.	X	.
Hoploscaphites constrictus (Sowerby, 1817) *crassus* (Łopuski, 1911)	.	.	.	.	.	X	.	.	.	.
Hoploscaphites constrictus (Sowerby, 1817) *johnjagti* Machalski, 2005b	.	.	.	.	X[b]	X	X	.	.	.
Hoploscaphites constrictus sp. ex gr. *waagei-angmartussutensis* of Machalski, 2005b	.	.	.	.	.	.	X	.	.	.

TABLE 4
(Continued)

Species	NJ	MD	MS, TE, MO	TX	DNK	POL	NLD	BISCAY	TUN	ATA
Hypophylloceras (Neophylloceras) velledaeforme (Schlüter, 1872)	.	.	.	.	X	.	.	.	.	.
Indoscaphites cunliffei (Forbes, 1846)	.	.	.	.	.	.	.	.	X	.
Indoscaphites pavana (Forbes, 1846)	.	.	.	.	.	.	.	.	X	.
Indoscaphites indet. of Goolaerts et al., 2004	.	.	.	.	.	.	.	.	X	.
Kitchinites (K.) laurae Macellari, 1986	.	.	.	.	.	.	.	.	.	X
Maorites densicostatus (Kilian and Reboul, 1909)	.	.	.	.	.	.	.	.	.	X
Menuites sp. of Goolaerts et al., 2004	.	.	.	.	.	.	.	.	X	.
Menuites terminus (Ward and Kennedy, 1993)	.	.	.	.	X	X	X	X	.	.
Pachydiscus (P.) armenicus Atabekian and Akopian, 1969	.	.	.	.	.	.	.	X	.	.
Pachydiscus (P.) jacquoti jacquoti Seunes, 1890	.	.	.	X	.	X	.	X	.	.
Pachydiscus (Neodesmoceras) mokotibensis Collignon, 1952	X	.	.	.	.	.	.	.	.	.
Phylloceras (Neophylloceras) ramosum (Meek, 1857)	.	.	.	.	.	.	.	X	.	.
Phylloptychoceras (P.) sp. of Machalski, 2005a	.	.	.	.	X	.	.	.	.	.
Phylloptychoceras cf. *P. sipho* (Forbes, 1846)	.	.	.	.	.	.	X	.	.	.
Pseudokossmaticeras duereri (Redtenbacher, 1873)	.	.	.	.	.	.	.	X	.	.
Pseudophyllites indra (Forbes, 1846)	.	.	.	.	.	.	.	X	.	.
Pseudophyllites loryi (Kilian and Reboul, 1909)	.	.	.	.	.	.	.	.	.	X
Pseudophyllites spp. 1, 2 of Goolaerts et al., 2004	.	.	.	.	.	.	.	.	X	.
Saghalinites, n.sp. of Birkelund, 1993	.	.	.	.	X	.	.	.	.	.
Saghalinites sp. of Goolaerts et al., 2004	.	.	.	.	.	.	.	.	X	.
Sphenodiscus binckhorsti Böhm, 1898	.	.	.	.	.	X	X	.	.	.
Sphenodiscus lobatus (Tuomey, 1856)	X	.	.	.	.	.	.	.	.	.
Sphenodiscus pleurisepta (Conrad, 1857)	X	.	X	.	.	.	.	.	.	.
Sphenodiscus sp. of Landman et al., 2004b	X	.	.	.	.	.	.	.	.	.
Zelandites varuna (Forbes, 1846)	.	.	.	.	.	.	.	.	.	X
Zelandites sp. of Goolaerts et al., 2004	.	.	.	.	.	.	.	.	X	.
Zelandites sp. of Ward and Kennedy, 1993	.	.	.	.	.	.	.	X	.	.

[a]Source: New Jersey (NJ): Kennedy and Cobban, 1996; Kennedy et al., 2000; Landman et al., 2004b, this report; Maryland (MD): Landman et al., 2004a; Mississippi, Tennessee, Missouri (MS, TE, MO): Stephenson, 1955; Kennedy and Cobban, 2000; Texas (TX): Kennedy et al., 2001; Denmark (DNK): Birkelund, 1979, 1993; Kennedy, 1993; Machalski, 2005a; Machalski and Heinberg, 2005; Poland (POL): Machalski and Walaszczyk, 1987, 1988; Machalski, 2005a, 2005b; Kennedy, 1993; Netherlands (NLD): Jagt and Kennedy, 1989; Jagt, 2002; Machalski, 2005b; Bay of Biscay, Spain, France (BISCAY): Wiedmann, 1987, 1988; Kennedy, 1993; Ward and Kennedy, 1993; Tunisia (TUN): Goolaerts et al., 2004; Antarctica (ATA): Macellari, 1986; Zinsmeister and Feldman, 1996; Zinsmeister, 1998.

[b]*Hoploscaphites constrictus* var. *johnjagti* is present at Stevns Klint, but the material from Kjølby Gård is too fragmentary to identify the variety (M. Machalski, personal commun. 2006).

merberg section near Limburg, southeast Netherlands. This horizon is generally interpreted as marking the K/T boundary. Because many of these baculites are preserved with their apertures intact, Jagt et al. (2003) suggested that they may represent early Danian survivors.

The Bay of Biscay region of southwestern France and northeastern Spain has received considerable attention because many K/T sections are apparently complete (Wiedmann, 1987, 1988; Kennedy, 1993; Ward and Kennedy, 1993; Rocchia et al., 2001). The strata consist of massive marls with rare turbidites deposited in an outer shelf setting with water depths of 100 to 500 m (Mathey, 1982). Ammonites are rare throughout most of the section. In Zumaya, Spain, Ward and Kennedy (1993) recorded a total of four specimens from approximately 1 m below the boundary, representing *Phylloceras* (*Neophylloceras*) *ramosum* (Meek, 1857), *Pachydiscus* (*P.*) *armenicus* Atabekian and Akopian, 1969, and *Zelandites*. In Sopelana, Spain, the highest ammonite (*Gaudryceras* sp.) occurs 10–15 m below the boundary. In Hendaye, France, a total of 11 species are present in the uppermost Maastrichtian *Menuites terminus* Zone. Four of these species extend to within 1 m of the boundary. In Bidart, France, six species are present in this same biostratigraphic zone. Rocchia et al. (2001) reported a poorly preserved ammonite from 5 cm below the boundary clay at this site containing Ni-rich spinel crystals and an anomalously high concentration of iridium. In total, there are approximately 30 specimens in the top 1 m in the combined sections at Zumaya, Hendaye, and Bidart representing nine or possibly ten species, although only one of these (the poorly preserved specimen mentioned above) is present in the top 10 cm of the section (table 4). Marshall and Ward (1996) used a statistical approach to evaluate the confidence intervals on the biostratigraphic ranges of these species. The hypothesis that all of these species actually persisted to the K/T boundary, even though there is no evidence of them at this level, could not be rejected according to their analysis.

Goolaerts et al. (2004) described the ammonites in the Cretaceous/Paleogene Global Stratotype Section and Point at El Kef, Tunisia. The ammonites occur in an interval between 7 and 2 m below the boundary, corresponding to the uppermost part of the *Abathomphalus mayaroensis* Zone. All of the ammonites were collected as surface float and may have moved slightly downslope. The ammonites consist of small septate inner whorls less than 20 mm in diameter, and, as a result, it is difficult to identify them to species or even genus level. Altogether, there are 19 taxa, of which 14 are in open nomenclature (table 4). The fauna is dominated by *Indoscaphites* (48% of the collection) and Desmoceratacea (27% of the collection). Goolaerts et al. (2004) speculated that the disappearance of the ammonites 2 m below the boundary was related to a local regressive event well before the end of the Cretaceous.

The section at Seymour Island in Antarctica has been studied by Macellari (1986, 1988), Zinsmeister and Feldman (1996), and Zinsmeister (1998). Macellari (1986) reported 15 ammonite species in the Maastrichtian part of the Lopez de Bertodano Formation. According to Zinsmeister (1998), five ammonite species are present 50 cm below the K/T boundary: *Maorites densicostatus* (Kilian and Reboul, 1909), *Diplomoceras maximum* Olivero and Zinsmeister, 1989, *Kitchinites (K.) laurae* Macellari, 1986, *Zelandites varuna* (Forbes, 1846), and *Pseudophyllites loryi* (Kilian and Reboul, 1909). Several studies have used a statistical approach to evaluate the biostratigraphic distribution of the ammonites in this section (Springer, 1990; Marshall, 1995; Wang and Marshall, 2004). The results of these studies are consistent with the possibility that most of these ammonite species extended to the K/T boundary.

The discussion of these 10 sections underscores the difficulties of compiling a list of ammonite species that lived at the end of the Cretaceous. [For additional data on late Maastrichtian ammonites from the Caucasus, West Kazakhstan, and the Crimea, see Kotetishvili (1999)]. In some areas, ammonites extend to the K/T boundary but the section is marked by a hiatus (e.g., Poland), and the amount of rock/time missing is difficult to determine. In other areas, the sections are reasonably complete but the ammonites disappear below the boundary

(e.g., El Kef), either because they did not live there or because they lived there but were not preserved at the site or because no one has yet been lucky enough to find them. On the other hand, statistical studies of the biostratigraphic ranges of the ammonites in some of these sections have demonstrated that the observed ranges tend to underestimate the actual ranges (Marshall, 1995; Wang and Marshall, 2004). These results suggest that the ammonite records even in sections in which some of the ammonites do not extend to the boundary still constitute a reasonable estimate of the number of species living at the end of the Maastrichtian.

With these caveats in mind, a tally of the species in these 10 sections reveals that a total of approximately 30 species were alive at the K/T boundary at various places on the planet (i.e., North America, Europe, North Africa, and Antarctica). [This figure is slightly higher than that reported by Kiessling and Claeys (2001) for the latest Maastrictian.] If we also include all of the species in open nomenclature, the number almost doubles. Studies in the Netherlands and Denmark, as well as our own in New Jersey, even suggest that some species may have survived into the early Danian.

The species at the end of the Maastrichtian represent all four suborders of post-Triassic ammonites. From an ecological perspective, they include relatively efficient swimmers, such as *Pachydiscus*, which may have actively hunted for prey, to more sluggish swimmers such as *Discoscaphites*, which may have passively fed on plankton. The worldwide disappearance of these species in a relatively short interval of time points toward a global catastrophe, i.e., the bolide impact and its aftermath.

SYSTEMATIC PALEONTOLOGY

Conventions

The cephalopods described in this paper are reposited in the Academy of Natural Sciences of Philadelphia (ANSP); the American Museum of Natural History (AMNH); the Monmouth Amateur Paleontologist's Society (MAPS), Long Branch, New Jersey; and the U.S. National Museum (USNM). Dimensions of the specimens are expressed in millimeters. Measurements of the nautilids, baculites, and scaphites are described in Landman et al. (2004b: fig. 16). Note that the formula to calculate the apical angle of baculites is misstated in that publication. The coefficient "2" is unnecessary (the values listed in the accompanying tables are correct). Of course, this formula does not take into account changes in the curvature of the shell during ontogeny (see Tsujino et al., 2003).

All specimens were photographed in life position (with the aperture near the bottom) except for the baculites. Arrows on the photos indicate the base of the body chamber, where visible. Suture terminology is that of Wedekind (1916), as reviewed by Kullmann and Wiedmann (1970).

CLASS CEPHALOPODA CUVIER, 1797
SUBCLASS NAUTILOIDEA AGASSIZ, 1847
ORDER NAUTILIDA AGASSIZ, 1847
SUPERFAMILY NAUTILITACEAE DE BLAINVILLE, 1825
FAMILY EUTREPHOCERATIDAE MILLER, 1951

Genus *Eutrephoceras* Hyatt, 1894

Type Species: *Nautilus Dekayi* Morton, 1834: 291, pl. 8, fig. 4, by original designation by Hyatt, 1894: 555.

Eutrephoceras dekayi (Morton, 1834)
figure 23

Nautilus Dekayi Morton, 1834: 291, pl. 8, fig. 4.
Nautilus Dekayi Morton. Whitfield, 1892: 243, pl. 37, figs. 1–6; pl. 38, figs. 1–4.
Eutrephoceras Dekayi. Hyatt, 1894: 556, pl. 13, figs. 4–8; pl. 14, fig. 1.
Eutrephoceras dekayi (Morton). Gardner, 1916: 372, pl. 13, fig. 9.
Eutrephoceras dekayi (Morton). Miller and Garner, 1962: 102, figs. 1, 2; pl. 65, figs. 1–6; pl. 66, figs. 1, 2; pl. 67, figs. 1–9 (with complete synonymy).
Eutrephoceras dekayi (Morton, 1834). Landman et al., 2004b: 41, figs. 17–21.

Type: The holotype ANSP 19484 is the original of Morton, 1834, pl. 8, fig. 4, from the "marls of Monmouth and Burlington counties, New Jersey," by subsequent designation by Whitfield (1892: 243, pl. 37, figs. 2, 3). See Landman et al. (2004b) for a more complete description of the holotype.

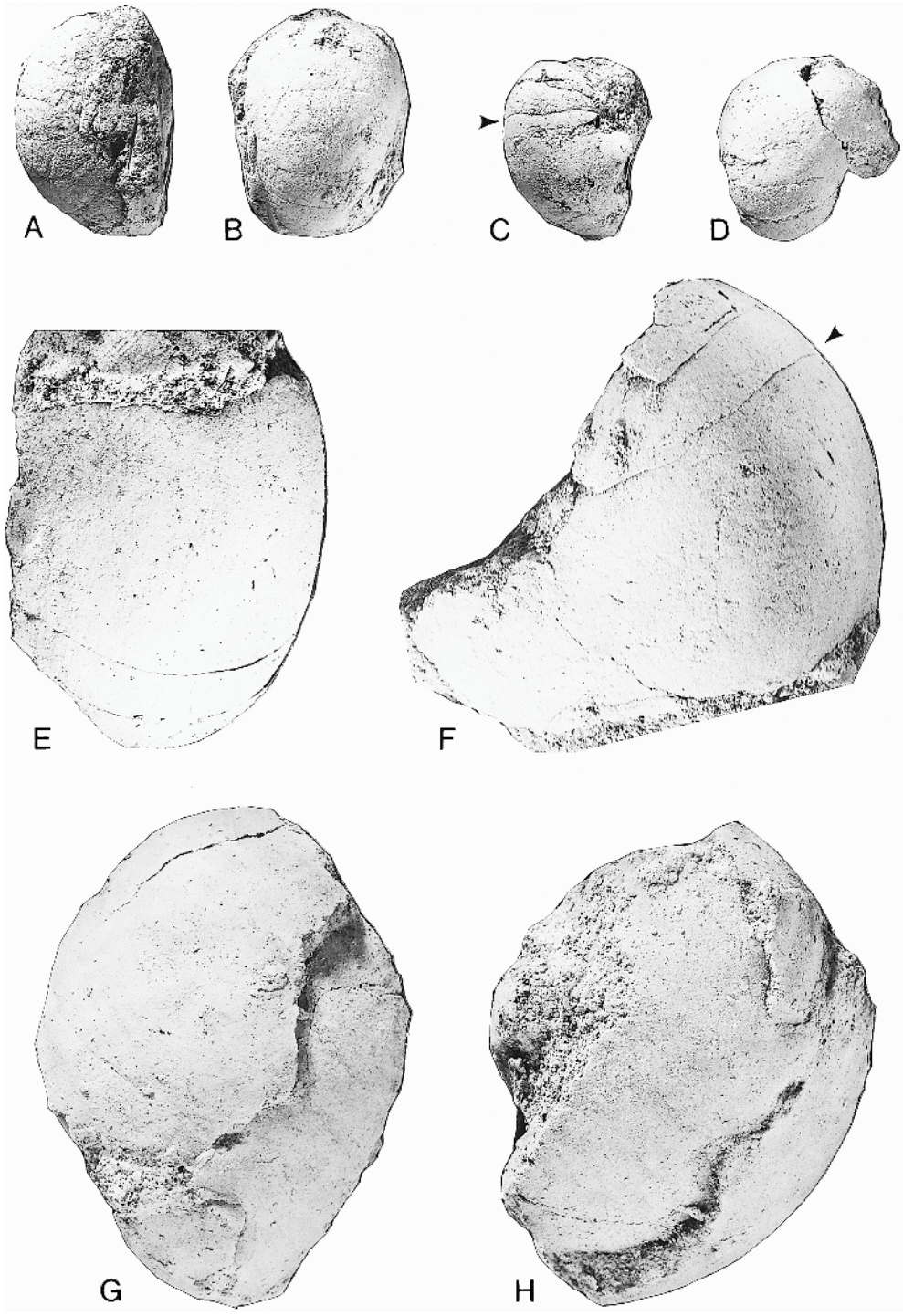

Fig. 23. *Eutrephoceras dekayi* (Morton, 1834), *Pinna* Layer, Tinton Formation, Manasquan River Basin, Monmouth County, New Jersey. **A, B.** MAPS A2012j1. **A.** Right lateral; **B.** ventral. **C, D.** MAPS A2012j2. **C.** Right lateral; **D.** ventral. **E, F.** MAPS A2012j4. **E.** Ventral; **F.** left lateral. **G, H.** AMNH 51295. **G.** Ventral; **H.** left lateral. All figures ×1.

MATERIAL: Seven specimens: MAPS A2012j1 and A2012j2 from the top of the Tinton formation just below the *Pinna* Layer at AMNH loc. 3335 and MAPS A2012j3–5, and AMNH 51295 and 51296 from the *Pinna* Layer at AMNH loc. 3335.

DESCRIPTION: All of the specimens are fragmentary internal molds exhibiting the depressed whorl section characteristic of this species. The smallest specimen (MAPS A2012j5) is a piece of a body chamber with a diameter of approximately 10 mm (not illustrated). AMNH 51296 is a broken phragmocone with a diameter of 16.1 mm (not illustrated). MAPS A2012j1 is a broken phragmocone with a diamter of 33.2 mm (fig. 23A,B). MAPS A2012j2 is a juvenile 25.6 mm in diameter, retaining part of the phragmocone and body chamber (fig. 23C,D). There are three larger specimens, all of which are incomplete. MAPS A2012j3 is a single chamber approximately 56.8 mm wide (not illustrated). MAPS A2012j4 is a fragment of a large specimen, with part of the phragmocone and body chamber preserved (fig. 23E,F). AMNH 51295 is a crushed piece of a large body chamber (fig. 23G,H).

DISCUSSION: These specimens represent a range of ontogenetic stages. The smallest specimen (MAPS A2012j5) is probably a newly hatched individual. Landman et al. (1983) demonstrated that the hatching size of this species is approximately 9 mm, based on a study of material from the U.S. Western Interior. On the other end of the spectrum, MAPS A2012j3 and A2012j4 and AMNH 51293 probably represent parts of adults.

The presence of a wide range of ontogenetic stages suggests that these animals lived at or close to this site, although some specimens may have drifted in from elsewhere after death. However, the nautilids in the Manasquan River Basin are rarer and more fragmentary than those from age-equivalent strata at Parkers Creek, northeastern Monmouth County, which may have represented a deeper water, more offshore environment. Landman et al. (2004b) described 27 specimens from the top of the New Egypt Formation and the base of the Hornerstown Formation at this site. The difference in abundance and state of preservation of the fossils between these two localities may indicate that the site at Parkers Creek was actually closer to the habitat of the living animals. Alternatively, it may simply reflect differences in taphonomic history.

OCCURRENCE: Top of the Tinton Formation, including the *Pinna* Layer, in the Manasquan River Basin, central Monmouth County, New Jersey. Elsewhere in New Jersey, this species occurs in the lower and upper parts of the Navesink Formation and the lower part of the New Egypt Formation in the Crosswicks Creek Basin, southwestern Monmouth County (Landman et al., in prep.); the Tinton Formation, near Tinton Falls, northeastern Monmouth County (Landman et al., 2004b); the top of the New Egypt Formation and as reworked material at the base of the Hornerstown Formation at Parkers Creek, northeastern Monmouth County (Landman et al., 2004b); the base of the Navesink Formation at Atlantic Highlands, northeastern Monmouth County; the Red Bank Sand, Monmouth County (Weller, 1907); and the Merchantville Formation, Burlington County [see Miller and Garner (1962: 109, 110) for additional localities in the Navesink Formation]. Outside of New Jersey, this species is widespread in Campanian to Maastrichtian strata on the Gulf and Atlantic Coastal Plains and in age-equivalent strata in the Western Interior.

ORDER AMMONOIDEA ZITTEL, 1884
SUBORDER AMMONITINA HYATT, 1889
SUPERFAMILY DESMOCERATACEAE ZITTEL, 1895
FAMILY PACHYDISCIDAE SPATH, 1922
Genus *Pachydiscus* Zittel, 1884

TYPE SPECIES: *Ammonites neubergicus* Hauer, 1858: 12, pl. 2, figs. 1–3; pl. 3, figs. 1,2, by the subsequent designation by de Grossouvre, 1894: 177.

Subgenus *Neodesmoceras* Matsumoto, 1947 (republished in English, 1951)

TYPE SPECIES: *Pachydiscus* (*Neodesmoceras*) *japonicus* Matsumoto, 1947: 39, by original designation.

Pachydiscus (*Neodesmoceras*) *mokotibensis* Collignon, 1952
figures 24, 25

Neodesmoceras mokotibense Collignon, 1952: 81, pl. 28, fig. 2.
Neodesmoceras mokotibense Collignon, 1955: 75, fig. 21; pl. 28, fig. 2.
Pachydiscus (*Neodesmoceras*) *mokotibensis* Collignon, 1971: 32, pl. 653, fig. 2410.
Pachydiscus (*Neodesmoceras*) *mokotibense* Collignon, 1952. Kennedy, 1986: 40, text-fig. 5.
Pachydiscus (*Neodesmoceras*) *mokotibensis* Collignon, 1952. Kennedy and Cobban, 1996: 799, figs. 2.7–2.12, 2.15–2.18.
Pachydiscus (*Neodesmoceras*) *mokotibense* Collignon, 1952. Kennedy and Klinger, 2006: 150, figs. 125–140.

TYPES: The holotype, by original designation, is that of Collignon (1952: pl. 28, fig. 2; 1955: pl. 28, fig. 2) from the Maastrichtian of Mokotibe, Madagascar. There are four paratypes from the same horizon and locality. The types are reposited in the collections of the École des Mines, now housed in the Université Claude Bernard, Lyon, France.

MATERIAL: One specimen (MAPS A2051a1) from the *Pinna* Layer, top of the Tinton Formation, AMNH loc. 3335, Manasquan River Basin, central Monmouth County, New Jersey.

DESCRIPTION: MAPS A2051a1 is a completely septate internal mold 90.7 mm in diameter missing approximately one-third of a whorl (fig. 24). The whorl cross section is compressed ovoid with a ratio of whorl width to height of 0.76 near the adoral end of the fragment. Coiling is involute. The umbilical wall is broadly rounded and the umbilical shoulder is narrowly rounded. The flanks are nearly flat and slightly convergent, the ventrolateral shoulder is narrowly rounded, and the venter is broadly rounded. Ornament is preserved on the adoral one-third of the whorl. It consists of relatively broad prorsiradiate ribs that are concave on the umbilical shoulder, nearly straight on the inner and middle flanks, and slightly concave on the outer flanks. They cross the venter with a weak adoral projection; there are approximately 2 ribs/cm on the venter. The suture is very incised (fig. 25).

OCCURRENCE: *Pinna* Layer, top of the Tinton Formation, Manasquan River Basin, central Monmouth County. Elsewhere in New Jersey, this species occurs in the upper part of the New Egypt Formation and as reworked material at the base of the Hornerstown Formation, Gloucester County (Kennedy and Cobban, 1996). Outside of New Jersey, it occurs in the upper Maastrichtian of Madagascar (Collignon, 1952, 1955, 1971), KwaZulu-Natal (South Africa) (Kennedy and Klinger, 2006), and the Cotentin Peninsula, Manche, France (Kennedy, 1986).

SUPERFAMILY ACANTHOCERATACEAE DE GROSSOUVRE, 1894
FAMILY SPHENODISCIDAE HYATT, 1900
Genus *Sphenodiscus* Meek, 1871

TYPE SPECIES: *Ammonites lenticularis* Owen, 1852: 579 (*non* Young and Bird, 1828: 269, fig. 5), by original designation, = *Ammonites lobata* Tuomey, 1856: 168.

Sphenodiscus lobatus (Tuomey, 1856)
figures 26–28

Ammonites lenticularis Owen, 1852: 579, pl. 8, fig. 5.
Ammonites lobatus Tuomey, 1856: 168.
Sphenodiscus lobatus (Tuomey, 1856). Cobban and Kennedy, 1995: 12, figs. 6.2, 6.3, 8.4, 8.6–8.11, 12.18, 12.19, 16.16, 16.17 (with full synonymy).
Sphenodiscus lobatus (Tuomey, 1856). Kennedy and Cobban, 1996: 802, fig. 2.4–2.6, 2.13, 2.14, 2.19, 2.21.
Sphenodiscus lobatus (Tuomey, 1856). Kennedy et al., 1997: 4, figs. 3–8, 9A–I, 10.
Sphenodiscus lobatus (Tuomey, 1856). Landman et al., 2004a: 28, fig. 12.
Sphenodiscus lobatus (Tuomey, 1856). Landman et al., 2004b: 51, figs. 23–25.

TYPE: The holotype, from Noxubee County, Mississippi, is lost (*fide* Stephenson, 1941: 434).

MATERIAL: Two specimens: MAPS A2002g1 and A2002g2 from the *Pinna* Layer from the top of the Tinton Formation, AMNH loc. 3335, Manasquan River Basin, central Monmouth County, New Jersey.

DESCRIPTION: MAPS A2002g2 is a large internal mold consisting of one septate whorl and a fragment of the body chamber, both of which fit together (figs. 26, 27). The specimen is smooth without any ornament. The diameter of the septate piece is 151 mm. The

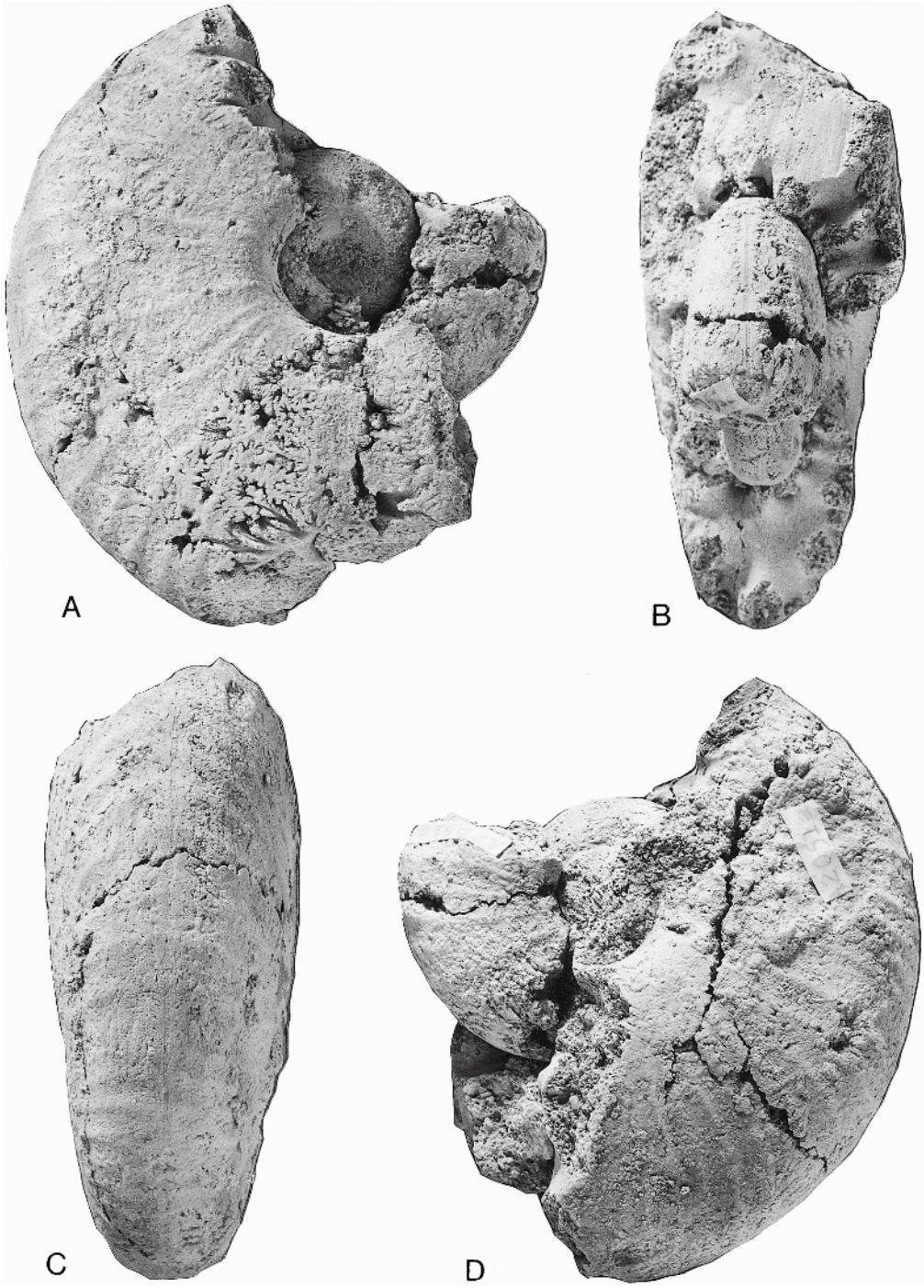

Fig. 24. *Pachydiscus* (*Neodesmoceras*) *mokotibensis* Collignon, 1952. MAPS A2051a1, *Pinna* Layer, Tinton Formation, Manasquan River Basin, central Monmouth County, New Jersey. **A.** Right lateral; **B.** apertural; **C.** ventral; **D.** left lateral. All figures ×1.

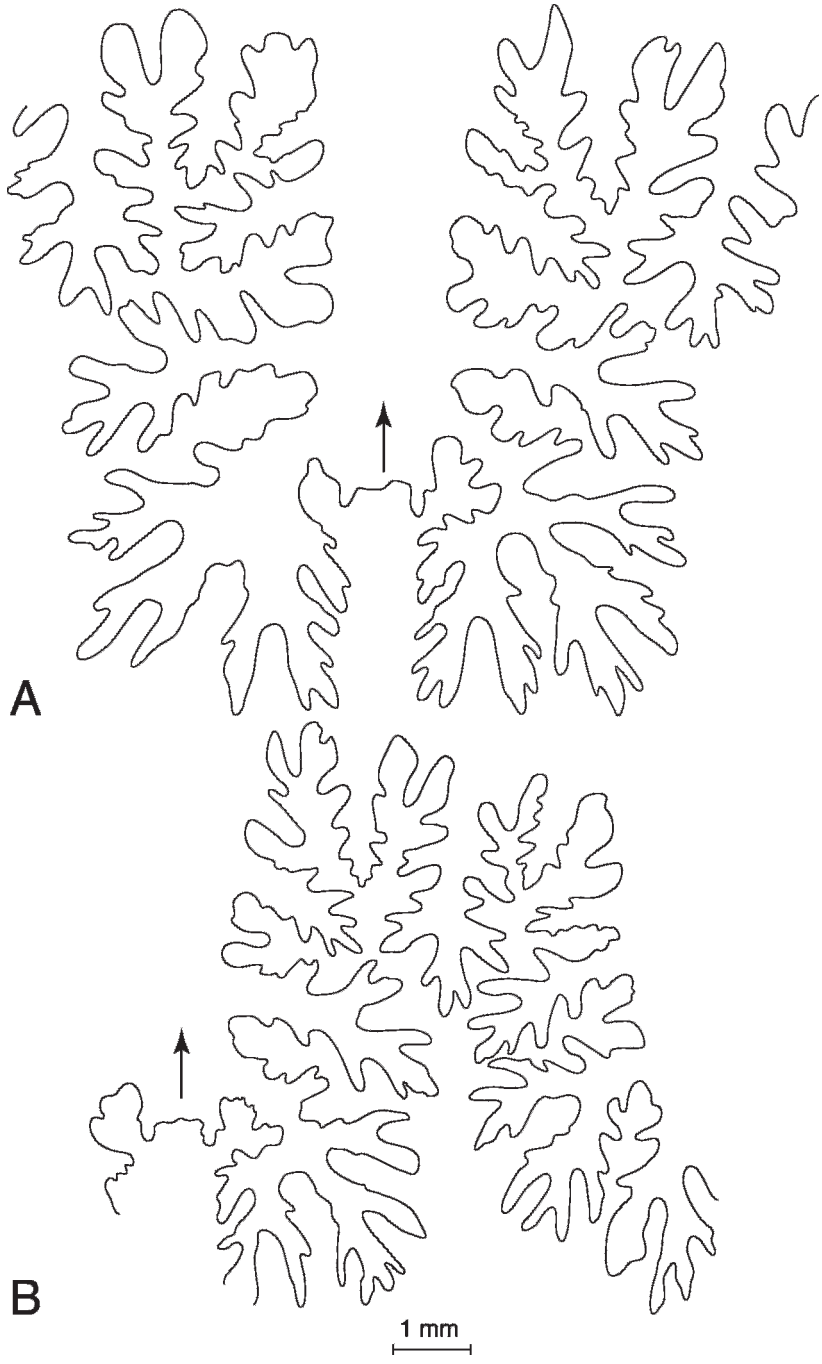

Fig. 25. *Pachydiscus (Neodesmoceras) mokotibensis* Collignon, 1952. MAPS A2051a1, *Pinna* Layer, Tinton Formation, Manasquan River Basin, central Monmouth County, New Jersey. **A, B.** Parts of consecutive sutures at a whorl height of approximately 13.5–15.0 mm.

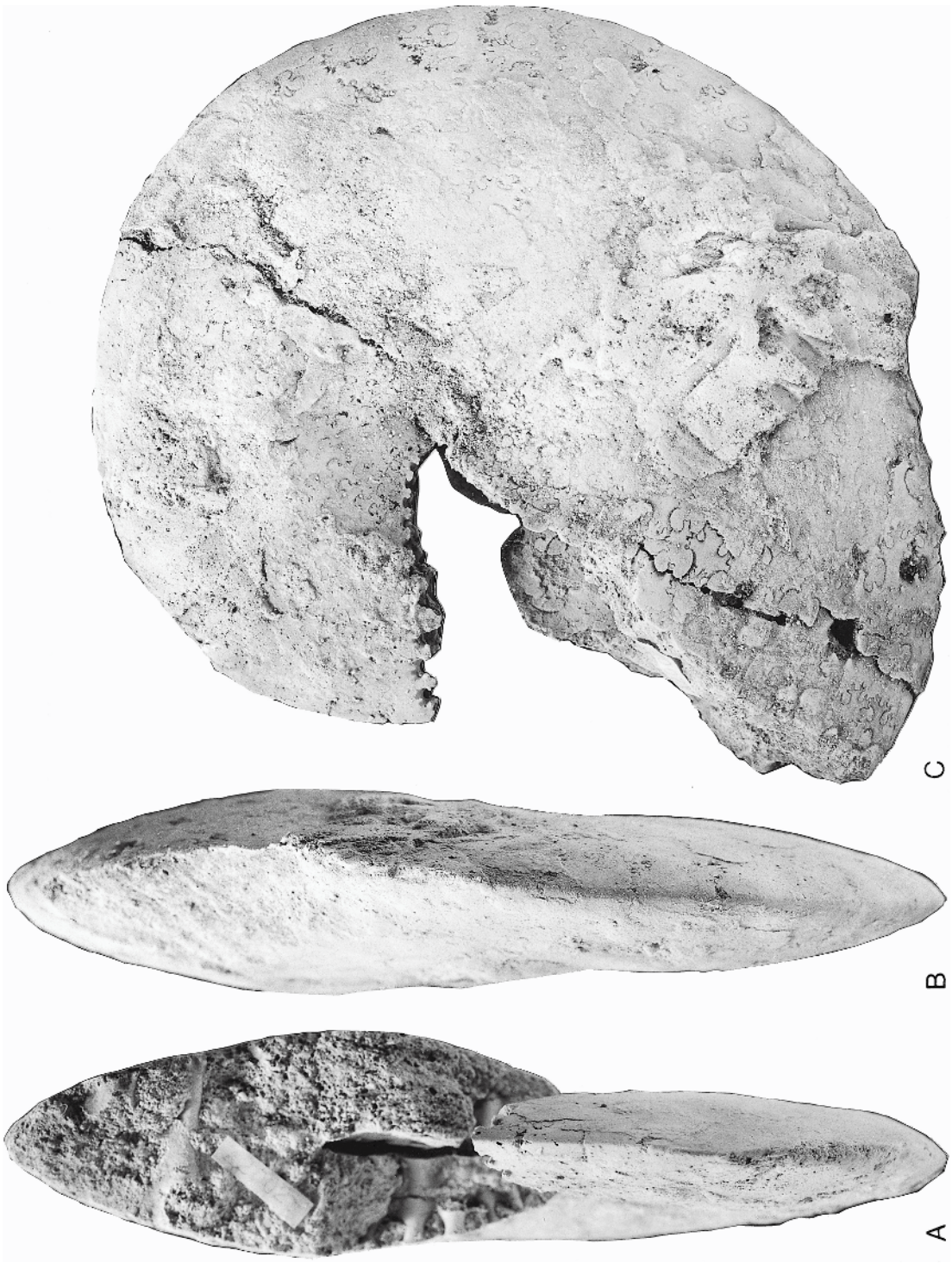

Fig. 26. *Sphenodiscus lobatus* (Toumey, 1856). MAPS A2002g2, *Pinna* Layer, Tinton Formation, Manasquan River Basin, Monmouth County, New Jersey. **A.** Apertural; B. ventral. **C.** left lateral. All figures ×1.

Fig. 27. *Sphenodiscus lobatus* (Toumey, 1856). MAPS A2002g2, *Pinna* Layer, Tinton Formation, Manasquan River Basin, Monmouth County, New Jersey. Right lateral with part of body chamber attached. Figure reduced × 0.71.

whorl width and height at the adoral end of the phragmocone are 34.8 and 87.3 mm, respectively; the ratio of whorl width to height is 0.40. The inner flanks are nearly flat and slightly divergent, the midflanks are broadly rounded and subparallel, and the outer flanks are nearly flat and converge to an acute venter.

The maximum whorl width of the piece of body chamber is approximately 62 mm. The venter is more rounded than it is on the phragmocone. There are several circles on the

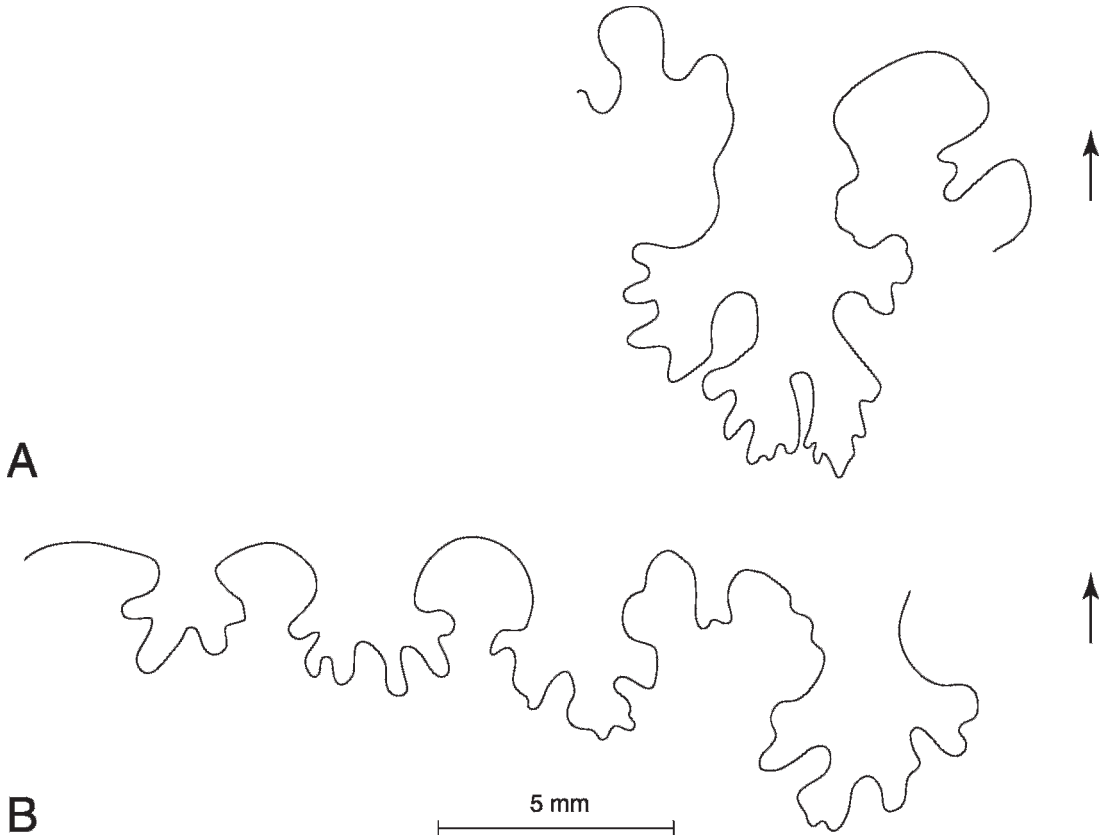

Fig. 28. *Sphenodiscus lobatus* (Toumey, 1856). MAPS A2002g2, *Pinna* Layer, Tinton Formation, Manasquan River Basin, Monmouth County, New Jersey. Parts of sutures at whorl heights of approximately 51 mm (**A**) and 63 mm (**B**), respectively.

left side (not illustrated), exposing the matrix below. These circles may represent the sites of limpet attachment or punctures produced by a mosasaur bite.

The suture has narrow-stemmed saddles with phylloidlike terminations (fig. 28).

OCCURRENCE: *Pinna* Layer, top of the Tinton Formation, Manasquan River Basin, central Monmouth County. This species also occurs in the Tinton Formation, near Tinton Falls, northeastern Monmouth County (Weller, 1907; Reeside, 1962; Gallagher, 1993; Landman et al., 2004b); the upper part of the Navesink Formation and the lower part of the New Egypt Formation in the Crosswicks Creek Basin, southwestern Monmouth County (Landman et al., in prep.); and at the Inversand Marl Pit, Gloucester County (Gallagher, 1993; Kennedy et al., 1995; Kennedy and Cobban, 1996). Specimens of *Sphenodiscus* occur in the top of the New Egypt Formation and as reworked material at the base of the Hornerstown Formation at Parkers Creek, northeastern Monmouth County, but they are too fragmentary for specific identification (Landman et al., 2004b). Elsewhere on the Gulf and Atlantic Coastal Plains, this species is known from the Corsicana Formation in northeast Texas (Kennedy and Cobban, 1993); the upper part of the Ripley Formation in Mississippi; the Prairie Bluff Chalk in Alabama and Mississippi (Cobban and Kennedy, 1995); the Providence Sand in the Chattahoochee River area, Alabama and Georgia; the upper part of the Peedee Formation in North Carolina (Landman et al., 2004a); and the Severn Formation in Prince Georges County, Maryland (Kennedy et al., 1997). It also occurs in the Escondido

Formation in Trans-Pecos Texas and northern Mexico (Stephenson, 1941, 1955). In the Western Interior, this species occurs in the *Hoploscaphites nicolletii* and *Jeletzkytes nebrascensis* Zones of the Fox Hills Formation in north-central South Dakota (Landman and Waage, 1993) and in the *J. nebrascensis* Zone of the Pierre Shale in southeastern South Dakota and northeastern Nebraska (Kennedy et al., 1998).

SUBORDER ANCYLOCERATINA WIEDMANN, 1966
SUPERFAMILY TURRILITACEAE GILL, 1871
FAMILY BACULITIDAE GILL, 1871
[= EUBACULITINAE BRUNNSCHWEILER, 1966]
Genus *Eubaculites* Spath, 1926

TYPE SPECIES: *Baculites vagina* Forbes var. *ootacodensis* Stoliczka, 1866: 199, pl. 90, figs. 14, ?15, by original designation by Spath, 1926: 80.

Eubaculites carinatus (Morton, 1834)
figures 29–35

Baculites carinatus Morton, 1834: 44, pl. 13, fig. 1.
Baculites lyelli d'Orbigny, 1847: pl. 1, figs. 3–7.
Baculites tippaensis Conrad, 1858: 334, pl. 3, fig. 27.
Baculites spillmani Conrad, 1858: 335, pl. 35, fig. 24.
Baculites sheromingensis Crick, 1924: 139, pl. 9, figs. 1–3.
Eubaculites lyelli (d'Orbigny, 1847). Kennedy, 1987: 195, pl. 27, figs. 5–8; pl. 32, figs. 13, 14 (with full synonymy).
Eubaculites carinatus (Morton, 1834). Klinger and Kennedy, 1993: 218, text-figs. 7a–e, 21–30, 31a–g, 32–35, 36e,f, 37, 38, 42a, 52g,h.
Eubaculites carinatus (Morton, 1834). Kennedy and Cobban, 2000: 180, pl. 2, figs. 1–23, 27, 28; text figs. 3, 4 (with additional synonymy).
Eubaculites carinatus (Morton, 1834). Kennedy et al., 2001: 168, fig. 4a,e.
Eubaculites carinatus (Morton, 1834). Landman et al., 2004a: 35, fig. 15P,Q.
Eubaculites carinatus (Morton, 1834). Landman et al., 2004b: 55, figs. 27–29, 30A,B, 33U–Y.

TYPE: The holotype, by monotypy, is ANSP 72866, the original of Morton, 1834: pl. 13, fig. 1, from the Maastrichtian Prairie Bluff Chalk of Alabama.

MATERIAL: Approximately 50 specimens in the AMNH collections and 55 specimens in the MAPS collections from the upper part of the Tinton Formation, mainly the *Pinna* Layer, and, more rarely, as reworked material at the base of the Hornerstown Formation, Manasquan River Basin, central Monmouth County. The majority of specimens consist of fragments of body chambers, nearly all of which are uncrushed. Most specimens are juveniles and range in length from 20 to 60 mm (fig. 35), but two specimens, probably parts of adults, are exceptionally long with lengths of 117 and 141 mm. Specimens in the *Pinna* Layer sometimes occur in clusters (fig. 6E), which are probably biological in origin.

DESCRIPTION: The apical angle ranges from 1.9 to 4.5° (table 5). The whorl cross section is compressed ovoid. The intercostal ratio of whorl width to height ranges from 0.68 to 0.77 and the costal ratio of whorl width to height ranges from 0.69 to 0.84 (table 5). These ratios are nearly constant throughout ontogeny. In a plot of whorl width versus height in intercostal section, the y-intercept is approximately 0 (at $x = 0$), indicating that the growth of whorl width versus height is nearly isometric (fig. 35).

The dorsum is almost flat to very broadly rounded and the dorsolateral margin is fairly abruptly rounded. The inner flanks are broadly rounded with maximum width at one-third whorl height both costally and intercostally. The outer flanks converge to a fastigiate to tabulate venter. The venter is bordered by a shallow, longitudinal groove on each side.

The inner one-half of the flanks are covered with weak to strong, slightly crescentic nodate swellings with a rib index of 1.2–2.8. The nodes are particularly well developed in the two largest specimens, MAPS A2058b1 (fig. 29) and AMNH 50766 (fig. 30A–E), but also occur in very small specimens such as AMNH 50771 (fig. 32E–I). In other specimens such as AMNH 50779 (fig. 33N–Q), the nodes are relatively weak. The venter is nearly smooth to strongly ornamented with transverse ribs that cross the venter with a slight adoral projection, producing a serrated appearance; the rib index ranges from 3.5 to 8.5 and averages 6 (table 5).

MAPS A2058b1 (fig. 29) and AMNH 50737 (fig. 31I) preserve a mature modification at the aperture. In both instances, there

Fig. 29. *Eubaculites carinatus* (Morton, 1834), MAPS A2058b1, mature macroconch with apertural modification, *Pinna* Layer, Tinton Formation, Manasquan River Basin, central Monmouth County, New Jersey. **A.** Right lateral; **B.** dorsal; **C.** ventral; **D.** left lateral. All figures ×1.

is a short dorsal and long ventral rostrum, each of which tapers gradually to a rounded tip. It is interesting that these two specimens are very different in size, with whorl heights at the aperture of 21.7 and 12.2 mm, respectivey, suggesting that they may represent antidimorphs.

One specimen (AMNH 50434), a small fragment with a whorl height of 16.8 mm at the adoral end, contains part of a convex structure inside the adoral end of the body chamber (fig. 32J–N). The structure looks suspiciously like part of a lower jaw (aptychus). It is ornamented with ribs that parallel the outer margin. However, the ribs are not as rugose as those on baculite lower jaws (Landman et al., in press) and, in any event, not enough of the structure is preserved to make a positive identification.

The suture shows a bifid E/L, a narrow, bifid L, a broad, bifid L/U, a bifid U, and a narrow I (fig. 34).

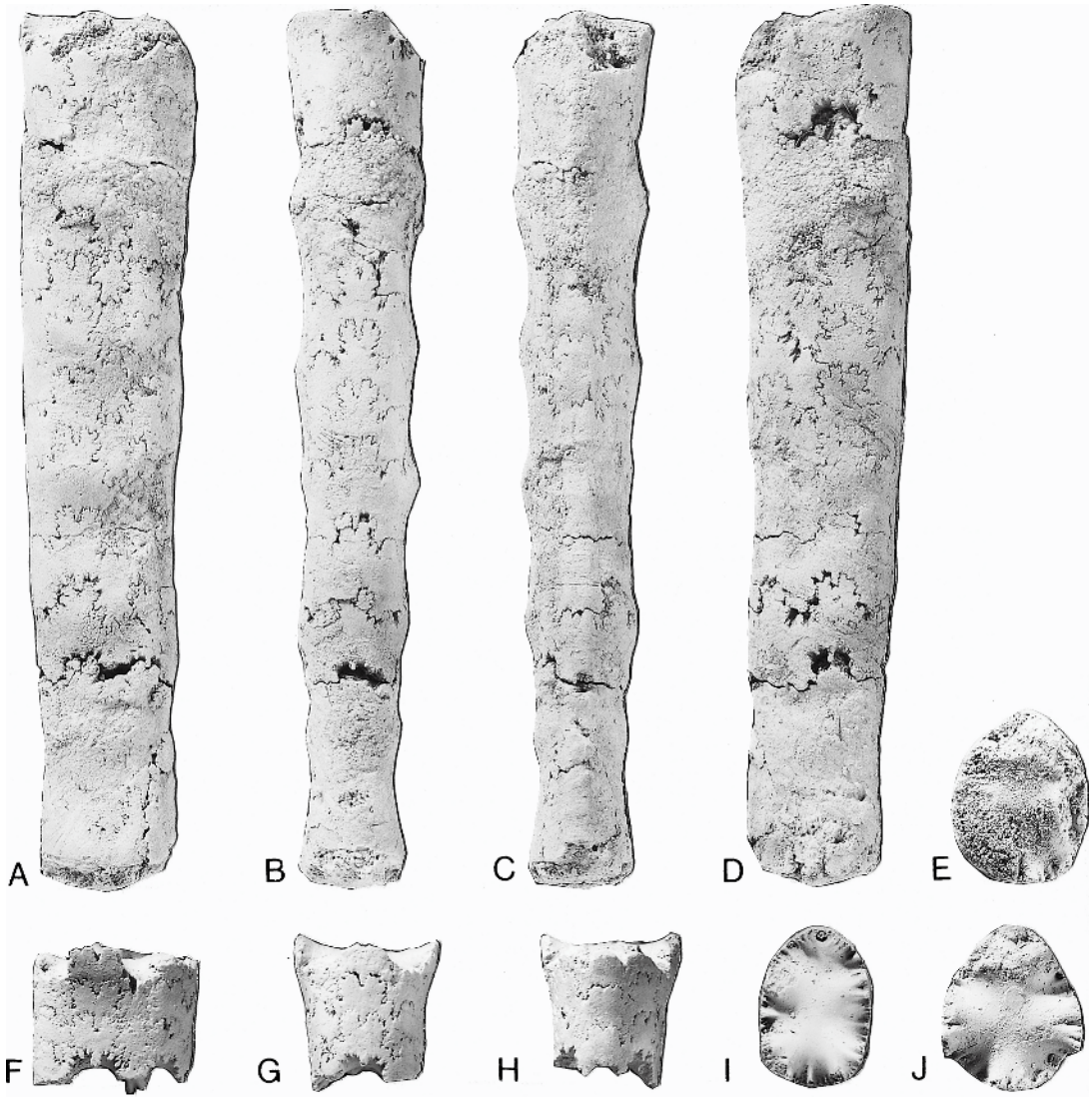

Fig. 30. *Eubaculites carinatus* (Morton, 1834), *Pinna* Layer, Tinton Formation, Manasquan River Basin, central Monmouth County, New Jersey. **A–E.** AMNH 50766, mature macroconch. **A.** Right lateral; **B.** dorsal; **C.** ventral; **D.** left lateral; **E.** whorl section at adoral end. **F–J.** AMNH 50778. **F.** right lateral; **G.** dorsal; **H.** ventral; **I.** whorl section at adapical end; **J.** whorl section at adoral end. All figures ×1.

DISCUSSION: The taphonomy of these specimens evidently favored gross ornament over fine ornament. Thus, delicate growth lines are missing but large nodes are well preserved. The fact that two specimens retain mature modifications at the aperture suggests that these animals lived nearby and did not suffer much postmortem transport. This is consistent with the observation that many specimens occur in monospecific clusters that may be related to group feeding or the result of nearly simultaneous death after spawning or mating. With the exception of one specimen (AMNH 51327) that bears a single thread of a bryozoan colony, there are no epizoans.

As summarized by Klinger and Kennedy (2001: 62), the adult size of this species in North America and Europe is much smaller than that in Argentina and Zululand. The maximum whorl height of a specimen from

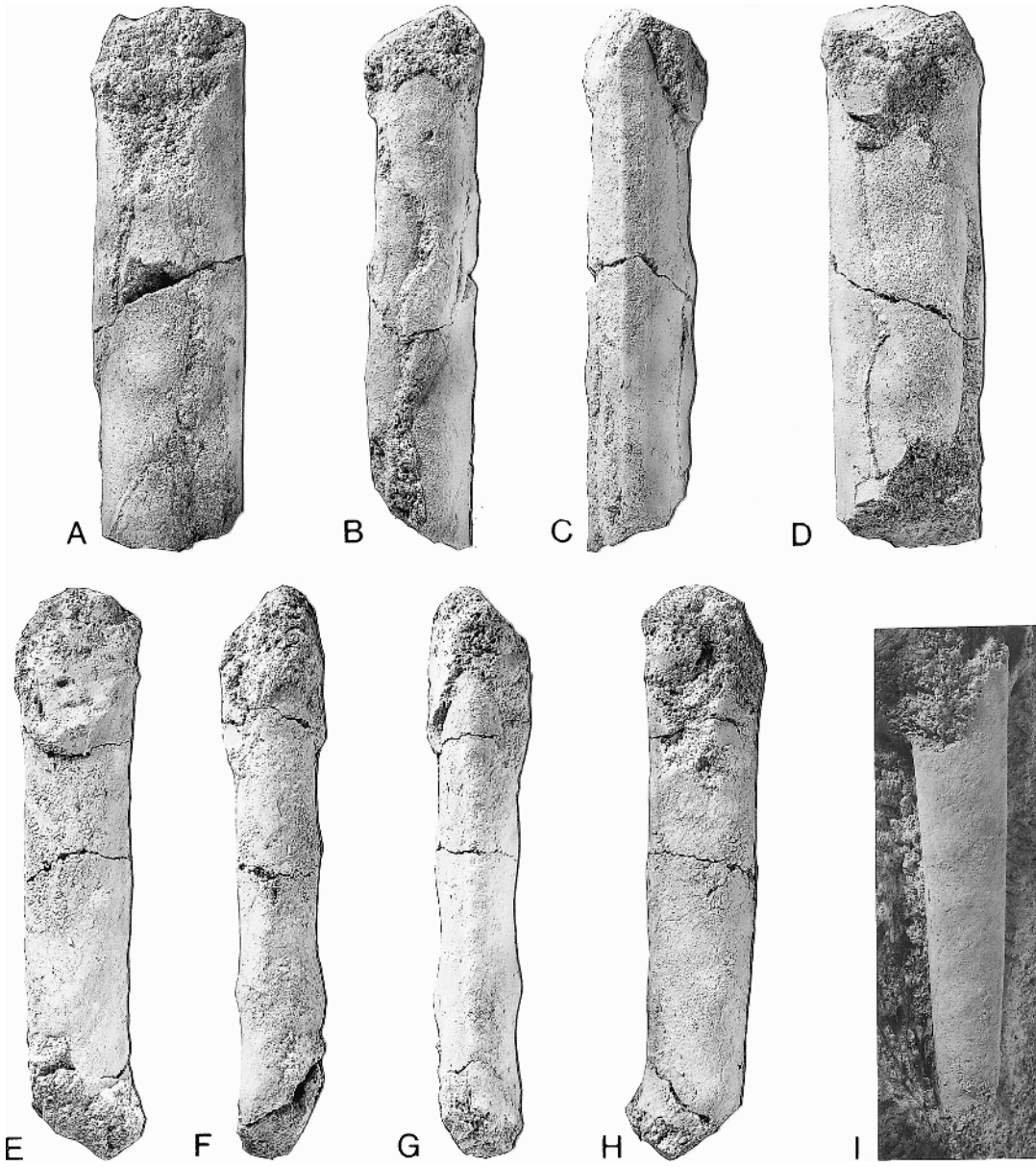

Fig. 31. *Eubaculites carinatus* (Morton, 1834), *Pinna* Layer, Tinton Formation, Manasquan River Basin, central Monmouth County, New Jersey. **A–D.** AMNH 50781. **A.** Right lateral; **B.** dorsal; **C.** ventral; **D.** left lateral. **E–H.** AMNH 50418. **E.** Right lateral; **F.** dorsal; **G.** ventral; **H.** left lateral. **I.** AMNH 50737, mature microconch in matrix, with a possible apertural modification, right lateral. All figures ×1.

the Manasquan River Basin is 25.4 mm whereas the maximum whorl heights of specimens from Argentina and Zululand are approximately 90 mm.

OCCURRENCE: Top of the Tinton Formation, mainly the *Pinna* Layer, and, rarely, as reworked material at the base of the Hornerstown Formation, Manasquan River Basin, central Monmouth County, New Jersey. Elsewhere in New Jersey, this species occurs in the upper part of the New Egypt Formation and as reworked material at the base of

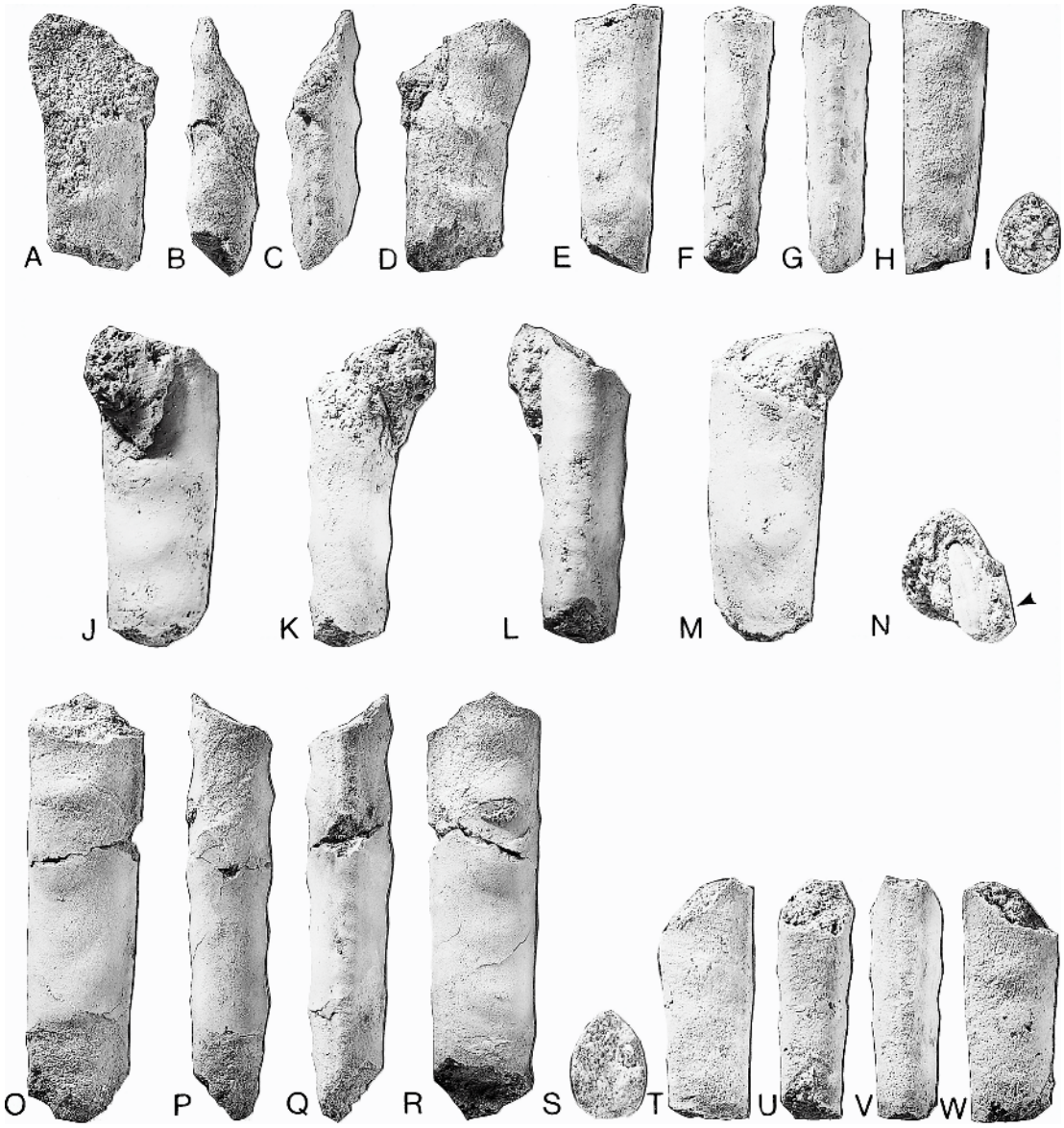

Fig. 32. *Eubaculites carinatus* (Morton, 1834), *Pinna* Layer, Tinton Formation, Manasquan River Basin, central Monmouth County, New Jersey. **A–D.** AMNH 50770. **A.** Right lateral; **B.** dorsal; **C.** ventral; **D.** left lateral. **E–I.** AMNH 50771. **E.** Right lateral; **F.** dorsal; **G.** ventral; **H.** left lateral; **I.** whorl section at adoral end. **J–N.** AMNH 50434. **J.** Right lateral; **K.** dorsal; **L.** ventral; **M.** left lateral; **N.** whorl section at adoral end with possible aptychus (arrow). **O–S.** AMNH 50765. **O.** Right lateral; **P.** dorsal; **Q.** ventral; **R.** left lateral; **S.** whorl section at adoral end. **T–W.** AMNH 50769. **T.** Right lateral; **U.** dorsal; **V.** ventral; **W.** left lateral. All figures ×1.

the Hornerstown Formation, near Eatontown, northeastern Monmouth County (Landman et al., 2004b); the top of the New Egypt Formation in the Crosswicks Creek Basin, southwestern Monmouth County (Landman et al., in prep.); and the New Egypt Formation and as reworked material at the base of the Hornerstown Formation at the

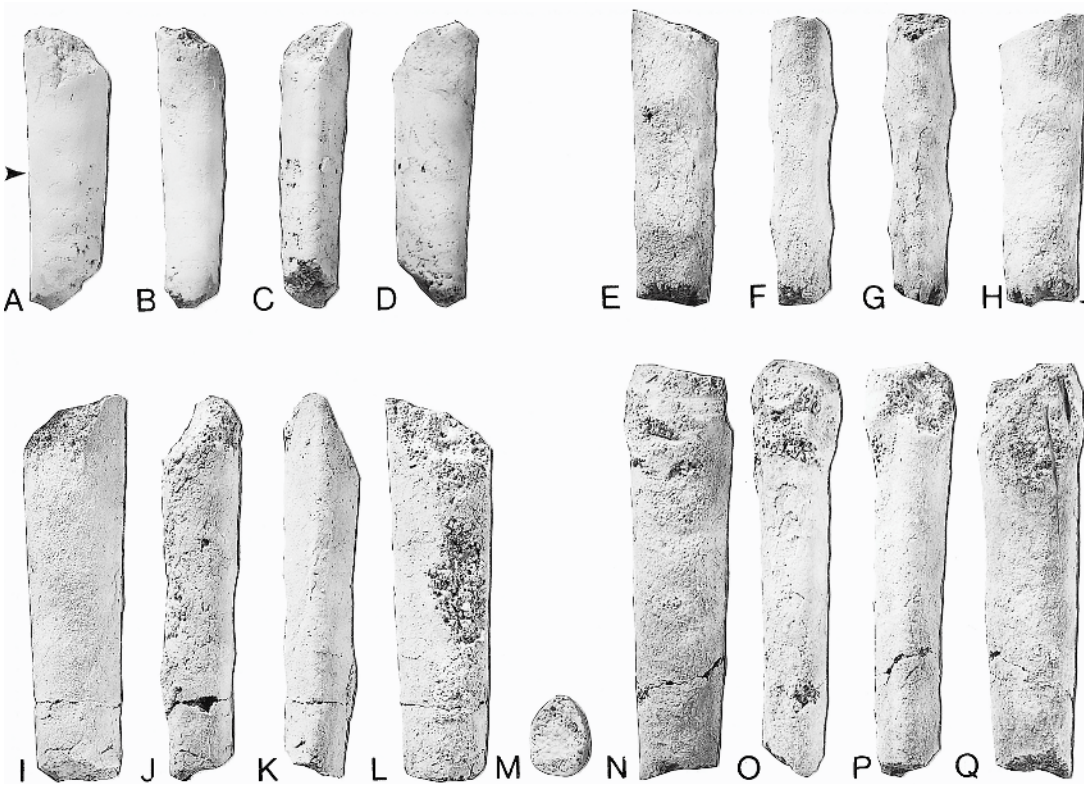

Fig. 33. *Eubaculites carinatus* (Morton, 1834), *Pinna* Layer, Tinton Formation, Manasquan River Basin, central Monmouth County, New Jersey. **A–D.** AMNH 50721. **A.** Right lateral; **B.** dorsal; **C.** ventral; **D.** left lateral. **E–H.** AMNH 50767. **E.** Right lateral; **F.** dorsal; **G.** ventral; **H.** left lateral. **I–M.** AMNH 50768. **I.** Right lateral; **J.** dorsal; **K.** ventral; **L.** left lateral; **M.** whorl section at adapical end. **N–Q.** AMNH 50779. **N.** Right lateral; **O.** dorsal; **P.** ventral; **Q.** left lateral. All figures ×1.

Inversand Pit, near Sewell, Gloucester County (Kennedy and Cobban, 1996). Kennedy and Cobban (1996: fig. 3.1–3.3, 3.7–3.12) recorded three specimens of this species (USNM 12691a–c), *ex* J.B. Marcou collection, labeled ''New Jersey,'' which they inferred to be from the base of the Hornerstown Formation. Elsewhere on the Atlantic Coastal Plain, this species occurs in the Severn Formation, Prince Georges County, Maryland (Kennedy et al., 1997), and Anne Arundel County, Maryland (Landman et al., 2004a). On the Gulf Coastal Plain, this species is reported from the top of the Corsicana Formation and as reworked material at the base of the Kincaid Formation, Falls County, Texas (Kennedy et al., 2001); the Owl Creek Formation, Mississippi, Missouri, and Tennessee (Kennedy and Cobban, 2000); and the Prairie Bluff Chalk, Alabama and Mississippi (Cobban and Kennedy, 1995). Klinger and Kennedy (2001) and Klinger et al. (2001) reported it from southeast and southwest France, northern Spain, Austria, the Netherlands, Zululand (South Africa), Mozambique, Madagascar, South India, Western Australia, Chile, Argentina, and California. It ranges from the upper lower to the upper upper Maastrichtian (Klinger et al., 2001). Henderson et al. (1992: 153) noted that this species was widely distributed but did not generally range beyond low to midlatitudes. They remarked that ''it is a useful indicator of middle to late Maastrichtian age and represents the last widely distributed heteromorph taxon to appear in the stratigraphic record.''

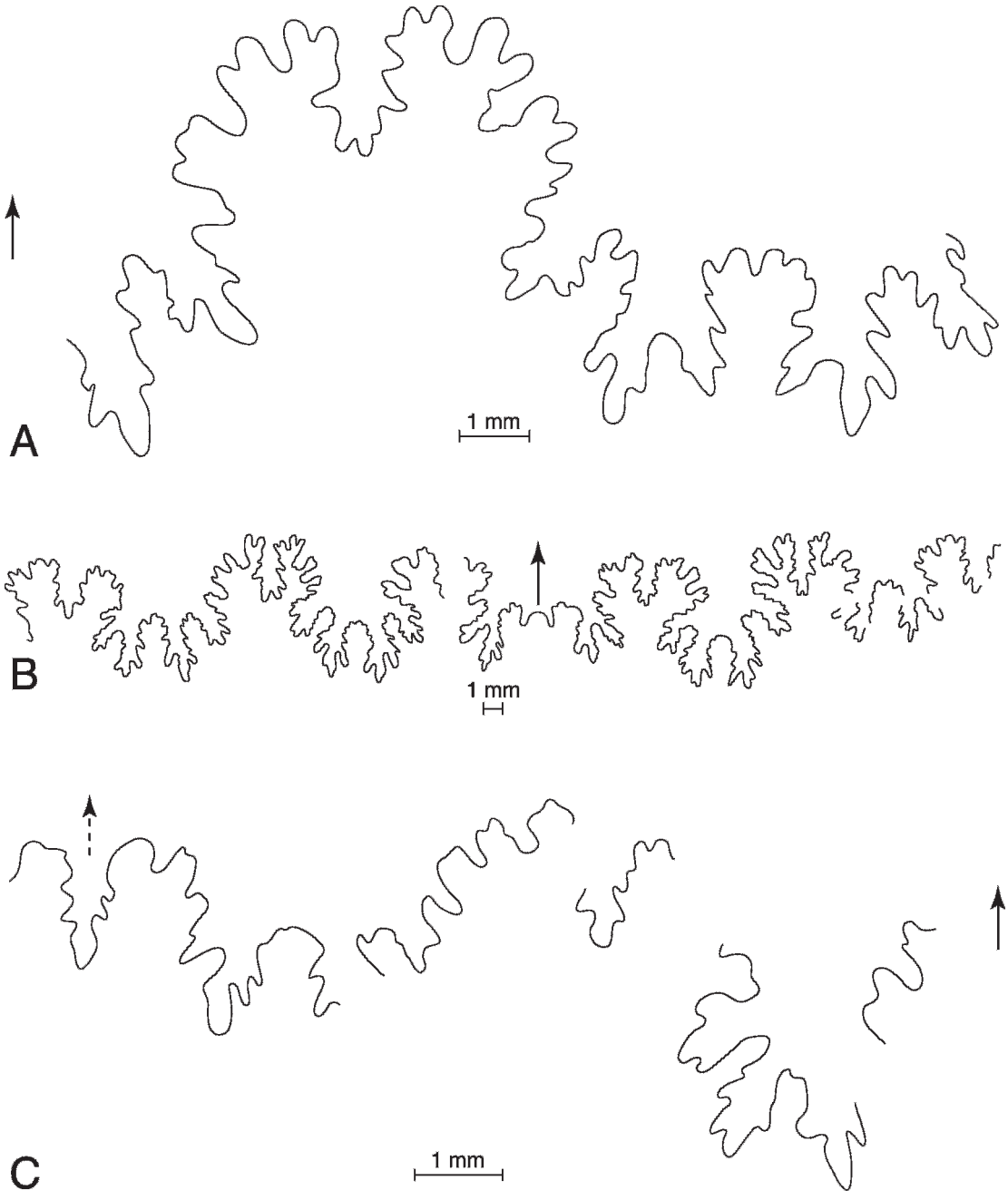

Fig. 34. *Eubaculites carinatus* (Morton, 1834), *Pinna* Layer, Tinton Formation, Manasquan River Basin, central Monmouth County, New Jersey. **A.** AMNH 50723, composite suture at WH = 16.7 mm. **B.** AMNH 50778, suture at WH = 22.2 mm. **C.** AMNH 50721, suture at WH = 9.9 mm.

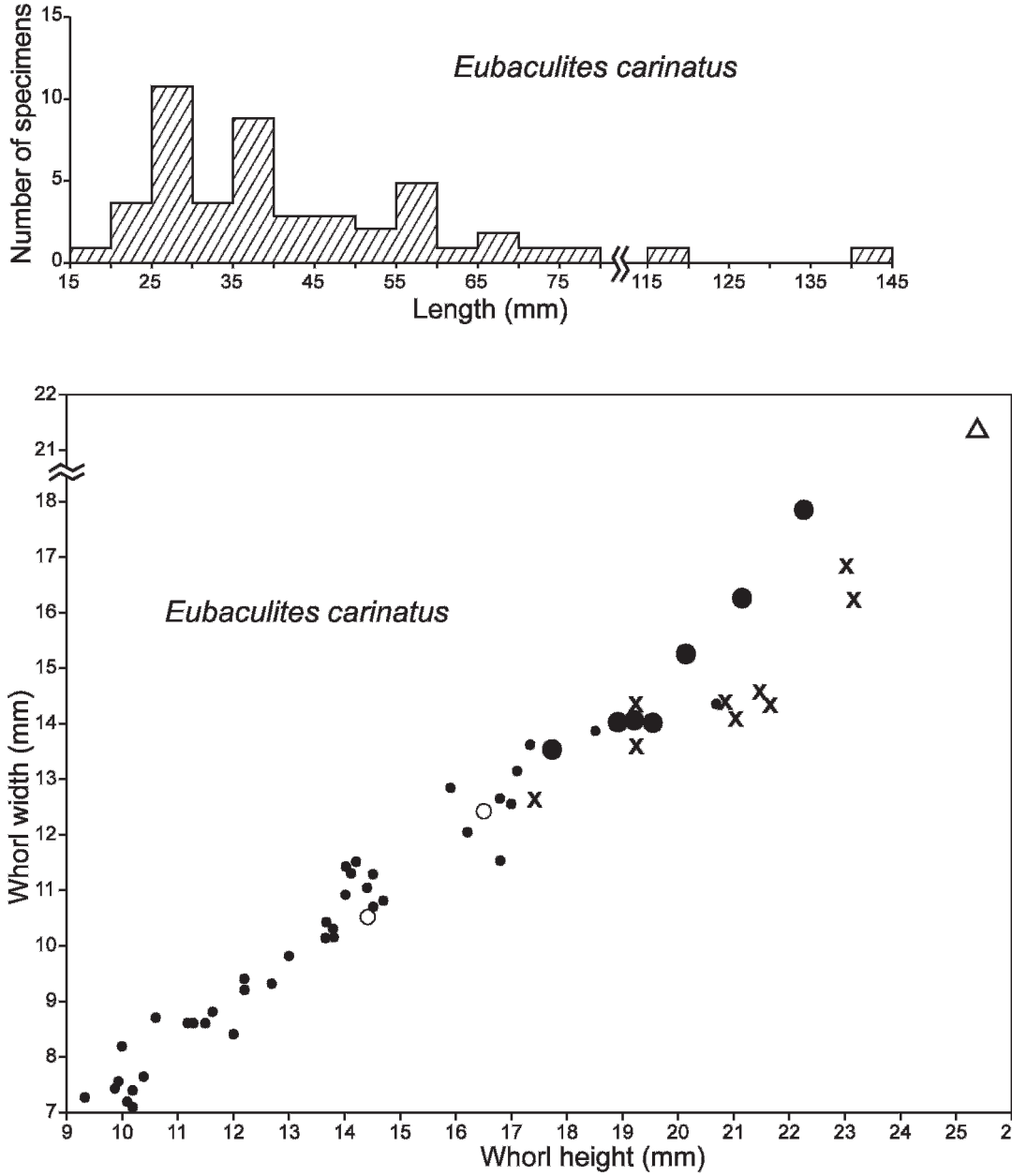

Fig. 35. **Top.** Size histogram of a sample of *Eubaculites carinatus* (Morton, 1834), *Pinna* Layer, Tinton Formation, Manasquan River Basin, central Monmouth County. Nearly all of the specimens are fragments of juvenile body chambers with some exceptions, notably the two largest specimens (AMNH 50766 and MAPS A2058b1), which are presumably mature macroconchs. **Bottom.** Scatter plot of whorl width versus height in intercostal section in the same sample of *E. carinatus*. All measurements are at the adoral ends of the specimens. The Xs and Os represent measurements through the ontogeny of AMNH 50766 and MAPS A2058b1, respectively (the open circles indicate the septate portion of MAPS A2058b1; AMNH 50766 is completely septate.) The triangle represents another large body chamber (MAPS A2058b2), presumably a macroconch.

TABLE 5
Measurements of *Eubaculites carinatus* (Morton, 1834)[a]

Specimen	M/m	L (mm)	WW/WH		Taper angle (°)	Rib index	
						Flanks	Venter
AMNH 50418		78.5	c	—	2.1	1.8	4.7
			ic	0.73			
AMNH 50432		44.6	c	0.81	—	2	7.2
			ic	0.77			
AMNH 50433		36.8	c	0.84	—	2.1	3.8
			ic	0.70			
AMNH 50434		45.0	c	0.77	—	2.8	5.8
			ic	0.74			
AMNH 50721		39.2	c	0.79	4.4	2.7	S
			ic	0.76			
AMNH 50737	m	59.4		—	—	2.8	S
AMNH 50765		62.8	c	0.74	3.0	2.7	7
			ic	0.68			
AMNH 50766	M?	117.3	c	0.75	3.6	2.1	4.8
			ic	0.71			
AMNH 50767		39.9	c	0.84	1.9	1.7	3.5
			ic	0.70			
AMNH 50768		52.7	c	0.75	2.9	2	S
			ic	0.75			
AMNH 50769		35.8	c	0.79	—	2.8	S
			ic	0.74			
AMNH 50770		39.5		—	—	2.2	5.2
AMNH 50771		39.3	c	0.76	4.5	2.3	6
			ic	0.75			
AMNH 50778		17.4		—	—	—	S
AMNH 50779		57.1	c	0.76	3.8	2.8	S
			ic	—			
AMNH 50781		74.7	c	0.69	—	2.5	S
			ic	—			
MAPS A2056b1	M	141.3	c	0.83	3.4	2.2	8.5
			ic	0.76			
MAPS A2056b2	M	67.8	c	0.80	—	2.2	—
			ic	—			

[a]M, macroconch; m, microconch; L, maximum length; WW/WH, ratio of whorl width to height at the adoral end of the specimen; c, costal section; ic, intercostal section; S, smooth or worn. If the specimen was partly broken, the length measurement used to calculate the taper angle was less than L.

Eubaculites latecarinatus (Brunnschweiler, 1966) figures 36–38

Eubaculites otacodensis (Stoliczka). Spath, 1940: 49 (*pars*), text-fig. 1c.

Giralites latecarinatus Brunnschweiler, 1966: 33, pl. 3, figs. 13, 14; pl. 4, figs. 1–5; text-figs. 17, 18.

Giralites quadrisulcatus Brunnschweiler, 1966: 35, pl. 4, figs. 11–14; text-fig. 20.

Eubaculites ambindensis Collignon, 1971: 18, pl. 646, fig. 2393.

Eubaculites latecarinatus (Brunnschweiler, 1966). Klinger, 1976: 91, pl. 40, fig. 1; pl. 41, fig. 3; pl. 42, figs. 2, 6; pl. 43, figs. 3, 4; text-figs. 11d,e.

Eubaculites latecarinatus (Brunnschweiler, 1966). Klinger and Kennedy *in* Klinger et al., 1980: 296, figs. 2a–c, 3a–d, 4a–c, 5d.

Eubaculites latecarinatus (Brunnschweiler, 1966). Henderson et al., 1992: 159, figs. 22L–N, 23N–P.

Eubaculites latecarinatus (Brunnschweiler, 1966). Klinger and Kennedy, 1993: 238, figs. 26A, 39–41, 42B,C, 43–49, 50A, 53A.

Fig. 36. *Eubaculites latecarinatus* (Brunnschweiler, 1966), *Pinna* Layer, Tinton Formation, Manasquan River Basin, central Monmouth County, New Jersey. **A,B.** AMNH 50419. **A.** Ventral; **B.** right lateral. **C–G.** AMNH 50435. **C.** Right lateral; **D.** dorsal; **E.** ventral; **F.** left lateral; **G.** whorl section at adapical end. **H–L.** AMNH 51888. **H.** Right lateral; **I.** dorsal; **J.** ventral **K.** left lateral; **L.** whorl section at adoral end. **M–P.** AMNH 51874. **M.** Right lateral; **N.** dorsal; **O.** ventral; **P.** left lateral. **Q–U.** AMNH 51864. **Q.** Right lateral; **R.** dorsal; **S.** ventral; **T.** left lateral; **U.** whorl section at adapical end. **V–Y.** AMNH 51863. **V.** Right lateral; **W.** dorsal; **X.** ventral; **Y.** left lateral. All figures ×1.

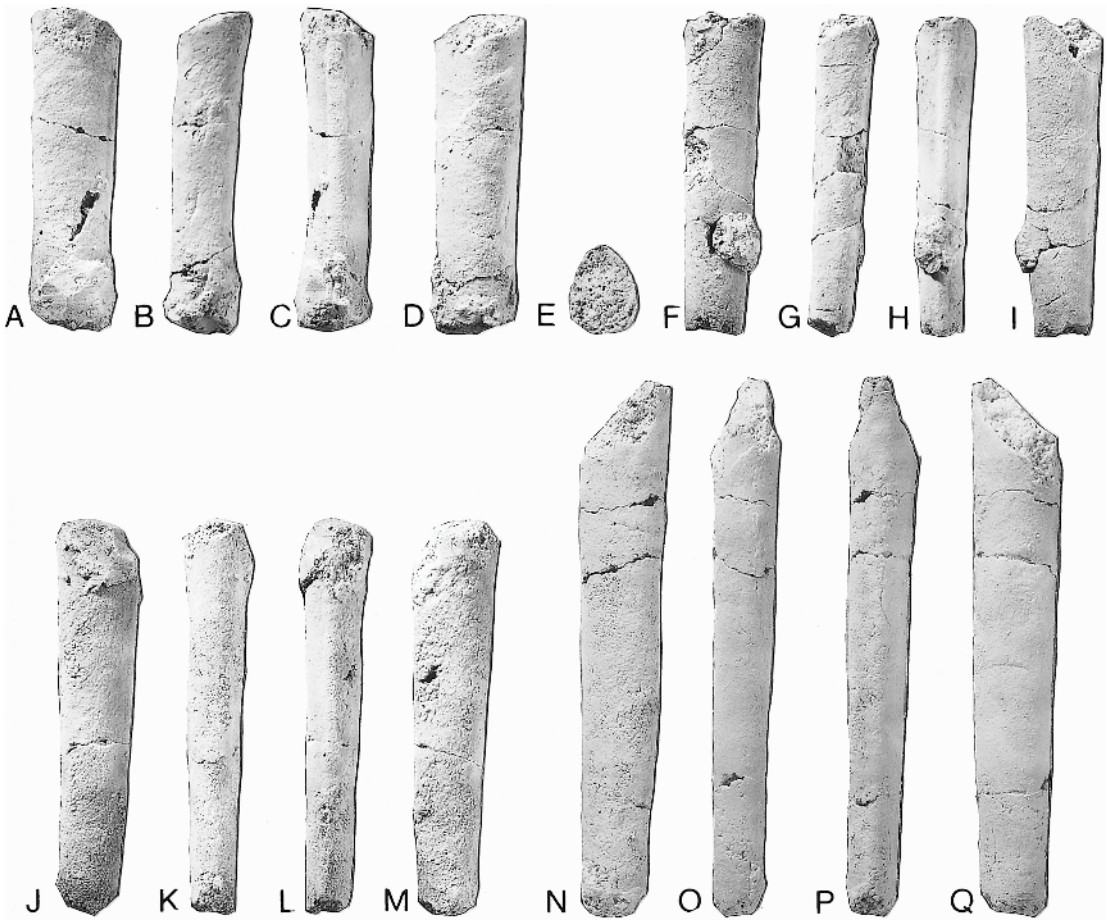

Fig. 37. *Eubaculites latecarinatus* (Brunnschweiler, 1966), *Pinna* Layer, Tinton Formation, Manasquan River Basin, central Monmouth County, New Jersey. **A–E.** AMNH 51877. **A.** Right lateral; **B.** dorsal; **C.** ventral; **D.** left lateral; **E.** whorl section at adoral end. **F–I.** AMNH 51876. **F.** Right lateral; **G.** dorsal; **H.** ventral; **I.** left lateral. **J–M.** AMNH 51862. **J.** Right lateral; **K.** dorsal; **L.** ventral; **M.** left lateral. **N–Q.** AMNH 51875. **N.** Right lateral; **O.** dorsal; **P.** ventral; **Q.** left lateral. All figures ×1.

Eubaculites latecarinatus (Brunnschweiler, 1966). Kennedy et al., 1997: 20, figs. 15A–D,K,L, 16G,H, 19.

Eubaculites latecarinatus (Brunnschweiler, 1966). Klinger and Kennedy, 2001: 234.

Eubaculites latecarinatus (Brunnschweiler, 1966). Klinger et al., 2001: 287, pl. 10, figs. 4–9; text-fig. 6.

Eubaculites latecarinatus (Brunnschweiler, 1966). Landman et al., 2004a: 34, figs. 13g–j, 14B.

Eubaculites latecarinatus (Brunnschweiler, 1966). Landman et al., 2004b: 63, figs. 30C,D, 31, 32.

TYPE: The holotype, by original designation, is that of Brunnschweiler (1966: pl. 4, figs. 2–4) from the lower Maastrichtian nodule bed at the top of the Korojong Calcarenite, Carnarvon Basin, Western Australia.

MATERIAL: Approximately 50 specimens in the AMNH collections and 45 specimens in the MAPS collections from the upper part of the Tinton Formation, mainly the *Pinna* Layer, and, more rarely, as reworked material from the base of the Hornerstown Formation, Manasquan River Basin, central Monmouth County, New Jersey. Most of the specimens are fragments of body chambers, nearly all of which are uncrushed. The largest fragment is 75 mm in length, but this is exceptional; the majority of specimens are 25–60 mm in length (fig. 38).

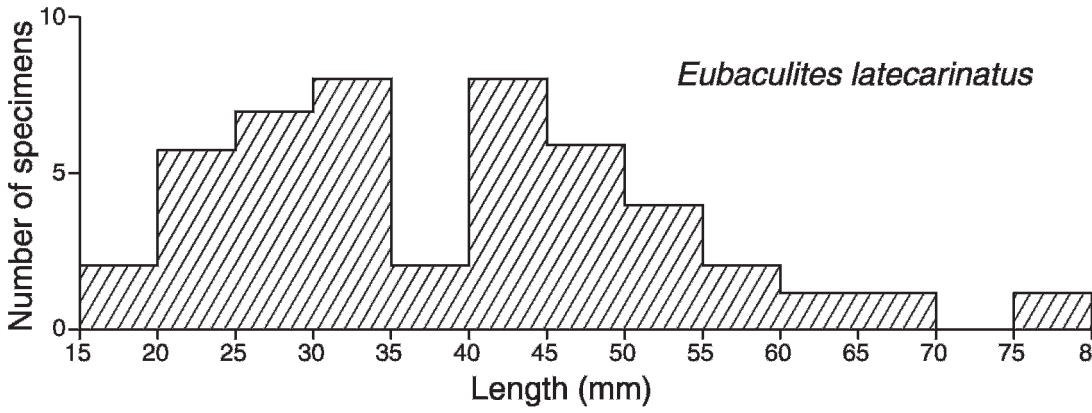

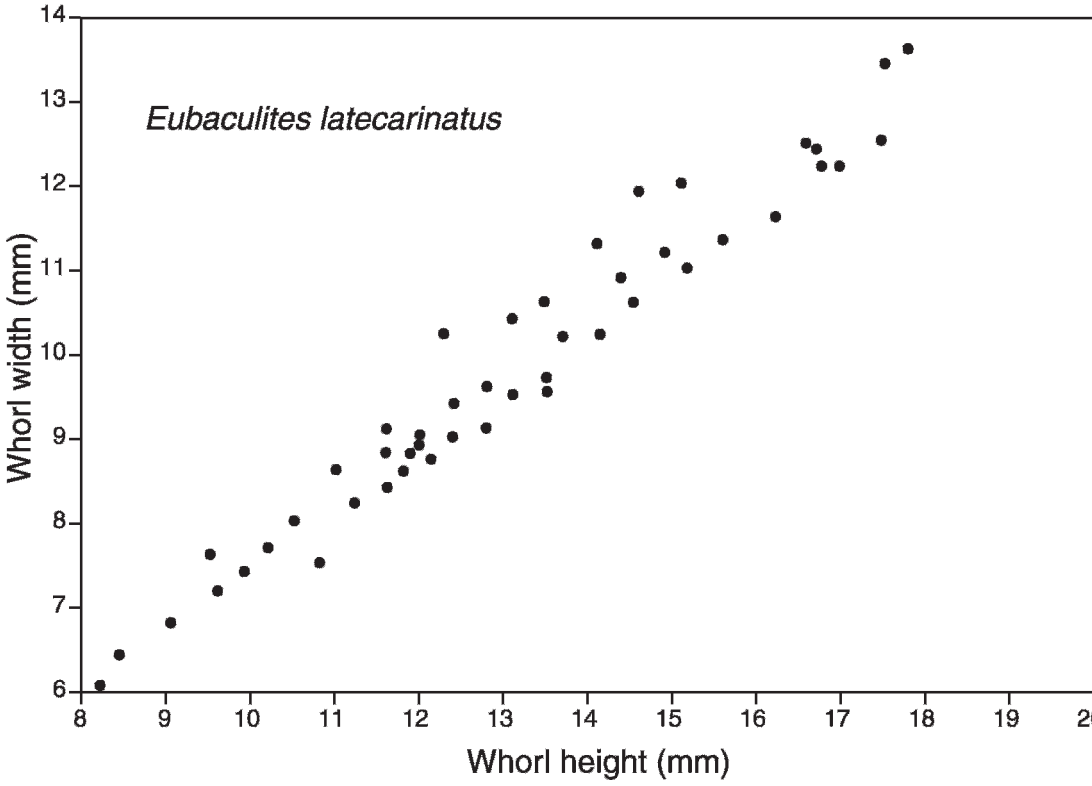

Fig. 38. **Top.** Size histogram of a sample of *Eubaculites latecarinatus* (Brunnschweiler, 1966), *Pinna* Layer, Tinton Formation, Manasquan River Basin, central Monmouth County, New Jersey. Most of the specimens are fragments of juvenile body chambers. **Bottom.** Scatter plot of whorl width versus height in the same sample of *E. latecarinatus.* Measurements are at the adoral ends of the specimens.

TABLE 6
Measurements of *Eubaculites latecarinatus* (Brunnschweiler, 1966)[a]

Specimen				Rib index	
AMNH	L (mm)	WW/WH	Taper angle (°)	Flanks	Venter
50419	45.0	—	—	S	~8
50435	41.8	0.71	3.9	S	7.3
51862	55.6	0.72	4.3	S	S
51863	57.4	0.73	4.0	2.1	S
51864	50.8	0.75	4.1	S	S
51874	63.2	0.75	4.0	2.4	6.7
51875	75.0	0.75	2.2	S	S
51876	45.1	0.73	3.6	S	8.5
51877	45.4	0.75	4.0	S	7.2
51888	69.2	0.73	2.6	S	S

[a]See table 5 for explanation of abbreviations.

DESCRIPTION: The angle of taper ranges from 2.2 to 4.3° (table 6). The whorl cross section is compressed ovoid with a ratio of whorl width to height of 0.71–0.75. The ratio is nearly constant throughout ontogeny. In a plot of whorl width versus height, the *y*-intercept is approximately 0 (at $x = 0$), indicating that the growth of whorl width versus height is nearly isometric (fig. 38). The dorsum is flat to broadly rounded and the dorsolateral shoulder is fairly sharply rounded. The inner flanks are broadly rounded with maximum width at midwhorl height. The outer flanks converge steeply to the venter, which is commonly bordered by a shallow longitudinal groove. The ventrolateral shoulder is fairly sharply rounded and the venter is flat.

Most of the specimens are smooth, although this may be due in part to preservation. However, some specimens bear weak convex folds on the dorsum, faint swellings on the inner flanks, and transverse ribs on the venter, with a rib index of approximately 7–8. No specimen is well enough preserved to illustrate the suture.

DISCUSSION: This species differs from *Eubaculites carinatus* in having weak or no ornament at all. It is possible that both species actually comprise a single polymorphic species with a gradation in ornament. The two species are approximately equally abundant in the Manasquan River Basin. Our collection of *E. latecarinatus* contains both slender and robust forms, which may correspond to microconchs and macroconchs, respectively, but without a complete ontogenetic series, this is difficult to demonstrate.

OCCURRENCE: Top of the Tinton Formation, mainly the *Pinna* Layer, and, rarely, as reworked material at the base of the Hornerstown Formation, Manasquan River Basin, central Monmouth County, New Jersey. Elsewhere in New Jersey, this species occurs in the upper part of the New Egypt Formation and as reworked material at the base of the Hornerstown Formation, near Eatontown, northeastern Monmouth County (Landman et al., 2004b) and at the top of the New Egypt Formation in the Crosswicks Creek Basin, southwestern Monmouth County (Landman et al., in prep.). This species is also known from the Severn Formation, Prince Georges County (Kennedy et al., 1997), and Kent County, Maryland (Landman et al., 2004a). In addition, Klinger and Kennedy (2001) and Klinger et al. (2001) reported this species from the upper lower to upper upper Maastrichtian of Zululand and the offshore Alphard Group (South Africa), Madagascar, and Western Australia.

SUPERFAMILY SCAPHITACEAE GILL, 1871
FAMILY SCAPHITIDAE GILL, 1871
SUBFAMILY SCAPHITINAE GILL, 1871
Genus *Discoscaphites* Meek, 1871

TYPE SPECIES: *Ammonites conradi* Morton, 1834: 39, pl. 16, fig. 3, by original designation.

DISCUSSION: The name *Discoscaphites* was originally used to describe a number of species now included in *Hoploscaphites* and *Jeletzkytes*, as well as those in *Discoscaphites*. Jeletzky and Waage (1978), based on a study of the type suite and other specimens of *Ammonites conradi* Morton, 1834, from the Prairie Bluff Chalk of Alabama and Mississippi, restricted the genus *Discoscaphites* to small to medium size, very involute, multituberculate scaphites, thus stabilizing the nomenclature.

The relationship of *Discoscaphites* to other scaphite genera is controversial. In an attempt to evaluate the phylogenetic relationships among *Discoscaphites*, *Hoploscaphites*, and *Jeletzkytes*, Landman and Waage (1993) performed a cladistic analysis of these three genera with *Scaphites* as the outgroup. The results of their analysis indicated that *Jeletzkytes* and *Hoploscaphites* are more closely related to each other than either is to *Discoscaphites*. Their study highlighted the importance of several characters, including the spacing between ventrolateral tubercles on either side of the venter, the apertural angle, and the degree of uncoiling of the body chamber.

Cooper (1994) did a much more extensive phylogenetic study of all scaphite genera but did not include an explicit data matrix. In his analysis, *Discoscaphites* forms a sister group with a clade containing *Hoploscaphites* and *Tovebirkelundites*. Cooper (1994) erected the latter taxon to include species of *Hoploscaphites* such as *Hoploscaphites schmidi* (Birkelund, 1982) and *Hoploscaphites pungens* (Binckhorst, 1861), which attain a very large size and develop a midventral row of tubercles. This three-taxon clade forms a sister group with *Indoscaphites*, and this expanded clade clusters with a clade containing *Jeletzkytes* and *Karlwaageites*. Cooper (1994) erected the latter taxon to include species of *Jeletzkytes* such as *Jeletzkytes criptonodosus* Riccardi, 1983, and *Jeletzkytes nebrascensis* (Owen, 1852), which develop multiple rows of tubercles on the phragmocone, some or all of which persist onto the body chamber. Cooper noted, as did Jeletzky and Waage (1978) before him, that these species converge on the morphology of *Discoscaphites*, but differ in their larger adult size, higher apertural angle, and more prominent ventrolateral tubercles on the body chamber.

Monks (2000) also did a phylogenetic study of all scaphite genera using a much more explicit parsimony-based analysis. His results are very different from those of Cooper (1994). According to Monks (2000), *Discoscaphites* forms a sister group with *Jeletzkytes*, and this clade forms a sister group, in turn, with *Rhaeboceras*. The clade containing these three genera forms a trichotomy with *Trachyscaphites* and *Acanthoscaphites*. *Hoploscaphites* occupies a basal position relative to these other genera.

Our own preliminary studies have suggested a different result, namely, that *Discoscaphites* and *Trachyscaphites* are sister taxa.[1] Both Cobban and Scott (1964) and Jeletzky and Waage (1978) have pointed out the close morphological resemblance between these two genera based on the presence of multiple rows of tubercles, with the inner and outer ventrolateral tubercles nearly equal in size. In addition, the ribs on the body chamber in both genera are simple and not differentiated into stronger primaries and weaker secondaries. The main difference is that the adult body chamber is more loosely coiled in *Trachyscaphites* than in *Discoscaphites*.

[1] *Trachyscaphites* is confined to the middle and upper Campanian, with the exception of two species from the upper Maastrichtian of the Gulf Coast, *Trachyscaphites alabamensis* Cobban and Kennedy, 1995, and *Trachyscaphites yorkensis* (Stephenson, 1941). The first species was attributed to *Trachyscaphites* based on the loose coiling of the body chamber, as exemplified by the holotype (USNM 463217; Cobban and Kennedy, 1995: fig. 21.14–17), which is a microconch. However, it is possible that an examination of the more tightly coiled macroconchs, if they were available, would indicate that this species actually belongs to *Discoscaphites*, which it otherwise resembles. The holotype of *T. yorkensis* (USNM 77308; Stephenson, 1941: pl. 90, fig. 9), on the other hand, is characterized by large ventrolateral tubercles on the body chamber, and probably belongs to *Jeletzkytes*.

The confusion about the higher level phylogeny of scaphites demonstrates the need for a thorough study of the generic relationships within this group. The purpose of the present study, however, is much more modest: to reconstruct the phylogenetic relationships among species of *Discoscaphites*.

The genus *Discoscaphites* contains eight recognized species: *D. conradi* (Morton, 1834), *D. gulosus* (Morton, 1834), *D. rossi* Landman and Waage, 1993, *D. iris* (Conrad, 1858), *D. sphaeroidalis* Cobban and Kennedy, 2000, *D. minardi* Landman et al., 2004a, *D. jerseyensis*, n.sp., *D. kambysis* (Quaas, 1902), and *D. acutituberculatus* (Tzankov, 1982). All of these species are from North America except *D. kambysis* and *D. acutituberculatus*, which are from Egypt and Bulgaria, respectively.

In our analysis, we relied on actual specimens as well as published descriptions of these species (e.g., Stephenson, 1955; Jeletzky and Waage, 1978; Kennedy and Cobban, 1993; Kennedy et al., 2001; Landman and Waage, 1993; Landman et al., 2004a, 2004b; Cobban and Kennedy, 1995, 2000). We excluded from our analysis *Discoscaphites acutituberculatus* and *D. kambysis* because these species are only represented by fragments.

We chose the genus *Trachyscaphites* as the outgroup, following the comments of Cobban and Scott (1964) and Jeletzky and Waage (1978) and our own preliminary investigations. Most of our observations were based on the type species, *T. redbirdensis* Cobban and Scott, 1964, but, where necessary, we examined other species such as *T. spiniger spiniger* (Schlüter, 1872) and *T. spiniger porchi* (Adkins, 1929). The choice of *Trachyscaphites* as an outgroup has some practical limitations. The majority of specimens in Europe are flattened and distorted and those in North America, while uncrushed, are generally incomplete.

We used nine characters (0–8) in our analysis. To the extent possible, all of them were based on macroconchs. Because of their larger size, macroconchs generally display a more complete suite of species-specific characters than microconchs (Riccardi, 1983; Landman and Waage, 1993; Machalski, 2005). Due to extensive intraspecific variation, as many specimens as possible were examined for each species. Several of our characters are quantitative and, as such, are difficult to subdivide into nonarbitrary character states (for a discussion of this controversial issue, see Archie, 1985; Chappill, 1989; Rae, 1998). We tried to identify natural gaps in the distribution of such characters to establish non-overlapping charcter states. However, we recognize that different subdivisions, based on a different approach, could lead to different results.

0. **Adult size** (LMAX): large (≈100 mm) (0); medium (50–90 mm) (1); small (40–45 mm) (2); very small (≈25 mm) (3). *Trachyscaphites redbirdensis* is large based on the holotype. *Discoscaphites gulosus* and *D. conradi* show a broad range of size from 50 to 90 mm. Specimens from the Western Interior are generally larger than those from the Gulf and Atlantic Coastal Plains (Jeletzky and Waage, 1978). Adults of *D. minardi*, *D. iris*, *D. sphaeroidalis*, and *D. jerseyensis* are small, and adults of *D. rossi* are very small.

1. **Coiling of the mature body chamber**: loosely coiled (0); moderately tightly coiled (1); very tightly coiled (2); extremely tightly coiled (3). This is also expressed by the degree of separation between the phragmocone and body chamber. The body chamber is loosely coiled in *Trachyscaphites redbirdensis*, moderately tightly coiled in *Discoscaphites conradi* and *D. gulosus*, very tightly coiled in *D. iris*, *D. sphaeroidalis*, *D. minardi*, and *D. jerseyensis*, and extremely tightly coiled in *D. rossi*.

2. **Apertural angle**: high (≈90°) (0); moderately high (40°–55°) (1); low (30°–40°) (2); very low (10°–20°) (3). The apertural angle usually correlates with the coiling of the body chamber, with higher apertural angles associated with more loosely coiled, and lower apertural angles with more tightly coiled body chambers. The apertural angle is ≈90° in *Trachyscaphites redbirdensis,* 40°–55° in *Discoscaphites conradi* and *D.* gulosus, 30°–40° in *D. iris*, *D. sphaeroidalis*, *D. minardi*, and *D. jerseyensis*, and 10°–20° in *D. rossi*.

3. **Whorl section of the body chamber at midshaft, defined by the intercostal ratio of whorl width to height** (WMS/HMS): equidimensional (WMS/HMS ≈1.0) (0); slightly depressed (WMS/HMS ≈1.15) (1); slightly compressed (WMS/HMS = 0.75–0.90) (2);

very compressed (WMS/HMS = 0.60–0.75) (3); extremely compressed (WMS/HMS = 0.50–0.60) (4). No macroconch of *Trachyscaphites redbirdensis* was complete enough to measure. Instead, we examined a macroconch of *T. spiniger spiniger* (USNM 441417; Cobban and Kennedy, 1992: pl. 7, figs. 1, 2, 5, 9) and a macroconch of *T. spiniger porchi* (USNM 132321; Cobban and Scott, 1964: pl. 3, figs. 10, 11), both of which displayed an equidimensional whorl section at midshaft. In contrast, the whorl section at midshaft is slightly depressed in *Discoscaphites sphaeroidalis* and *D. jerseyensis*, slightly compressed in *D. gulosus* and *D. iris*, very compressed in *D. minardi* and *D. conradi*, and extremely compressed in *D. rossi*.

4. **Curvature of the whorl flanks of the body chamber at midshaft**: slightly curved (0); strongly curved (1); nearly flat (2). The whorl flanks at midshaft are slightly curved in *Trachyscaphites redbirdensis*, *Discoscaphites gulosus*, and *D. iris*, strongly curved in *D. sphaeroidalis* and *D. jerseyensis*, and nearly flat in *D. conradi*, *D. rossi*, and *D. minardi*.

5. **Maximum number of tubercle rows on the body chamber**: ≥ 5 (0); 4 (1); 3 (2). Tubercle rows are labeled as umbilicolateral, flank (inner, middle, outer), inner and outer ventrolateral, and ventral. There is sometimes a discrepancy in usage, with one author referring to a row of tubercles as umbilical and another author referring to it as umbilicolateral. We use these latter two terms interchangeably for the row nearest the umbilical margin. Similarly, some authors refer to the outer ventrolateral row as ventral. We restrict the term ventral to the midventral or siphonal row of tubercles.

All species display two ventrolateral rows, but vary in the number of flank rows. A total of five tubercle rows is present in *Trachyscaphites redbirdensis*. There are as many as seven rows in *D. gulosus* and *D. conradi*, depending on the height of the whorl section. In *D. rossi*, five tubercle rows are present on the largest specimens (see Landman and Waage, 1993: fig. 181F,G), but in smaller specimens, the umbilicolateral tubercles are reduced to weak bullae and the inner ventrolateral tubercles do not develop at all. There are four rows in *D. iris* and *D. sphaeroidalis* and three rows in *D. minardi* and *D. jerseyensis*.

6. **Number of tubercles (X) in the outer ventrolateral row of the body chamber**: $15 < X \leq 20$ (0); $10 \leq X \leq 15$ (1); $25 \leq X \leq 45$ (2). What constitutes a tubercle sometimes becomes an issue, especially near the aperture. According to our criterion, a feature qualifies as a tubercle, even if it is very small or elongate, as long as it shows a conical projection.

There are 19 or 20 ventrolateral tubercles on the holotype of *Trachyscaphites redbirdensis* (referred to as ventral nodes by Cobban and Scott, 1964). The number of ventrolateral tubercles is approximately the same ($15 < X \leq 20$) in *Discoscaphites gulosus*. In contrast, the number of ventrolateral tubercles ranges from 25 to 45 in *D. conradi* and *D. rossi* and from 10 to15 in *D. iris*, *D. sphaeroidalis*, *D. minardi*, and *D. jerseyensis*.

7. **Ventral ribbing on the shaft of the body chamber**: Present (0); absent (1). Ribs are present on the venter of the shaft of the body chamber on *Trachyscaphites redbirdensis*, but they are absent or indistinct in this area on *Discoscaphites*.

8. **Spacing of ventral ribs on the hook, defined as the number of ventral ribs/cm (X)**: widely spaced ($X < 5$) (0); closely spaced ($5 \leq X \leq 10$) (1); very closely spaced ($X \approx 15$) (2). This character is sometimes difficult to assess because the ribs are indistinct on the hook. The spacing of ribs also varies within a species and, therefore, we treated this character as polymorphic. The ribs are widely spaced in *Trachyscaphites redbirdensis* and *Discoscaphites sphaeroidalis*, closely to widely spaced in *D. iris*, closely spaced in *D. gulosus*, closely to very closely spaced in *D. conradi*, and very closely spaced in *D. jerseyensis*, *D. minardi*, and *D. rossi*.

The data matrix (table 7) was analyzed using the data management analysis algorithm Winclada (Nixon, 2002) and the parsimony-based tree-search program NONA ver. 2.0 (Goloboff, 1993). Multistate characters were treated as nonadditive (unordered). All characters were equally weighted. We used a heuristic search, with 1,000 replications of random taxon addition, holding up to 100 trees, with up to 10 starting

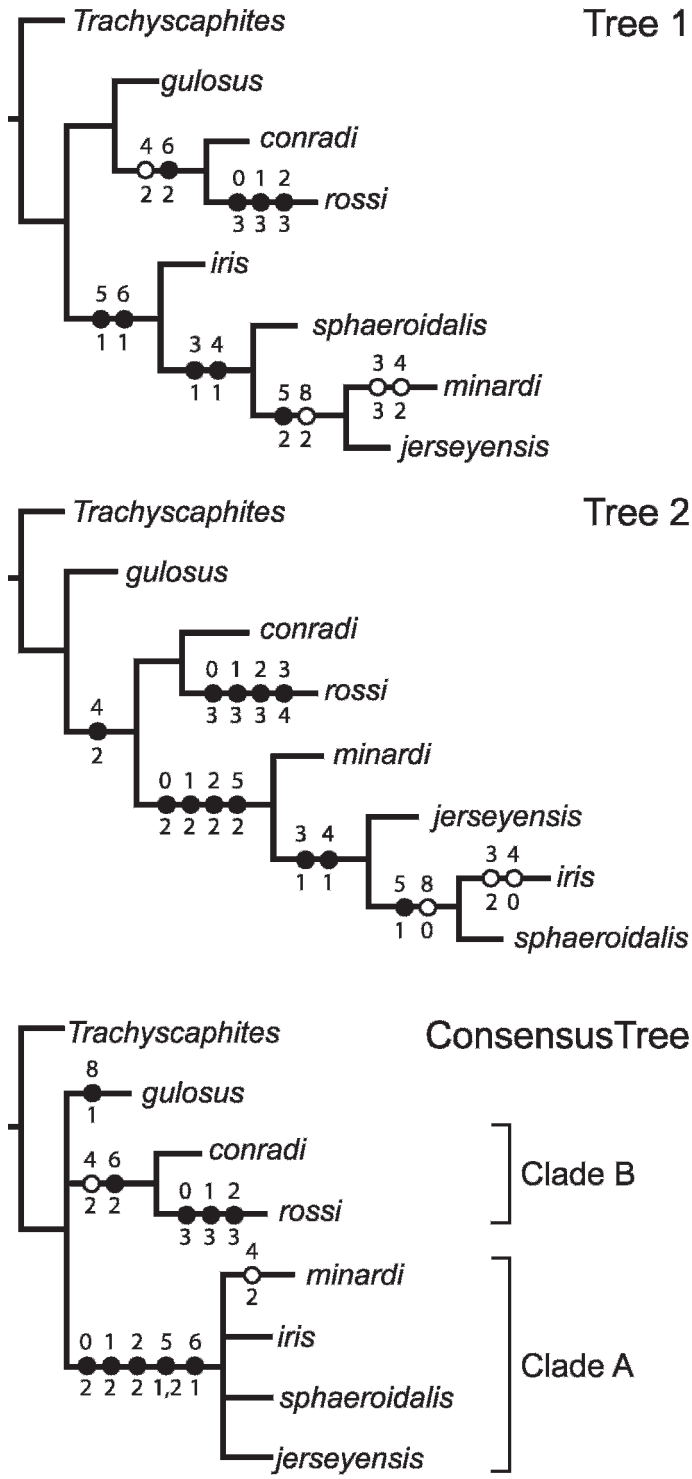
Tree 1
Trachyscaphites
gulosus
conradi
rossi
iris
sphaeroidalis
minardi
jerseyensis
4 6
2 2
0 1 2
3 3 3
5 6
1 1
3 4
1 1
5 8
2 2
3 4
3 2
Tree 2
Trachyscaphites
gulosus
conradi
rossi
minardi
jerseyensis
iris
sphaeroidalis
4
2
0 1 2 3
3 3 3 4
0 1 2 5
2 2 2 2
3 4
1 1
5 8
1 0
3 4
2 0
ConsensusTree
Trachyscaphites
gulosus
conradi
rossi
minardi
iris
sphaeroidalis
jerseyensis
8
1
4 6
2 2
0 1 2
3 3 3
4
2
0 1 2 5 6
2 2 2 1,2 1
Clade B
Clade A

TABLE 7
Matrix of Character States for *Trachyscaphites* and *Discoscaphites*

Taxon	Characters[a]								
	0	1	2	3	4	5	6	7	8
Trachyscaphites	0	0	0	0	0	0	0	0	0
D. conradi	1	1	1	3	2	0	2	1	1,2
D. gulosus	1	1	1	2	0	0	0	1	1
D. iris	2	2	2	2	0	1	1	1	0,1
D. jerseyensis	2	2	2	1	1	2	1	1	2
D. minardi	2	2	2	3	2	2	1	1	2
D. rossi	3	3	3	4	2	0	2	1	2
D. sphaeroidalis	2	2	2	1	1	1	1	1	0

[a]Defined in text.

trees per replicate, and the branch-swapping option multi*max*.

The analysis produced two equally most parsimonious trees (1 and 2) with lengths of 25 steps, CI = 0.88, and RI = 0.78 (fig. 39). In both trees, *Discoscaphites minardi*, *D. jerseyensis*, *D. iris*, and *D. sphaeroidalis* form a monophyletic clade (clade A) supported by small adult size, very tightly coiled body chamber with an apertural angle of 30–40°, a reduced number of tubercle rows (three or four), and 10–15 outer ventrolateral tubercles on the body chamber. The relationships within this clade vary between the two trees, with *D. minardi* and *D. jerseyensis* grouping as sister taxa in tree 1, and *D. iris* and *D. sphaeroidalis* grouping as sister taxa in tree 2. In both trees, there is a sister group relationship between *D. conradi* and *D. rossi* (clade B), which is supported in tree 1 by the large number of outer ventrolateral tubercles on the body chamber (25–45). In tree 1, *D. gulosus* clusters with the clade containing *D. conradi* and *D. rossi*, whereas in tree 2, *D. gulosus* is basal to the rest of the *Discoscaphites*. Because of the topological differences between these two trees, clades A and B and *D. gulosus* collapse to form a trichotomy in the strict consensus tree (fig. 39).

The phylogenetically informative characters in our analysis relate to adult size, degree of uncoiling of the body chamber, apertural angle, and ornament, that is, the number of tubercle rows and the number of outer ventrolateral tubercles on the body chamber. In contrast, the shape of the whorl section (depressed, compressed, equidimensional) and the curvature of the flanks (slightly curved, broadly curved, flat) are subject to homoplasy.

The species in Clade A occur on the Gulf and Atlantic Coastal Plains, with the exception of *Discoscaphites minardi*, which has not yet been documented on the Gulf Coastal Plain. These species represent the youngest scaphites in North America. Analyses of dinoflagellates at sites in New Jersey where all four species co-occur indicate the uppermost Maastrichtian *Palynodinum grallator* Zone, probably the Tpe Subzone of Schiøler and Wilson (1993), corresponding to the upper part of calcareous nannofossil Subzone CC26b. *Discoscaphites minardi* also occurs in Maryland and New Jersey in a stratigraphically slightly lower interval corresponding to the upper part of calcareous nannofossil Subzone CC26a and the lower part of Subzone CC26b (Landman et al., 2004a, 2004b).

The other three species of *Discoscaphites* show slightly different geographic and stratigraphic distributions. *Discoscaphites conradi* and *D. gulosus* are present in the U.S. Western Interior and the Gulf and Atlantic Coastal Plains. Analyses of dinoflagellates at sites in South Dakota and Maryland where both species co-occur indicate the lower part

←

Fig. 39. Phylogenetic relationships among species of *Discoscaphites* from North America based on the data matrix in table 7. The analysis produced two equally most parsimonious trees (1 and 2) with lengths of 25 steps, CI = 0.88, and RI = 0.78. In both trees, *Discoscaphites minardi*, *D. jerseyensis*, *D. iris*, and *D. sphaeroidalis* form a monophyletic clade (clade A) supported by small adult size, very tightly coiled body chamber with an apertural angle of 30°–40°, a reduced number of tubercle rows (three or four), and 10–15 outer ventrolateral tubercles on the body chamber. Symbols: numbers above the line refer to characters 0–8; numbers below the line refer to character states; closed circles indicate synapomorphies or autapomorphies; open circles indicate homoplasies.

of the upper Maastrichtian, corresponding to calcareous nannofossil Subzone CC25b (Palamarczuk et al., 2003; Landman et al., 2004a, 2004b). Two specimens of *D. gulosus* have also been reported from New Jersey from a higher stratigraphic interval in association with *D. iris*. This interval corresponds to the upper part of calcareous nannofossil Subzone CC26b (Landman et al., 2004b; this report), suggesting that *D. gulosus* has a relatively long stratigraphic range. [Another specimen of this species has been reported from the Inversand Marl Pit, Gloucester County, New Jersey, but its biostratigraphic position has not yet been resolved (Landman et al., 2004b)]. *Discoscaphites rossi* co-occurs with *D. gulosus* and *D. conradi* in the Timber Lake Member of the Fox Hills Formation in South Dakota (Landman and Waage, 1993: 232).

Although we did not consider the species of *Discoscaphites* outside of North America, studies in progress by Machalski et al. suggest that *D. acutituberculatus* is conspecific with *D. gulosus*. It is reported from the upper Maastrichtian of Bulgaria (Tzankov, 1982). *Discoscaphites kambysis* is only known from phragmocones, but it is very compressed, with as many as five rows of tubercles, suggesting a close affinity with *D. conradi*. It occurs in the upper Maastrichtian calcareous nannofossil Subzone CC25c in the Eastern Desert, Egypt (Kennedy and Kulbrok, 2003).

Discoscaphites iris (Conrad, 1858)
figures 40–46, 47A–C

Scaphites iris Conrad, 1858: 335, pl. 35, fig. 23.
Scaphites iris Conrad. Whitfield, 1892: 265, pl. 44, figs. 4–7.
Discoscaphites iris (Conrad). Stephenson, 1955: 134, pl. 23, figs. 23–30.
Discoscaphites iris (Conrad, 1858). Kennedy and Cobban, 2000: 183, fig. 5; pl. 3, figs. 3–35.
Discoscaphites iris (Conrad, 1858). Landman et al., 2004a: 39, figs. 15A,B,G–O, 17A–G, 18R.
Discoscaphites iris (Conrad, 1858). Landman et al., 2004b: figs. 34E–W (*non* A–D = *Discoscaphites sphaeroidalis* Kennedy and Cobban, 2000), 35, 36A–H,K–Q,S–Z,l–p, 37A–l, 38, 39A–P, 41A–D.

TYPE: The holotype is the original illustrated in Conrad, 1858: 335, pl. 35, fig. 23, labeled ANSP 50989, from the bluffs of Owl Creek, Tippah County, Mississippi. See Landman et al. (2004b) for a more complete description of this specimen.

MATERIAL: Approximately 300 specimens, consisting of most of the body chamber or parts of the phragmocone and body chamber, plus numerous fragments, in the AMNH and MAPS collections. All of the specimens are from the Manasquan River Basin. They are primarily derived from the *Pinna* Layer at the top of the Tinton Formation (≈90% of the specimens). The rest of them were collected from the underlying 25 cm of the Tinton Formation below the *Pinna* Layer (≈7%) and as reworked material in the basal Hornerstown Formation (< 3%). (These percentages may reflect variation in the degree of collecting effort. It was much easier and more rewarding to collect in the *Pinna* Layer than in the other two intervals.)

The preservation of the scaphites in each of these layers is different. Specimens from the Tinton Formation below the *Pinna* Layer are black, those from the *Pinna* Layer are orange-brown and occasionally sideritized, and those from the basal Hornerstown Formation are black and almost always sideritized. Some of the phragmocones in the *Pinna* Layer and the basal Hornerstown Formation are hollow, with parts of the siphuncle exposed.

As indicated previously, many of the specimens occur in clusters. In one of the clusters (fig. 6), almost all of the specimens are mature microconchs. In other clusters,

→

Fig. 40. *Discoscaphites iris* (Conrad, 1858), macroconchs, *Pinna* Layer, Tinton Formation, Manasquan River Basin, Monmouth County, New Jersey. **A–D.** AMNH 50545. **A.** Right lateral; **B.** apertural; **C.** ventral; **D.** left lateral. **E–H.** AMNH 50540. **E.** Right lateral; **F.** apertural; **G.** ventral; **H.** left lateral. **I–L.** AMNH 47430. **I.** Right lateral; **J.** apertural; **K.** ventral; **L.** left lateral. **M–P.** AMNH 50396, with midventral row of tubercles. **M.** Right lateral; **N.** apertural; **O.** ventral; **P.** left lateral. All figures ×1.

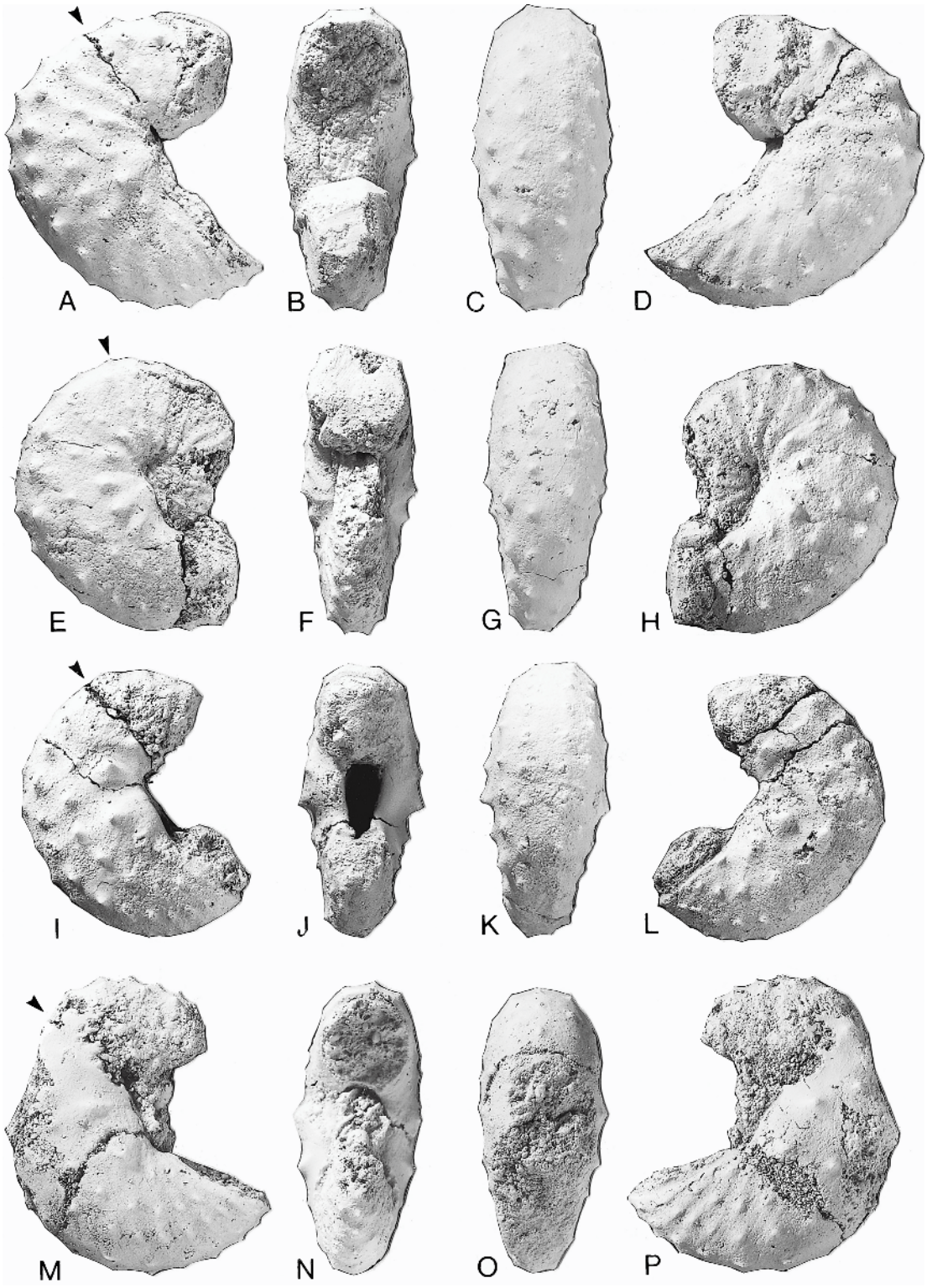
A
B
C
D
E
F
G
H
I
J
K
L
M
N
O
P

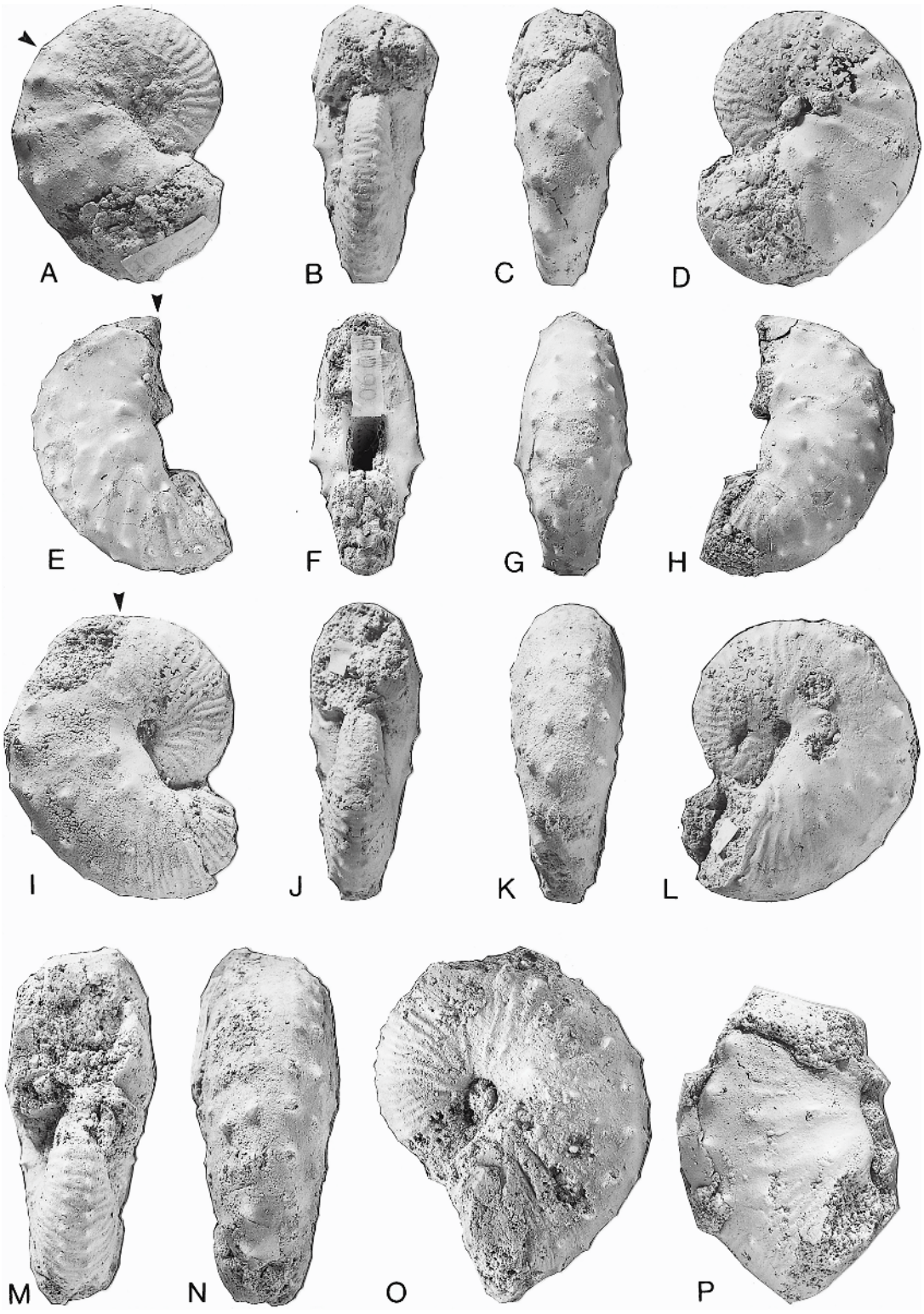
A
B
C
D
E
F
G
H
I
J
K
L
M
N
O
P

there is a mixture of dimorphs, but microconchs are almost always more common. Still other clusters are mostly made up of juveniles.

In the Manasquan River Basin, microconchs are more abundant than macroconchs. In a sample of nearly complete specimens (n = 131), there are 78 microconchs and 53 macroconchs. If we expand our sample to include all fragments in which the dimorph can be identified, the numbers increase to 139 microconchs and 80 macroconchs. (These numbers may be slightly inflated because some fragments may represent parts of the same individual, but presumably this bias would affect microconchs and macroconchs equally.) The ratio of microconchs to macroconchs in the total sample is 1.7. The predominance of microconchs may reflect ecological preferences or, more likely, taphonomic processes that favored microconchs, for example, massive die-offs after mating, assuming that microconchs represented males and displayed the same reproductive behavior as modern coleoids (see Boyle and Rodhouse, 2005).

DESCRIPTION: As documented in other scaphites (Cobban, 1969; Landman and Waage, 1993), this species is strongly dimorphic. It also displays a range of variation, from more robust specimens with prominent tubercles such as AMNH 50545 (fig. 40A–D) to more compressed specimens with weaker tubercles such as AMNH 50755 (fig. 41I–L). However, it is noteworthy that the variation in size and ornament within a single cluster is much smaller than that in the whole sample.

MACROCONCH DESCRIPTION: Specimens are tightly coiled with a tiny umbilicus. They range in maximum length from 32 to 54 mm, with most specimens between 38 and 46 mm; the average size is 43 mm (fig. 46, table 8). In side view, the venter of the phragmocone passes smoothly into that of the body chamber. The body chamber occupies approximately one-half whorl and shows a bulge on the umbilical shoulder. There is no gap between the body chamber and the phragmocone. The apertural angle is low and ranges from approximately 20 to 43° (table 8). The apertural margin is constricted and the venter and dorsum are slightly projected.

The phragmocone is slender with a ratio of whorl width to height of approximately 0.6 to 0.7 at the ultimate septum (table 8). The whorl section is compressed ovoid with maximum width at one-quarter whorl height. The umbilical wall is steep and inclined slightly outward and the umbilical shoulder is gently rounded. In intercostal section, the flanks are flat to broadly rounded and gradually converge toward the venter, becoming more steeply convergent at the site of the inner ventrolateral tubercles. The ventrolateral shoulder is sharply rounded and the venter is nearly flat.

The body chamber is fairly robust. The intercostal ratio of whorl width to height at midshaft ranges from approximately 0.8 to 0.9 (table 8). The whorl section is compressed ovoid with maximum width at one-third whorl height. The umbilical wall is steep and convex and the umbilical shoulder is broadly rounded. The inner flanks are nearly flat and inclined outward, the mid-flanks are nearly flat to broadly rounded, and the outer flanks between the inner and outer ventrolateral tubercles are flat and converge toward the venter. The ventrolateral shoulder is sharply rounded and the venter is nearly flat.

As in other scaphites, the body chamber undergoes a series of modifications in passing from the midshaft to the aperture. Both the whorl width and height decrease, but not at the same rate, so that the whorl section becomes nearly subquadrate. The ratio of

←

Fig. 41. *Discoscaphites iris* (Conrad, 1858), macroconchs, *Pinna* Layer, Tinton Formation, Manasquan River Basin, Monmouth County, New Jersey. **A–D.** MAPS A2060b2. **A.** Right lateral; **B.** apertural; **C.** ventral; **D.** left lateral. **E–H.** MAPS A2060b5, sideritized. **E.** Right lateral; **F.** apertural; **G.** ventral; **H.** left lateral, with an extra tubercle between the flank and inner ventrolateral rows of tubercles. **I–L.** AMNH 50755. **I.** Right lateral, with a hole in the adapical end of the body chamber; **J.** apertural; **K.** ventral; **L.** left lateral. **M–O.** MAPS A2060b3. **M.** Apertural; **N.** ventral; **O.** left lateral. **P.** AMNH 50406, right lateral. All figures ×1.

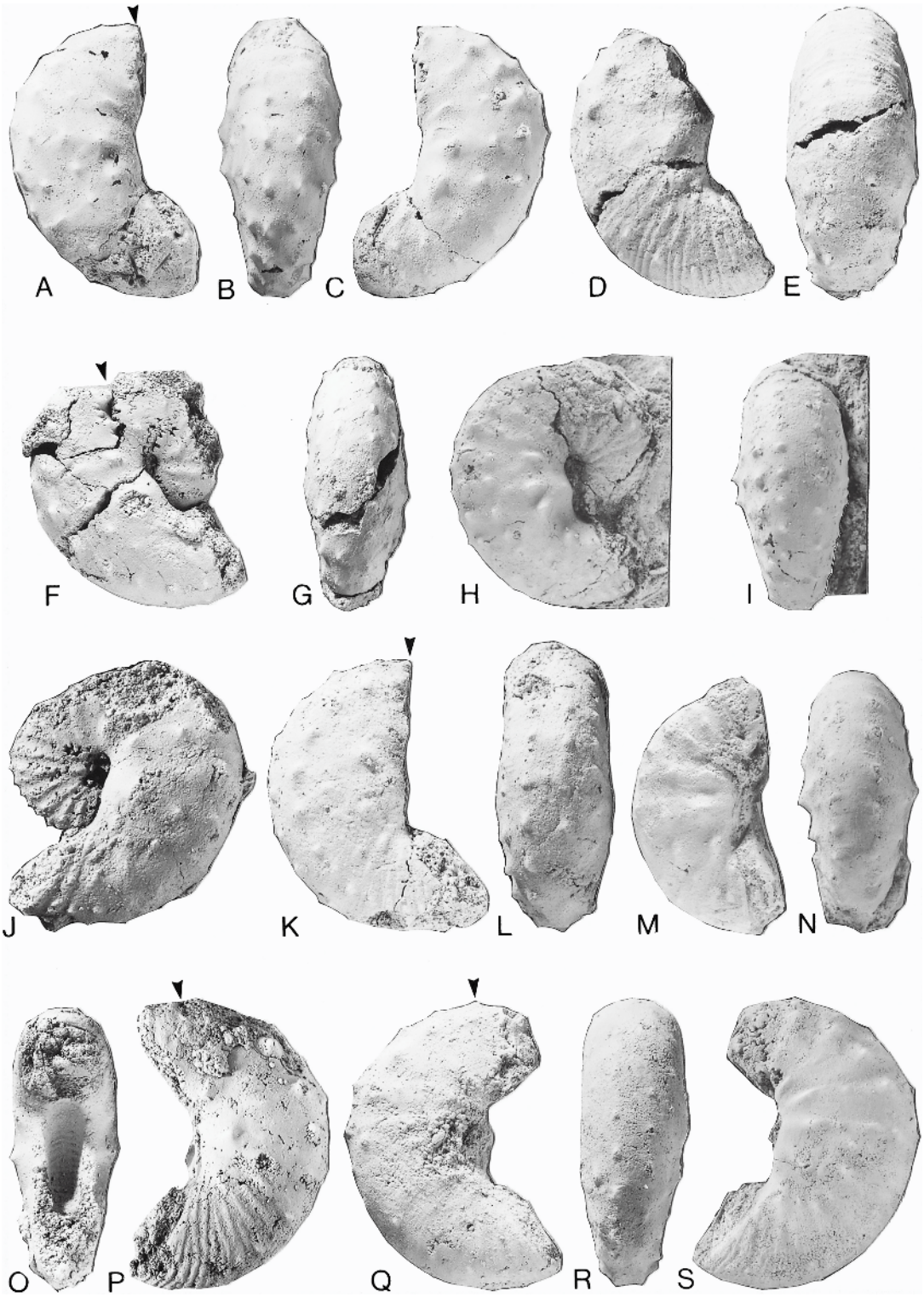
A
B
C
D
E
F
G
H
I
J
K
L
M
N
O
P
Q
R
S

whorl width to height at the aperture ranges from approximately 0.9 to 1.0 (table 8).

The ribs on the phragmocone are rectiradiate to prorsiradiate. In coarsely ornamented specimens such as AMNH 50710 (fig. 42J), the ribs are straight and barlike at the adapical end of the exposed phragmocone. In contrast, in more finely ornamented specimens such as AMNH 50755 (fig. 41I–L), the ribs are slightly flexuous, curving backward on the inner flanks, forward and then backward on the midflanks, and forward again on the outer flanks, crossing the venter with a slight adoral projection. There are 10 ribs/cm on the venter of the adapical part of the phragmocone in MAPS A2060b2 (fig. 41A–D). Intercalation and branching occur at one-third and two-thirds whorl height. The ribs become broader, straighter, and more widely spaced toward the adoral end of the phragmocone. They weaken on the venter, forming indistinct swellings, before disappearing altogether.

In coarsely ornamented specimens, all four rows of tubercles—umbilicolateral, flank, and inner and outer ventrolateral tubercles—are already present on the adapical end of the exposed phragmocone. In more finely ornamented specimens, only the outer ventrolateral tubercles are present at this point. The other three rows appear soon thereafter, although the flank tubercles sometimes do not appear until the adapical end of the body chamber.

The ornament on the body chamber consists of four rows of tubercles on low, broad, convex ribs. The ribs are indistinct on the shaft but more prominent on the hook, where they range from coarse to relatively fine. For example, there are 3 ventral ribs/cm on the hook of AMNH 50392 (fig. 43N,O) and 9 ventral ribs/cm on the hook of MAPS A2060b22 (not illustrated). The ribs cross the venter with a broad convexity.

All of the tubercles on the body chamber are fairly sharp, even on relatively compressed specimens. The number of umbilicolateral tubercles averages 5 and ranges from 4 to 7. The one or two tubercles on the midshaft just below the umbilical bulge are the most prominent tubercles on the shell. The midflank row of tubercles is generally equidistant between the umbilicolateral and inner ventrolateral rows. It is slightly subdued relative to the umbilicolateral row and consists of 5 to 11 tubercles, averaging 7. The midflank tubercles are more or less evenly spaced but become slightly approximated near the aperture, where they diminish in size and, occasionally, disappear altogether, as in AMNH 50755 (fig. 41I–L) and AMNH 50395 (fig. 43P–S). The inner ventrolateral tubercles are more pronounced than the midflank tubercles. The number of inner ventrolateral tubercles averages 12 and ranges from 8 to 15. They are more or less evenly spaced, with some approximation near the aperture. The strongest inner ventrolateral tubercles occur on the midshaft, and the weakest ones occur on the hook; they rarely ever disappear. These tubercles sometimes develop a clavate shape on the shaft, as in AMNH 50398 (fig. 43A–D). The inner and outer ventrolateral rows of tubercles are closely spaced together. The number of tubercles in the outer ventrolateral row is approximately the same as or slightly greater than that in the inner ventrolateral row. The outer ventrolateral tubercles are slightly weaker than the inner ventrolateral tubercles and, in rare specimens such as AMNH 50398 (fig. 43A–D), they develop a clavate shape on the shaft. The outer ventrolateral tubercles become slightly smaller and more closely spaced on the hook. They

←

Fig. 42. *Discoscaphites iris* (Conrad, 1858), macroconchs, *Pinna* Layer, Tinton Formation, Manasquan River Basin, Monmouth County. **A–C.** AMNH 50754. **A.** Right lateral; **B.** ventral; **C.** left lateral. **D,E.** AMNH 50773. **D.** Right lateral; **E.** ventral. **F,G.** AMNH 50409. **F.** Right lateral; **G.** ventral. **H,I.** MAPS A2060b21. **H.** Right lateral; **I.** ventral. **J.** AMNH 50710, left lateral, with a hole in the adapical end of the body chamber. **K,L.** AMNH 50753. **K.** Right lateral; **L.** ventral. **M,N.** MAPS A2060b24. **M.** Right lateral; **N.** ventral. **O,P.** AMNH 50391. **O.** Apertural; **P.** left lateral. **Q–S.** AMNH 50782. **Q.** Right lateral; **R.** ventral; **S.** left lateral. All figures ×1.

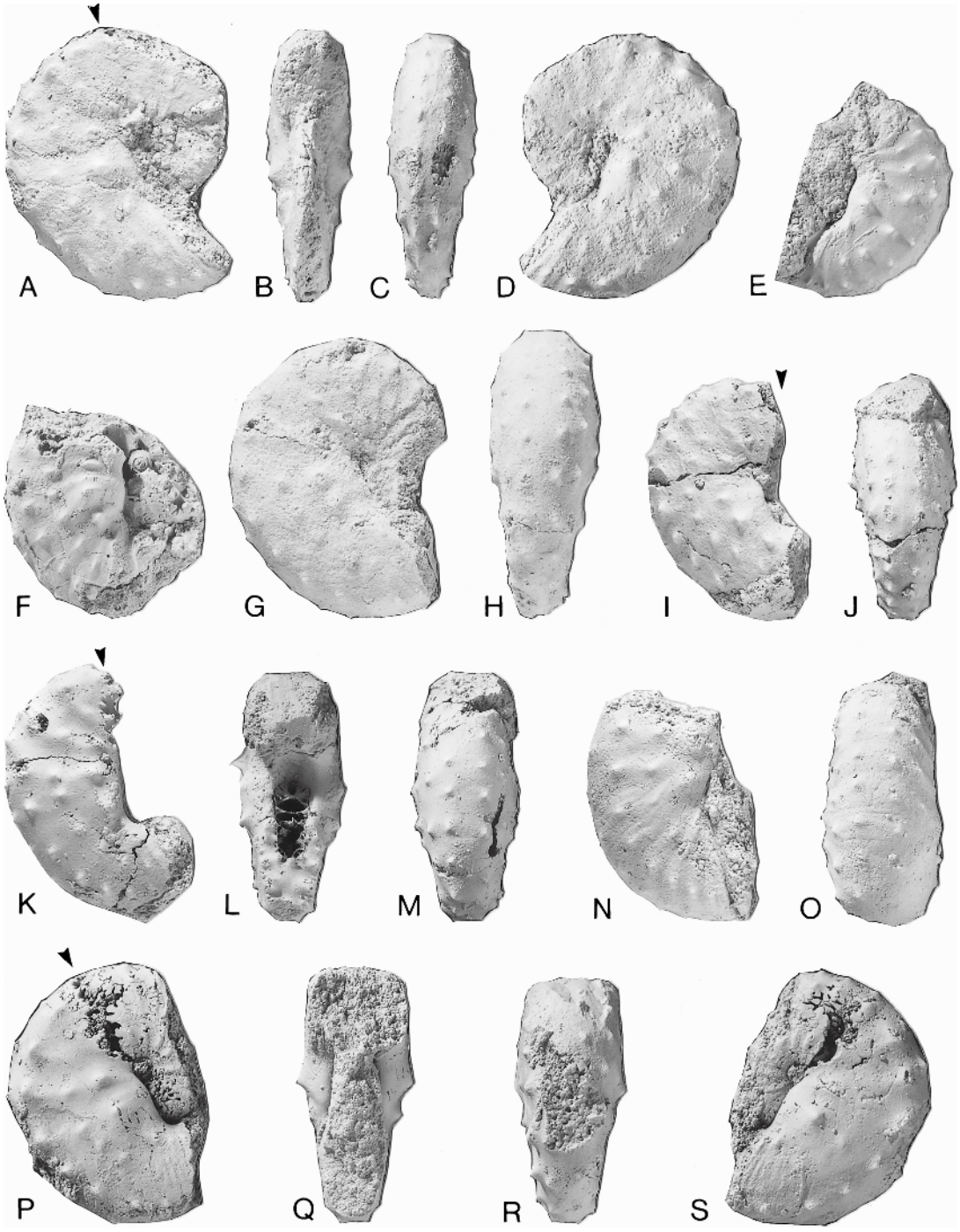

Fig. 43. *Discoscaphites iris* (Conrad, 1858), macroconchs. **A–E, G–S.** *Pinna* Layer and the underlying part of the Tinton Formation (as indicated), Manasquan River Basin, Monmouth County, New Jersey. **A–D.** AMNH 50398, slightly crushed, underlying part of the Tinton Formation. **A.** Right lateral; **B.** apertural; **C.** ventral; **D.** left lateral. **E.** AMNH 50387, small specimen, partially sideritized, left lateral. **G,H.** AMNH 50756. **G.** Right lateral; **H.** ventral. **I,J.** AMNH 50389. **I.** Right lateral; **J.** ventral. **K–M.**

are sometimes paired and sometimes offset on either side of the venter.

There are several exceptions to this general pattern of ornament on the body chamber: (1) In AMNH 50396 (fig. 40M–P), a midventral row of tubercles appears on the phragmocone and extends to the aperture. The tubercles are evenly spaced and similar in size to the outer ventrolateral tubercles. (2) In MAPS A2060b24 (fig. 42M,N), only three rows of tubercles are present on each side of the specimen. A single row of ventrolateral tubercles replaces the usual double row. This is matched by microconchs with only three rows of tubercles. (3) Two specimens display additional tubercles besides those in the four tubercle rows. In MAPS A2060b5 (fig. 41E,H), a single tubercle occurs between the rows of flank and inner ventrolateral tubercles and in AMNH 50782 (fig. 42Q–S), two tubercles occur between the rows of umbilicolateral and flank tubercles and a single tubercle occurs between the rows of flank and inner ventrolateral tubercles. (4) In AMNH 50391 (fig. 42O,P), AMNH 50753 (fig. 42K,L), and AMNH 50773 (fig. 42D,E), the flank tubercles are weak and develop into ribs or bullae on the hook, which is covered with relatively fine ribbing. These features are similar to those in *Discoscaphites minardi* but the shape of the whorl section is very different. The flanks of the body chamber are inflated in these specimens, whereas they are flat and subparallel in *D. minardi*.

The suture is similar to that of other species of *Discoscaphites*, with a broad first lateral saddle and an asymmetrically bifid first lateral lobe (fig. 47A, B).

MICROCONCH DESCRIPTION: Microconchs are generally smaller than macroconchs. The maximum length averages approximately 35 mm and ranges from approximately 29 to 41 mm (fig. 46, table 8). The ratio of the average size of macroconchs to that of microconchs is 1.2. The shell is tightly coiled but, unlike macroconchs, the umbilical seam of microconchs follows the curvature of the venter. There is a very small gap between the phragmocone and body chamber. The end of the phragmocone occurs at the line of maximum length and the body chamber occupies approximately one-half whorl. The aperture is constricted and the venter and dorsum are slightly projected.

The whorl section of the phragmocone is compressed ovoid. The intercostal ratio of whorl width to height at the ultimate septum averages approximately 0.7 and ranges from approximately 0.6 to 0.9 (table 8). The umbilical wall is steep and subvertical and the umbilical shoulder is sharply rounded. The inner flanks are flat and slightly divergent, the midflanks are flat to broadly rounded, and the outer flanks between the inner and outer ventrolateral tubercles are flat and gently converge to the venter. The ventrolateral shoulder is relatively sharply rounded and the venter is nearly flat.

In passing into the body chamber, whorl width expands more rapidly than whorl height, producing a swollen whorl section at midshaft. The intercostal whorl section is subquadrate and ranges from slightly compressed to slightly depressed, with maximum width at the umbilical shoulder. The ratio of whorl width to height averages approximately 1.0 and ranges from approximately 0.7 to 1.2 (table 8). The umbilical wall is broad, steep, and subvertical and the umbilical shoulder is abruptly rounded. The inner flanks are flat and slightly divergent, the midflanks are flat to broadly rounded, and the outer flanks are flat and convergent. The ventrolateral shoulder is broadly to sharply rounded and the venter is nearly flat. The whorl dimensions are approximately the same at the aperture, with the ratio of whorl width to height averaging approximately 1.0 (table 8).

The phragmocone is covered with prorsiradiate straight ribs. In coarsely ornamented forms, e.g., MAPS A2060b8 (fig. 45E), the

←

AMNH 50399, partially sideritized, with a hollow phragmocone. **K.** Right lateral; **L.** apertural; **M.** ventral. **N,O.** AMNH 50392. **N.** Right lateral; **O.** ventral. **P–S.** AMNH 50395, partially sideritized. **P**. Right lateral; **Q.** apertural; **R.** ventral; **S.** left lateral. **F.** AMNH 8916/1, sideritized, with a hollow phragmocone, right lateral, collected in the late 19th or early 20th century, ?New Jersey. All figures ×1.

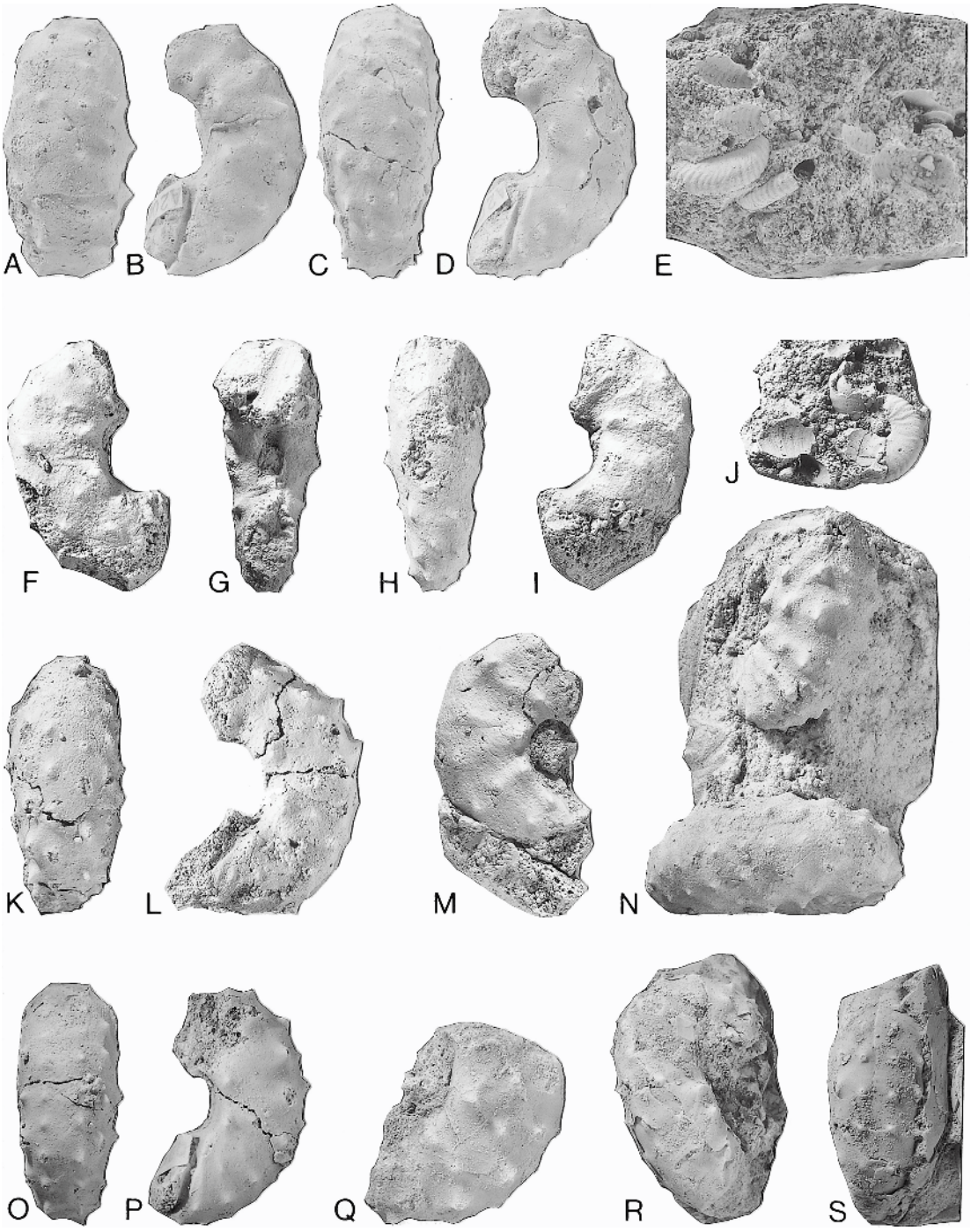

Fig. 44. *Discoscaphites iris* (Conrad, 1858). **A–Q.** *Pinna* Layer, Tinton Formation, and reworked material at the base of the Hornerstown Formation (as indicated), Manasquan River Basin, Monmouth County, New Jersey. **A,B.** MAPS A2060b34, a microconch. **A.** Ventral; **B.** left lateral. **C,D.** MAPS A2060b33, a microconch. **C.** Ventral; **D.** left lateral. **E.** MAPS A2060b1, part of a cluster of juveniles, with the bottom side down. **F–I.** AMNH 50711, a microconch. **F.** Right lateral; **G.** apertural; **H.** ventral; **I.** left

ribs are barlike, whereas in more finely ornamented forms, e.g., MAPS A2060b9 (fig. 45K–N), the ribs are slightly flexuous. Branching and intercalation occur at one-third and two-thirds whorl height. The ventral ribs are faint, straight, and swollen and join ventrolateral tubercles on either side of the venter. Both rows of ventrolateral tubercles are present at the adapical end of the exposed phragmocone and the other two rows appear soon thereafter. Tubercles in all four rows gradually become more widely spaced toward the adoral end of the phragmocone.

The ornament on the body chamber consists of swollen, poorly defined prorsiradiate ribs bearing four rows of tubercles. Ribs are only conspicuous near the aperture. There are 3 to 5 umbilicolateral tubercles, averaging 4, perched on the umbilical shoulder, which attain their greatest height just adoral of midshaft. The number of midflank tubercles is higher, ranging from 6 to 9, averaging 7. These tubercles also attain their greatest height just adoral of midshaft and usually become bullate near the aperture. In contrast, the inner ventrolateral tubercles attain their greatest height just adapical of midshaft where they sometimes assume a clavate shape. There are 8 to 16 inner ventrolateral tubercles, averaging 11, with more coarsely ornamented specimens having fewer, larger tubercles—compare AMNH 50401 (fig. 44K,L) with AMNH 50772 (fig. 45P–S). The outer ventrolateral tubercles are slightly more numerous, and like the inner ventrolateral tubercles, are smaller and more closely spaced on the hook. The outer ventrolateral tubercles are matched or offset on either side of the venter.

The suture is the same as that in macroconchs (fig. 47C).

DISCUSSION: *Discoscaphites iris* is characterized by four rows of tubercles, but in rare specimens, a midventral row is present or one of the four rows is absent, either the midflank row or one of the two ventrolateral rows. *Discoscaphites iris* differs from the closely related species *D. minardi* in having a more robust body chamber with inflated flanks, more sharply pointed, conical tubercles, and coarser ribbing at the aperture. The distinction between the two species is reminiscent of that between *D. gulosus* and *D. conradi*, as discussed by Jeletzky and Waage (1978).

The specimens of *Discoscaphites iris* from the Manasquan River Basin are very similar to those described from the Owl Creek Formation and as reworked material at the base of the Clayton Formation in Mississippi, Tennessee, and Missouri (Stephenson, 1955: pl. 23, figs. 23–30; Sohl, 1960, 1964; Kennedy and Cobban, 2000: pl. 3, figs. 3–35) and from the top of the New Egypt Formation and as reworked material at the base of the Hornerstown Formation in northeastern Monmouth County, New Jersey (Landman et al., 2004b: figs 34E–W, 35, 36A–H,K–Q,S–Z,l–p, 37A–l, 38, 39A–P, 41A–D). There are only two significant differences. The collections from the Manasquan River Basin contain a specimen with a midventral row of tubercles and several very large specimens, the largest of which is incomplete but, if entire, would have been at least 54 mm in maximum length. These differences probably reflect the expanded size of our collections, which undoubtedly include more rare specimens.

With *Discoscaphites iris* as abundant as it is in New Jersey, albeit from only a few localities, it is surprising that it has never been described before. In fact, it has occasionally been mentioned from New Jersey, but never in a definitive way. Whitfield (1892) described *D. iris* in his publication on the fossils of the Greensand Marls. He cited Meek as having included this species in his list of New Jersey

←

lateral. **J.** AMNH 50403, juvenile with body chamber, left lateral. **K,L.** AMNH 50401, a microconch. **K.** ventral, **L.** left lateral. **M.** AMNH 50407, a microconch, right lateral. **N.** MAPS A2060b29a,b, two microconchs in the same cluster. **O,P.** MAPS A2060b31, a microconch, with a subdued row of flank tubercles. **O.** Ventral; **P.** left lateral. **Q.** AMNH 50733, a microconch, left lateral, reworked, base of the Hornerstown Formation. **R,S.** Holotype, a microconch, ANSP 50989, bluffs along Owl Creek, Mississippi. **R.** Right lateral; **S.** ventral. All figures ×1.

fossils (the list was, in fact, compiled by Conrad, not Meek). However, the specimens Whitfield described and illustrated are from Mississippi, although he noted that the specimen of *D. iris* originally figured by Conrad (the holotype) was in a tray marked "*S. reniformis* Cret. N.J.," a coincidence he discounted. Whitfield (1892: 266, 267) added, with an eye toward the future, that "I have seen no example from New Jersey myself that could be referred to this species, although Mr. Meek [actually Conrad] cites it as from the State, probably basing his identification on those mentioned above. I give the species here to help in the identification should specimens of it be found in future, that the record may be as perfect as possible."

As a curious footnote, the collection of fossil invertebrates at the American Museum of Natural History includes a specimen (AMNH 8916/1) labeled "*Scaphites conradi* Morton sp. Cretaceous, Lower Green Marls ?New Jersey." It is, in fact, a macroconch of *Discoscaphites iris* embedded in a siderite nodule and consisting of a hollow phragmocone and part of the body chamber (fig. 43F). It is black in color and is probably from the top of the New Egypt Formation or the base of the Hornerstown Formation, possibly from an abandoned borrow pit near Tinton Falls, New Jersey (see Gallagher, 1993, for a short discussion of the borrow pits that were active in New Jersey in the late 19th century). This specimen is not listed in the catalog of fossil invertebrates prepared by Whitfield and Hovey (1898). However, the specimen number is part of a sequence of numbers assigned to ammonites and other fossils from New Jersey that are illustrated in Whitfield (1892).

OCCURRENCE: Upper part of the Tinton Formation and as reworked material at the base of the Hornerstown Formation, Manasquan River Basin, central Monmouth County, New Jersey. Elsewhere in New Jersey, this species occurs in the upper part of the New Egypt Formation and as reworked material at the base of the Hornerstown Formation, Parkers Creek, near Eatontown, northeastern Monmouth County (Landman et al., 2004b) and in the upper part of the New Egypt Formation in the Crosswicks Creek Basin, southwestern Monmouth County (Landman et al., in prep.). Elsewhere on the Atlantic Coastal Plain, it occurs in the upper part of the Severn Formation, Kent and Anne Arundel Counties, Maryland (Landman et al., 2004a). On the Gulf Coastal Plain, it occurs in the Owl Creek Formation and as reworked material at the base of the Clayton Formation in Mississippi, Tennessee, and Missouri (Stephenson, 1955; Sohl, 1960, 1964; Kennedy and Cobban, 2000). G. Keller (personal commun., 2005) also reported it from a core in the upper part of the Corsicana Formation along the Brazos River, Falls County, Texas. It is the name bearer of the *Discoscaphites iris* Zone on the Gulf and Atlantic Coastal Plains, which represents the upper part of the upper Maastrichtian, corresponding to the upper part of calcareous nannofossil Subzone CC26b.

Discoscaphites sphaeroidalis Kennedy and Cobban, 2000
figures 47D, 48

Discoscaphites sp. Stephenson, 1955: 135, pl. 23, figs. 20–22.

Discoscaphites sphaeroidalis Kennedy and Cobban, 2000: 185, pl. 1, figs. 1–11, text-fig. 6.

→

Fig. 45. **A–U.** *Discoscaphites iris* (Conrad, 1858), microconchs, *Pinna* Layer, Tinton Formation, Manasquan River Basin, Monmouth County, New Jersey. **A–D.** AMNH 50703. **A.** Right lateral, with a hole in the adapical end of the body chamber; **B.** apertural; **C.** ventral; **D.** left lateral. **E.** MAPS A2060b8, left lateral. **F–H.** MAPS A2060b7. **F.** Right lateral; **G.** ventral; **H.** left lateral. **I,J.** AMNH 50397. **I.** Right lateral; **J.** ventral. **K–N.** MAPS A2060b9. **K.** Right lateral; **L.** apertural; **M**. ventral; **N.** left lateral. **O.** AMNH 50390, small specimen, right lateral. **P–S.** AMNH 50772. **P.** Right lateral; **Q.** apertural; **R.** ventral; **S.** left lateral. **T.** AMNH 50405, small specimen, left lateral. **U.** AMNH 50400, right lateral. **V–a.** *Discoscaphites minardi* Landman et al., 2004a, same locality as **A–U**. **V–Y.** AMNH 50693, a microconch. **V.** Right lateral, with a hole in the body chamber; **W.** apertural; **X.** ventral; **Y.** left lateral. **Z.** AMNH 50402, a microconch, left lateral. **a.** AMNH 51326, part of hook, left lateral. All figures ×1.

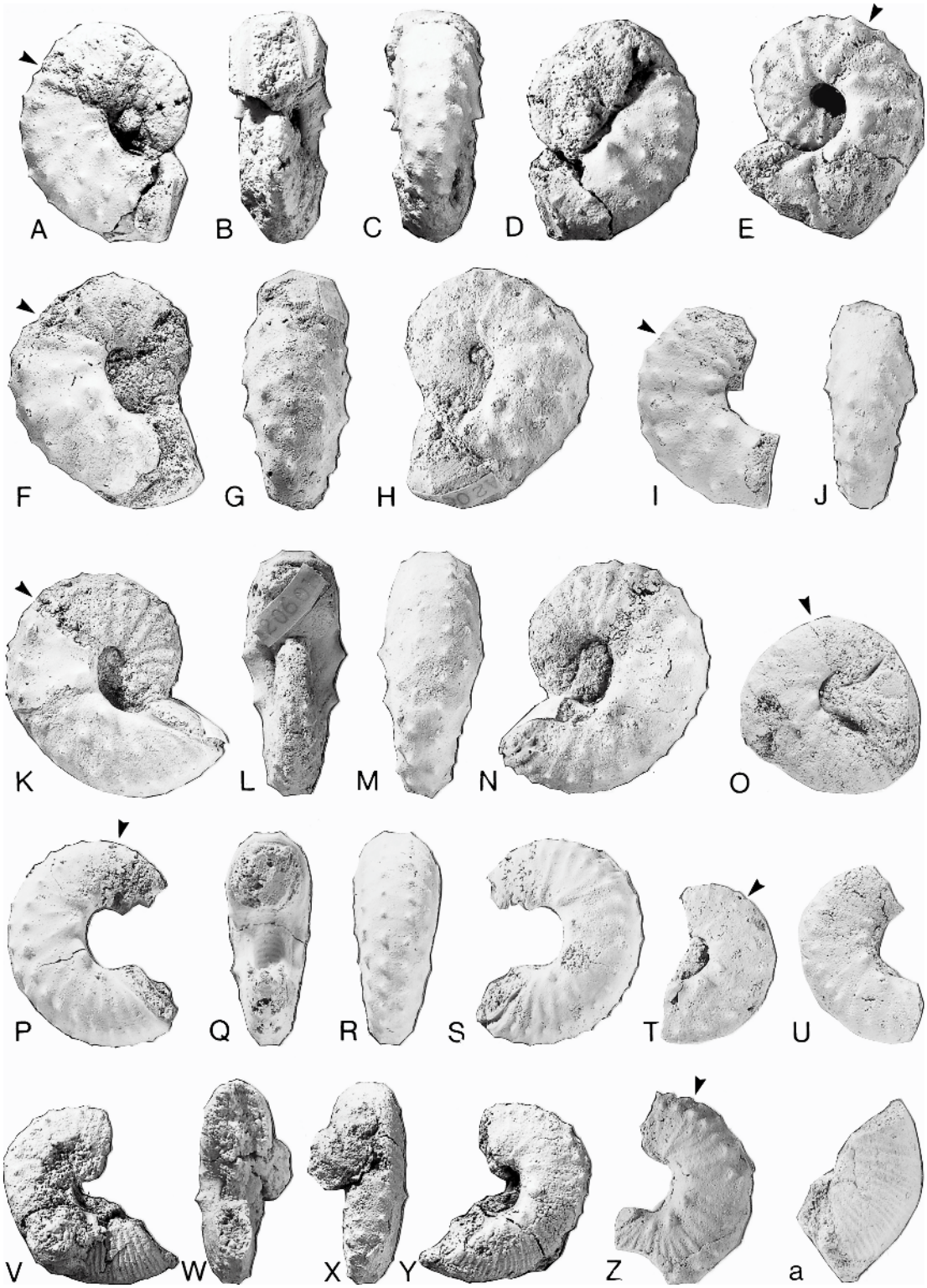
A
B
C
D
E
F
G
H
I
J
K
L
M
N
O
P
Q
R
S
T
U
V
W
X
Y
Z
a

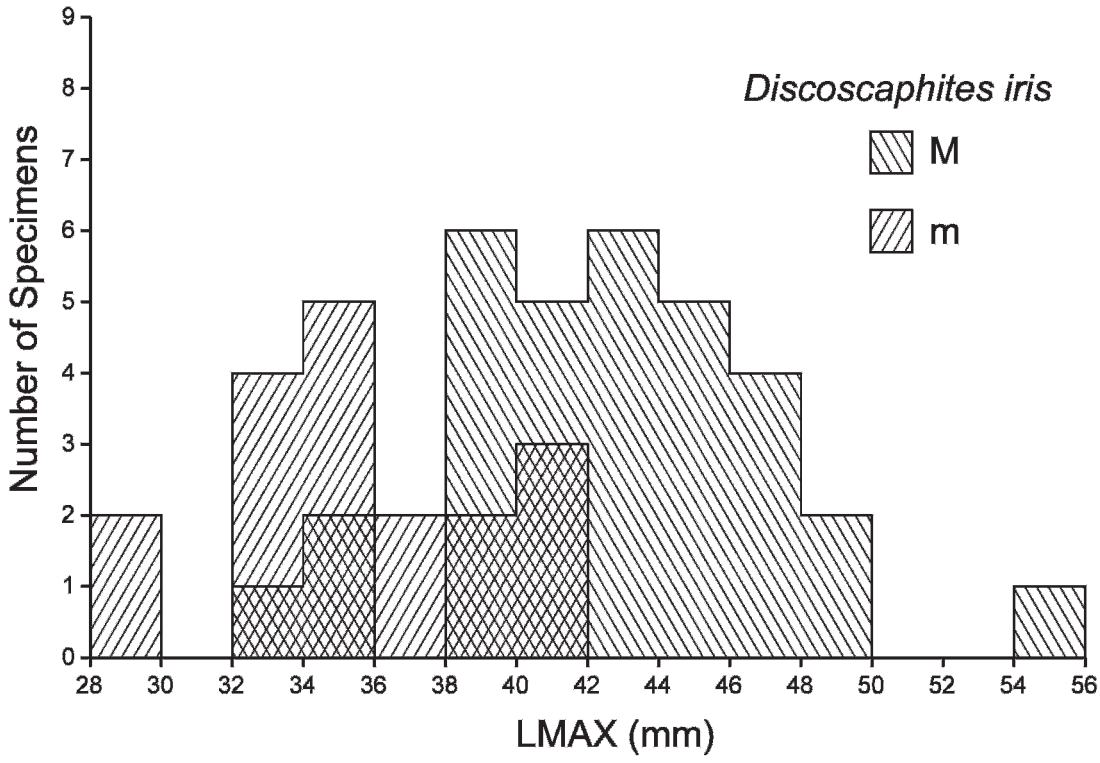

Fig. 46. Size frequency histogram of a sample of *Discoscaphites iris* (Conrad, 1858) from the upper part of the Tinton Formation, mostly the *Pinna* Layer, Manasquan River Basin, Monmouth County, New Jersey.

Discoscaphites sphaeroidalis Kennedy and Cobban, 2000. Kennedy et al., 2001: 169, figs. 4b,c.

Discoscaphites iris (Conrad, 1858). Landman et al., 2004b: 71, fig. 34A–D.

TYPE: The holotype is USNM 465615, a macroconch missing part of the hook, from the Owl Creek Formation at its type locality, 4 km northeast of Ripley, Tippah County, Mississippi.

MATERIAL: Five specimens consisting of four macroconchs (MAPS A2063a1, 2, and 3 and AMNH 50752) and one microconch (AMNH 50713) from the *Pinna* Layer at the top of the Tinton Formation, Manasquan River Basin, Monmouth County, New Jersey.

MACROCONCH DESCRIPTION: The two nearly complete specimens range from 39.3 to 49.7 mm in maximum length (table 9). The shell is inflated with a tiny umbilicus. The umbilical diameter is 3.1 mm in AMNH 50752; the ratio of umbilical diameter to phragmocone diameter is 0.09. The ultimate

→

Fig. 47. **A–C.** *Discoscaphites iris* (Conrad, 1858), *Pinna* Layer, Tinton Formation, Manasquan River Basin, Monmouth County, New Jersey. **A.** AMNH 50395, macroconch, suture at WH = 16.0 mm. **B.** MAPS A2060b43, macroconch, suture at WH = 15.5 mm. **C.** AMNH 50715, microconch, suture at WH = 7.8 mm. **D.** *Discoscaphites sphaeroidalis* Kennedy and Cobban, 2000, AMNH 50752, macroconch, same loc. as **A–C,** suture at WH = 20.3 mm. **E.** *Discoscaphites minardi* Landman et al., 2004a, MAPS A2059c3, macroconch, same loc. as **A–C,** suture at WH = 12.0 mm. **F.** *Discoscaphites jerseyensis*, n.sp., AMNH 51312, fragment, same loc. as **A–C**, suture at WH = 15.8 mm. The dashed line demarcates the umbilical shoulder.

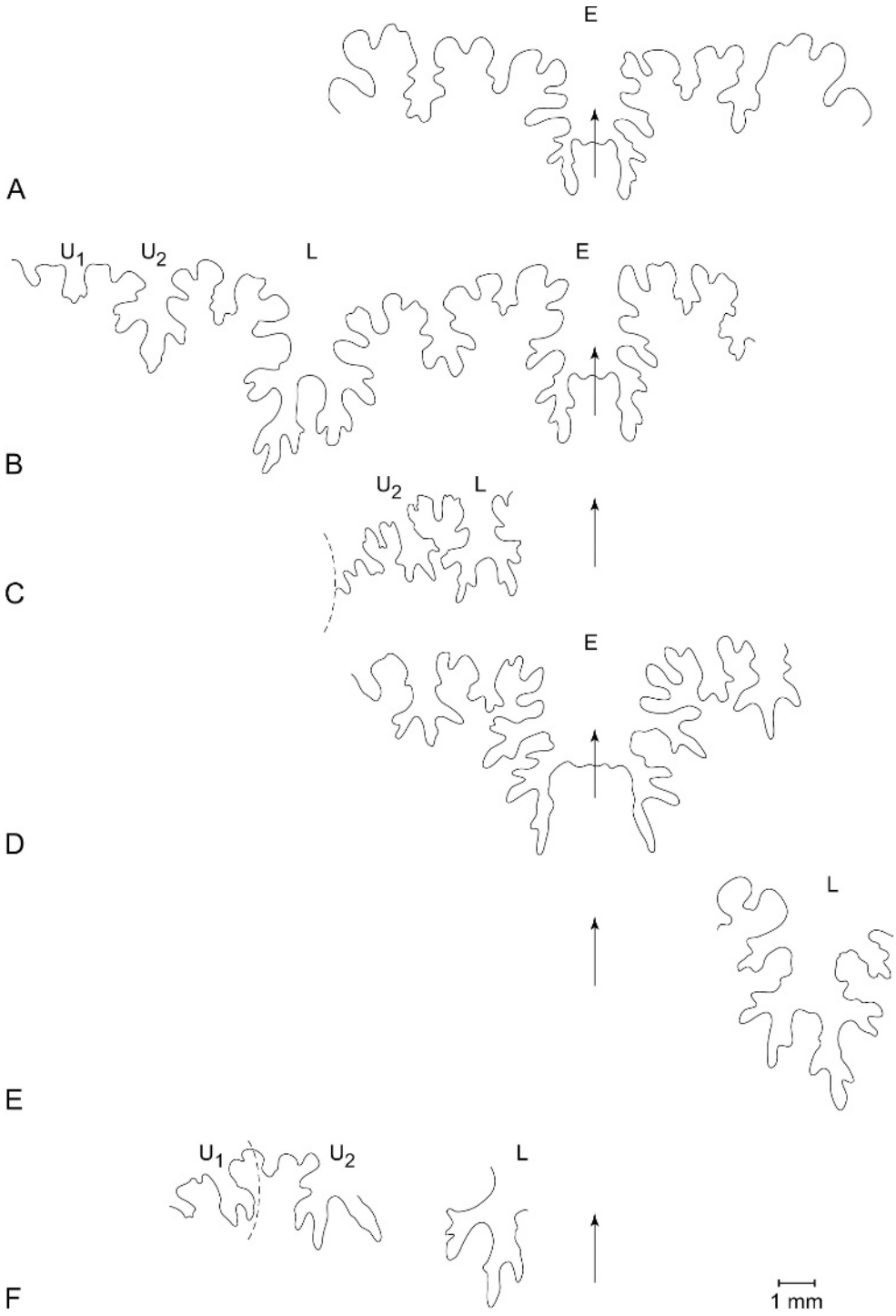
A
E
B
U1
U2
L
E
C
U2
L
D
E
E
L
F
U1
U2
L
1 mm

TABLE 8
Measurements of *Discoscaphites iris* (Conrad, 1858) [a]

Specimen	M/m	LMAX	Angle (°)	WUS	HUS	WUS/HUS	WMS	HMS	WMS/HMS	WAPT	HAPT	WAPT/HAPT
AMNH 47430	M	41.8	20.5	11.0	17.7	0.62	18.6	20.4	0.91	14.7	15.8	0.93
AMNH 50387	M	34.0	—	11.2	15.1	0.74	12.0	15.1	0.79	—	—	—
AMNH 50389	M	—	—	—	—	—	15.2	18.5	0.82	—	—	—
AMNH 50391	M	45.0	33.5	—	—	—	17.0	20.6	0.82	15.7	15.7	1.00
AMNH 50395	M	39.6	—	11.4	17.2	0.66	16.6	20.6	0.80	—	—	—
AMNH 50396	M	47.0	38.5	—	—	—	19.1	21.2	0.90	16.4	17.8	0.92
AMNH 50398	M	41.5	27.0	12.3	20.0	0.62	11.8	14.7	0.80	—	—	—
AMNH 50399	M	39.5	—	11.2	15.9	0.70	15.2	17.8	0.85	—	—	—
AMNH 50406	M	—	—	—	—	—	25.0	30.5	0.82	—	—	—
AMNH 50409	M	42.6*	—	—	—	—	16.0	18.7	0.86	—	—	—
AMNH 50540	M	43.6*	—	10.3	17.7	0.58	17.0	20.7	0.82	—	—	—
AMNH 50545	M	46.6	28.3	13.2	20.4	0.65	19.3	24.2	0.80	17.5	18.1	0.99
AMNH 50710	M	45.4	—	—	—	—	19.0	20.6	0.92	—	—	—
AMNH 50753	M	44.1	39.0	11.8	—	—	17.4	22.0	0.79	15.4	16.4	0.94
AMNH 50754	M	43.7	—	11.3	16.2	0.70	15.9	19.6	0.81	—	—	—
AMNH 50755	M	45.1*	35.0	—	—	—	16.7	21.3	0.78	—	—	—
AMNH 50756	M	42.7	—	—	—	—	15.0	19.9	0.75	—	—	—
AMNH 50763	M	43.4*	—	—	—	—	16.3	20.6	0.79	—	—	—
AMNH 50773	M	39.2*	—	—	—	—	19.7	22.0	0.90	18.0	16.8	1.07
AMNH 50782	M	45.9	42.8	10.9	16.0	0.68	16.1	21.4	0.74	15.4	16.7	0.92
AMNH 51301	M	41.8	—	8.7	—	—	13.1	18.2	0.72	12.4	14.2	0.87
MAPS A2060b2	M	—	—	11.4	16.4	0.70	16.5	20.8	0.79	—	—	—
MAPS A2060b3	M	54.2*	—	—	—	—	22.1	24.1	0.92	—	—	—
MAPS A2060b5	M	41.5	24.0	11.0	16.5	0.67	16.7	19.6	0.85	13.9	15.6	0.89
MAPS A2060b19	M	41.6	34.0	10.3	14.4	0.72	15.9	19.6	0.81	14.8	16.7	0.89
MAPS A2060b20	M	38.2	—	7.2	14.1	0.51	15.2	17.2	0.88	13.2	13.5	0.98
MAPS A2060b21	M	38.5	—	—	16.0	—	16.5	19.0	0.88	—	—	—
MAPS A2060b22	M	45.6	—	—	—	—	—	—	—	14.7	16.3	0.90
MAPS A2060b23	M	44.3	—	12.4	18.3	0.68	16.3	20.9	0.78	—	—	—
MAPS A2060b24	M	40.1	—	—	—	—	16.0	17.6	0.91	13.4	14.7	0.91
MAPS A2060b26	M	48.0	—	—	—	—	18.2	19.7	0.92	—	—	—
MAPS A2060b27	M	43.4	—	11.5	—	—	17.1	21.3	0.80	—	—	—
MAPS A2060b28	M	—	—	—	—	—	15.4	15.4	1.00	—	—	—
MAPS A2060b29	M	39.8	—	—	—	—	15.3	17.9	0.85	—	—	—
MAPS A2060b30	M	46.8	—	—	—	—	17.2	20.4	0.84	—	—	—

TABLE 8
(Continued)

Specimen	M/m	LMAX	Angle (°)	WUS	HUS	WUS/HUS	WMS	HMS	WMS/HMS	WAPT	HAPT	WAPT/HAPT
MAPS A2060b42	M	48.2	—	13.4	19.3	0.69	19.5	23.5	0.83	17.4	17.4	1.00
MAPS A2060b43	M	46.6	—	—	—	—	18.5	20.0	0.92	16.5	16.2	1.02
AMNH 50314	m	29.7*	—	—	—	—	—	—	—	—	—	—
AMNH 50390	m	29.0	—	—	—	—	—	—	—	—	—	—
AMNH 50397	m	—	—	—	—	—	12.2	13.9	0.88	—	—	—
AMNH 50400	m	—	—	6.2	11.2	0.55	9.2	12.5	0.74	—	—	—
AMNH 50401	m	40.0	—	—	—	—	15.9	14.4	1.10	—	13.6	—
AMNH 50405	m	—	—	5.9	10.1	0.58	7.7	10.8	0.71	—	—	—
AMNH 50407	m	—	—	—	—	—	12.2	14.3	0.85	—	—	—
AMNH 50703	m	35.1*	—	9.2	13.6	0.68	13.0	14.4	0.90	—	—	—
AMNH 50711	m	—	—	8.3*	13.4*	0.62*	14.0	14.3	0.98	—	—	—
AMNH 50715	m	—	—	9.2	11.2	0.82	—	—	—	—	—	—
AMNH 50772	m	33.2	—	7.7	10.5	0.73	11.2	12.1	0.92	13.1	12.8	1.02
AMNH 50775	m	33.2	—	9.0	10.2	0.88	13.5	11.4	1.18	12.7	12.4	1.02
MAPS A2060b7	m	35.2	—	9.1	12.3	0.74	14.9	15.0	0.99	—	—	—
MAPS A2060b8	m	34.1	—	10.9	—	—	—	12.3	—	—	—	—
MAPS A2060b9	m	38.9	—	9.2	13.8	0.67	14.0	14.3	0.98	13.7	14.7	0.93
MAPSA2060b29a	m	—	—	—	—	—	—	13.5	—	—	—	—
MAPSA2060b29b	m	38.4	—	—	—	—	—	—	—	—	14.6	—
MAPS A2060b31	m	—	—	—	—	—	13.7	13.4	1.02	14.1	13.8	1.02
MAPS A2060b32	m	36.2	—	—	—	—	13.2	13.1	1.01	13.0	14.0	0.93
MAPS A2060b33	m	40.5	—	—	—	—	16.8	13.9	1.21	15.2	15.1	1.01
MAPS A2060b34	m	—	—	—	—	—	17.6	14.7	1.20	16.4	15.0	1.09
MAPS A2060b35	m	—	—	—	—	—	17.1	15.0	1.14	15.1	15.5	0.97
MAPS A2060b36	m	36.3*	—	—	—	—	12.8	12.7	1.01	—	—	—
MAPS A2060b37	m	40.9*	—	—	—	—	15.8	16.0	0.99	—	—	—
MAPS A2060b38	m	32.5*	—	—	—	—	12.0	12.3	0.98	11.8	13.2	0.89
MAPS A2060b39	m	34.7*	—	—	—	—	—	—	—	—	—	—
MAPS A2060b40	m	32.4*	—	—	—	—	—	—	—	—	—	—
MAPS A2060b41	m	34.1*	—	—	—	—	—	—	—	—	—	—

[a]M = macroconch; m = microconch; LMAX = maximum length; Angle = apertural angle; WUS = whorl width at ultimate septum (mm) in intercostal section; HUS = whorl height at ultimate septum (mm) in intercostal section; WMS = whorl width at midshaft (mm) in intercostal section; HMS = whorl height at midshaft (mm) in intercostal section; WAPT = whorl width at aperture (mm) in intercostal section; HAPT = whorl height at aperture (mm) in intercostal section; * = estimate. See Landman et al. (2004b: fig. 16) for an illustration of measurements.

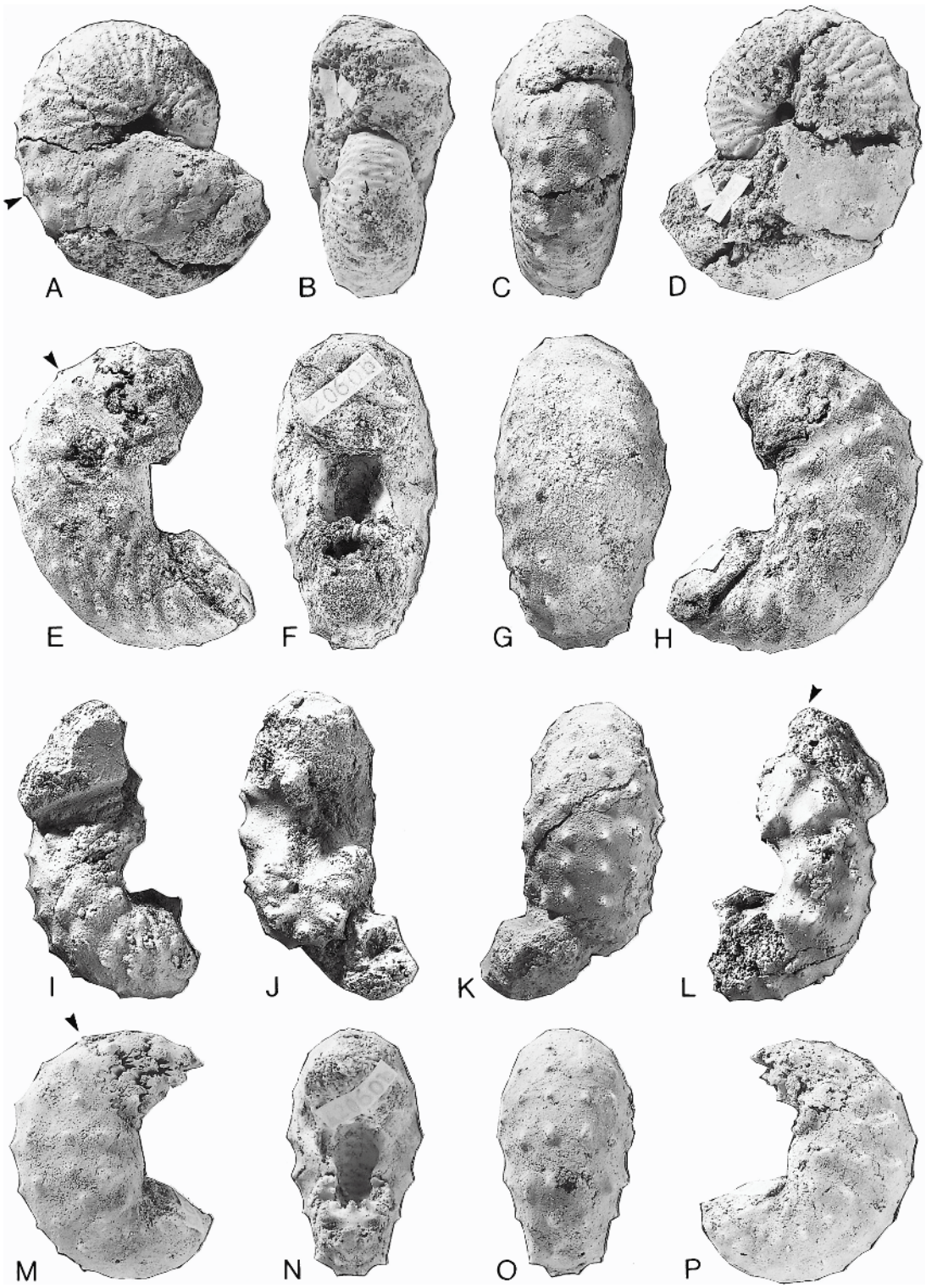
A
B
C
D
E
F
G
H
I
J
K
L
M
N
O
P

TABLE 9
Measurements of *Discoscaphites sphaeroidalis* Kennedy and Cobban, 2000[a]

Specimen	M/m	LMAX	Angle (°)	WUS	HUS	WUS/HUS	WMS	HMS	WMS/HMS	WAPT	HAPT	WAPT/HAPT
AMNH 50752	M	—	—	17.2	18.9	0.91	—	—	—	—	—	—
MAPS A2063a1	M	49.7	39.0	17.9	20.2	0.89	26.8	21.7	1.24	20.8	18.0	1.15
MAPS A2063a2	M	39.3	40.5	13.5	16.3	0.83	20.3	19.5	1.04	16.3	14.4	1.13
AMNH 50713	m	—	—	—	—	—	19.9	14.0	1.42	15.6	—	—

[a]See table 8 for explanation of abbreviations.

septum occurs approximately 30° adoral of the line of maximum length and the body chamber occupies approximately one-half whorl. There is no gap between the phragmocone and body chamber. The apertural angle is 39.0° and 40.5° in MAPS A2063a1 and 2, respectively. The apertural margin is constricted with weak ventral and dorsal projections.

The phragmocone is inflated with a narrow venter, as shown in AMNH 50752 (fig. 48A–D). The intercostal ratio of whorl width to height at the ultimate septum ranges from 0.83 to 0.91 with maximum width at one-third whorl height (table 9). The umbilical wall is steep and subvertical and the umbilical shoulder is sharply rounded. The inner flanks are flat and slightly divergent, the midflanks are broadly rounded and slightly convergent, and the outer flanks between the inner and outer ventrolateral tubercles are flat and steeply convergent. The ventrolateral shoulder is fairly sharply rounded and the venter is flat to broadly rounded.

The body chamber is swollen at midshaft with an intercostal ratio of whorl width to height ranging from 1.04 to 1.24 (table 9). Maximum width occurs at the umbilicolateral margin. The umbilical wall is steep and convex and the umbilical shoulder is fairly abruptly rounded. The inner flanks are nearly flat and steeply divergent, the midflanks are broadly rounded, and the outer flanks are flat and steeply convergent. The ventrolateral shoulder is fairly abruptly rounded and the venter is flat. Whorl width increases toward the adoral end of the shaft and then decreases toward the aperture. The ratio of whorl width to height at the aperture averages 1.14.

The ornament on the phragmocone is only preserved in AMNH 50752 (fig. 48A–D). The ribs are slightly flexuous on the adapical end of the phragmocone but straighten out adorally. They are very long, with branching and intercalation at one-third and two-thirds whorl height. They cross the venter with a slight adoral projection. There are 10 ribs/cm on the venter of the middle one-third of the phragmocone. The ventral ribs weaken and disappear toward the adoral end of the phragmocone. All four rows of tubercles are already present at the point of exposure. The outer ventrolateral tubercles are matched on either side of the venter and are linked to each other by one or two ribs.

The ornament on the body chamber consists of coarse ribs bearing four rows of tubercles. The ribs are indistinct on most of the body chamber except the hook. The ribs

←

Fig. 48. *Discoscaphites sphaeroidalis* Kennedy and Cobban, 2000, *Pinna* Layer, Tinton Formation, Manasquan River Basin, Monmouth County, New Jersey. **A–D.** AMNH 50752, macroconch. **A.** Right lateral; **B.** apertural; **C.** ventral; **D.** left lateral. **E–H.** MAPS A2063a1, macroconch. **E**. Right lateral; **F.** apertural; **G.** ventral; **H.** left lateral. **I–L.** AMNH 50713, microconch, with piece of matrix attached. **I.** Right lateral; **J.** apertural; **K.** ventral; **L.** left lateral. **M–P.** MAPS A2063a2. **M**. Right lateral; **N**. apertural; **O**. ventral; **P**. left lateral. All figures ×1.

on the hook are prorsiradiate and cross the venter with a slight adoral projection. There are 5 ribs/cm on the venter of the hook in MAPS A2063a1. The number of umbilicolateral tubercles ranges from 4 to 6. These tubercles attain their greatest height just adoral of midshaft. There are 8 flank tubercles midway between the umbilicolateral and inner ventrolateral tubercles. The number of inner ventrolateral tubercles (10–13) is equal to or slightly less than the number of outer ventrolateral tubercles (12 or 13). Both rows of ventrolateral tubercles extend to the aperture. The tubercles are more widely spaced on the shaft and more closely spaced on the hook. The outer ventrolateral tubercles are matched on either side of the venter.

The suture consists of a broad first lateral saddle and bifid first lateral lobe (fig. 47D).

MICROCONCH DESCRIPTION: The only microconch is AMNH 50713, an incomplete body chamber missing part of the hook on the left side (fig. 48I–L). The specimen is very robust, with an intercostal ratio of whorl width to height at midshaft of 1.42. The ornament consists of coarse, indistinct ribs bearing four rows of tubercles. The umbilicolateral and flank tubercles on the adoral part of the shaft are the largest tubercles on the specimen.

DISCUSSION: This species closely resembles *Discoscaphites iris* but differs in having a more inflated phragmocone with relatively narrow venter and a more robust body chamber with maximum whorl width just adoral of midshaft. In addition, the flanks of the phragmocone are covered with narrow, long ribs. *Discoscaphites sphaeroidalis* differs from *D. minardi* and *D. jerseyensis* in having coarser and more widely spaced ribs on the hook.

OCCURRENCE: *Pinna* Layer, upper part of the Tinton Formation, Manasquan River Basin, central Monmouth County, New Jersey. Elsewhere in New Jersey, this species occurs at the top of the New Egypt Formation, near Eatontown, northeastern Monmouth County (Landman et al., 2004b). On the Gulf Coastal Plain, this species occurs in the Owl Creek Formation, northern Mississippi and southeastern Missouri (Kennedy and Cobban, 2000) and at the top of the Corsicana Formation, along the Brazos River, Falls County, Texas (Kennedy et al., 2001).

Discoscaphites minardi Landman et al., 2004a
figures 47E, 49, 50

Discoscaphites minardi Landman et al., 2004a: 44, figs. 17H–M, 18A–Q,S–Y, 19–22.

Discoscaphites minardi Landman et al., 2004a. Landman et al., 2004b: 89, figs. 39Q–T, 40A–D,J–P.

TYPE: The holotype is AMNH 47288, a macroconch, from the top of the Severn Formation, Kent County, Maryland.

MATERIAL: There are approximately 30 specimens in the AMNH and MAPS collections from the upper part of the Tinton Formation, mainly the *Pinna* Layer, Manasquan River Basin, Monmouth County, New Jersey. Most of the specimens are fragments of body chambers. In specimens in which the dimorph can be identified ($n = 22$), there are 20 macroconchs and 2 microconchs. Two macroconchs (MAPS A2059c6, 7) occur together in the same cluster with two baculites, six echinoids, fragments of a specimen of *Pinna laqueata*, and several small snails.

DESCRIPTION: Our collection includes many specimens with nearly intact body chambers, allowing a more complete picture of the fine ribbing near the aperture than was previously possible based on fragmentary specimens.

→

Fig. 49. *Discoscaphites minardi* Landman et al., 2004a, macroconchs, *Pinna* Layer, and underlying part of the Tinton Formation (as indicated), Manasquan River Basin, Monmouth County, New Jersey. **A,B.** MAPS A2059c1. **A.** Right lateral; **B.** ventral. **C–E.** MAPS A2059c2, underlying part of the Tinton Formation. **C.** Right lateral; **D.** ventral; **E.** left lateral. **F,G.** MAPS A2059c3. **F.** Ventral; **G.** left lateral. **H,I.** MAPS A2059c4. **H.** Right lateral; **I.** ventral. **J,K.** MAPS A2059c5. **J.** Ventral; **K.** left lateral. **L,M.** MAPS A2059c6, part of the same cluster as MAPS A2059c7. **L.** Ventral; **M.** left lateral. **N,O.** MAPS A2059c7. **N.** Ventral; **O.** left lateral. **P,Q.** AMNH 50697. **P.** Right lateral; **Q.** ventral. All figures ×1.

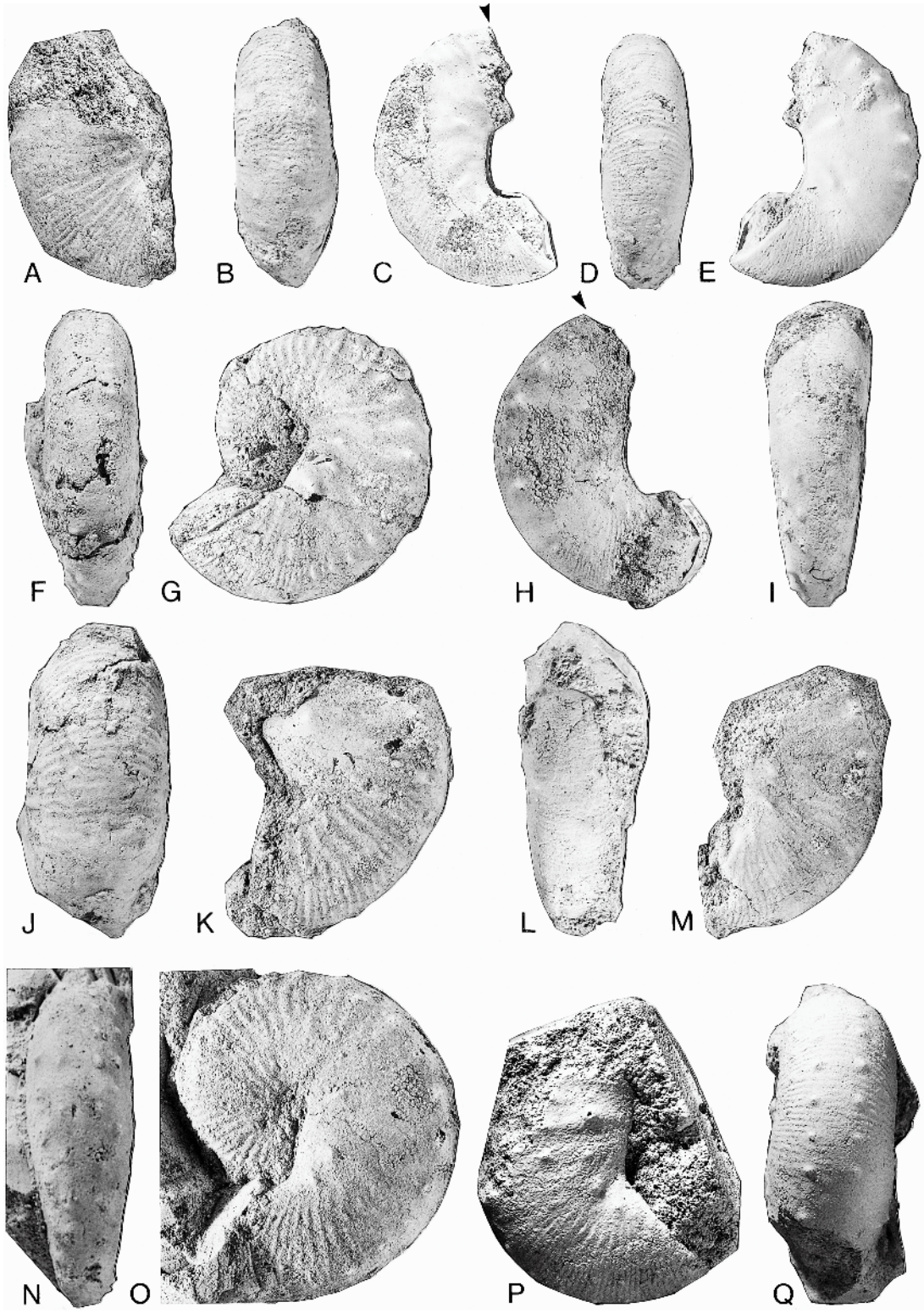
A
B
C
D
E
F
G
H
I
J
K
L
M
N
O
P
Q

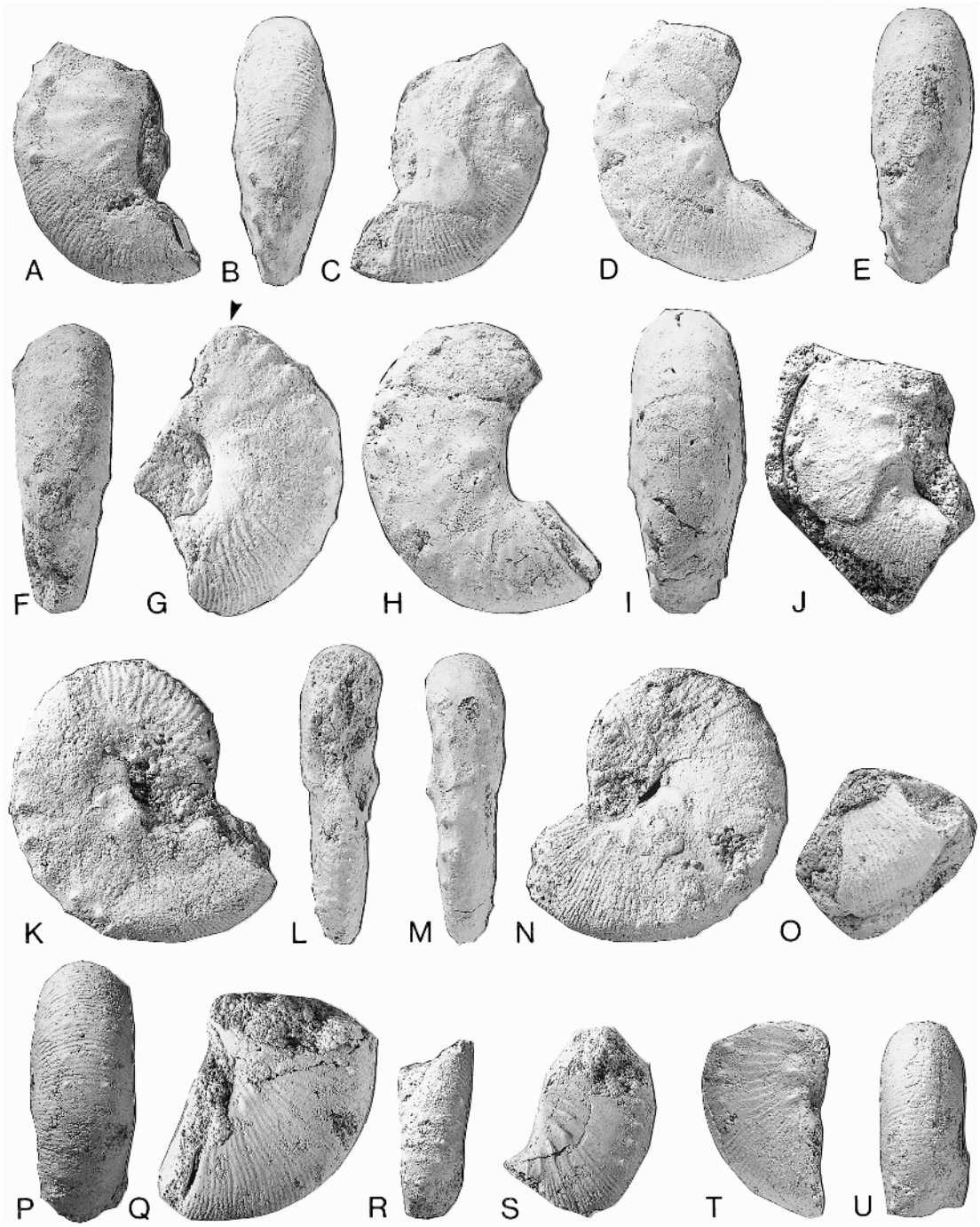

Fig. 50. *Discoscaphites minardi* Landman et al., 2004a, macroconchs, or indeterminate (as indicated), *Pinna* Layer, and underlying part of Tinton Formation (as indicated), Manasquan River Basin, Monmouth County, New Jersey. **A–C.** AMNH 50760, underlying part of the Tinton Formation. **A.** Right lateral; **B.** ventral; **C.** left lateral. **D,E.** AMNH 50759. **D.** Right lateral; **E.** ventral. **F,G.** AMNH 50758, dimorph indeterminate, but probably a microconch. **F**. Ventral; **G.** left lateral. **H,I.** AMNH 50761.

TABLE 10
Measurements of *Discoscaphites minardi* Landman et al., 2004a[a]

Specimen	M/m	LMAX	Angle (°)	WUS	HUS	WUS/HUS	WMS	HMS	WMS/HMS	WAPT	HAPT	WAPT/HAPT
AMNH 50411	M	45.3	—	—	—	—	—	21.1	—	—	—	—
AMNH 50697	M	—	43.5	—	—	—	—	—	—	18.5	19.0	0.97
AMNH 50758	M	—	—	—	—	—	13.7	20.1	0.68	—	—	—
AMNH 50759	M	—	35.5*	—	—	—	14.7	19.3	0.76	—	14.3	—
AMNH 50760	M	—	36.0*	—	—	—	—	—	—	13.4	12.6	1.02
AMNH 50761	M	46.4	37.2	—	—	—	16.6	21.6	0.77	15.3	15.9	0.97
MAPS A2059c2	M	40.2	42.5	9.4	16.0	0.59	12.9	17.5	0.75	12.2	14.3	0.85
MAPS A2059c3	M	44.6	29.5	9.6	17.8	0.54	14.6	20.7	0.70	13.6	16.3	0.83
MAPS A2059c4	M	47.2*	—	—	—	—	14.3	20.2	0.71	—	—	—
MAPS A2059c7	M	51.2	—	—	—	—	—	25.0	—	—	—	—
AMNH 50693	m	30.6	—	6.3	10.2	0.62	8.2	10.5	0.78	10.5	11.6	0.90
AMNH 50402	m	30.4*	—	6.7	10.8	0.62	—	13.0	—	—	—	—

[a]See table 8 for explanation of abbreviations.

MACROCONCH DESCRIPTION: Maximum length ranges from approximately 40 to 51 mm (table 10). The shell is closely coiled with a tiny umbilicus. There is hardly any gap between the phragmocone and body chamber. The body chamber occupies approximately one-half whorl. The hook is slightly reflected; the apertural angle ranges from 29.5° to 43.5°. The aperture is constricted and the dorsum and venter are slightly projected.

The phragmocone is very compressed. The intercostal ratio of whorl width to height at the ultimate septum ranges from 0.54 to 0.59 in two specimens (table 10). The umbilical wall is steep and convex and the umbilical shoulder is sharply rounded. The inner flanks are flat and slightly divergent, the midflanks are flat and slightly convergent, and the outer flanks are flat and more steeply convergent. The ventrolateral shoulder is sharply rounded and the venter is flat.

The body chamber is slender with subparallel flanks. The intercostal ratio of whorl width to height at midshaft averages 0.73 and ranges from 0.68 to 0.77 (table 10). The umbilical wall is vertical and steeply convex and the umbilical shoulder is fairly sharply rounded. The inner flanks are flat and divergent, the midflanks are flat and gently convergent, and the outermost flanks, between the inner and outer ventrolateral tubercles, are flat and more steeply convergent. The ventrolateral shoulder is fairly sharply rounded and the venter is nearly flat. Whorl height decreases more rapidly than width, producing a more depressed whorl section at the aperture with an intercostal ratio of whorl width to height ranging from 0.83 to 1.02 (table 10).

The ornament on the phragmocone consists of rectiradiate to prorsiradiate slightly flexuous ribs. Intercalation and branching occur at one-third and two-thirds whorl height. The ribs are short and straight on the venter. There are 8 ventral ribs/cm on the adapical one-third and 5 ventral ribs/cm on the adoral one-third of the phragmocone in MAPS A2059c3 (fig. 49F,G). Both rows of ventrolateral tubercles are already present at the point of exposure.

With the exception of the tubercles, the ornament on the body chamber is subdued.

←

H. Right lateral; **I.** ventral. **J.** AMNH 50691, right lateral. **K–N.** AMNH 50411, slightly crushed, underlying part of the Tinton Formation. **K.** Right lateral, **L.** apertural; **M.** ventral; **N.** left lateral. **O.** AMNH 51315, dimorph indeterminate, left lateral. **P,Q.** AMNH 50394. **P.** Ventral; **Q.** left lateral. **R,S.** AMNH 50410. **R.** Ventral; **S.** left lateral. **T,U.** AMNH 50408. **T.** Right lateral; **U.** ventral. All figures ×1.

There are 4 to 7 weakly to strongly arcuate umbilicolateral tubercles/bullae. In some specimens, e.g., MAPS A2059c3 (fig. 49F,G), these tubercles are the most prominent tubercles on the shell, whereas in other specimens, e.g., AMNH 50760 (fig. 50A–C), these tubercles are surpassed in size by the inner ventrolateral tubercles. The umbilicolateral tubercles give rise to weak rectiradiate to prorsiradiate ribs, which are slightly convex on the flanks, as shown in AMNH 50410 (fig. 50R,S), AMNH 50760 (fig. 50A,C), and MAPS A2059c3 (fig. 49F,G). The ribs become increasingly prorsiradiate and more closely spaced adorally so that the hook is covered with fine, dense ribbing. The ribs cross the venter with a slight adoral projection; there are 14 and 15 ribs/cm on the venter of the hook in AMNH 50760 and 50394, respectively. The flank tubercles are either absent, as in MAPS A2059c2 (fig. 49C,E) and AMNH 50410 (fig. 50R,S), or appear as elongate swellings that weaken adorally, as in AMNH 50760 (fig. 50A–C) and AMNH 50761 (fig. 50H,I). The inner ventrolateral tubercles are more or less evenly spaced on the shaft. There are 13 such tubercles on the preserved piece of body chamber in AMNH 50761 (fig. 50H, I). These tubercles sometimes become smaller and more closely spaced on the hook, as shown in AMNH 50761 (fig. 50H, I). More commonly, however, they disappear on the adoral end of the shaft, as shown in AMNH 50411 (fig. 50K–N), AMNH 50759 (fig. 50D, E), and MAPS A2059c4 (fig. 49H, I). The outer ventrolateral tubercles are smaller than the inner ventrolateral tubercles. They sometimes disappear on the adoral end of the shaft, as in AMNH 50410 (fig. 50R, S), AMNH 50411 (fig. 50K–N), AMNH 50760 (fig. 50A–C), and MAPS A2059c4 (fig. 49H, I). Other times, however, they persist to the aperture, with or without the inner ventrolateral tubercles, as in AMNH 50759 (fig. 50D,E), AMNH 50761 (fig. 50H,I), and MAPS A2059c2 (fig. 49C–E).

Part of the suture is preserved in MAPS A2059c3 and shows an asymmetrically bifid first lateral lobe (fig. 47E).

MICROCONCH DESCRIPTION: The two best microconchs, AMNH 50402 (fig. 45Z) and AMNH 50693 (fig. 45V–Y), are incomplete body chambers. Both of them are difficult to measure. AMNH 50693 has a piece of matrix attached to the midshaft, possibly concealing a hole in the shell. AMNH 50402 is pushed in on the right side, probably the result of an injury.

The maximum length is approximately 30 mm in both specimens (table 10). The whorl section at the ultimate septum is compressed ovoid with maximum width at one-third whorl height. The intercostal ratio of whorl width to height is 0.62 in both specimens.

Whorl width increases slightly more than whorl height in passing into the body chamber and, therefore, the whorl section at midshaft is more depressed. The intercostal ratio of whorl width to height is 0.78 in AMNH 50693. The umbilical wall is broadly rounded and inclined outward and the umbilical shoulder is fairly abruptly rounded. The inner flanks are broadly rounded and slightly divergent, the midflanks are nearly flat and slightly convergent, and the outer flanks are flat and more steeply convergent. The ventrolateral shoulder is fairly abruptly rounded and the venter is nearly flat. The whorl section is slightly more depressed at the aperture with an intercostal ratio of whorl width to height of 0.90 in AMNH 50693.

As in macroconchs, the body chamber is ornamented with only three rows of tubercles. The flank tubercles are either absent or expressed as bullate swellings. There are five umbilicolateral tubercles in both AMNH 50402 and 50693; these are the most prominent tubercles on the shell. They give rise to weak rectiradiate ribs that become increasingly prorsiradiate toward the aperture. The hook is covered with fine, dense ribbing. There are 12 ribs/cm on the venter of the hook in AMNH 50693. Both rows of ventrolateral tubercles are present. However, in AMNH 50693, only the outer ventrolateral row of tubercles persists to the aperture.

DISCUSSION: *Discoscaphites minardi* differs from *D. iris* in subtle but significant ways. In *D. minardi*, the flanks of the body chamber are flat and nearly subparallel, the umbilicolateral tubercles are arcuate, the flank tubercles are absent or weak, and the ribs are fine and closely spaced near the aperture. *Discoscaphites minardi* is less abun-

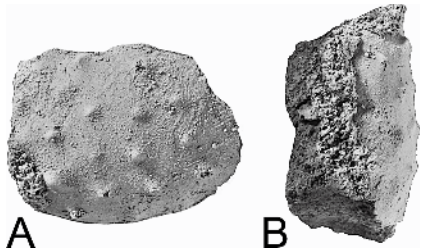

Fig. 51. *Discoscaphites gulosus* (Morton, 1834), macroconch, MAPS A2025c1, *Pinna* Layer, top of the Tinton Formation, Manasquan River Basin, Monmouth County, New Jersey. **A**. Lateral view of part of the shaft; **B**. ventral view. Both figures ×1.

dant than *D. iris* in the Manasquan River Basin, representing approximately only 10% of the total collection of scaphites. In contrast, *D. minardi* is the only species of *Discoscaphites* present in the underlying *D. minardi* Zone in northeastern Monmouth County, New Jersey (Landman et al., 2004b) and Kent County, Maryland (Landman et al., 2004a).

OCCURRENCE: Upper part of the Tinton Formation, mainly the *Pinna* Layer, Manasquan River Basin, central Monmouth County, New Jersey. Elsewhere in New Jersey, *Discoscaphites minardi* occurs in the upper part of the New Egypt Formation and as reworked material at the base of the Hornerstown Formation, near Eatontown, northeastern Monmouth County (Landman et al., 2004b). This species was originally described from the top of the Severn Formation, Kent County, Maryland (Landman et al., 2004a). It is the name bearer of the *D. minardi* Zone, which occurs below the *D. iris* Zone, and indicates the lower part of the upper Maastrichtian, corresponding to the upper part of calcareous nannofossil Zone CC26a and the lower part of calcareous nannofossil Zone CC26b.

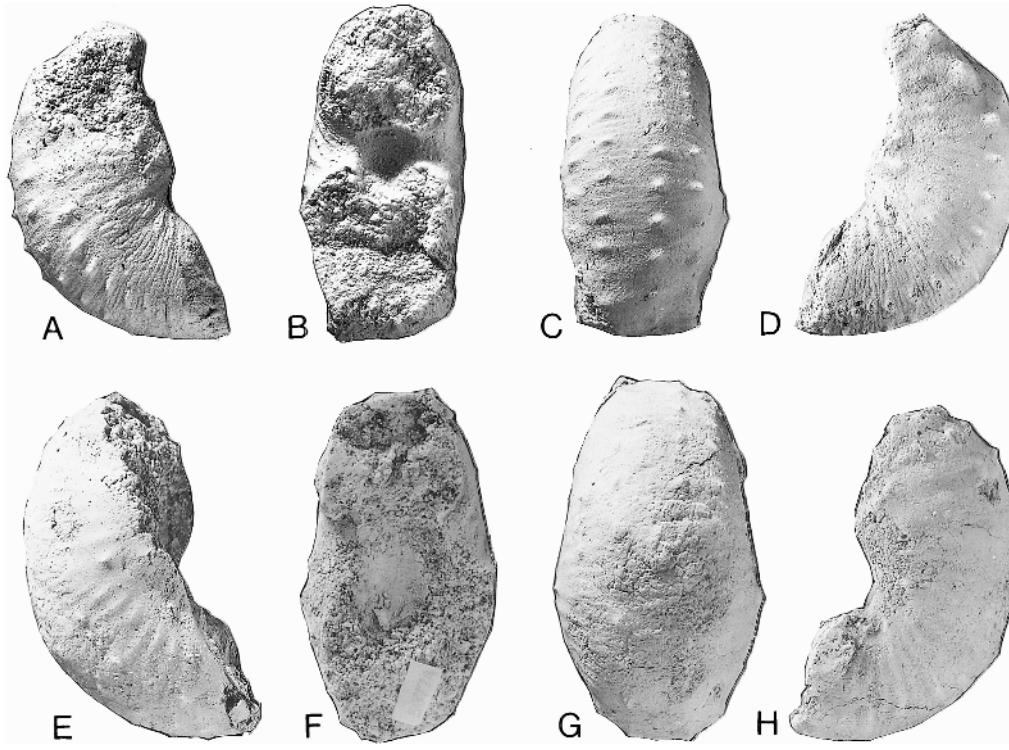

Fig. 52. *Discoscaphites jerseyensis*, n.sp., macroconchs, *Pinna* Layer, top of the Tinton Formation, Manasquan River Basin, Monmouth County, New Jersey. **A–D.** AMNH 50393, holotype. **A.** Right lateral; **B.** apertural; **C.** ventral; **D.** left lateral. **E–H.** AMNH 50774, paratype. **E.** Right lateral; **F.** apertural; **G.** ventral; **H.** left lateral. All figures ×1.

TABLE 11
Measurements of *Discoscaphites jerseyensis*, n.sp.[a]

Specimen	M/m	LMAX	Angle (°)	WUS	HUS	WUS/HUS	WMS	HMS	WMS/HMS	WAPT	HAPT	WAPT/HAPT
AMNH 50393	M	44.8*	35.5	—	—	—	21.9	20.4	1.07	19.4	17.2	1.13
AMNH 50774	M	46.3*	41.0	—	—	—	26.7	22.4	1.19	21.0*	18.0*	1.17*

[a]See table 8 for explanation of abbreviations.

Discoscaphites gulosus (Morton, 1834)
figure 51

Ammonites conradi var. *petechialis* Morton, 1834: 39, 40, pl. 16, fig. 1.
Ammonites conradi var. *gulosus* Morton, 1834: 39, 40, pl. 16, fig. 2.
Ammonites conradi var. *navicularis* Morton, 1834: 40, pl. 19, fig. 4.
Discoscaphites conradi gulosus (Morton, 1834). Jeletzky and Waage, 1978: 1129, pl. 2, figs. 1–19; pl. 3, figs. 1–15; text-fig. 1B, C, E, F.
Discoscaphites gulosus (Morton, 1834). Landman and Waage, 1993: 212, figs. 156, 157, 159, 160, 167–180 (with full synonymy).
Discoscaphites gulosus (Morton, 1834). Cobban and Kennedy, 1995: 29, figs. 10.4, 10.5, 19.20–19.24, 20.8–20.12, 20.14–20.17, 21.18–21.21.
Discoscaphites gulosus (Morton, 1834). Kennedy et al., 1997: figs. 20K–O, 21D, E.
Discoscaphites gulosus (Morton, 1834). Landman et al., 2004a: 37, figs. 12C–J, 16.
Discoscaphites gulosus (Morton, 1834). Landman et al., 2004b: 92, figs. 39Y, Z, a, b, 41E.

TYPE: The holotype is ANSP 51552 from the Prairie Bluff Chalk at Prairie Bluff, Alabama.

MATERIAL: MAPS A2025c1, *Pinna* Layer, Manasquan River Basin, Monmouth County, New Jersey.

DESCRIPTION: MAPS A2025c1 is part of the shaft of a body chamber of a large macroconch (fig. 51). The midflanks are broadly rounded and slightly convergent and the outer flanks are nearly flat and more steeply convergent. There are five equally spaced rows of small, round tubercles. The most prominent tubercle on the specimen is near the umbilical margin.

DISCUSSION: Macroconchs of *Discoscaphites gulosus* from the *D. iris* Zone on the Altantic Coastal Plain display five tubercle rows (fig. 51; Kennedy et al., 2000: fig. 9G–I). [This also applies to an incomplete specimen of this species in which the dimorph is indeterminate (Landman et al., 2004b: fig. 39Y, Z, a, b). Similarly, the specimen of *Discoscaphites* sp. cf. *gulosus* reported from the *D. iris* Zone of Texas displays five tubercle rows (Kennedy et al., 2001: fig. 4f)]. In contrast, macroconchs of *D. gulosus* from the stratigraphically lower *D. conradi* Zone on the Gulf and Atlantic Coastal Plains exhibit either five or six tubercle rows (e.g., Jeletzky and Waage, 1978: pl. 2, figs. 8–11, 16–19; pl. 3, figs. 1–3; Cobban and Kennedy, 1995: figs. 19.20–19.24, 20.1, 20.2, 20.8–20.12; Kennedy et al., 1997: fig. 20K–M; Landman et al., 2004a: 12C,D,H–J, 16). The *D. conradi* Zone is approximately equivalent to the *Hoploscaphites nicolletii* and *Jeletzkytes nebrascensis* Zones of the Western Interior (Landman et al., 2004a). Macroconchs from these two zones also display either five or six rows of tubercles (Landman and Waage, 1993: figs. 167A–C, 168A–C, 169A–F, 170A–C, 171A–F, 172A–E). Thus, these data suggest a temporal reduction in the number of tubercle rows, with younger forms of *D. gulosus* having one fewer row.

→

Fig. 53. Lower jaws (aptychi) of *Discoscaphites iris* (Conrad, 1858), *Pinna* Layer, top of the Tinton Formation, Manasquan River Basin, Monmouth County, New Jersey. **A–C**. Lower jaw, MAPS A2062a7, closely associated with a macroconch of *D. iris*. **D,E**. Macroconch of *D. iris*, MAPS A2060b11, with its lower jaw (arrow), MAPS A2062a8, preserved inside the adoral part of the body chamber. **D**. Right lateral, ×1; **E**. close-up of the lower jaw. **F**. Large microconch of *D. iris*, MAPS A2060b10, with lower jaw (arrow), MAPS A2062a9, preserved nearby. Scale bar = 1 mm.

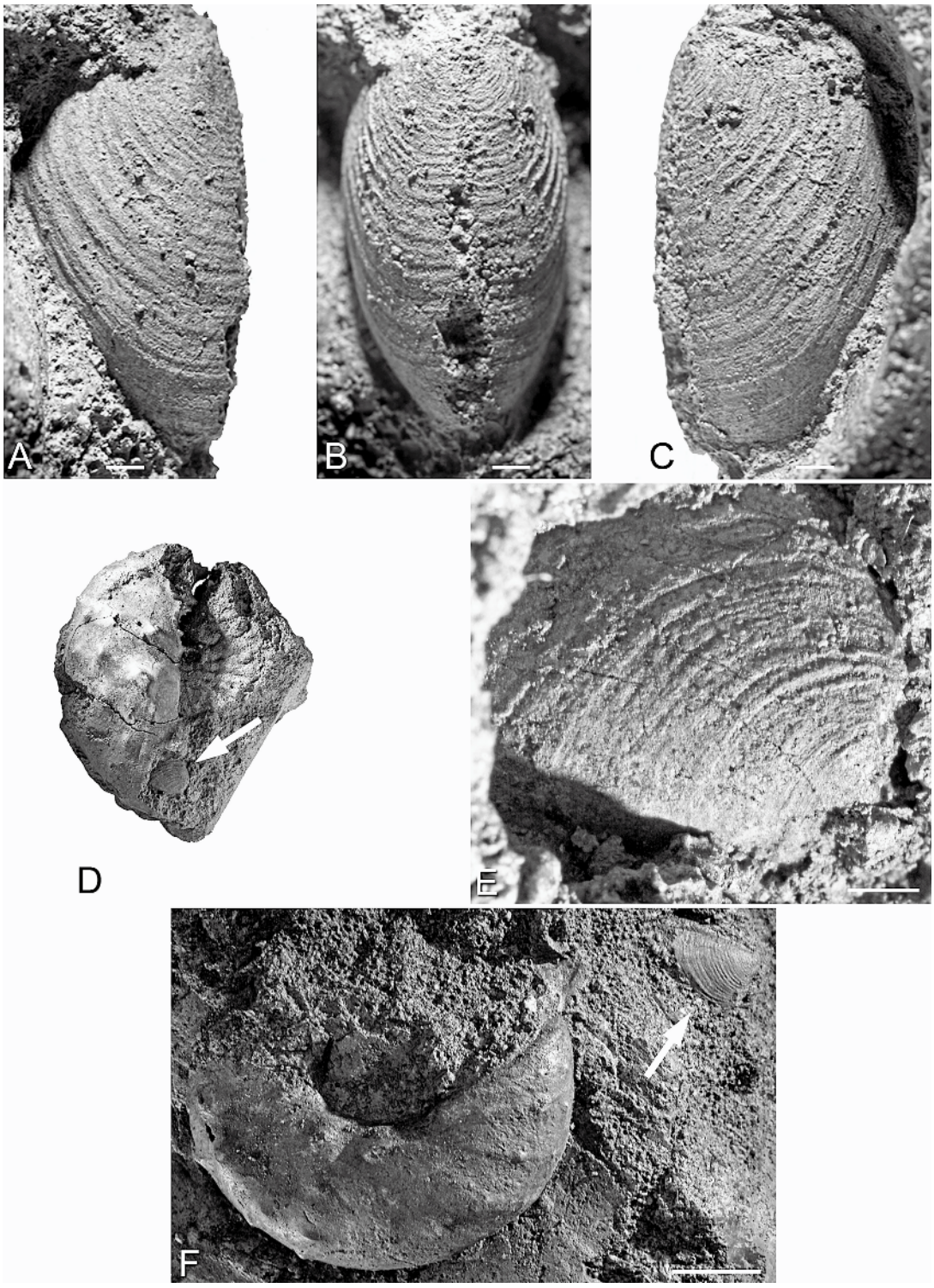
A
B
C
D
E
F

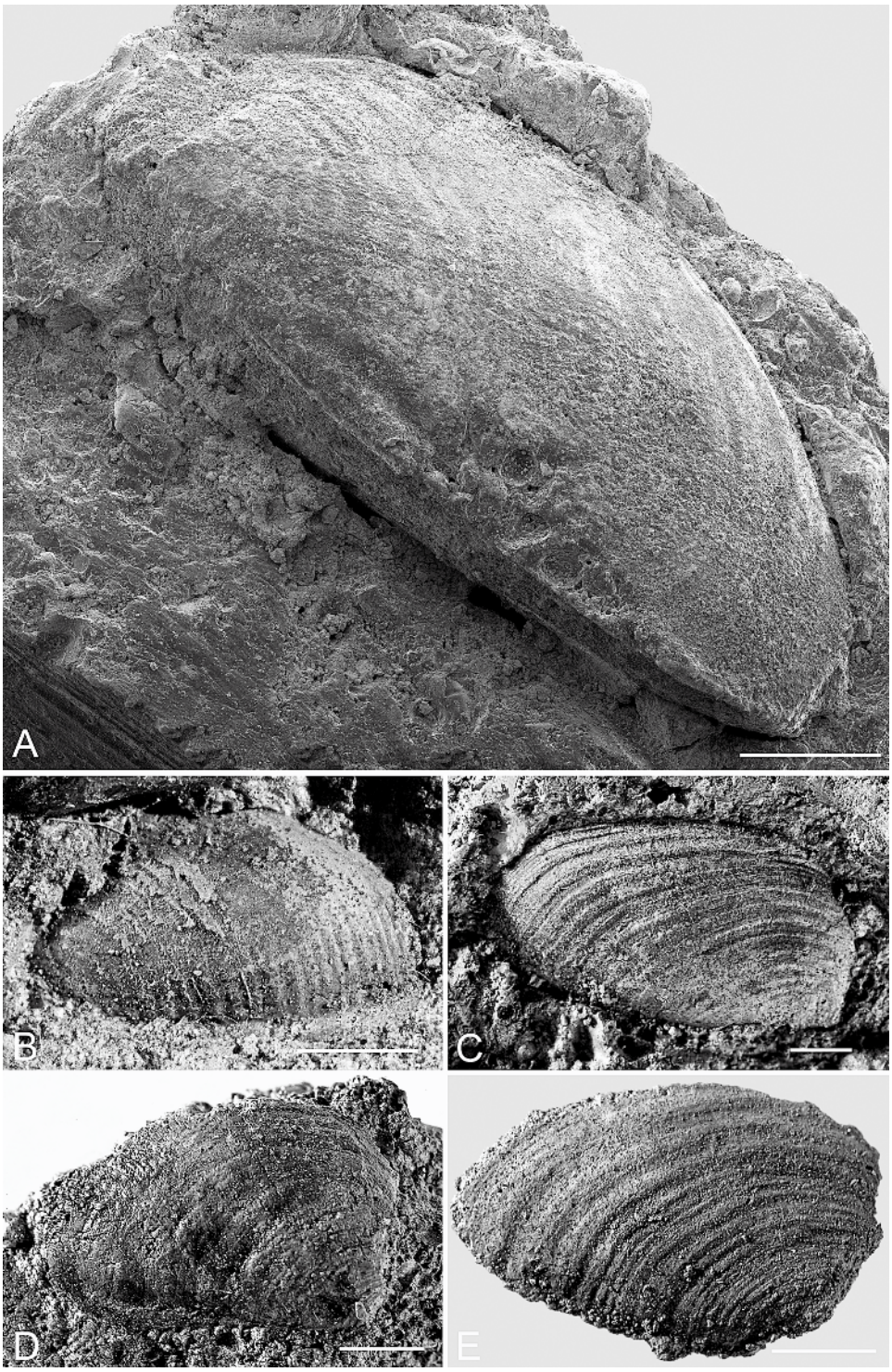
A
B
C
D
E

OCCURRENCE: *Pinna* Layer, Tinton Formation, Manasquan River Basin, New Jersey. Elsewhere in New Jersey, this species occurs at the top of the New Egypt Formation and as reworked material at the base of the Hornerstown Formation, near Eatontown, Monmouth County (Landman et al., 2004b), and in the Navesink Formation (New Egypt Formation according to our usage) at the Inversand Marl Pit, Gloucester County (Kennedy et al., 2000). This species also occurs in several localities on the Gulf and Atlantic Coastal Plains including the Severn Formation, Prince Georges County, Maryland (Kennedy et al., 1997); the Peedee Formation, Brunswick County, North Carolina (Landman et al., 2004a); and the Prairie Bluff Chalk, Alabama (Cobban and Kennedy, 1995). In the Western Interior, *D. gulosus* occurs in both the *Hoploscaphites nicolletii* and *Jelezkytes nebrascensis* Zones of the Fox Hills Formation, South Dakota (Landman and Waage, 1993).

Discoscaphites jerseyensis, new species
figures 47F, 52

ETYMOLOGY: Named after the state of New Jersey, which has produced more scaphites than anyone would have dreamed of just a few years ago.

TYPES: The holotype and paratype are AMNH 50393 and 50774, respectively, from the *Pinna* Layer at the top of the Tinton Formation, Manasquan River Basin, Monmouth County, New Jersey. Both specimens are macroconch body chambers. In AMNH 50393, there is a small healed injury at the adapical end.

MATERIAL: Two incomplete macroconch body chambers (AMNH 50393 and 50774), part of a hook of a microconch (MAPS A2061a1), and a piece of a phragmocone (AMNH 51312), possibly of a macroconch, from the *Pinna* Layer at the top of the Tinton Formation, Manasquan River Basin, Monmouth County, New Jersey.

DIAGNOSIS: Body chamber with very depressed whorl section. Ornament consists of three rows of small tubercles (umbilicolateral and inner and outer ventrolateral tubercles), a single row of small midflank bullae, and long, straight, closely spaced ribs on the hook.

MACROCONCH DESCRIPTION: The body chamber is very depressed. The intercostal ratio of whorl width to height at midshaft is 1.07 and 1.19 in AMNH 50393 and AMNH 50774, respectively (table 11). The umbilical wall is broad and convex and the umbilical shoulder is fairly abruptly rounded. The inner flanks are broadly rounded and divergent, the midflanks are broadly rounded and convergent, and the outer flanks are nearly flat and more steeply convergent. Maximum width occurs at the umbilicolateral margin. The ventrolateral shoulder is broadly rounded and the venter is nearly flat. Both whorl width and height decrease adorally, producing a depressed whorl section at the aperture. The intercostal ratio of whorl width to height at the aperture is 1.13 and 1.17 in AMNH 50393 and 50774, respectively.

The small piece of phragmocone (AMNH 51312) bears long narrow ribs with four rows of tubercles (not illustrated). The body chamber is ornamented with umbilicolateral tubercles that give rise to straight rectiradiate to prorsiradiate ribs bearing weak midflank bullae. In AMNH 50393 (fig. 52A–D), these bullae disappear at the adoral end of the shaft, but in AMNH 50774 (fig. 52E–H), they persist to the aperture. Inner and outer ventrolateral tubercles are present on the entire body chamber. In AMNH 50393, in which the tubercles can easily be counted, there are 15 inner and 15 outer ventrolateral tubercles, although the body chamber is incomplete. These tubercles are strongest and most widely spaced on the adapical part of the body chamber, and weaker and more closely spaced on the hook; they develop into bullae in AMNH 50393. The hook is covered with fine dense ribbing. The ribs are prorsiradiate

←

Fig. 54. Isolated lower jaws (aptychi) attributed to *Discoscaphites iris* (Conrad, 1858), *Pinna* Layer, top of the Tinton Formation, Manasquan River Basin, Monmouth County, New Jersey. The jaw is covered with fine ridges that parallel the posterior margin. **A**. AMNH 51298. **B**. MAPS A2062a6. **C**. MAPS A2062a1. **D**. MAPS A2062a3. **E**. MAPS A2062a2. Scale bar = 2 mm.

on the flanks and straight on the venter; there are 15 ribs/cm on the venter of the hook in AMNH 50393. Part of the suture is preserved in AMNH 51312 and is similar to that of other species of *Discoscaphites* (fig. 47F).

DISCUSSION: *Discoscaphites jerseyensis*, n. sp., differs from *D. sphaeroidalis* in having very fine ribbing on the hook and a row of midflank bullae instead of tubercles. It differs from *D. minardi* in having a much more robust body chamber. The difference between *D. jerseyensis* and *D. minardi* is analogous to that between *D. sphaeroidalis* and *D. iris*.

OCCURRENCE: *Pinna* Layer, top of the Tinton Formation, Manasquan River Basin, central Monmouth County, New Jersey.

APTYCHI (LOWER JAWS)
figures 53, 54

MATERIAL: There are 17 aptychi in the AMNH and MAPS collections (AMNH 51298, 51300, 51313, MAPS A2062a1–14) from the *Pinna* Layer at the top of the Tinton Formation, Manasquan River Basin, central Monmouth County, New Jersey. Based on their shape and ornament, these specimens are interpreted as the lower jaws of scaphites. MAPS A2062a8 is preserved inside the body chamber of a macroconch of *Discoscaphites iris* (fig. 53D, E). MAPS A2062a7 (fig. 53A–C) and MAPS A2062a9 (fig. 53F) are closely associated with a macroconch and microconch of the same species, respectively. The rest of the jaws are isolated (fig. 54), but were probably associated with the shells from which they were derived, although this was not noted at the time they were collected. We attribute all of the isolated jaws to *D. iris* because this is the most abundant scaphite in the *Pinna* Layer. In general, the jaws are preserved with only one of the wings exposed, although the other wing is probably embedded in the matrix. Sometimes, the jaw is folded together [''folio'' preservation of Seilacher (1993)] exposing both wings of the jaw. In two specimens (MAPS A2062a7, 10), the lower jaw forms a U-shaped structure, which probably approximates its shape in life.

DESCRIPTION: In well preserved specimens, the length of the jaw ranges from 8.4 to 12.6 mm, and averages 10.3 mm (table 12). The width of the wing ranges from 5.4 to 7.6 mm, and averages 6.2 mm. The ratio of jaw width (= twice wing width) to length ranges from 0.98 to 1.48, and averages 1.23. The symphysal edge is straight and forms a flange that increases in height posteriorly. The anterior margin is nearly straight, the lateral margin is broadly rounded, and the posterior margin is sharply rounded. The wings are ventrally convex and covered with small folds that parallel the posterior margin.

TABLE 12
Measurements of the Lower Jaws of *Discoscaphites iris* (Conrad, 1858), Tinton Formation, Manasquan River Basin, Monmouth County, New Jersey[a]

Specimen	Width (W)	Length (L)	2W/L
AMNH 51298	5.6	10.4	1.08
AMNH 51313	6.6	10.7	1.23
MAPS A2062a1	6.7	12.0	1.12
MAPS A2062a2	6.0	8.7*	1.38*
MAPS A2062a3	6.2	9.3	1.33
MAPS A2062a4	4.0*	6.5*	1.23*
MAPS A2062a5	5.4	7.6*	1.42*
MAPS A2062a6	4.2*	6.5*	1.29*
MAPS A2062a7	6.2	12.6	0.98
MAPS A2062a8	6.5	7.8*	1.67*
MAPS A2062a9	7.6	10.3	1.48
MAPS A2062a10	5.2	8.4	1.24
MAPS A2062a11	6.2	9.6*	1.29*
MAPS A2062a12	6.1	8.8	1.39

[a]W = maximum width of the wing, measured perpendicular to the symphysis; L = maximum length of the jaw, measured parallel to the symphysis; 2W/L = ratio of jaw width to length; * = estimate. All measurements in millimeters.

DISCUSSION: This is the first record of the lower jaws of ammonites from the Upper Cretaceous strata of the Atlantic Coastal Plain. These specimens closely resemble the lower jaws of scaphites illustrated from Maastrichtian deposits of South Dakota (Landman and Waage, 1993: figs. 37–41, 167E–I) and northern Europe (Birkelund, 1982: pl. 2, figs. 6, 7; Birkelund, 1993: pl. 17, figs. 2–4; Machalski, 2005: fig. 26). The presence of these jaws in the *Pinna* Layer suggests minimal transport and relatively rapid burial.

ACKNOWLEDGMENTS

Peter J. Harries (University of South Florida), John A. Chamberlain, Jr. (Brook-

lyn College), and Marcin Machalski (Institute of Paleobiology, Warsaw) reviewed an earlier draft of this manuscript and made many valuable suggestions. At the AMNH, Susan Klofak helped in the field, prepared specimens, and drew sutures; Kathy Sarg helped in the field, did the sedimentological analysis, and helped prepare the figures; Steve Thurston photographed the specimens and helped prepare the figures; Jay Biederman photographed the jaws; Yumiko Iwasaki helped in the field; Stephanie Crooms word-processed the manuscript; George E. Harlow, Denton Ebel, and Charles Mandeville kindly examined sediment samples and identified minerals; and John Maisey helped identify fish teeth. At Stony Brook, Kirk Cochran helped in the interpretation of the geochemical data, Robert Aller provided information on the formation of glauconite, and Josie Aller helped in the interpretation of burrows. At the U.S.Geological Survey (Reston, Virginia), Colleen Durand prepared the dinoflagellate samples. We thank Paul Calloman (Academy of Natural Sciences of Philadelphia), Copeland MacClintock and Susan Butts (Yale Peabody Museum), William B. Gallagher (New Jersey State Museum), William A. Cobban (U.S. Geological Survey, Denver), and Dan Levin (National Museum of Natural History) for providing access to specimens in their care. Penny Chapman (Ridgefield, New Jersey), Bill Beck (Bridgeton, New Jersey), and Michelle Carter (Brooklyn College) assisted in field work. We are grateful to the construction crew at the original bridge site on the Manasquan River for their generous help. We also thank the owner of the McNeil Farm at Ivanhoe Brook who dug a pit on his property for us to study the geology. Field work was supported by the Norman D. Newell Fund of the American Museum of Natural History. F.T. Kyte was supported by NASA grants NAG5-12895 and NNA04CC10A.

Dedicated to the memory of Norman D. Newell (1909–2005), Curator of Invertebrate Paleontology at the American Museum of Natural History, whose work on mass extinctions, and their influence on the history of life, has inspired generations of paleontologists.

REFERENCES

Adbel-Gawad, G.I. 1986. Maastrichtian noncephalopod mollusks (Scaphopoda, Gastropoda, and Bivalvia) of the Middle Vistula Valley, Central Poland. Acta Geologica Polonica 36(1–3): 69–224.

Agassiz, L. 1847. An introduction to the study of natural history, in a series of lectures delivered in the hall of the College of Physicians and Surgeons. New York: 1–58.

Aller, R.C. 2004. Conceptual models of early diagenetic processes: The muddy seafloor as an unsteady, batch reactor. Journal of Marine Research 62: 815–835.

Arenillas, I., J.A. Arz, J.M. Grajales-Nishimura, G. Murillo-Muñetón, W. Alvarez, A. Camargo-Zanoguera, E. Molina, and C. Rosales-Domínguez. 2006. Chicxulub impact event is Cretaceous/Paleogene boundary in age: New micropaleontological evidence. Earth and Planetary Science Letters 249: 241–257.

Atabekian, A.A., and V.T. Akopian. 1969. Late Cretaceous ammonites of the Armenian SSR (Pachydiscidae). Izvestiya AN Armyanskoj SSR Nauki o Zemle 6: 3–20. [In Russian]

Beesley, P.L., G.J.B. Ross, and A. Wells (editors). 1998. Mollusca: The Southern Synthesis. Fauna of Australia. Vol. 5, Part B: 565–1234. Melbourne: CSIRO Publishing.

Bensen, D.G. 1976. Dinoflagellate taxonomy and biostratigraphy at the Cretaceous-Tertiary boundary, Round Bay, Maryland. Tulane Studies in Geology and Paleontology 12(4): 169–233.

Berggren, W.A., D.V. Kent, C.C. Swisher, III, and M.-P. Aubrey. 1995. A revised Cenozoic geochronology and chronostratigraphy. *In* W.A. Berggren and J. Hardenbol (editors), Geochronology, time scales and global stratigraphic correlation. SEPM Special Publication 54: 130–212. Tulsa, OK: Society for Sedimentary Geology.

Birkelund, T. 1979. The last Maastrichtian ammonites. *In* Cretaceous-Tertiary boundary events symposium. Vol. 1. The Maastrichtian and Danian of Denmark: 51–57. University of Copenhagen.

Birkelund, T. 1993. Ammonites from the Maastrichtian White Chalk in Denmark. Bulletin of the Geological Society of Denmark 40: 33–81.

Blainville, H.-M.D. de. 1825. Manuel de malacologie et de conchyliologie…. Paris: F.G. Levrault, 1825–1927.

Böhm, J. 1898. Über *Ammonites pedernalis* von Buch: Zeitschrift der Deutschen Geologischen Gesellschaft 50: 183–201.

Boyle, P., and P. Rodhouse. 2005. Cephalopods: ecology and fisheries. Oxford: Blackwell.

Bralower, T.J., C.K. Paull, and R.M. Leckie. 1998. The Cretaceous-Tertiary boundary cocktail: Chicxulub impact triggers margin collapse and extensive sediment gravity flows. Geology 26: B331–334.

Bralower, T.J., S. Geleskie, M.A. Arthur, and L. Eccles. 2006. Quantification of plankton size and flux changes across the Cretaceous/Paleocene Extinction. 2006 Geological Society of America Annual Meeting Abstracts with Programs 38(7): 473.

Brinkhuis, H., S. Sengers, A. Sluijs, J. Warnaar, and G.L. Williams. 2003. Latest Cretaceous-earliest Oligocene and Quaternary dinoflagellate cysts, ODP Site 1172, East Tasman Plateau. *In* N.F. Exon, J.P. Kennett, and M.J. Malone (editors), Proceedings of the Ocean Drilling Program, Scientific Results, 189 (Online) www.odp.tamu.edu/publications/189_SR/106/106.htm

Brunnschweiler, R.O. 1966. Upper Cretaceous ammonites from the Carnarvon Basin of Western Australia. 1. The heteromorph Lytoceratina. Bureau of Mineral Resources Geology and Geophysics Bulletin 58: 1–58.

Bryan, J.R., and D.S. Jones. 1989. Fabric of the Cretaceous-Tertiary marine macrofaunal transition at Braggs, Alabama. Palaeogeography, Palaeoclimatology, Palaeoecology 69: 279–301.

Bucher, H., N.H. Landman, S.M. Klofak, and J. Guex. 1996. Mode and rate of growth in ammonoids. *In* N.H. Landman, K. Tanabe, and R.A. Davis (editors), Ammonoid Paleobiology: 407–461. New York: Plenum Press.

Chauris, H., J. Lerousseau, B. Beadoin, S. Propson, and A. Montanari. 1998. Inoceramid extinction in the Gubbio basin (northeastern Apennines of Italy) and relations with mid-Maastrichtian environmental changes. Palaeogeography, Palaeoclimatology, Palaeoecology 139: 177–193.

Chinzei, K., E. Savazzi, and A. Seilacher. 1982. Adaptational strategies of bivalves living as infaunal secondary soft bottom dwellers. Neues Jahrbuch für Geologie und Paläontologie 164: 229–244.

Clark, W.B. 1891. A revision of the Cretaceous Echinoidea of North America. Johns Hopkins University Circulars 10(87): 75–77.

Clark, W.B. 1916. Upper Cretaceous deposits of Maryland. *In* W.B. Clark et al., Upper Cretaceous. Maryland Geological Survey Systematic Report 4(2): 749–752.

Clarke, R.F.A., and J.-P. Verdier. 1967. An investigation of microplankton assemblages from the Chalk of the Isle of Wight, England. Koninklijke Nederlandse Akademie van Wetenschappen Verhandelingen, Afdeling Natuurkunde Eerste Reeks 24(3): 1–96.

Cobban, W.A. 1969. The late Cretaceous ammonites *Scaphites leei* Reeside and *Scaphites hippocrepis* (DeKay) in the western interior of the United States. U.S. Geological Survey Professional Paper 619: 1–29.

Cobban, W.A., and W.J. Kennedy. 1995. Maastrichtian ammonites chiefly from the Prairie Bluff Chalk in Alabama and Mississippi. Paleontological Society Memoir 44: 1–40.

Collignon, M. 1952. Ammonites néocrétacées du Menabe (Madagascar). II-Les Pachydiscidae. Travaux du Bureau Géologique de Madagascar 41: 1–114.

Collignon, M. 1955. Ammonites néocrétacées du Menabe (Madagascar). II-Les Pachydiscidae. Annales Géologiques du Service des Mines de Madagascar 21: 1–98.

Collignon, M. 1971. Atlas des fossils caractéristiques de Madagascar (Ammonites). XVII. (Maestrichtien). Tananarive: Service Géologique.

Conrad, T.A. 1853. Article XXVI—Descriptions of new fossil shells of the United States. Journal of the Academy of Natural Sciences of Philadelphia, 2nd ser, 2: 273–276.

Conrad, T.A. 1857. Descriptions of Cretaceous and Tertiary fossils. *In* W.H. Emory (editor), Report on the United States and Mexican boundary survey. United States 34th Congress, 1st Session, Senate Ex Document 108 and House Ex Document 1351(2): 141–174.

Conrad, T.A. 1858. Observations on a group of Cretaceous fossil shells found in Tippah County, Mississippi, with descriptions of fifty-six new species. Journal of the Academy of Natural Sciences of Philadelphia, 2nd ser., 3: 323–336.

Conrad, T.A. 1860. Art. VIII—Description of new species of Cretaceous and Eocene fossils of Mississippi and Alabama. Journal of the Academy of Natural Sciences of Philadelphia, 2nd ser., Part III. 4: 275–298.

Conrad, T.A. 1868. Appendix A. Synopsis of the invertebrate fossils of the Cretaceous Formation of New Jersey. Geological Survey of New Jersey 1868: 721–732.

Conrad, T.A. 1870. Notes on recent and fossil shells, with descriptions of new species. American Journal of Conchology 6: 71–78.

Cookson, I.C. 1965. Microplankton from the Paleocene Pebble Point Formation, south-western Victoria. Proceedings of the Royal Society of Victoria 78: 137–141.

Cookson, I.C., and A. Eisenack. 1958. Microplankton from Australian and New Guinea Upper Mesozoic sediments. Proceedings of the Royal Society of Victoria 70(1): 19–79.

Cookson, I.C., and A. Eisenack. 1960. Microplankton from Australian Cretaceous sediments. Micropaleontology 6(1): 1–18.

Cookson, I.C., and A. Eisenack. 1962. Additional microplankton from Australian Cretaceous sediments. Micropaleontology 8(4): 485–507.

Cooper, M.R. 1994. Towards a phylogenetic classification of the Cretaceous ammonites. III. Scaphitaceae. Neues Jahrbuch für Geologie und Palaeontologie Abhandlung 193(2): 165–193.

Cope, K.H., J.E. Utgaard, J.M. Masters, and R.M. Feldmann. 2005. The fauna of the Clayton Formation (Paleocene, Danian) of southern Illinois: a case of K/P survivorship and Danian recovery. Bulletin of the Mizunami Fossil Museum 32: 97–108.

Cowie, J.W., W. Ziegler, and J. Remane. 1989. Stratigraphic Commission accelerates progress, 1984 to 1989. Episodes 12(2): 79–83.

Crick, G.C. 1924. On Upper Cretaceous Cephalopoda from Portuguese East Africa. Transactions of the Geological Society of South Africa 26: 130–140.

Cuvier, G. 1797. Tableau élémentaire de l' histoire naturelle des animaux. Paris: Baudouin, XVI, 710 pp.

Davey, R.J., and G.L. Williams. 1966. V. The genus *Hystrichosphaeridium* and its allies. *In* R.J. Davey, C. Downie, W.A.S. Sarjaent, and G.L. Williams (editors), Studies on Mesozoic and Cainozoic dinoflagellate cysts. Bulletin of the British Museum (Natural History). Geology Supplement 3: 53–106.

Davis, R.A., N.H. Landman, J.-L. Dommergues, D. Marchand, and H. Bucher. 1996. Mature modifications and dimorphism in ammonoid cephalopods. *In* N.H. Landman, K. Tanabe, and R.A. Davis (editors), Ammonoid Paleobiology: 463–539. New York: Plenum Press.

Deflandre, G. 1937. Microfossiles des silex crétacés. Deuxième partie. Flagellés incertae sedis. Hystrichosphaeridés. Sarcodinés. Organismes divers. Annales de Paléontologie 25: 151–191.

Deflandre, G., and I.C. Cookson. 1955. Fossil microplankton from Australian Late Mesozoic and Tertiary sediments. Australian Journal of Marine and Freshwater Research 6(2): 242–313.

Defrance, M.J.L. 1816. Dictionnaire des sciences naturelles, dans lequel on traite méthodiquement des differents Etres de la Nature…, Vol. 3. Paris and Strassbourg: Levrault.

D'Hondt, S. 2005. Consequences of the Cretaceous/Paleogene mass extinction for marine ecosystems. Annual Review of Ecology, Evolution, and Systematics 36: 295–317.

Downie, C., and W.A.S. Sarjeant. 1965. Bibliography and index of fossil dinoflagellates and acritarchs. Geological Society of America Memoir 94: 1–180. (Cover date: December, 1964; issue date: January, 1965.)

Drugg, W.S., and A.R. Loeblich, Jr. 1967. Some Eocene and Oligocene phytoplankton from the Gulf Coast, U.S.A. Tulane Studies in Geology 5(4): 181–194.

Duxbury, S. 1980. Barremian phytoplankton from Speeton, east Yorkshire. Palaeontographica Abteilung B 173(4–6): 107–146.

Edwards, L.E., G.S. Gohn, J.M. Self-Trail, D.C. Prowell, L.M. Bybell, L.P. Bardot, J.V. Firth, B.T. Huber, N.O. Frederiksen, and K.G. MacLeod. 1999. Physical stratigraphy, paleontology, and magnetostratigraphy of the USGS-Santee Coastal Reserve core (CHN-803), Charleston County, South Carolina. United States Geological Survey Open-File Report: 99-0308-A: 1–36.

Edwards, L.E., D.K. Goodman, and R.J. Witmer. 1984. Lower Tertiary (Pamunkey Group) dinoflagellate biostratigraphy, Potomac River area, Virginia and Maryland. *In* N.O. Frederiksen and K. Krafft (editors), Cretaceous and Tertiary stratigraphy, paleontology, and structure, southwestern Maryland, and northeastern Virginia. American Association of Stratigraphic Palynologists Field Trip Volume and Guidebook October 17, 1984: 137–152.

Eisenack, A. 1954. Mikrofossilien aus Phosphoriten des samländischen Unteroligozäns und über Einheitlichkeit der Hystrichosphaerideen. Palaeontographica Abteilung A 105: 49–95.

Eisenack, A., and H. Gocht. 1960. Neue Namen für einige Hystrichosphären der Bernsteinformation Ostpreussens. Neues Jahrbuch für Geologie und Paläontologie, Monatschefte 11: 511–518.

Fenton, C.L., and M.A. Fenton. 1932. A new species of *Cliona* from the Cretaceous of New Jersey. American Midland Naturalist 13: 54–62.

Firth, J.V. 1987. Dinoflagellate biostratigraphy of the Maastrichtian to Danian interval in the U.S. Geological Survey Albany Core, Georgia, U.S.A. Palynology 11: 199–216.

Firth, J.V. 1993. Dinoflagellate assemblages and sea-level fluctuations in the Maastrichtian of southwest Georgia. Review of Palaeobotany and Palynology 79: 179–404.

Forbes, E. 1846. Report on the fossil Invertebrata from southern India, collected by Mr. Kaye and Mr. Cunliffe. Transactions of the Geological Society of London, 2nd ser., 7: 97–174.

Gabb, W.M. 1859. Art. IX-Descriptions of some new species of Cretaceous fossils. Journal of the Academy of Natural Sciences of Philadelphia, 2nd ser., Pt. III, 4: 299–305.

Gabb, W.M. 1860. Art. XIV-Descriptions of new species of American Tertiary and Cretaceous fossils. Journal of the Academy of Natural Sciences of Philadelphia, 2nd ser., Pt. IV, 4: 375–406.

Gabb, W.M. 1861. Description of new species of Cretaceous fossils from New Jersey, Alabama and Mississippi. Proceedings of the Academy of Natural Sciences of Philadelphia 13: 318–330.

Gaffney, E.S. 1975. A revision of the side-necked turtle *Taphrosphys sulcatus* (Leidy) from the Cretaceous of New Jersey. American Museum Novitates 2571: 1–24.

Gallagher, W.B. 1986. Depositional environments, paleo-oceanography, and paleoecology of the Upper Cretaceous-Lower Tertiary sequence in the New Jersey Coastal Plain. *In* R. Talkington (editor), Geological investigations of the coastal plain of southern New Jersey. Part 2. B. Paleontologic investigations. 2nd Annual Meeting of the Geological Association of New Jersey, Stockton State College, Pomona, New Jersey: 1–17.

Gallagher, W.B. 1993. The Cretaceous/Tertiary mass extinction event in the northern Atlantic Coastal Plain. Mosasaur 5: 75–155.

Gallagher, W.B. 2002. Faunal change across the Cretaceous-Tertiary (K-T) boundary in the Atlantic coastal plain of New Jersey: restructuring the marine community after the K-T mass-extinction event. *In* C. Koeberl and K.G. MacLeod (editors), Castastrophic events and mass extinctions: impacts and beyond. Geological Society of America Special Paper 356: 291–301.

Gallagher, W.B., D.C. Parris, and E.E. Spamer. 1986. Paleontology, biostratigraphy, and depositional environments of the Cretaceous-Tertiary transition in the New Jersey Coastal Plain. Mosasaur 3: 1–35.

Ganapathy, R., S. Gartner, and M.-J. Jiang. 1981. Iridium anomaly at the Cretaceous/Tertiary boundary in Texas. Earth and Planetary Science Letters 54: 393–396.

Gardner, J. 1916. Upper Cretaceous systematic paleontology: Mollusca. *In* W.B. Clark et al., Upper Cretaceous. Maryland Geological Survey Systematic Report 6(1–2): 371–733.

Gill, T. 1871. Arrangement of the families of mollusks. Smithsonian Miscellaneous Collections 227: 1–49.

Gocht, H. 1970. Dinoflagellaten-Zysten aus einem Geschiebefeuerstein und ihr Erhaltungszustand. Neues Jahrbuch für Geologie und Paläontologie, Monatshefte 3: 129–140.

Goloboff, P. 1993. *NONA, version 2.0, Program and Documentation*. Tucumán, Argentina: P. Goloboff, Also available online at http://www.cladistics.com.

Goolaerts, S., W.J. Kennedy, C. Dupuis, and E. Steurbaut. 2004. Terminal Maastrichtian ammonites from the Cretaceous – Paleogene Global Stratotype Section and Point, El Kef, Tunisia. Cretaceous Research 25: 313–328.

Grossouvre, A. de. 1894. Recherches sur la craie supérieure 2: Paléontologie. Les ammonites de la Craie supérieure. Mémoires pour Servir à l'Explication de la Carte Géologique Détaillée de la France: 1–264. (misdated 1893).

Guinasso, N.L., Jr., and D.R. Schink. 1975. Quantitative estimates of biological mixing rates in abyssal sediments. Journal of Geophysical Research 80(21): 3023–3043.

Habib, D., and W.S. Drugg. 1987. Palynology of sites 603 and 605, Leg 93, Deep Sea Drilling Project. *In* J.E. van Hinte, S.W. Wise, Jr. et al., Initial reports, Deep Sea Drilling Project 92(2): 751–776.

Hallam, A., and P.B. Wignall. 1997. Mass extinctions and their aftermath. New York: Oxford University Press.

Hansen, H.J. 1990. Diachronous extinctions at the K/T boundary; a scenario. Geological Society of America Special Paper 247: 417–423.

Hansen, J.M. 1977. Dinoflagellate stratigraphy and echinoid distribution in Upper Maastrichtian and Danian deposits from Denmark. Bulletin of the Geological Society of Denmark 26: 1–26.

Hansen, J.M. 1979. A new dinoflagellate zone at the Maastrichtian/Danian boundary in Denmark. Danmarks Geologiske Understø-gelse, Årboog 1978: 131–140.

Hansen, T.A., R.B. Farrand, H.A. Montgomery, H.G. Billman, and G. Blechenschmidt. 1987. Sedimentology and extinction patterns across the Cretaceous-Tertiary boundary interval in east Texas. Cretaceous Research 8: 229–252.

Hansen, T.A., B. Upshaw III, E.G. Kauffman, and W. Gose. 1993a. Patterns of molluscan extinction and recovery across the Cretaceous-Tertiary boundary in east Texas; report on new outcrops. Cretaceous Research 14: 685–706.

Hansen, T.A., B.R. Farrell, and B. Upshaw III. 1993b. The first 2 million years after the Cretaceous-Tertiary boundary in east Texas: rate and paleoecology of the molluscan recovery. Paleobiology 19(2): 251–265.

Harries, P.J. 2006. What does the "Lilliput Effect" mean? 2006 Geological Society of America Annual Meeting Abstracts with Programs 38(7): 473.

Harris, G.D. 1894. The Tertiary geology of southern Arkansas. Arkansas Geological Survey Annual Report for 1892. 2: 1–207.

Hauer, F.von. 1858. Uber die Cephalopoden aus der Gosauschichten. Beiträge zur Paläontologie von Osterreich 1: 7–14.

Heinberg, C. 1999. Lower Danian bivalves, Stevns Klint, Denmark: continuity across the K/T boundary. Palaeogeography, Palaeoclimatology, Palaeoecology 154: 87–106.

Henderson, R.A., W.J. Kennedy, and K.J. McNamara. 1992. Maastrichtian heteromorph ammonites from the Carnarvon Basin, Western Australia. Alcheringa 16: 133–170.

Hewitt, R. 1996. Architecture and strength of the ammonoid shell. *In* N.H. Landman, K. Tanabe, and R.A. Davis (editors), Ammonoid Paleobiology. 297–343. New York: Plenum Press.

Histon, K. 2002. Telescoping in orthoconic nautiloids: An indication of high or low energy hydrodynamic regime? *In* H. Summesberger, K. Histon, and A. Daurer (editors), Cephalopods-Present and Past. Abhandlungen der Geologischen Bundesanstalt 57: 431–442.

Hsü, K.J., and J.A. McKenzie. 1985. A "Strangelove Ocean" in earliest Tertiary. In E.T. Sundquist and W. Broecker (editors), American Geophysical Union Monograph 32: 487–492.

Hultberg, S.U. 1986. Danian dinoflagellate zonation, the C-T boundary and the stratigraphical position of the fish clay in southern Scandinavia. Journal of Micropalaeontology 5: 37–47.

Hultberg, S.U., and B.A. Malmgren. 1985. Dinoflagellate and planktonic foraminiferal paleobathymetrical indices in the Boreal uppermost Cretaceous. Micropaleontology 32: 316–323.

Hultberg, S.U., and B.A. Malmgren. 1987. Quantitative biostratigraphy based on Late Maastrichtian dinoflagellates and planktonic foraminifera from southern Scandinavia. Cretaceous Research 8: 211–228.

Hyatt, A. 1889. Genesis of the Arietidae. Smithsonian Contributions to Knowledge 26(637): 1–239.

Hyatt, A. 1894. Phylogeny of an acquired characteristic. Proceedings of the American Philosophical Society 32: 349–647.

Hyatt, A. 1900. Cephalopoda. *In* K.A. von Zittel (editor), Textbook of palaeontology, translated by C.R. Eastman, pp. 502–604. London: Macmillan, 1896–1900.

Ifrim, C., W. Stinnesbeck, and A. Schafhauser. 2005. Maastrichtian shallow-water ammonites of northeastern Mexico. Revista Mexicana de Ciencias Geologicas 22(1): 48–64.

Jablonski, D., and D.T. Bottjer. 1983. Soft-bottom epifaunal suspension feeding assemblages in the Late Cretaceous: Implications for the evolution of benthic paleocommunities. *In* M.J.S. Tevesz and P.L. McCall (editors), Biotic interactions in Recent and fossil benthic communities: 747–812. New York: Plenum Press.

Jagt, J.W.M. 1996. Late Maastrichtian and Early Palaeocene index macrofossils in the Maastrichtian type area (SE Netherlands, NE Belgium). Geologie en Mijnbouw 75: 153–162.

Jagt, J.W.M. 2002. Late Cretaceous ammonite faunas of the Maastrichtian type area. *In* H. Summesberger, K. Histon, and A. Daurer (editors), Cephalopods–Present and Past. Abhandlungen der Geologischen Bundesanstalt Wien 57: 509–522.

Jagt, J.W.M., and W.J. Kennedy. 1989. *Acanthoscaphites varians* (Lopuski, 1911) (Ammonoidea) from the Upper Maastrichtian of Haccourt, N.E. Belgium. Geologie en Mijnbouw 68: 237–240.

Jagt, J.W.M., S. Goolaerts, E.A. Jagt-Yazykova, G. Cremers, and W. Verhesen. 2006. First record of *Phylloptychoceras* (Ammonoidea) from the Maastrichtian type area, The Netherlands. Bulletin de l'Institut royal des Sciences naturelles de Belgique. Sciences de la Terre 76: 97–103.

Jagt, J.W.M., J. Smit, and A.S. Schulp. 2003. ?Early Paleocene ammonites and other molluscan taxa from the Angerpoort-Curfs quarry (Geulhem, southern Limburg, the Netherlands). *In* M.A. Lamolda (editor), Bioevents: their stratigraphical records, patterns and causes. Caravaca, 3rd–8th June 2003, p. 113. Ayuntamiento de Caravaca de la Cruz.

Jeletzky, J.A., and K.M. Waage. 1978. Revision of *Ammonites conradi* Morton 1834, and the concept of *Discoscaphites* Meek 1870. Journal of Paleontology 52(5): 1119–1132.

Katsamevakis, S. 2005. Population ecology of the endangered fan mussel *Pinna nobilis* in a marine lake. Endangered Species Research 1: 1–9.

Kauffman, E.G., B.B. Sageman, J.I. Kirkland, W.P. Elder, P.J. Harries, and T. Villamil. 1993. Molluscan biostratigraphy of the Cretaceous Western Interior Basin, North America. *In* W.G.E. Caldwell and E.G. Kauffman (editors), Evolution of the Western Interior Basin, Geological Association of Canada, Special Paper 39: 397–434.

Keller, G., W. Stinnesbeck, T. Adatte, and D. Stüben. 2003. Multiple impacts across the Cretaceous-Tertiary boundary. Earth-Sciences Reviews 1283: 1–37.

Keller, G., T. Adatte, W. Stinnesbeck, M. Rebolledo-Vieyra, J. Fucugauchi, U. Kramar, and D. Stüben. 2004. Chicxulub impact predates the K-T boundary mass extinction. Proceedings of the National Academy of Sciences 101(11): 3753–3758.

Kennedy, W.J. 1986. The ammonite fauna of the Calcaire à *Baculites* (Upper Maastrichtian) of the Cotentin Peninsula (Manche, France). Palaeontology 29: 25–83.

Kennedy, W.J. 1987. The ammonite fauna of the type Maastrichtian with a revision of *Ammonites colligatus* Binkhorst, 1861. Bulletin de l'Institut Royal des Sciences Naturelles de Belgique 56: 151–267 (1986 imprint).

Kennedy, W.J. 1993. Ammonite faunas of the European Maastrichtian, diversity and extinction. *In* The Ammonoidea: Environment, Ecology, and Evolutionary Change, M.R. House (editor), Systematics Association Special Volume No. 47: 285–326. Oxford: Clarendon Press.

Kennedy, W.J., and W.A. Cobban. 1993. Maastrichtian ammonites from the Corsicana Formation in northeast Texas. Geological Magazine 130(1): 57–67.

Kennedy, W.J., and W.A. Cobban. 1996. Maastrichtian ammonites from the Hornerstown Formation in New Jersey. Journal of Paleontology 70(5): 798–804.

Kennedy, W.J., and W.A. Cobban. 2000. Maastrichtian (Late Cretaceous) ammonites from the Owl Creek Formation in northeastern Mississippi, U.S.A. Acta Geologica Polonica 50(1): 175–190.

Kennedy, W.J., W.A. Cobban, and N.H. Landman. 1997. Maastrichtian ammonites from the Severn Formation of Maryland. American Museum Novitates 3210: 1–30.

Kennedy, W.J., A.S. Gale, and T.A. Hansen. 2001. The last Maastrichtian ammonites from the Brazos River sections in Falls County, Texas. Cretaceous Research 22: 163–171.

Kennedy, W.J., R.O. Johnson, and W.A. Cobban. 1995. Upper Cretaceous ammonite faunas of New Jersey. *In* J.E.B. Baker (editor), Contributions to the Paleontology of New Jersey 12: 24–55. Trenton: The Geological Association of New Jersey.

Kennedy, W.J., and H.C. Klinger. 2006. Cretaceous faunas from Zululand and Natal, South Africa. The ammonite family Pachydiscidae Spath, 1922. African Natural History 2(2006): 17–166.

Kennedy, W.J., and F. Kulbrok. 2003. An Upper Maastrichtian ammonite faunule from the Eastern Desert, Egypt. Neues Jahrbuch für Geologie und Paläontologie Monatshefte 2003: 449–462.

Kennedy, W.J., N.H. Landman, W.K. Christensen, W.A. Cobban, and J.M. Hancock. 1998. Marine connections in North America during the late Maastrichtian: palaeogeographic and palaeobiogeographic significance of *Jeletzkytes nebrascensis* Zone cephalopod fauna from the Elk Butte Member of the Pierre Shale, SE South Dakota and NE Nebraska. Cretaceous Research 19: 745–775.

Kennedy, W.J., N.H. Landman, W.A. Cobban, and R.O. Johnson. 2000. Additions to the ammonite fauna of the Upper Cretaceous Navesink Formation of New Jersey. American Museum Novitates 3306: 1–30.

Keupp, H. 2006. Sublethal punctures in body chambers of Mesozoic ammonites (forma *aegra fenestra* n.f.), a tool to interpret synecological relationships, particularly predator-prey interactions. Palaeontologische Zeitschrift 80/2: 112–123.

Kiessling, W., and P. Claeys. 2001. A geographic database approach to the KT boundary. *In* E. Buffetaut and C. Koeberl (editors), Geological and biological effects of impact events: 83–140. New York: Springer.

Kilian, W., and P. Reboul. 1909. Les Céphalopodes néocrétacées des Îles Seymour et Snow Hill. Wissenschaftliche Ergebnisse der Schwedischen Südpolar-Expedition 1901–1903 3(6): 1–75.

Kineke, G.C., and R.W. Sternberg. 1995. Distribution of fluid muds on the Amazon continental shelf. Marine Geology 125: 193–233.

Kineke, G.C., R.W. Sternberg, J.H. Trowbridge, and W.R. Geyer. 1996. Fluid-mud processes on the Amazon continental shelf. Continental Shelf Research 16(536): 667–696.

Klinger, H.C. 1976. Cretaceous heteromorph ammonites from Zululand. Memoirs of the Geological Survey of South Africa 69: 1–142.

Klinger, H.C., E.G. Kauffman, and W.J. Kennedy. 1980. Upper Cretaceous ammonites and inoceramids from the off-shore Alphard Group of South Africa. Annals of the South African Museum 82: 293–320.

Klinger, H.C., and W.J. Kennedy. 1993. Cretaceous faunas from Zululand and Natal, South Africa. The heteromorph ammonite genus *Eubaculites* Spath, 1926. Annals of the South African Museum 102: 185–264.

Klinger, H.C., and W.J. Kennedy. 2001. Stratigraphic and geographic distribution, phylogenetic trends and general comments on the ammonite family Baculitidae Gill, 1871 (with an annotated list of species referred to the family). Annals of the South African Museum 107: 1–290.

Klinger, H.C., W.J. Kennedy, J.A. Lees, and S. Kitto. 2001. Upper Maastrichtian ammonites and nannofossils and a Palaeocene nautiloid from Richards Bay, Kwa Zulu, South Africa. Acta Geologica Polonica 51(3): 273–291.

Koch, C.F., and N.F. Sohl. 1983. Preservational effects in paleoecological studies: Cretaceous mollusc examples. Paleobiology 9(1): 26–34.

Koeberl, C. and K.G. MacLeod (editor). 2002. Catastrophic events and mass extinctions: Impacts and beyond. Boulder, CO: Geological Society of America.

Kossmat, F. 1895. Untersuchungen über die Südindische Kreideformation. Beiträge zur Paläontologie Österreich-Ungarns und des Orients 9(1895): 97–203 (1–107).

Kotetishvili, E. 1999. Upper Cretaceous ammonites and their extinction: interpretation of data

from the Caucasus and comparison with Mangyshlak, the Crimea and the Maastricht area. Bulletin de l'Institut royal des Sciences naturelles de Belgique. Sciences de la Terre 69: 167–172.

Kullmann, J., and J. Wiedmann. 1970. Significance of sutures in phylogeny of Ammonoidea. University of Kansas, Paleontological Contributions 44: 1–32.

Kump, L.R. 1991. Interpreting carbon-isotope excursions: Strangelove oceans. Geology 19: 299–302.

Lamarck, J.P. 1801. Système des animaux sans vertèbres. Paris: Deterville.

Lamarck, J.P. 1822. Histoire naturelle des animaux sans vertèbres. Paris: Verdière.

Landman, N.H., R.O. Johnson, and L.E. Edwards. 2004a. Cephalopods from the Cretaceous/Tertiary boundary interval on the Atlantic Coastal Plain, with a description of the highest ammonite zones in North America. Part 1. Maryland. American Museum Novitates 3454: 1–64.

Landman, N.H., R.O. Johnson, and L.E. Edwards. 2004b. Cephalopods from the Cretaceous/Tertiary boundary interval on the Atlantic Coastal Plain, with a description of the highest ammonite zones in North America. Part 2. Northeastern Monmouth County, New Jersey. Bulletin of the American Museum of Natural History 287: 1–107.

Landman, N.H., R.O. Johnson, M.P. Garb, and L.E. Edwards. In prep. Cephalopods from the Cretaceous/Tertiary boundary in New Jersey and Maryland, with a description of the highest ammonite zones in North America. Part 4. Crosswicks Creek Basin, Monmouth County, New Jersey.

Landman, N.H., N.L. Larson, and W.A. Cobban. In press. Jaws and radula of baculites from the Upper Cretaceous (Campanian) of North America. Cephalopods-Past and Present. New York: Springer Verlag.

Landman, N.H., D.M. Rye, and K.L. Shelton. 1983. Early ontogeny of *Eutrephoceras* compared to Recent *Nautilus* and Mesozoic ammonites: evidence from shell morphology and light stable isotopes. Paleobiology 9(3): 269–279.

Landman, N.H., and K.M. Waage. 1993. Scaphitid ammonites of the Upper Cretaceous (Maastrichtian) Fox Hills Formation in South Dakota and Wyoming. Bulletin of the American Museum of Natural History 215: 1–257.

Lejeune-Carpentier, M. 1938. L'étude microscopique des silex. Areoligera : nouveau genre d'Hystrichosphaeridée. (Sixième note.). Annales de la Société Géologique de Belgique 62: B163–B174.

Lejeune-Carpentier, M. 1942. L'étude microscopique des silex. Péridiniens nouveaux ou peu connnus (Dixième note). Annales de la Société Géologique de Belgique 65: B181–B192.

Lentin, J.K., and T.F. Vozzhennikova. 1990. Fossil dinoflagellates from the Jurassic, Cretaceous and Paleogene deposits of the USSR—a re-study. American Association of Stratigraphic Palynologists Contribution Series 23: 1–221.

Lentin, J.K., and G.L. Williams. 1973. Fossil dinoflagellates: index to genera and species. Geological Survey of Canada Paper 73–42: 1–176.

Lentin, J.K., and G.L. Williams. 1976. A monograph of fossil peridinoid dinoflagellate cysts. Bedford Institute of Oceanography Report Series BI-R-75-16: 1–237.

Lewis, J.V., and H.B. Kümmel. 1910–1912 (revised 1950). Geologic map of New Jersey: New Jersey Geological Survey, scale 1:250,000.

Lockwood, R. 2006. Trends in body size across the end-Cretaceous and Early Cenozoic extinctions in veneroid bivalves. 2006 Geological Society of America Annual Meeting Abstracts with Programs 38(7): 473.

Łopuski, C. 1911. Przyczynki do znajomosci fauny kredowej guberni Lubelskiej. Sprawozdania Towarzystwa Naukowego Warszawskiego 4: 104–140.

Luterbacher, H.P., J.R. Ali, H. Brinkhuis, F.M. Gradstein, J.J. Hooker, S. Monechi, J.G. Ogg, J. Powell, U. Röhl, A. Sanfilippo, and B. Schmitz. 2004. The Paleogene Period. *In* F.M. Gradstein, J.G. Ogg, and A.G. Smith (editors), A geologic time scale 2004: 384–408. New York: Cambridge University Press.

Lyell, C., and E. Forbes. 1845. On the fossil shells collected by Mr. Lyell from the Cretaceous formations of New Jersey. Quarterly Journal of the Geological Society of London 1: 61–64.

Macellari, C.E. 1986. Late Campanian-Maastrichtian ammonites from Seymour Island (Antarctic Peninsula). Paleontological Society Memoir 18. Journal of Paleontology 60 (2 supp.): 1–55.

Macellari, C.E. 1988. Stratigraphy, sedimentology, and paleontology of Upper Cretaceous/Paleocene shelf-deltaic sediments of Seymour Island. *In* R.M. Feldman and M.O. Woodburne (editors), Geology and Paleontology of Seymour Island, Antarctic Peninsula. Geological Society of America Memoir 169: 25–53.

Machalski, M. 1998. The Cretaceous-Tertiary boundary in Central Poland. Przegląd Geologiczny 46: 1153–1161. [In Polish]

Machalski, M. 2002. Danian ammonites: A discussion. Bulletin of the Geological Society of Denmark 49: 49–52.

Machalski, M. 2005a. The youngest Maastrichtian ammonite faunas from Poland and their dating by scaphitids. Cretaceous Research 26: 813–836.

Machalski, M. 2005b. Late Maastrichtian and earliest Danian scaphitid ammonites from central Europe: Taxonomy, evolution, and extinction. Acta Palaeontologica Polonica 50(4): 653–696.

Machalski, M., and C. Heinberg. 2005. Evidence for ammonite survival into the Danian (Paleogene) from the Cerithium Limestone at Stevns Klint, Denmark. Bulletin of the Geological Society of Denmark 52: 97–111.

Machalski, M., and I. Walaszczyk. 1987. Faunal condensation and mixing in the uppermost Maastrichtian/Danian greensand (Middle Vistula Valley, central Poland). Acta Geologica Polonica 37: 75–91.

Machalski, M., and I. Walaszczyk. 1988. The youngest (uppermost Maastrichtian) ammonites in the middle Vistula Valley, central Poland. Bulletin of the Polish Academy of Sciences, Earth Sciences 36: 67–70.

MacLeod, K.G., B.T. Huber, and P.D. Ward. 1996. The biostratigraphy and paleobiogeography of Maastrichtian inoceramids. *In* G. Ryder, D. Fastovsky, and S. Gartner (editors), The Cretaceous-Tertiary Event and other catastrophes in Earth history. Geological Society of America, Special Paper 307: 361–373.

MacLeod, N. 2006. Size, extinction, survivorship and phylogeny in Foraminifera. 2006 Geological Society of America Annual Meeting Abstracts with Programs 38(7): 473.

Maeda, H., and A. Seilacher. 1996. Ammonoid taphonomy. *In* N.H. Landman, K. Tanabe, and R.A. Davis (editors), Ammonoid Paleobiology: 544–578. New York: Plenum Press.

Marshall, C.R. 1995. Distinguishing between sudden and gradual extinctions in the fossil record: predicting the position of the Cretaceous – Tertiary iridium anomaly using the ammonite fossil record on Seymour Island, Antarctica. Geology 23(8): 731–734.

Marshall, C.R., and P.D. Ward. 1996. Sudden and gradual molluscan extinctions in the latest Cretaceous of Western European Tethys. Science 274: 1360–1363.

Mathey, B. 1987. The paleogeographical evolution of the Basco - Cantabrian domain during the Upper Cretaceous. *In* M.A. Lamolda (editor), Field-guide excursion to the K/T Boundary at Zumaya and Biarritz. III Jornadas de Paleontologia - Paleontologia y evolución: fenómenos de extinción: 1–16. Vasco: Universidad del Pais.

Matsumoto, T. 1947. A note on the Japanese Pachydiscinae. Scientific Reports of the Department of Geology, Faculty of Sciences, Kyushu University 2: 34–46 [In Japanese]

May, F.E. 1977. Functional morphology, paleoecology, and systematics of *Dinogymnium* tests. Palynology 1: 103–121.

May, F.E. 1980. Dinoflagellate cysts of the Gymnodiniaceae, Peridiniaceae, and Gonyaulacaceae from the Upper Monmouth Group, Atlantic Highlands, New Jersey. Palaeontographica Abteilung B 172: 10–116.

Meek, F.B. 1857. Descriptions of new organic remains from the Cretaceous rocks of Vancouver Island. Transactions of the Albany Institute 4: 37–49.

Meek, F.B. 1871. Preliminary paleontological report, consisting of lists of fossils, with descriptions of some new types, etc. Preliminary Report of the United States Geological Survey of Wyoming (Hayden) 4: 287–318.

Miller, A.K. 1951. Tertiary nautiloids of westcoastal Africa. Annales du Musée Royal du Congo Belge Série.8, Sciences Géologiques 8: 1–88.

Miller, A.K., and H.F. Garner. 1962. Cretaceous nautiloids of New Jersey. *In* H.G. Richards *et al.* (editors), The Cretaceous fossils of New Jersey. New Jersey Department of Conservation and Economic Development Bulletin 61. Part 2: 101–111.

Miller, K.G., P.J. Sugarman, J.V. Browning, M.A. Kominz, R.K. Olsson, M.D. Feigenson, and J.C. Hernández. 2004. Upper Cretaceous sequences and sea-level history, New Jersey Coastal Plain. Geological Society of America Bulletin 116(3/4): 368–393.

Miller, K.G., Sr., J.V. Browning, M.A. Kominz, P.J. Sugarman, P.P. McLaughlin, T.G. Hayden, and A.A. Kulpecz. 2006. Tectonic and sediment supply effects on eustatically controlled sequences of the Mid Atlantic Region. 2006 Geological Society of America Annual Meeting. Abstracts with Programs 38(7): 128.

Minard, J.P., P. Owens, N.F. Sohl, H.E. Gill, and J.F. Mello. 1969. Cretaceous-Tertiary boundary in New Jersey, Delaware, and eastern Maryland. United States Geology Survey Bulletin 1274-H: 1–33.

Monks, N. 2000. Functional morphology, ecology, and evolution of the Scaphitaceae Gill, 1871 (Cephalopoda). Journal of Molluscan Studies 66: 205–216.

Morgenroth, P. 1966. Mikrofossilien und Konkretionen des nordwesteuropäischen Untereozäns. Palaeontographica Abteilung B 119: 1–53.

Morgenroth, P. 1968. Zur Kenntnis der Dinoflagellaten und Hystrichosphaeridien des Danien. Geologisches Jahrbuch Hannover 86: 533–578.

Morton, S.G. 1830. Synopsis of the organic remains of the Ferruginous Sand Formation of the United States, with geographical remarks. American Journal of Science and Arts 17: 274–295.

Morton, S.G. 1833. Article X-Supplement to the "Synopsis of the organic remains of the Ferruginous Sand Formation of the United States," contained in Vols. XVII and XVIII of this journal. American Journal of Science and Arts 23: 288–294.

Morton, S.G. 1834. Synopsis of the organic remains of the Cretaceous group of the United States. Illustrated by nineteen plates, to which is added an appendix containing a tabular view of the Tertiary fossils hitherto discovered in North America. Philadephia: Key and Biddle.

Moshkovitz, S., and D. Habib. 1993. Calcareous nannofossil and dinoflagellate stratigraphy of the Cretaceous-Tertiary boundary, Alabama and Georgia. Micropaleontology 39: 167–191.

Nittrouer, C.A., D.J. Demaster, S.A. Kuehl, B.A. McKee, and K.W. Thorbjarnarson. 1984. Some questions and answers about the accumulation of fine-grained sediment in continental margin environments. Geo-Marine Letters 4(3–4): 211–213.

Nixon, K.C. 2002. WinClada, version 1.00.08, Program and Documentation. Ithaca, New York: K.C. Nixon. Also available online at http://www.cladistics.com.

Olivero, E.B., and W.J. Zinsmeister. 1989. Large heteromorph ammonites from the Upper Cretaceous of Seymour Island, Antarctica. Journal of Paleontology 63(5): 626–636.

Olsson, R.K. 1960. Foraminifera of latest Cretaceous and earliest Tertiary age in the New Jersey Coastal Plain. Journal of Paleontology 34: 1–58.

Olsson, R.K. 1963. Latest Cretaceous and earliest Tertiary stratigraphy of New Jersey Coastal Plain. American Association of Petroleum Geologists Bulletin 47(4): 643–665.

Olsson, R.K. 1975. Upper Cretaceous and Lower Tertiary stratigraphy, New Jersey coastal plain. New York, New York: Petroleum Exploration Society.

Olsson, R.K. 1987. Cretaceous stratigraphy of the Atlantic Coastal Plain, Atlantic Highlands of New Jersey. Geological Society of America Centennial Field Guide-Northeastern Section: 87–90.

Olsson, R.K., K.G. Miller, J.V. Browning, D. Habib, and P.J. Sugarman. 1997. Ejecta layer at the Cretaceous-Tertiary boundary, Bass River, New Jersey (Ocean Drilling Program Leg 174AX). Geology 25: 759–762.

Olsson, R.K., K.G. Miller, J.V. Browning, J.D. Wright, and B.S. Cramer. 2002. Sequence stratigraphy and sea-level change across the Cretaceous-Tertiary boundary on the New Jersey passive margin. *In* C. Koeberl and K.G. MacLeod (editors), Catastrophic events and mass extinctions: impacts and beyond. Geological Society of America Special Paper 356: 97–100.

Orbigny, A.d'. 1847. Paléontologie. *In* D. d'Urville, Voyage au pole sud et dans l'Océanie sur les corvettes l'Astrolabe et la Zélée, exécuté par ordre du roi pendant les années 1837–1838–1839–1840, sous le commandement de M. J. Dumont d'Urville, capitaine de vaisseau …. Paris: Gide, 1842–1854.

Owen, D.D. 1852. Report of a geological survey of Wisconsin, Iowa, and Minnesota and incidentally of a portion of Nebraska Territory. Philadelphia: Lippincott, Grambo.

Owens, J.P., and N.F. Sohl. 1969. Shelf and deltaic paleoenvironments in the Cretaceous-Tertiary formations of the New Jersey coastal plain. *In* S. Subitzky (editor), Geology of selected areas in New Jersey and eastern Pennsylvania, pp. 235–278. New Brunswick: Rutgers University Press.

Owens, J.P., P.J. Sugarman, N.F. Sohl, R.A. Parker, H.F. Houghton, R.A. Volkert, A.A. Drake, Jr., and R.C. Orndorff. 1998. Bedrock geologic map of central and southern New Jersey. United States Geological Survey. Miscellaneous Investigations Series Map I-2540-B.

Pannella, G., C. MacClintock, and M.N. Thompson. 1968. Paleontological evidence of variations in length of synodic month since Late Cambrian. Science 162: 792–796.

Pervinquière, L. 1907. Etudes de paléontologie tunisienne. I. Céphalopodes des terrains secondaires. Carte Géologique de la Tunisie. Paris: De Rudeval.

Pilsbry, H.A. 1901. Crustacea of the Cretaceous Formation of New Jersey. Proceedings of the Academy of Natural Sciences of Philadelphia 53: 111–118.

Pope, K.O., K.H. Baines, A.C. Ocampo, and B.A. Ivanov. 1997. Energy, volatile production, and climatic effects of the Chicxulub Cretaceous/Tertiary impact. Planets 102(E9): 21, 645.

Quaas, A. 1902. Beitrag zur Kenntnis der Fauna der obersten Kreidebildungen in der Libyschen wüste (Overwegi-Schichten und Blättertone). Palaeontographica 30: 153–397.

Rae, T.C. 1998. The logical basis for the use of continuous characters in phylogenetic systematics. Cladistics 14: 221–228.

Redtenbacher, A. 1873. Die Cephalopodenfauna der Gosauschichten in den nordöstlichen Alpen. Abhandlungen der Kaiserlich-Königlichen Geologischen Reichsanstalt 5: 91–140.

Reeside, J.B., Jr. 1962. Cretaceous ammonites of New Jersey. *In* H.G. Richards et al. (editor), The

Cretaceous fossils of New Jersey. New Jersey Department of Conservation and Economic Development Bulletin 61. Part 2: 113–137.

Richardson, C.A., H. Kennedy, C.M. Duarte, D.P. Kennedy, and S.V. Proud. 1999. Age and growth of the fan mussel (*Pinna nobilis*) from south-east Spanish Mediterranean seagrass (*Posidonia oceanica*) meadows. Marine Biology 133: 205–212.

Roberts, H.B. 1962. The Upper Cretaceous decapod crustaceans of New Jersey and Delaware. *In* H.G. Richards et al. (editors), The Cretaceous fossils of New Jersey. New Jersey Department of Conservation and Economic Development Bulletin 61. Part 2: 163–191.

Robertson, D.S., M.C. McKenna, O.B. Toon, S. Hope, and J.A. Lillegraven. 2004. Survival in the first hours of the Cenozoic. Geological Society of America Bulletin 116(5/6): 760–768.

Rocchia, R., and E. Robin. 1998. L'iridium à la limite Crétacé-Tertiare du site d'El Kef, Tunisie. Bulletin de la Société Géologique de France 169(4): 515–526.

Rocchia, R., E. Robin, J. Smit, O. Pierrard, and I. Lefevre. 2001. K/T impact remains in an ammonite from the uppermost Maastrichtian of Bidart section (French Basque Country). *In* E. Buffetaut and C. Koeberl (editors), Geological and biological effects of impact events: 159–166. Berlin: Springer.

Roemer, F. 1849. Texas. Mit besonderer Rücksicht auf deutsche Aus-Wanderung und die physischen Verhältnisse des Landes nach eigener Beobachtung Geschildert von Ferdinand Roemer. 464 pp. Bonn: A. Marcus.

Rosewater, J. 1961. The family Pinnidae in the Indo-Pacific. Indo-Pacific Mollusca 1(4): 175–226.

Say, T. 1820. Observations on some species of zoophytes, shells, &c. principally fossil. The American Journal of Science and Arts 2(2): 34–45.

Sawlowicz, Z. 1993. Iridium and other platinum-group elements as geochemical markers in sedimentary environments. Palaeogeography, Palaeoclimatology, Palaeoecology 104: 253–270.

Schellenberg, S.A., H. Brinkhuis, C.F. Stickley, M. Fuller, F.T. Kyte, and G.L. Williams. 2004. The Cretaceous/Paleogene transition on the East Tasman Plateau, Southwestern Pacific. *In* N. Exon, J.P. Kennett, and M. Malone (editors), The Cenozoic Southern Ocean: tectonics, sedimentation, and climate change between Australia and Antarctica. Geophysical Monograph Series 151: 93–112. Washington, D.C.: American Geophysical Union.

Schindel, D.E. 1980. Microstratigraphic sampling and the limits of paleontologic resolution. Paleobiology 6(4): 408–426.

Schiøler, P., and G.J. Wilson. 1993. Maastrichtian dinoflagellate zonation in the Dan Field, Danish North Sea. Review of Palaeobotany and Palynology 78(3–4): 321–351.

Schlüter, C. 1871–1876. Cephalopoden der oberen deutschen Kreide. Palaeontographica 21: 1–120; 24: 1–144.

Seilacher, A. 1984. Constructional morphology of bivalves: evolutionary pathways in primary versus secondary soft-bottom dwellers. Paleontology 27: 207–237.

Seilacher, A. 1993. Ammonite aptychi: how to transform a jaw into an operculum. American Journal of Science 293A: 20–32.

Seunes, J. 1890. Contributions à l'étude des cephalopods du Crétacé Supérieur de France. L. Ammonites du Calcaire à Baculites du Cotentin. Mémoires de la Société Géologique de France. Paléontologie 1, Mémoire 2, 1–7.

Signor, P.W., and J.H. Lipps. 1982. Sampling bias, gradual extinction patterns and catastrophes in the fossil record. Geological Society of America Special Paper 190: 291–296.

Slimani, H. 1994. Les dinokystes des craies du Campanien au Danien à Halembaye (Belgique) et à Beutenaken (Pays-Bas). Mémoires pour Servir à l'Explication des Cartes Géologiques et Minières de la Belgique 37: 1–173.

Smit, J. 1999. The global stratigraphy of the Cretaceous-Tertiary boundary impact ejecta. Annual Review of Earth and Planetary Sciences 27: 75–113.

Smit, J., and H. Brinkhuis. 1996. The Geulhemmerberg Cretaceous/Tertiary boundary section (Maastrichtian type area, SE Netherlands); summary of results and a scenario of events. Geologie en Mijnbouw 75: 283–293.

Smit, J., T.B. Roep, W. Alvarez, A. Montanari, P. Claeys, J.M. Grajales-Nishmura, and J. Bermudez. 1996. Coarse-grained, clastic sandstone complex at the K/T boundary around the Gulf of Mexico: Deposition by tsunami waves induced by the Chicxulub impact? *In* G. Ryder, D. Fastovsky, and S. Gartner (editors), The Cretaceous-Tertiary event and other catastrophes in Earth history. Geological Society of America Special Paper 307: 151–182.

Sohl, N.F. 1960. Archeogastropoda, Mesogastropoda and stratigraphy of the Ripley, Owl Creek, and Prairie Bluff Formations. United States Geological Survey Professional Paper 331A: 1–151.

Sohl, N.F. 1964. Neogastropoda, Opisthobranchia, and Basommatophora from the Ripley, Owl Creek, and Prairie Bluff Formations. United States Geological Survey Professional Paper 331-B: 153–344.

Sowerby, J. 1812–1822. The Mineral Conchology of Great Britain. London: The author.

Spath, L.F. 1922. On the Senonian ammonite fauna of Pondoland. Transactions of the Royal Society of South Africa 10: 113–147.

Spath, L.F. 1926. New ammonites from the English Chalk. Geological Magazine 63: 77–83.

Spath, L.F. 1940. On Upper Cretaceous (Maastrichtian) Ammonoidea from Western Australia. Journal of the Royal Society of Western Australia 26: 41–57.

Speden, I. 1970. Generic status of the *Inoceramus? tegulatus* species group (Bivalvia) of the latest Cretaceous of North America and Europe. Postilla 145: 1–45.

Springer, M.S. 1990. The effect of random range truncations on patterns of evolution in the fossil record. Paleobiology 16: 512–520.

Stanley, E.A. 1965. Upper Cretaceous and Paleocene plant microfossils and Paleocene dinoflagellates and hystrichosphaerids from northwestern South Dakota. Bulletins of American Paleontology 49(222): 179–384.

Stephenson, L.W. 1941. The larger invertebrates of the Navarro Group of Texas (exclusive of corals and crustaceans and exclusive of the fauna of the Escondido Formation). University of Texas Bulletin 4101: 1–641.

Stephenson, L.W. 1955. Owl Creek (Upper Cretaceous) fossils from Crowley's Ridge, southeastern Missouri. United States Geological Survey Professional Paper 274: 97–140.

Stoliczka, F. 1863–1866. The fossil Cephalopoda of the Cretaceous rocks of southern India. Ammonitidae with revision of the Nautilidae etc. Memoirs of the Geological Survey of India. Palaeontologica. Indica 3 1(1863): 41–56; 2–5(1864): 57–106; 6–9(1865): 107–154; 10–13(1866): 155–216.

Stover, L.E., and W.R. Evitt. 1978. Analyses of pre-Pleistocene organic–walled dinoflagellates. Stanford University Publications 15: 1–300.

Surlyk, F., and T. Birkelund. 1977. An integrated stratigraphical study of fossil assemblages from the Maastrichtian White Chalk of Northwestern Europe. *In* E.G. Kauffman and J.E. Hazel (editors), Concepts and Methods of Biostratigraphy. Stroudsburg: Dowden, Hutchinson and Ross, Inc., pp. 257–281.

Surlyk, F., and J.M. Nielsen. 1999. The last ammonite? Bulletin of the Geological society of Denmark 46: 115–119.

Trowbridge, J.H., and G.C. Kineke. 1994. Structure and dynamics of fluid muds on the Amazon continental shelf. Journal of Geophysical Research 99(C1): 865–874.

Tsujino, Y., H. Naruse, and H. Maeda. 2003. Estimation of allometric shell growth by fragmentary specimens of *Baculites tanakae* Matsumoto and Obata (a Late Cretaceous heteromorph ammonoid). Paleontological Research 7(3): 245–255.

Tuomey, M. [1854] 1856. Description of some new fossils from the Cretaceous rocks of the southern States. Proceedings of the Academy of Natural Sciences of Philadelphia 7: 167–172.

Turner, R., and J. Rosewater. 1958. The family Pinnidae in the western Atlantic. Johnsonia 3(38): 285–325.

Twitchett, R.J. 2006. The palaeoclimatology, palaeoecology, and palaeoenvironmental analysis of mass extinction events. Palaeogeography, Palaeoclimatology, Palaeoecology 232: 190–213.

Tzankov, V. (Cankov, V.) 1982. Cephalopoda (Nautiloidea, Ammonoidea) et Echinodermata (Echinoidea). Les fossiles de Bulgarie. Va. Crètacé supérieur. Sofia: Editions de l'Académie Bulgarie des Sciences.

Waage, K.M. 1964. Origin of repeated fossiliferous concretion layers in the Fox Hills Formation. Kansas Geological Survey Bulletin 169: 541–563.

Wade, B. 1926. The fauna of the Ripley Formation on Coon Creek, Tennessee. United States Geological Survey Professional Paper 137: 1–272.

Wang, S.C., and C.R. Marshall. 2004. Improved confidence intervals for estimating the position of a mass extinction boundary. Paleobiology 30(1): 5–18.

Ward, P.D., and W.J. Kennedy. 1993. Maastrichtian ammonites from the Biscay region (France, Spain). The Paleontological Society Memoir 34: 1–58.

Wedekind, R. 1916. Über Lobus, Suturallobus und Inzision. Zentralblatt für Mineralogie, Geologie und Paläontologie B 1916: 185–195.

Weller, S. 1907. A report on the Cretaceous paleontology of New Jersey. Geological Survey of New Jersey. Paleontology Series Vol. 4, Part 1. Text: 1–870.

Wetzel, O. 1933. Die in organischer Substanz erhaltenen Mikrofossilien des baltischen Kreide-Feuersteins mit einem sediment-petrographischen und stratigraphischen Anhang. Palaeontographica Abteilung A 78: 1–110.

Whitfield, R.P. 1886. Brachiopoda and Lamellibranchiata of the Raritan Clays and Greensand Marls of New Jersey. U.S. Geological Survey Monograph, Volume 9 (=New Jersey Geological Survey Paleontological Series, Volume 1).

Whitfield, R.P. 1892. Gasteropoda and Cephalopoda of the Raritan Clays and Greensand Marls of New Jersey. United States Geological Survey Monograph 18: 1–402.

Whitfield, R.P., and E.O. Hovey. 1898. Catalogue of the types and figured specimens in the Paleontological Collection of the Geological Department, American Museum of Natural

History. Bulletin of the American Museum of Natural History 11: 1–500.

Wiedmann, J. 1966. Stammesgeschichte und System der postriadischen Ammonoideen: ein Überblick. Neues Jahrbuch für Geologie und Paläontologie. Abhandlungen 125: 49–79; 127: 13–81.

Wiedmann, J. 1987. The K/T boundary section of Zumaya, Guipuzcoa. *In* M.A. Lamola (editor), Field-guide excursion to the K/T Boundary at Zumaya and Biarritz. III Jornadas de Paleontologia - Paleontologia y evolución: fenómenos de extinción: 17–23. Vasco: Universidad del Pais.

Wiedmann, J. 1988. Ammonite extinction and the "Cretaceous-Tertiary Boundary Event". *In* J. Wiedmann and J. Kullmann (editors), Cephalopods– Past and Present, pp. 117–140. E. Schweizerbart'sche Verlagsbuchhandlung, Stuttgart.

Williams, G.L., J.K. Lentin, and R.S. Fensome. 1998. The Lentin and Williams Index of fossil dinoflagellates. American Association of Stratigraphic Palynologists, Contributions Series 34: 1–817.

Williams, G.L., H. Brinkhuis, M.A. Pearce, R.A. Fensome, and J.W. Weegink. 2004. Southern ocean and global dinoflagellate cyst events compared: index events for the Late Cretaceous-Neogene. *In* N.F. Exon, J.P. Kennett, and M.J. Malone (editors), Proceedings of the Ocean Drilling Program, Scientific Results 189: 1–98.

Yonge, C.M. 1953. Form and habit in *Pinna carnes* Gmelin. Philosophical Transactions of the Royal Society of London B Biological Sciences 237: 335–374.

Young, G., and J. Bird. 1828. A geological survey of the Yorkshire coast: describing the strata and fossils occurring between the Humber and the Tees, from the German ocean to the plain of York. 2nd ed.: 1–368. Whitby: R. Kirby.

Yun, H. 1981. Dinoflagellaten aus der Oberkreide (Santon) von Westfalen. Palaeontographica Abteilung B 177: 1–89.

Zinsmeister, W.J. 1998. Discovery of fish mortality horizon at the K-T Boundary on Seymour Island: Re-evaluation of events at the end of the Cretaceous. Journal of Paleontology 72(3): 556–571.

Zinmeister, W.J., and R.M. Feldmann. 1996. Late Cretaceous faunal change in the high southern latitudes: a harbinger of biotic global catastrophe? *In* N. MacLeod and G. Keller (editors), Cretaceous-Tertiary Mass Extinction: Biotic and Environmental Changes, pp. 356–378. W.W. Norton & Co., New York.

Zittel, K.A. von. 1884. Handbuch der Paläontologie. Abt. 1. Band 2: 329–522. Munich: R. Oldenbourg.

Zittel, K.A. von. 1895. Grundzüg der Palaeontologie (Palaeozologie). Munich: R. Oldenbourg: 1–972.